REPORT NO.
UCB/SEMM-88/14

STRUCTURAL ENGINEERING,
MECHANICS AND MATERIALS

ANALYTICAL AND EXPERIMENTAL STUDIES OF DOUBLE-ANGLE FRAMING CONNECTIONS

by

KURT M. McMULLIN

ABOLHASSAN ASTANEH-ASL

AUGUST 1988

DEPARTMENT OF CIVIL ENGINEERING
UNIVERSITY OF CALIFORNIA AT BERKELEY
BERKELEY, CALIFORNIA

ANALYTICAL AND EXPERIMENTAL STUDIES OF DOUBLE-ANGLE FRAMING CONNECTIONS

by

Kurt M. McMullin, Graduate Research Assistant

and

Abolhassan Astaneh-Asl, Assistant Professor

Department of Civil Engineering

University of California, Berkeley

AUGUST 1988

TABLE OF CONTENTS

PAGE

LIST OF TABLES

LIST OF FIGURES

ABSTRACT

by K.M. McMullin and A. Astaneh

Seven full scale experiments of steel shear connections were performed. Four experiments were typical double-angle connections and three were a new lambda connection. All seven connections were bolted to the beam web and welded to the column flange. Shear, moment and rotation quantities were obtained for incremental steps during monotonic loading.

Each specimen was loaded in two cycles. First a ductility cycle loading was applied. This test measured the rotational flexibility of the connection and was performed with a cantilever testing procedure. The second cycle measured ultimate strength and was applied using a new testing procedure. The new procedure was a realistic simulation of the actual conditions for a shear connector. This loading was applied until failure of the connection occurred.

The results obtained from the experimental work were compared to predictions based on various models. Comparison with the Richard's model, and an analysis based on plastic methods were also performed. Guidelines and analytical models were developed to be used to predict the ultimate strength and to design the double-angle shear connection.

ACKNOWLEDGMENT

The research project reported here was primarily sponsored by the Department of Civil Engineering, University of California at Berkeley as CE-299 Individual Study of the first author for his Master of Science degree. The authors wish to thank Professor F. Filippou for his assistance in reviewing this report.

The original concept of Lambda connections presented in Chapters 5 and 6 of this report, was invented and developed by the second author. The research reported here was conducted to verify its validity by testing and studying behavior of actual specimens.

The specimens were fabricated by the laboratory technicians at the University of California, Berkeley. The authors recognize the valuable assistance given by the laboratory staff particularly Roy Stephen and Mike Pitrola, without whose help the experimental work could not have been completed. The authors also wish to thank graduate student Marwan N. Nader for his assistance in teaching the first author about the testing equipment.

Finally, the first author wishes to thank the two people who have inspired him to reach this goal: his parents Eugene and Joan McMullin.

CHAPTER ONE

INTRODUCTION

1.1 Introduction

A common type of construction of steel buildings is the use of simple connections between the beams and columns. Simple connections (designated as Type II) are expected to act like hinges; they should carry vertical shear, but not bending moment, from the beam and to the column. The Eighth edition of the AISC Steel Manual (20) lists double-angle connections as one type of simple framing connection.

A typical double-angle connection is shown in Figure 1.1. Double-angle connections attach the web of the beam to the support. Figure 1.2 shows three common applications of the double-angle connection: a beam-to-beam, a beam-to-column, and a beam-to-wall joint.

Strength and ductility are the two most important criteria for any simple connection (15). The shear strength of the connection must be sufficient to transfer the load from the beam and to the column. However, unlike a rigid connection the simple connection must be ductile enough to rotate without transferring a significant moment into the column. Normally, engineers consider a connection to be simple if less than 20% of the fixed end moment of a beam is developed in the connection (18).

Double-angle connections have several advantages over other simple connections. First, they allow for over or under cutting

the length of the beam (10). Also, they are stronger and more ductile than shear tabs, allowing for heavier loads to be carried by the beam. One major disadvantage of double-angle connections is that the beam flange should be coped to aid in erection.

The purpose of this report is to determine the characteristics of double-angle connections depending on changes of their geometry. Also an added objective is to outline the common modes and paths that lead to failure of this type of connection.

1.2 Scope of the Research Project

This experimental study was proposed after considering the past work on simple connections and the overall behavior of double-angle connections. There were two broad objectives for this study. First to investigate the current connections and their characteristics. Second to look at alternative designs to improve these characteristics. It was hoped that information would be gained through the experimental testing of several connections. This information is expected to allow designers to more accurately estimate the strength and ductility limits of a double-angle connection.

The objectives of this study were accomplished by testing seven full size, double-angle connection details. Figure 1.3 presents the various parameters that define the double-angle geometry. These geometric parameters were varied within the limits shown in Table I to establish a testing schedule.

The testing measured the strength and ductility of each specimen. This report contains moment-rotation and shear-

rotation curves for all seven connections. This information may be used to develop analytical models of rotational stiffness of connections.

1.3 Literature Survey

Though double-angles are in common use as structural shear connections there is little available information about their mechanical behavior and characteristics. The two main criteria for shear connections are strength and ductility (1,15). Strength capacity is required to transfer the beams end reaction to the column. Ductility is required for bending to allow the beam to rotate. Any restraint to that rotation would reduce the connections free rotational flexibility.

This reaction is dominated by vertical shear in most connections. The beam reaction also includes a small moment due to the rotational stiffness of the connection. This moment is dependent on the location of the beam's inflection point and the shear on the connection. The connection's flexibility is an important factor in the location of this point. This is described in more detail in Section 4.3. Unfortunately, very little information is available in the literature about the location of the point of inflection and the magnitude of these reactions during the life of the connection. This experimental program provides evidence of where the point of inflection of a simply supported beam will develop.

Testing performed by past investigators provides some information about these connections (4),(5),(8),(11),(15),(16),(19). However, the results obtained from past research are

limited and tend to measure only one parameter (strength or rotational ductility) due to the testing procedure used. This limitation is explained in Section 2.4. Still, information from past research provides an important starting point when investigating connections. A series of 33 double angle tests are documented in the research which show the excellent ductility of this connection (13). These tests measured rotational capacities of 0.08 radians and developed moments of only 5-15% of the beam's plastic moment.

During design it is normally assumed that a double-angle connection will behave like a perfect pin; transfer no moment into the column. However in real applications this is never the case and the designer must be aware of the effects. In fact, moments transferred into columns can be significant, as high as 57% of the column's plastic moment (13). This transfer of moment affects the supporting column in two ways. It is a factor of both the column's effective length and load carrying capacity. The lateral stiffness and strength are higher for a column restrained by flexible connections than one supported by pins. In fact, assuming that double angles are perfect pins has been shown to underestimate the capacity of a column by up to 40% (13).

Previous research indicates that the assumption of no moment being transferred into the column is conservative. If the beam is supported by a girder, the connection moment will act as a torque on the girder. This torque will cause torsional stresses and twist the girder. Disregarding this torque would be unconservative, and therefore designers must note the detrimental

effect of a connection on supporting elements.

Much work has been done in the past to model rigid connections but the amount of published information on simple and semi-rigid connections has been small. Modelling these connections is difficult due to the complex stress patterns that develop. This complex pattern is due to the coupling action between shear and moment as well as significant inelasticity in the connection. Also, it must be noted that shear and moment do not increase at a constant ratio (1,3).

This coupling action usually is not considered in structural design because normal design practices in steel structures tend to separate load-carrying members into distinct elements. Each element is then designed to carry one type of force. In the double-angle connection one element carries both the shear and the moment, unlike a W shape that carries shear in the web and moment in the flanges (3).

Another problem in modelling simple connections is the effect of large deformations in the connection which cause the development of strain and kinematic hardening. These hardenings create a significant non-linearity in the response of the connection that must be considered in design.

Ralph Richard and his colleagues (16) have developed an analytical model to predict the moment-rotation relationship for a double-angle connection. This model is non-linear and neglects the effects due to shear. The model is based on a discretized rigid bar held by horizontal springs. As the bar rotates each spring develops a force resisting the rotation of the connection. These forces create a moment which will be transferred into the

support. Appendix C contains a more detailed explanation of the Richard Equation and contains relevant references.

Other attempts have been made in the past to develop empirical models to predict the moment-rotation curves obtained from laboratory testing. Analytical models have been proposed by Lothers et al (12), and by Lewitt et al (11). These models are listed by Morris and Packer (13).

CHAPTER TWO

EXPERIMENTAL PROGRAM

2.1 Introduction

Seven full scale double-angle connection specimens were tested during the experimental phase. Each test consisted of subjecting a double-angle beam-to-column connection to a combination of shear, moment, and rotation that would realistically simulate a simply supported beam. The following sections explain the parameters of study, test specimens, loading history and test procedures. Test results are given in Chapters Three and Five.

2.2 Parameters of Study

There were two main objectives of this study. First, investigate shear strength and rotational ductility of the connection. In other words, find the shear capacity which corresponds to a certain amount of required rotation for a double-angle connection. Second, to see if this relationship is improved by a new connection geometry denoted as the Lambda connection (2). Improvement was defined as the lowering of the moment transferred to the column while increasing the total shear capacity of the connection.

2.3 Test Specimens

Each specimen consisted of a W 24x68 beam connected to a W10x77 column with a double-angle connection. Table II lists properties of these double-angle connections. All specimens were fabricated in the laboratory.

All bolts used were A325 with threads excluded from both shear planes. Two different nominal diameters of bolts were used. In test specimens 4,5 and 6 the bolts were 3/4" diameter and in tests 7,8,9, and 10 the bolts were 7/8" diameter The bolt spacing for all specimens was three inches center-to-center of bolts. The edge distance of the bolts for all specimens was 1.25 inches from the top and bottom. This edge distance and spacing satisfied the requirements of current AISC specifications (1).

Each angle was welded to the column using E-70XX electrodes resulting in a nominal strength of 70 ksi for the welds. The nominal weld size for each specimen was 1/4 inch.

The column used was a W10x77 and the beam was a W24X68. These sections were selected to ensure that they would remain elastic during the experiments and would not enter as a major parameter of the study.

2.4 Test Set-up

As discussed in Section 1.3, the moment and shear are coupled in a Type II connection. The complexity of the problem is increased due to large rotations in the connection area that cause significant strain hardening and geometric non-linearities. Because the connection is very flexible, a small moment applied to a beam will create large rotations. In a testing lab it is

physically impossible to apply a large shear on a connection with no eccentricity, if only one load applying actuator is used. Yet large shear forces with small eccentricities will develop moments high enough to cause unrealistically large rotations for a double-angle connection.

A laboratory test must simulate the actual shear, moment and rotation values of a loaded beam as closely as possible in order to study the actual behavior of a connection. Some researchers have used a typical cantilever beam specimen (15) as shown in Figure 2.1(a). Although this test arrangement provides valuable information on moment-rotation characteristics, it fails to accurately measure the strength of a connection for shear. Upon loading by a small shear, a large rotation takes place and the specimen fails in bending due to the high flexibility of the connection. This happens even though the shear stresses in the connection are still quite small. Therefore, the results of the cantilever test specimens measure only the rotational ductility of Type II connections and not the shear strength.

In order to measure shear strength of the connection, test set-up of Figure 2.1(b) or similar set-ups have been developed by researchers (15). Usually in these tests a short span beam is used, in order to fail the connection before the beam fails. The use of a short span beam in this test set-up results in a very small end rotation of the beam. Therefore, the rotation experienced by the connection during the test will be unrealistically smaller than the actual rotation in a structure.

Consequently, since the realistic rotations are not imposed on connections, the measured shear strength at best is an upper

limit of strength and not the actual strength at failure. Particularly in welded framing connections, the rotation of a connection generates large strains in the welds that can significantly reduce the direct shear strength capacity of the connection.

To perform a more realistic test and to simulate the combined effects of shear, moment and rotation in a Type II connection, one way is to fabricate a typical beam specimen and its end connections and test the specimen to failure. In this case the cost of fabricating the specimens is prohibitive and very few tests can be performed.

A. Astaneh (1,3) has developed a test set-up as shown in Figure 2.2 to overcome these difficulties. This set-up can be used to test any flexible or semi-rigid connection.

The main components of the test set-up are a permanent beam, two actuators, and support blocks. Actuator S, which is close to the column support, is force controlled and provides the bulk of the shear force on the connection. Actuator R, which is displacement controlled, regulates and provides the rotation of the connection. Any desired shear and rotation combination can be developed in the connection by adjusting these two actuators. The support blocks are concrete and steel dead weights that have been pre-stressed to the floor of the laboratory.

2.5 Loading History

The objective in conducting each test was to simulate the shear and rotation induced in a flexible connection when a beam

is subjected to gravity loading. It was desired to test each specimen under two different cycles of loading. The first cycle, denoted as the ductility cycle, was performed by applying a small shear with actuator R. The loading and test procedures are similar to the common cantilever test procedure and shows the available ductility in the connection.

The second cycle, denoted as the ultimate cycle, was used to measure the ultimate shear of the connection. A. Astaneh used the computer program ENDROT and a further modified ENDGEN program to establish a realistic end rotation demand of a beam (3). These computer programs, explained in the cited reference, calculate the necessary rotation that must develop at the midspan of a simply supported beam if the beam is to achieve its plastic moment.

By using ENDGEN, it was found that the ratio of end rotation at failure to rotation at yield is almost constant for a beam as it forms a mid-span plastic hinge. This constant was found to be conservatively less than two and was independent of the beam's span or size. ENDGEN showed that for beams with spans of 50 feet or less, the end rotation of the beam will be less than 0.05 radians when the midspan moment reaches 97% of plastic moment. Typically the end rotation of the connection was in a 1:1000 ratio to the span length in units of feet.

A rotation of 0.03 radians was chosen as a desirable lower limit for the double-angle connection. This value was chosen for two primary reasons. First because it is an average value for end rotations of common spans (10, 30, and 50 feet). Second it exceeds the normal requirement for rotation capacity of Type II

flexible connections that is usually set to 0.02 radians in the literature (10).

A predicted shear failure load was calculated considering all possible modes of failure based on the AISC-LRFD manual (2) procedures and the expected behavior of these connections. This failure load was calculated when subjecting the double-angle framing connection to pure shear. These calculations are made for each test specimen in Section 4.2.

This failure load (V_{ult}) and 0.03 radian rotation were plotted as a target point for each ultimate cycle test. During the ultimate cycle of each test the connection was subjected to a monotonic shear load and rotation such that the slope of the shear-rotation curve was Vult/0.03. Figure 2.3 shows a graph of this desired loading path. Once the connection approaches its ultimate capacity this loading path begins to level off and the shear to rotation ratio can no longer be maintained. This behavior is well documented in the graphs of test data in Appendix B.

In summary, each specimen was subjected to two cycles of loading. First a ductility cycle was performed to a maximum rotation exceeding 0.05 radians. Second, an ultimate cycle was run with a linear loading rate between shear and rotation. Figure 2.4 shows a computer graph of the loading cycles during a test.

2.6 Instrumentation

Figure 2.5 shows the instrumentation for this experimental program. The instrumentation consisted of three Linear Variable

Displacement Transducers (LVDT), three Linear Potentiometers (LP), and two load cells. LVDT #7 measured the separation of the top of the angle relative to the column flange. LVDT's 5,6,8 and 9 were used to measure the relative displacement between the beam flanges and the column flange. The rotation of the beam can be calculated from these readings, especially at low (less than 0.02 rad.) rotations. The calculation is:

$$\text{Rotation} = \frac{\text{LVDT5} + \text{LVDT6} + \text{LVDT8} + \text{LVDT9}}{2 \text{ x (distance between LVDT centerlines)}}$$

LP #3 was used to measure the deflection at the end of the beam, direcly across from actuator R. LP #4 was used to measure the deflection across from actuator S while LP #10 measured the displacement at the boltline in the direction of the applied shear load. LP #1 and #3 were used to calculate the rotation of the beam, especially at values above 0.01 radians. This calculation is:

$$\text{Rotation} = \frac{\text{LP3 - LP10}}{\text{separation}}$$

Load cell R was used to measure the force in actuator R which controlled the rotation of the connection. Load cell S measured the force supplied by the A actuator. These two forces were added together to obtain the total shear on the connection.

The data acquisition system for the experiments consisted of an IBM-PC based system with capability of real-time recording and processing. Another IBM-PC was used to maintain a plot of the shear rotation curve as loading proceeded. Slides, photographs and notes were taken at frequent points to record the qualitative aspects of the research.

2.7 Test Procedures

Table II contains the schedule of test specimens used for this project. The following is a step by step listing of the testing procedure:

1. The specimen was fabricated, assembled and prepared for testing.
2. Instrumentation was placed and connected to the data acquisition system.
3. Specimen was coated with a light covering of whitewash which would crack to show when the specimen yielded.
4. By applying a small load the instrumentation was checked to confirm that everything was working.
5. A ductility cycle was performed with a maximum rotation exceeding 0.05 radians.
6. An ultimate cycle was performed until the connection failed. Failure was defined as significant cracking of the weld.
7. A test summary was written and graphs of data plotted.

CHAPTER THREE

EXPERIMENTAL RESULTS OF DOUBLE-ANGLE CONNECTION TESTS

3.1 Introduction

This chapter presents the quantitative and qualitative data from the first series of tests in the experimental study. The specimens in this test series were standard double-angles welded to the column and bolted to the beam web. Each specimen was tested under two separate cycles as described in Chapter Two.

The first cycle was a ductility cycle and the second an ultimate strength cycle. The objective of this test series was to gain insight about the behavior of double-angle connections under actual field conditions. Figure 3.1 shows the nomenclature used to describe the different areas of the double-angle connection. Table III contains the overall results for each test.

3.2 Behavior of Test Number Four

The first test performed was for a seven bolt connection. This connection was welded to the column and bolted to the beam with seven 3/4" bolts spaced every three inches. During the ductility cycle yielding was observed along the top of the weld and near the middle bolt. During the ultimate cycle a maximum load of 230 kips was achieved before the weld sheared in the heat affected zone.

This failure occurred well below the expected capacity of

280 kips. Also the slope of the shear vs. rotation graph remained relatively constant, indicating that the connection stiffness was not changing. When yielding occurs this stiffness will decrease. Apparently, the weld was of poor quality, having poor penetration into the base metal. This caused the weld to shear free from the base metal before the connection could yield and develop its capacity.

The slope of the loading line in this test was not as described in Section 2.5. The reason for the discrepancy in the slope was due to an instrumentation error. Unfortunately this error was not found until after the test was completed. However it is believed that the steeper load path did not contribute to the premature failure of this specimen.

3.3 Behavior of Test Number Five

The next test was of a five bolt connection. This connection was similar to test number Four's, except only five bolts were used. During the ductility cycle a small crack developed in the weld return. The weld dimension's consistency on this specimen was poor but the overall weld quality appeared to be much better than Test 4.

At 110 kips into the ultimate cycle yielding began to appear on some of the thinner parts of the weld. At 197 kips the top third of the weld length cracked but the connection still held 205 kips of shear load before finally failing. Bearing damage of the beam was observed when this connection was dismantled.

3.4 Behavior of Test Number Six

The last test of this series was number six, a three bolt connection. On this specimen the ductility cycle could only be taken to 0.0310 radians. The reason for this limit was that the rotation caused the beam flange to come in contact with the column due to the depth of the beam. Continuing the ductility cycle beyond this point would have caused damage to the connection. This damage is due to the higher stiffness of the connection once contact is made between the beam and the column flange. Even though this is a possible failure mode of simple connections, it was not a mode we were investigating so we concluded the ductility cycle.

During the ultimate cycle yielding was seen to occur at several locations in the connection. These areas were the weld return, the shear beam area of the back-to-back legs, and along the length of the outstanding leg. After reaching 113 kips, the weld cracked from the top down. By increasing the rotation, but without an increase in the load, the entire length of the weld finally cracked.

3.5 Behavior of Test Number Nine

Test number Nine was part of the second series of tests. The test is explained in Chapter Five, because it was the control specimen for this later test series. However, the specimen was detailed with the same connection geometry as Tests number 4,5 and 6 and so the results are used to support the information gained through this first series of tests.

This specimen used 4x4x3/8" angles, five 7/8" A325-X bolts,

and was 14.5 inches long. During the ductility cycle the weld return cracked, the outstanding leg showed compression yielding and the top portion of the weld yielded. During the ultimate cycle, yielding was seen to begin in the shear beam area of the back-to-back leg when the load reached 72 kips. The weld cracked at 190 kips and the ultimate load obtained was 192 kips, corresponding to an ultimate rotation of 0.0332 radians.

3.6 Typical Failure Mode of Double-Angle Connections

Double-angle connections tend to follow a very similar behavior during testing, independent of their geometric parameters. Before the connection fails the outstanding leg can normally be seen to operate as three distinct regions. Figure 3.2 shows a sketch of these regions on a double-angle connection.

The top portion of the leg behaves similar to a tee-hanger. A tee-hanger is defined as an angle welded to a plate with a pure tension load applied to the outstanding leg. This tension load acts to pull the angle from the support. The tee-hanger region covers the top few inches of a connection. Figure 3.3 shows an actual connection as the angle fillets pull away from the column in the tee-hanger portion.

The second portion of the connection behaves as a shear beam. This portion covers the majority of the length of the connection. In this region the shear load of the beam is carried from the beam web, through the bolts, into the shear beam region of the bolted leg, through the shear beam region of the outstanding leg and finally to the weld and into the column. This region normally deforms similar to the traditional shear

stress block of elementary mechanics of materials, in that it deforms as a parallelogram.

The third portion of the connection behaves similar to a plate under the forces of compression. This occurs in the lower region of the connection, normally in the bottom few inches. This compression develops due to the Out-of-plane moment which tends to push the bottom of the angle's outstanding leg out from the beam web. Compressive stresses normally increase until the region fails by buckling the outstanding leg away from the column flange as shown in Figure 3.4.

Traditionally the double-angle connection fails in the following sequence:

- -at low shears, but high rotations (during the ductility cycle), the weld return cracks
- -yielding appears to concentrate around the weld return region of the angle, and near the top portion of the weld
- -the top of the angles begin to pull away from the column flange and the bottom edge bulges away from the column due to compression
- -the weld cracks at the top as shown in Figure 3.5 and as more load is applied, this crack propogates along the length of the weld
- -at the same time stresses in the bottom of the weld cause a crack to develop and propogate toward the middle

Figure 3.6 shows a specimen after complete failure. Notice that the weld has cracked throughout its entire length. Also

notice the heavy yielding (indicated by the whitewash broken loose from the specimen) which has occurred in the outstanding leg.

3.7 Other Failure Modes of Double-Angle Connections

Other possible failure modes for double-angle connections exist but they do not seem likely to occur in common designs. Bearing of the bolt against the beam web can be a problem. This is especially true if light beams (thin webs), or small (less than 3/4") bolts are used. Bearing is seldom a failure of catastrophic proportions, but can cause excessive deflections and serviceability problems. Figure 3.7 shows bearing damage on the beam web. Note the bulge occurring around the bottom hole of the connection.

Shear failure of the bolts is another problem, but this is extremely rare since the bolts are loaded in double shear and commonly the threads are excluded from the shear planes.

Failure of the bolted leg due to shear is another unlikely mode. The even distribution of yielding throughout the shear beam area of the bolted leg, seen in most tests, causes this failure mode to be rare. Another reason this is an uncommon failure mode is because each angle must carry only half the shear on the connection. In contrast, a shear tab connection must carry the total shear with a single thickness of plate.

Another failure mode can occur if the connection rotates excessively. This failure mode happens when the bottom flange of the beam rotates and touches the column. This action pulls the neutral axis of the connection down and sharply increases the

slope of the shear-rotation graph. This increase in the slope is documented in current research (10). It occurs because the connection suddenly becomes much stiffer than before. This increase in stiffness will correspond to a higher moment being transferred into the column.

Block shear of the beam web, especially for coped beams, is a potential failure mode that should not be overlooked. This failure mode was beyond the scope of this study and so no information is provided from this investigation. This failure mode has been reported in the past and design specifications have considerations for this problem (20,21).

3.8 Summary of Failure Modes of Double-Angle Connections

Several failure modes exist for double-angle connections as mentioned in the previous section. The following failure modes were considered as part of this investigation.

1-) Fracture of weld

2-) Bolt bearing on web bolt holes

3-) Bolt shear failure

4-) Failure of the back-to-back legs of the angles

The last two modes were found to be unlikely with most double-angle connection details.

Two more failure modes exist for double-angle connections but these are predominantly dependent on the beam geometry, not the double-angle. These failure modes are:

5-) Excessive rotation of the connection, allowing the beam flange to contact the column

6-) Block shear failure of the beam web, especially when the beam has been coped

These six are considered to be all the possible failure modes, or at least the most significant.

3.9 Test Results

After each test a summary containing the qualitative information obtained was written. These summaries are contained in Appendix A. Also in this Appendix are tables containing the data obtained and calculated for each test. Tensile tests were made of coupons machined from the steel used to fabricate the connection angles. These tests were performed to obtain the material properties of the steel. The results are listed in Table IV and reflect the properties of A36 steel.

For both cycles of each test the following variables were plotted against each other:

Shear on Connection vs. Rotation of Beam
Shear on Connection vs. Deflection at Boltline
Moment at Boltline vs. Rotation of Beam
Moment at Weld vs. Rotation of the Angle
Moment at Weld vs. Shear on Connection
Moment at Boltline vs. Shear on Connection

These graphs are contained in Appendix B. Figure 3.8 shows the sign convention used for each graph.

By comparing the results of the tests, certain characteristics of double-angle connections were found to occur. These characteristics were the location of the inflection point during loading, the estimated stress distribution, the equivalent stress calculated by von Mises' criteria, and the interaction of shear and moment by plastic analysis of the weld.

CHAPTER FOUR

ANALYSIS OF EXPERIMENTAL RESULTS

4.1 Introduction

After observing the test specimens during the actual testing the following ideas have been developed and are explained in the following sections of this chapter:

1. The inflection point in a beam supported by double-angle connections moves toward the support during the loading history.
2. At low loads, the inflection point is in the beam, and has not moved to the connection.
3. Yielding of the connection causes the inflection point to move into the connection, this behavior began to occur at loads below the expected service capacity of the connection.
4. Elastic theory estimates concentrated stresses that are unrealistically large.
5. Plastic analysis based on an inelastic stress distribution predicts the failure capacity of a connection with reasonable accuracy.
6. Connection strength predictions based on allowable stress design methods of AISC are conservative with regard to service loads, but may not have a consistent factor of safety.

7. Fracturing of the weld is by far the most common mode of failure for double-angle connections.
8. Double-angle connections are superior to shear tabs because they have less rotational stiffness and so transfer less moment into the column or other supporting members.
9. The Richard equation appears to predict the test results reasonably well but should possibly be modified to include shear effects.

Table V contains the predicted and actual failure loads for each test.

4.2 Failure Prediction Used During Testing

The predicted failure of each specimen was originally calculated as failure due to pure shear as shown in Chapter 2. These calculations are shown in Section 4.6 This prediction was used because of the lack of knowledge about the actual location of the inflection point during the loading of a double-angle connection. Since some restraining moment is developed in the connection the beam is not simply supported and so an inflection point will occur in the beam as shown in Figure 4.1. If the location of this inflection point is known, the moment transferred can be approximated as:

$$M = V\ e$$

However due to the complexity of the connection it is impossible to determine e, the eccentricity, before testing is performed.

The strength of each connection was predicted using appropriate design equations from the AISC-LRFD Manual (21). To predict the nominal ultimate load of each connection the ø resistance factor used in the LRFD format was excluded. These predictions were used to plot the loading line as described in Section 2.5. However after observing the testing a better understanding of the connection behavior was developed. With this better understanding a model was created for determining weld failure.

4.3 Determination of Location of Inflection Point

A perfect pin supported beam develops an inflection point at its support. A beam with completely rigid connections develops an inflection point near the quarter span point. A double-angle connection is idealized as a simple support but actually provides a small restraining moment to the beam. For this study we consider the moment which develops at the weld of the connection as the moment transferred into the column.

From the experimental results obtained in these tests the actual location of the inflection point could be obtained by static analysis for any load during the loading history. Figures 4.2 through 4.5 are graphs of the location of the inflection point as a function of the normalized shear on the connection. The boltline has a two inch eccentricity from the weld. By observing the graphs it may be seen that the location of the inflection point remains near the back of the bolt hole, especially when the load is above 50% of ultimate capacity (the normal allowable stress limit).

Figure 4.6 shows graphs obtained from two tests (#6 and #9). These graphs have been normalized to the maximum shear and an original eccentricity. The first graph uses an original eccentricity for loads nearly equal to zero. Three theoretical curves, based on elliptical functions are plotted on this graph. These curves predict the location of the inflection point for a given loading. The linear curve is conservative but easy to use. The better prediction is given by the middle curve. The equation of this graph is:

$$\left(\frac{V}{V_{max}} - 1\right)^{1.5} + \left(\frac{e}{e_o} - 1\right)^{1.5} = 1.0$$

where:

V/V_{max} = shear normalized to the measured capacity

e/e_o = eccentricity normalized to original eccentricity

The second graph shows the same data normalized to an original eccentricity when V = 0.4 Vmax, roughly the point where the eccentricity becomes constant. This graph shows how well the two tests match each other.

The difficulty upon using these curves is determining the original eccentricity of the connection. The values used here were obtained by studying the test data. One important fact the graphs show is that at low loads (less than 30% of ultimate)

enough yielding has occurred to cause the inflection point to move well into the connection.

Based upon the results of this investigation, when using ultimate strength design procedures, assuming an eccentricity of three inches is justified for three, five and seven bolt double-angle connections.

4.4 Distribution of Stresses in Connection Weld by Elastic Theory

Figure 4.7 shows the distribution of bending stresses that is assumed to develop in a double-angle connection. The shear stress is assumed to follow the parabolic distribution for a rectangular section.

The In-plane bending stress has a neutral axis far below the midline of the connection. The tension region remains linear through the mid-portion of the connection but grows dramatically at the weld return. This rapid increase is due to the stress concentration at the end of the weld. Since the neutral axis is near the bottom of the weld, a large compression force must develop to balance the force resultant of the tension region. Although the force is large, it is transferred into the column mostly by bearing and the weld is relatively free of stress. An approximation of this stress distribution is shown in part b of Figure 4.7. The stress distribution is idealized as a triangular linear function with a neutral axis at one/sixth the height of the connection.

The Out-of-plane bending stress is distributed similarly to the In-plane except that the compression force is carried almost entirely by the weld and will develop high compression stresses

at the bottom of the connection. These high stresses create the buckling of the compression zone of the leg, which is commonly seen at ultimate failure. This stress is idealized with a triangular linear distribution with the neutral axis located at mid-height. This location is an approximation based on observation of the connection behavior.

4.5 Stress Calculation by von Mises Criterion

Using these idealized stress distributions and the location of the inflection point as determined in Section 4.2, the stress in the weld can be calculated using linear elastic methods. The use of linear elastic stress distribution is very common in current design methods of welds (6,18,21).

These stresses are tabulated in Table V for Tests 4,5,6 and 9. The three independent stresses were combined into an equivalent stress by using von Mises' criterion (7). These equivalent stresses were calculated at three different points in the weld: point A, at the top; point B, at the mid-depth; and point C at the bottom of the weld. The welding electrode was E70XX so a reasonable estimate of the yield stress is 60 ksi with an ultimate strength about 70 ksi.

The loads can be compared to the shear load as it is normalized to the maximum capacity during the test. For each test yielding should occur at the given normalized shear as shown by the table on the following page.

Test Number	Normalized Shear (V_y/V_{max}) by von Mises	by observation during testing
4	0.728	1.000
5	0.582	0.529
6	0.586	0.239
9	0.650	0.375

These values show that von Mises' criterion predicts yielding to occur at a load different than the one observed during the actual testing. The above values also show that yielding can be observed in the connection well below the service capacity, normally considered to be 50% of the ultimate load.

Once yielding begins, the connection stiffness decreases and linear elastic analysis is no longer valid. If this analysis is used it will overestimate the stress in the weld. The values that are in the tables for failure loads show stresses of over 100 ksi. These values are unreasonably high for E70XX electrode. Table V contains the load when a value of 70 ksi is calculated by von Mises' criterion. This would be the failure load as predicted by linear elastic methods. It is evident that linear elastic analysis will significantly under-estimate the capacity of the connection.

4.6 Calculation of Ultimate Strength

The AISC Load and Resistance Factor (LRFD) specification (21) was used to make the original estimate of ultimate capacity for each specimen. Three criteria were checked as follows:

1. Weld fracture

The capacity of welds subjected to Out-of-plane shear parallel to the weld's axis can be calculated as :

$$V_u = C \times C1 \times D \times L$$

This formula is based on Table XVIII, page 5.91 of the LRFD Manual. The factors in this formula are:

C = coefficient from Table XVIII which is a function of two variables (k,a)

k = 0 for shear applied out of plane

a = e/L

e = eccentricity of shear from weld

L = length of each weld

D = number of sixteenth of an inch in fillet weld size

C1 = 1 for E70XX electrodes

Therefore this formula becomes:

$$V_u = 1\ (C \times 1 \times D \times L)$$

for this series of tests.

2. Bolt bearing against web of beam

The bearing strength for a bolt fulfilling the requirements of Section J3.6 (page 6-68) of the LRFD Specification (21) is given as:

$$R_n = 2.4 \times d \times t \times F_u$$

where:

d = nominal diameter of the bolt

t = thickness of the connected part

F_u = specified ultimate strength of the connected part

For this series of tests:

t = 0.375 in. = the web thickness of a W24x68 beam

F_u = 58 ksi = the ultimate strength for A36 steel as given by the AISC Manual

Substituting in these variables gives:

R_n = 39.2 kips for each 3/4" bolt

R_n = 45.7 kips for each 7/8" bolt

The shear capacity of the connection for failure due to bolt bearing can be calculated as:

$$Vu = \phi \, Rn \, (\# \text{ of bolts})$$

where ϕ is equal to 0.75

3. Shearing of bolts

The shearing stength of a bolt which fulfills the requirements of Section J3.3 (page 6-66) of the LRFD Specification (21) is given as:

$$R_n = A_b \times \text{Nominal Strength} \times 2$$

where:

A_b = area of the bolt based on the nominal diameter

Nominal strength = value from Table J3.2

For this series of tests, using A325-X bolts, the nominal strength is 72.0 ksi/shear plane. Substituting these values into the above equation gives:

R_n = 63.6 kips for each 3/4" bolt

R_n = 86.6 kips for each 7/8" bolt

As in the bearing calculation presented above, the shear strength

of the connection is calculated as:

$$V_u = \phi \text{ Rn (\# of bolts)}$$

where ϕ in this case is equal to 0.65.

After calculating the nominal capacity, an estimate of the expected failure capacity was obtained by dividing the above capacity by the corresponding ϕ factor. The strength for each connection was also determined according to the AISC 1978 Specification (20). These values were found in Table II-A on page 4-25 of the AISC Manual. The values used were for 3/4" bolts and 5/16" angles.

Table V lists the calculated value for each mode of failure for each of the test specimens based on these various methods. The ultimate load actually achieved in each test and a factor of safety, expressed as a percentage, is also shown.

4.7 Evaluation of Strength by Plastic Analysis

Plastic analysis was used to develop a prediction model for strength of double-angle connections. Plastic methods were chosen because of the high degree of inelastic behavior observed during the experimental tests. The plastic methods used were developed using methods presented by Neal (14).

The ultimate plastic capacity of a weld was calculated for moment and shear acting independently. These calculations were made for each connection as:

$$M_{ult} = 0.707 \text{ D } (L/2)^2 F_{u-e}$$

$$V_{ult} = 0.707 \text{ D L } F_{u-e}$$

where:

D = weld size (1/4 inch)

L = length of weld

F_{u-e} = ultimate strength of weld (70 ksi)

The moment at any loading point can be calculated as:

$$M = (e_i^2 + e_o^2)^{0.5} V$$

where:

e_i = eccentricity of the In-plane bending

e_o = eccentricity of the Out-of-plane bending

The value of e_i used was the same as was calculated earlier in Section 4.3. The Out-of-plane bending is indeterminant for a double-angle connection. For this reason the location of the Out-of-plane inflection point is unknown. To be conservative a value of four inches was used. This is the dimension of the outstanding leg, a value common in design literature (6) as the eccentricity.

The moment and shear load can be normalized for each experiment by dividing by the corresponding ultimate plastic capacity. Graphs of Moment vs. Shear for Tests 4,5,6 and 9 are presented in Figures 4.8-4.11. Two failure surfaces were considered to represent the ultimate capacity of the connection. A linear combination of shear and moment and a circular interaction equation (9) were each plotted for an individual specimen. The circular interaction curve was plotted with the normalized moment, m, and shear, s, as:

$$m = \coth w - w / \cosh^2 w$$

$$s = w / \cosh w$$

w = geometric parameter determined by procedures given in Reference (9).

Tests 5,6 and 9 are very near the expected failure as

predicted by the interaction equations. The linear interaction forms a lower bound and the circular equation forms an upper bound. However, there are two concerns to be considered with the plastic analysis. First, the Out-of-plane eccentricity is believed to also move during the testing. This eccentricity would shorten, and therefore would cause a smaller moment to be calculated in the above equation. This would lower the loading path compared to those shown in the graphs.

The second concern is that plastic analysis demands that a material have enough ductility to develop a plastic hinge before tearing. Since a weld does not have the ductility that most connection materials contain, this will be a limiting factor. This is especially important in very deep connections with long welds. For these two reasons it is proposed that the linear model be used until more testing can be performed to verify the model. These tests indicate that weld failure for double-angle connections may be predicted by the use of plastic analysis methods and a moment-shear failure surface. Test 4 is below the linear surface, supporting the argument that because of the welds poor quality it failed at a load much below its expected capacity.

4.8 Weld Fracture Failure Mode

Two modes of failure governed the test specimens in both the expected and the actual ultimate load. These two modes were:

1. Weld Fracture
2. Bolt Bearing

In all the tests it was apparent that the weld was the weakest

part of the connection. During the rotation of the connection the angle was pulled away from the column. This displacement tended to crack the weld from the root of the weld toward the surface. This is commonly considered the critical and governing failure mode of a weld.

This bending action could be seen very easily in the first series of tests. The stresses induced in the weld return were large enough to cause the weld return to crack very early, often during the ductility cycle. Figure 4.12 shows specimen number 9 at the end of the ductility cycle. This photograph shows some yielding along the full length of the outstanding leg. However, it is apparent that heavy yielding has occurred along the top of the weld. This yielding indicates the extreme stress concentration which develops around the weld return.

4.9 Predicted Results

The first three test specimens, (Test 4,5 and 6) were run using the standard connection detail as shown in the AISC Manual (A). All three of these tests failed by weld fracture although in the second test some bearing damage was done on the beam. These three tests all followed the traditional failure path as outlined in Section 3.6.

All three tests showed heavy stress concentration around the weld return. These test specimens failed with much of the weld showing little yielding. The connection with seven bolts (specimen 4) failed at 82% of its expected load. All of these connections resisted the loads predicted by the AISC 8th Edition (1) and LRFD Specifications (2). However, as Table V indicates,

the factors of safety were occasionally less than 2.0, the value generally desired for connections.

Both the five and three bolt specimens (Test 5 and 6) were accurately predicted. It is believed this is because the shorter length of connection does not place as high of percentage of the shear load on the weld return. The reason for this is most likely that the moment arm between the tension stress component and the compression stress component as shown in Figure 4.7 is shorter.

4.10 Rotational Ductility of Double-Angle Connection

The double-angle connection shows excellent rotation capabilities. From the ENDGEN program (3) it was seen that 0.05 radians rotation will allow a beam to develop its plastic moment. All of the test specimens, except number 6, were easily rotated beyond 0.05 radians during the ductility cycle. The reason that number 6, the three bolt connection, was not taken this far was because of the test fixture limitations as described in Section 3.4. The condition of all the specimens was excellent at the maximum point of the ductility cycle.

Double-angle connections rotate much more than shear tabs as can be seen by comparing the graphs of beam rotation to those of angle rotation. The angle rotation was calculated as the top separation divided by the length of the angle. This measurement is possibly low since the angle normally pivots at a point a few inches above the base of the angle. The top separation is the displacement of the top corner of the angle away from the column flange. This rotation would not occur in a shear tab connection

since the tab would be welded directly to the column. This additional flexibility of a double-angle connection causes a smaller moment to be transferred into the column.

4.11 Moment-Rotation Prediction Models

A rough comparison of the test data and the results from the Richard's model (16) was made at the conclusion of these tests. Figure 4.13 shows the test results plotted against theoretical predictions for similar connections. The test results shown were obtained in the first cycle of loading. Therefore this data represents the moment-rotation curve developed by the cantilever test set-up. Traditionally, this curve is considered as the connection's behavior. However, as was shown in Chapter Two, this does not accurately resemble the behavior seen in actual applications.

It should be noted that the theoretical curves are for all-welded connections and for slightly different lengths. However the shape of the curves is similar and the model predicts the ultimate moment reasonably well. Figure 4.14 outlines a flowchart which could be used to develop a computer program to calculate the Richard-LeBouton model (16).

However, by observing the behavior of these tests, two additional changes are proposed to improve the model. First the Richard's equation does not take into account effects of shear. During the testing of the specimens it was clear that shear was the predominant deformation developing throughout most of the connection.

Figure 4.15 offers a change to improve the model. Instead

of using a roller as the vertical support a spring can be used. The spring constant would be the slope of the graph of shear vs boltline deflection during the ultimate strength cycle. This slope remains constant throughout the test and was determined by linear regression. The result of the spring constant calculation for each test is shown in Table VI. The spring constant varied from 1192 k/in to 207.9 k/in.

This vertical spring should be considered since vertical movement of the support will directly increase the deflection at the middle of the beam. Also if an indeterminate beam is supported by different connections this vertical flexibility may significantly change the distribution of bending stresses along the span of the beam.

The second proposed modification to the Richard's model is the discretization size. The Richard-LeBouton (16) model requires that at least the bottom spring be in compression to satisfy equilibrium. The model uses a three inch segment as the discretization length. When using a three inch segment this bottom spring occurs at the bottom bolt. In longer connections this is most likely sufficient. However for shorter connections, especially three bolt, it was observed that the compression region of the connection may be entirely below the bottom bolt.

CHAPTER FIVE

TESTING OF NEW LAMBDA CONNECTION DETAIL

5.1 Introduction

This chapter presents the quantitative and qualitative data collected during the second series of tests. These tests were performed to study the actual behavior of a modified double-angle connection (2). When looking at the column, the modification can be seen as a 45 degree cut along the outstanding legs. The connection now resembles the upper case Greek letter lambda, and so is called the lambda connection. A photograph showing this connection, along with a common double-angle connection is shown in Figure 5.1.

5.2 Testing of Lambda Connection

The last three test specimens (Tests 8, 9 and 10) were identical to each other except for the shape of the outstanding leg and the welding detail. These tests were run to fulfill the second objective of this project. Three ideas were to be tried with the lambda connection. First, by cutting a 45 degree angle from the back-to-back legs the tee-hanger region of the outstanding leg is removed. Usually in double-angle connections, weld cracks initiate in this tee-hanger region.

Second, it is expected that a more even distribution of strain will allow for a given length of weld to support a higher load. Third, the compression zone of the outstanding leg is

strenghtened to resist buckling, by extending the outstanding leg below the back-to-back leg. This strengthening is created by a larger portion of the total weld being contained in this area.

Figure 5.2 shows drawings of the three different connection details that were tested. The first (Test 9) was a typical double-angle connection with 7/8" bolts and 4x4x3/8" angle. The second (Test 10) specimen was a lambda connection cut at a 45 degree angle from the top. For this connection the weldline is along the length of the angle but ends at the bottom point. The third connection (Test 8) is also a lambda connection and is similar to the second but the weld is continued around the bottom edge of the angle. These three connection specimens should provide insight into the effectiveness of the three concepts in the above paragraphs.

5.3 Test Results

The lambda connections behaved similarly to the previous tests of double-angle connections as explained in Chapter Three. The lambda connections exhibited higher strengths and higher rotational flexibility. A yield line was evident which formed between the weld return region of the angle and the bottom corner of the angle. Although this line was evident in the previous tests, it did not show to be as well developed. The new connection also appeared to create a plastic hinge in the top edge of the leg, about midway between the top corners. In the traditional connection this hinge normally formed very close to the angle fillet.

The biggest advantage seen in the lambda connection was the

ability to distribute the load more uniformly, and to yield very large areas of the connection before the weld cracked. On some tests, the weld return did not crack during the ductility cycle, instead holding until very high shear loads were applied during the ultimate cycle. This absence of cracking during high rotations indicates the lack of stress concentration at the weld return.

After observing the testing of this series of specimens, the following conclusions are added to those mentioned in Chapter Four:

1. Changing the geometry of the outstanding leg and welding detail can benefit the overall behavior of the connection.
2. The beams inflection point remains very near the boltline during the service loads of a structure.
3. At ultimate loads, the inflection point moves to the weld line, so that the ultimate fracture strength may be calculated based on zero eccentricity.

5.4 Analysis of Experimental Results

The experiments showed that the effects due to the tee-hanger region were significantly reduced. In a double-angle connection a large catenary force can develop in this region. Figure 5.3 shows the effect of removing this region. Without the catenary forces the corners of the angles were free to close in upon themselves and wrap around the beam web. It is believed

that a double-angles catenary forces tend to resist the beam rotation by restricting the movement of the beams top flange away from the column.

Because of the complex and predominantly inelastic strains developed in these specimens, no estimates of the distribution will be offered. This allows only qualitative analysis of the tests.

Spreading the shear force over a larger portion of the weld appeared to have benefited the connections strength. Specimens 9 and 10 had the same weld dimensions and therefore the same predicted failure load. Specimen 10 carried 217 kips while specimen 9 carried only 192 kips. Also specimen 10 had an ultimate rotation of 0.0344 radians while specimen 9 had a 0.0332 radian ultimate rotation. Specimen 8 had an ultimate strength of 243 kips and a 0.0326 ultimate rotation. Specimen 8 had a higher predicted failure load because it had the additional weld at the base of the outstanding leg.

Figure 5.4 shows the progression of failure for specimen 10. An even distribution of yielding can be seen in part a. Note that yielding is not apparent about the weld return but is carried throughout the outstanding leg. In part b, the yielding has covered the outstanding leg, has moved up toward the weld and a small crack has developed from the weld return. This point is already at 205 kips, higher than the ultimate load of specimen 9. The photo in part c is taken after the specimen has failed at 217 kips. The weld had cracked four inches down the length and will not resist any increase in load.

CHAPTER SIX

CONCLUSIONS

6.1 General

The two major objectives of this experiment were to study the behavior of simple framing connections made with double-angles and to test the performance of a new double-angle connection. The new connection, denoted the lambda connection, was designed to change the geometry to reduce strain concentrations (2). Chapters Three, Four and Five of this report provided detailed information on these two objectives. This chapter will give a general overview of the main conclusions.

6.2 Conclusions and Recommendations

Based on observing and analyzing the behavior of these specimens during the actual testing the following conclusions have been reached:

1. Double-angle connections show three distinct regions of behavior during their use: a tee-hanger region, a shear beam region and compression region.
2. The inflection point of a beam supported by double-angle connections moves during the loading history. Yielding of the connection is what causes this movement, which normally occurs at loads below the expected service capacity of the connection.

3. Using elastic stress distribution resulted in stresses that were unrealistically large.
4. Plastic analysis and shear-moment yield surface can be used to predict the failure capacity of a connection reasonably well.
5. Connection strength predictions based on AISC (20) methods are conservative, but may not have the factor of safety that is commonly assumed.
6. Fracturing of the weld at the top of the connection is by far the most common mode of failure for double-angle connections.
7. Double-angle connections are superior to shear tabs because they have less rotational stiffness and so transfer less moment into the column.
8. The Richard equation appears to accurately predict the test results but should possibly be modified to include shear effects.
9. Response characteristics can be improved by making minor changes to the geometry of the connection.
10. Overall performance of double-angle connections is very good, because they resist high shears, allow rotation of the beam end and pass negligible moment to the column.

11. Performance of the Lambda double-angle connection was better than traditional designs. The new connection behaved almost as a perfect pin with very small (negligible) moments developed in the connection.
12. Strength of the Lambda double-angle connection was higher than the traditional connection and the distribution of yielding was more uniform.

REFERENCES

1 Astaneh-Asl, A., "Ductility and Strength of Steel Shear Connections," in review, Journal of Construction Steel Research (April, 1988).

2 Astaneh-Asl, A., "A New Shear Connection for Steel Structures," submitted to Lincoln Arc Welding Foundation, April, 1988.

3 Astaneh-Asl, A., Experimental Investigation of Tee-Framing Connection. Progress Report to American Institute of Steel Construction. Berkeley, CA.: April 1987.

4 Bennetts, I.D., I.R. Thomas, and P. Grundy. "Shear Connections for Beams to Columns." Metal Structures Conference, Institution of Engineers. Perth, Australia: November, 1978:70-75

5 Bergquist, D.J. "Tests on Columns Restrained by Beams with Simple Connections." Report No. 1, American Iron and Steel Institute Project No. 189. Austin, TX.: University of Texas, January, 1977.

6 Blodgett, O.W. Design of Welded Structures. James F. Lincoln Arc Welding Foundation, 1966.

7 Boresi, A.P., and O.M. Sidebottom. Advanced Mechanics of Materials, 4th ed. New York: John Wiley and Sons, March, 1978

8 Bose, B. "Moment Rotation Characteristics of Semi-Rigid Joints in Steel Structures." Journal of Institution of Engineers (India) 62. Part C1 Civil Engineering Division (September, 1981):128-132

9 Hodge, P.G. Plastic Analysis of Structures. New York: McGraw-Hill, 1959

10 Kennedy, D.J.L. "Moment-Rotation Characteristics of Shear Connections." AISC Engineering Journal (October, 1969)

11 Lewitt, C.W., E. Chesson, and W.H. Munse. Restraint Characteristics of Flexible Riveted and Bolted Beam-to-Column Connections. Bulletin no. 500. Chicago: Engineering Experiment Station, University of Illinois, 1969.

12 Lothers, J.E. "Elastic Restraint Equations for Semi-rigid Connections." American Society of Civil Engineers Transactions 116 (1951):480-502.

13 Morris, G.A., and J.A. Packer. "Beam-to-Column Connections in Steel Frames." Canadian Journal of Civil Engineering 14 (1987).

14 Neal, B.G. The Plastic Methods of Structural Analysis, 3rd ed. London: Chapman and Hall, 1977.

15 Nethercot, D.A. "Utilisation of Experimentally Obtained Connection Data in Assessing the Performance of Steel Frames." Connection Flexibility and Steel Frames ed. Wai-Fah Chen. New York: American Society of Civil Engineers, October, 1985

16 Richard, R.M., and M.C. LeBouton. "Welded-Welded Double Framing Angle Connection Moments." Report to American Institute of Steel Construction. Tucson: University of Arizona, June, 1987.

17 Sommer, W.H. "Behaviour of Welded Header Plate Connections." Masters Thesis, University of Toronto, January, 1969

18 Tall, L., and J.L. Rumpf. Structural Steel Design, 2nd ed. Malabar, FL.: Robert E. Krieger, 1974.

19 Thompson, L.E., R.J. McKee, and D.A. Visintainer. "An Investigation of Rotation Characteristics of Web Shear Framed Connections Using A-36 and A-441 Steels." Department of Civil Engineering, Rolla, MO: University of Missouri-Rolla, 1970

20 _____. American Institute of Steel Construction. Manual of Steel Construction. 8th ed. Chicago: 1980.

21 _____. American Institute of Steel Construction. Load and Resistance Factor Design. Chicago: 1986.

TABLE I

VARIATION OF
GEOMETRIC PARAMETERS

Parameter*	Low Value	High Value
Angle Thickness (t)	3/8	3/8
Bolt Eccentricity (b-L_h)	2	2.5
Bolt Diameter	3/4	7/8
Number of Bolts	3	7
Type of Bolts	A325-X	A325-X
Weld Size	1/4	3/8
Weld Length	8.5	26
Weld Type	AWS E70XX	AWS E70XX
Edge Distance	1.25	1.25
Center-to-Center Bolt Spacing	3	3

* Parameters defined in Figure 1.3

TABLE II

SCHEDULE OF TESTING

Test No.	# of Bolts	Bolt Size	Weld Size	Conn. Length	Weld Length	Angle Size	Conn.* Detail
4	7	3/4	1/4	20.5	20.5	4x3.5x3/8	I
5	5	3/4	1/4	14.5	14.5	4x3.5x3/8	I
6	3	3/4	1/4	8.5	8.5	4x3.5x3/8	I
7	7	7/8	5/16	20.5	26.0	4x4x3/8	III
8	5	7/8	5/16	14.5	20.0	4x4x3/8	III
9	5	7/8	5/16	14.5	14.5	4x4x3/8	I
10	5	7/8	5/16	14.5	14.5	4x4x3/8	II

* Connection Details

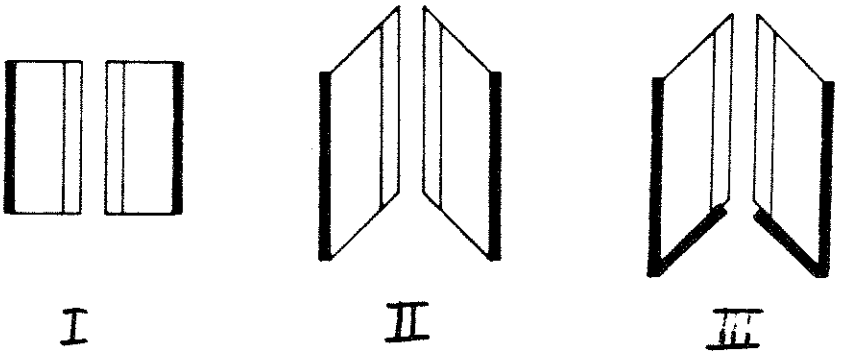

TABLE III

MAXIMUM SHEAR FORCE AND ROTATION

Ductility Cycle				
TEST NO.	ROTATION RAD.	SHEAR KIPS	M-weld K-IN	M-bolt K-IN
4	0.0514	10.2	697	676
5	0.0573	5.3	369	360
6	0.0310	3.11	171	165
7	0.0602	8.62	612	570
8	0.0562	3.88	245	236
9	0.0563	8.17	507	487
10	0.0535	5.66	285	272

Ultimate Cycle						
	at Ultimate Load		at Max Rotation		Max During Test	
TEST NO.	ROTATION RAD.	SHEAR KIPS	ROTATION RADS	SHEAR KIPS	M-weld K-IN	M-bolt K-IN
4	0.0257	230	0.0467	184	404	−68
5	0.0315	205	0.0367	172	248	−477
6	0.0414	117	0.0449	107	203	−348
7	0.0301	300	0.0309	114	547	−1046
8	0.0326	243	0.0331	207	195	−661
9	0.0332	192	0.0341	189	265	−581
10	0.0344	217	0.0423	196	−265	−808

TABLE IV

MATERIAL TENSILE TEST RESULTS

COUPON	1-3	1-4	2-3	2-4
WIDTH INCH	1.502	1.504	1.503	1.506
THICKNESS INCH	0.376	0.376	0.374	0.379
AREA SQ. IN.	0.565	0.565	0.563	0.571
YIELD LOAD KIPS	24.7	25.3	25.3	25.2
YIELD STRESS KSI	43.7	44.7	44.8	44.1
UPPER YIELD	44.3	46.0	45.3	45.5
LOWER YIELD	43.5	44.2	44.0	43.8
ULTIMATE LOAD KIPS	34.8	35.0	34.7	34.8
ULTIMATE STRESS KSI	61.6	61.9	61.6	60.9
ELONGATION PERCENT - 8" GAGE LENGTH	29.7	29.7	28.1	28.9

TABLE V

PREDICTION OF CONNECTION FAILURE LOAD

TEST NO.	Failure Load								
	ACT.	LRFD Method				ASD Method		von Mises'	
		Q x NOM.		NOMINAL		ALLOW		ULTIMATE	
		LOAD	% FS	LOAD	% FS	LOAD	% FS	LOAD	% FS
4	230	210	109	280	82	130	177	202	114
5	208	143	146	190	110	93	224	144	145
6	117	71	165	94	125	56	210	80	147
9	192	148	130	197	98	93	207	142	136

TABLE VI

SHEAR STIFFNESS OF CONNECTION

Test No.	No. of Bolts	Spring constant (k, kips/in)	Maximum shear (kips)
4	7	1089.9	230
5	5	1192.0	208
6	3	207.9	117

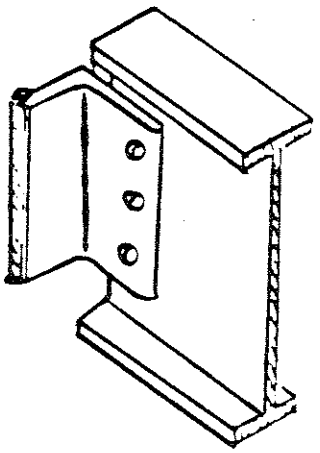

Figure 1.1 Double-Angle Connection

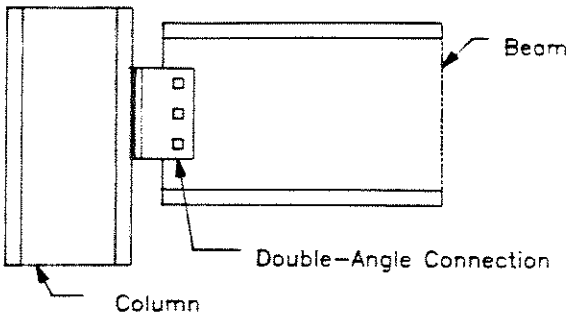

Beam-to-Column Connection

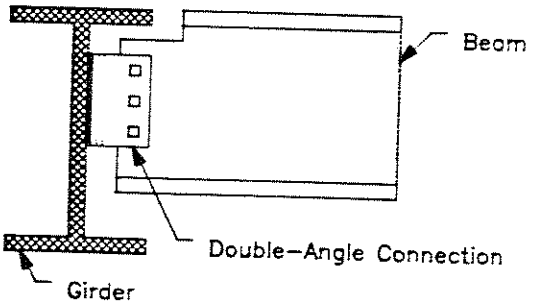

Beam-to-Beam Connection

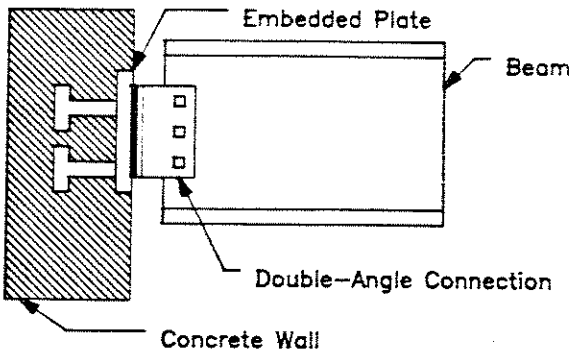

Beam-to-Wall Connection

Figure 1.2 Uses of Double Angle Connection

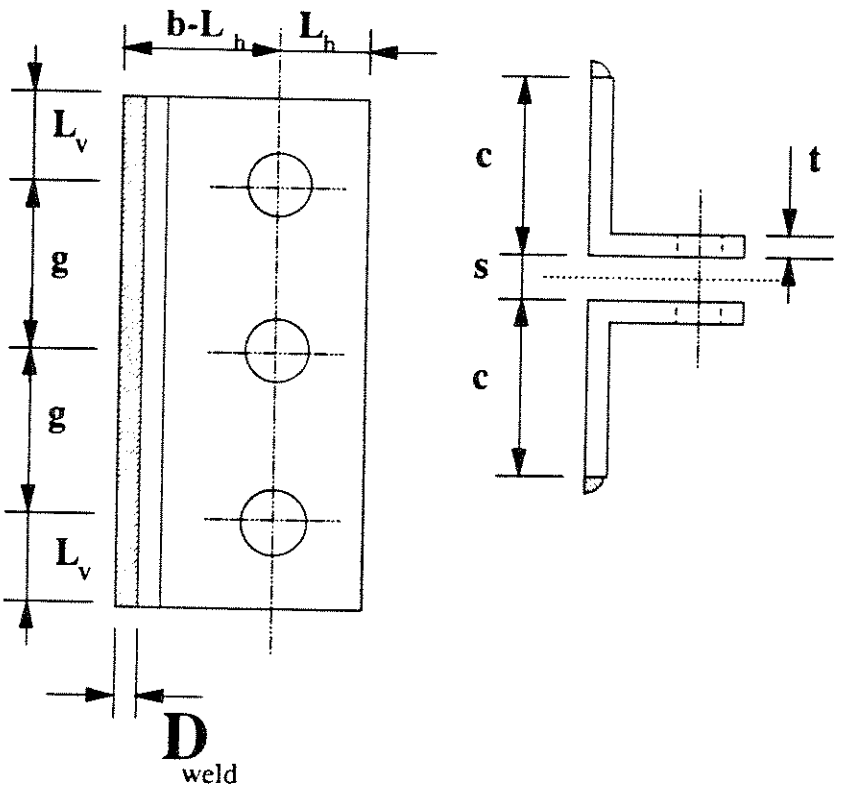

Figure 1.3 Geometric Parameters

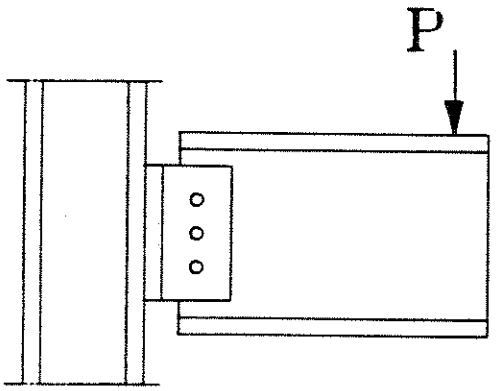

(a) Contilever Test Set-up

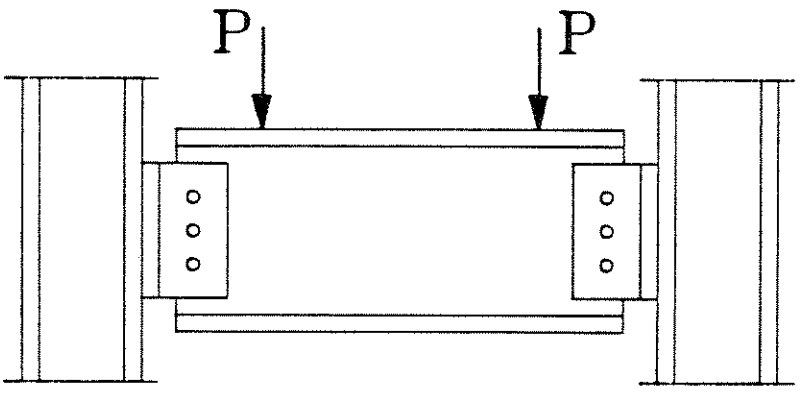

(b) Shear Beam Test Set-up

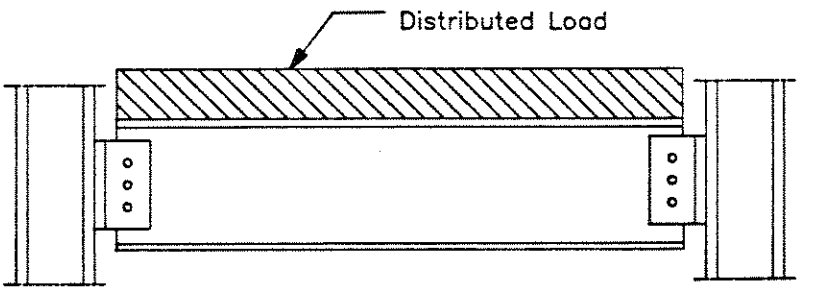

(c) Actual Loading on Beam

Figure 2.1 Test Specimens

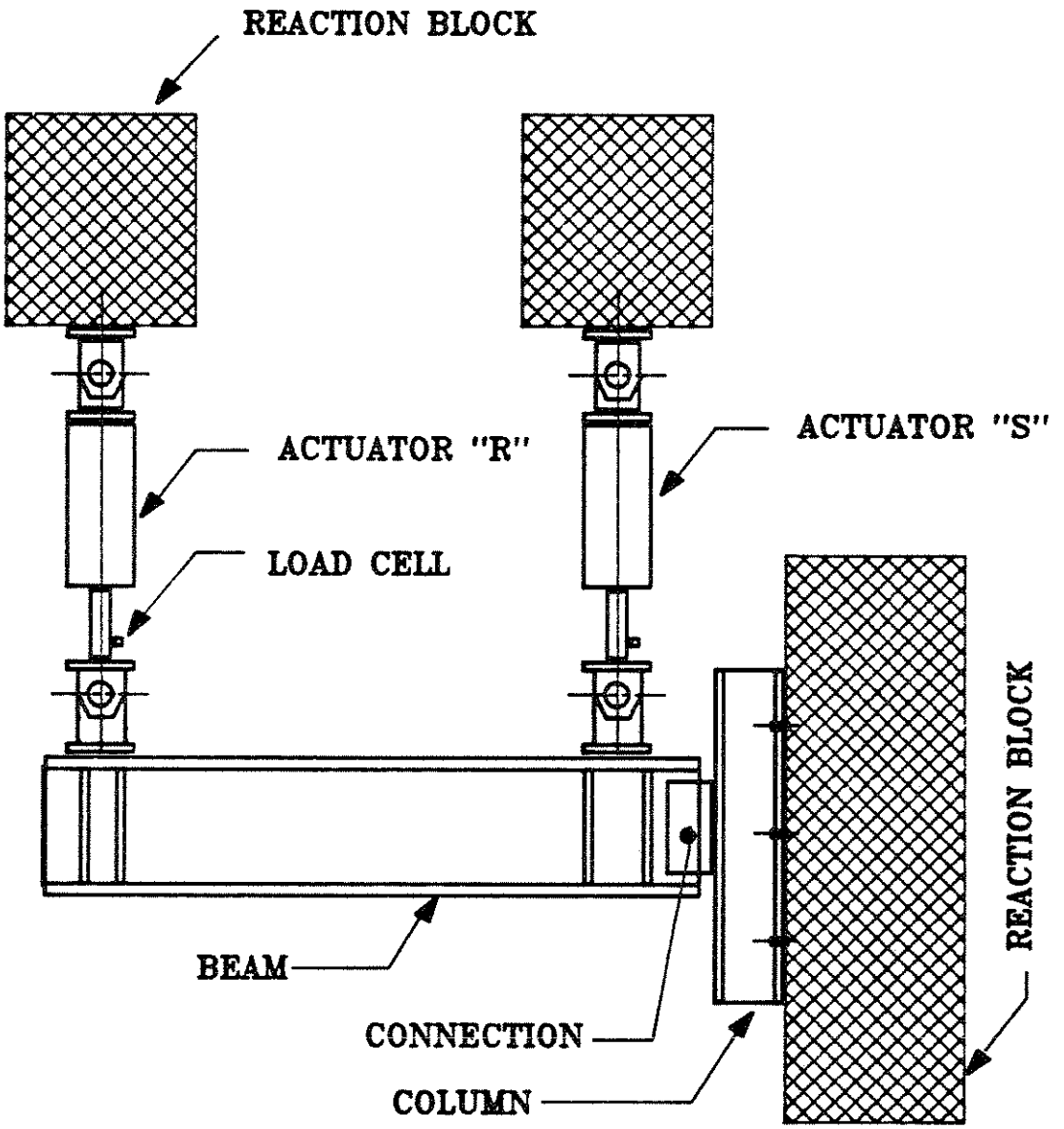

Figure 2.2 Test Set-up

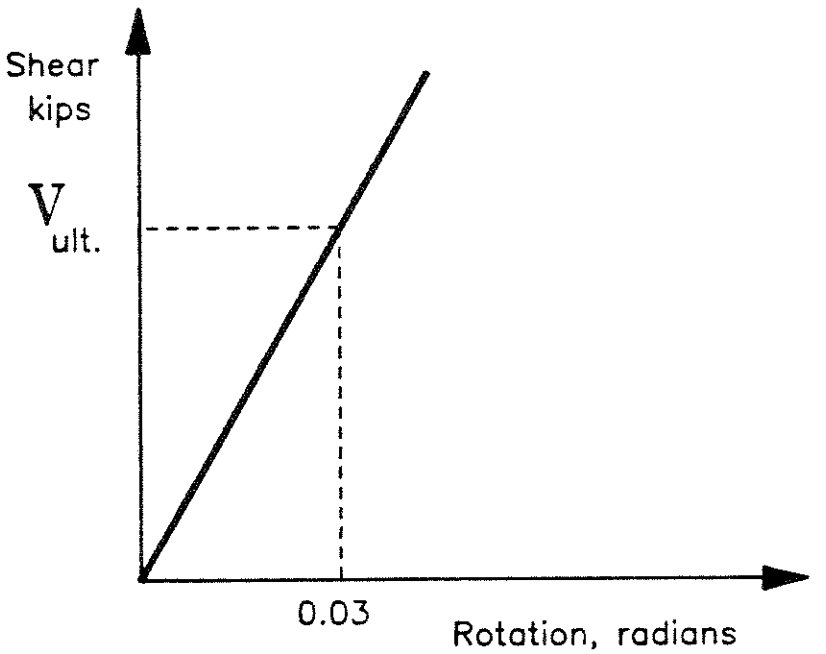

Figure 2.3 Path of Loading Cycle

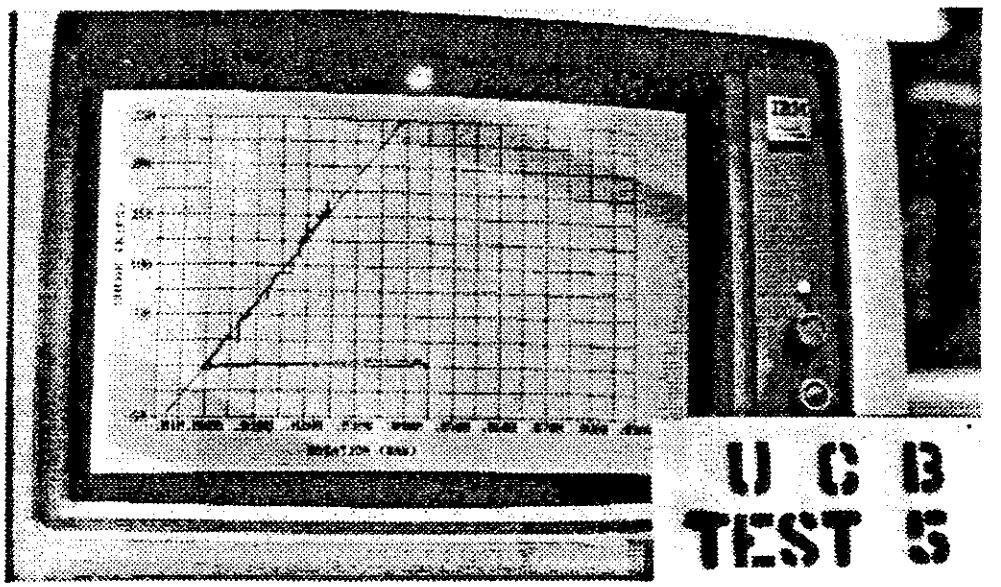

Figure 2.4 Loading Cycle During a Test

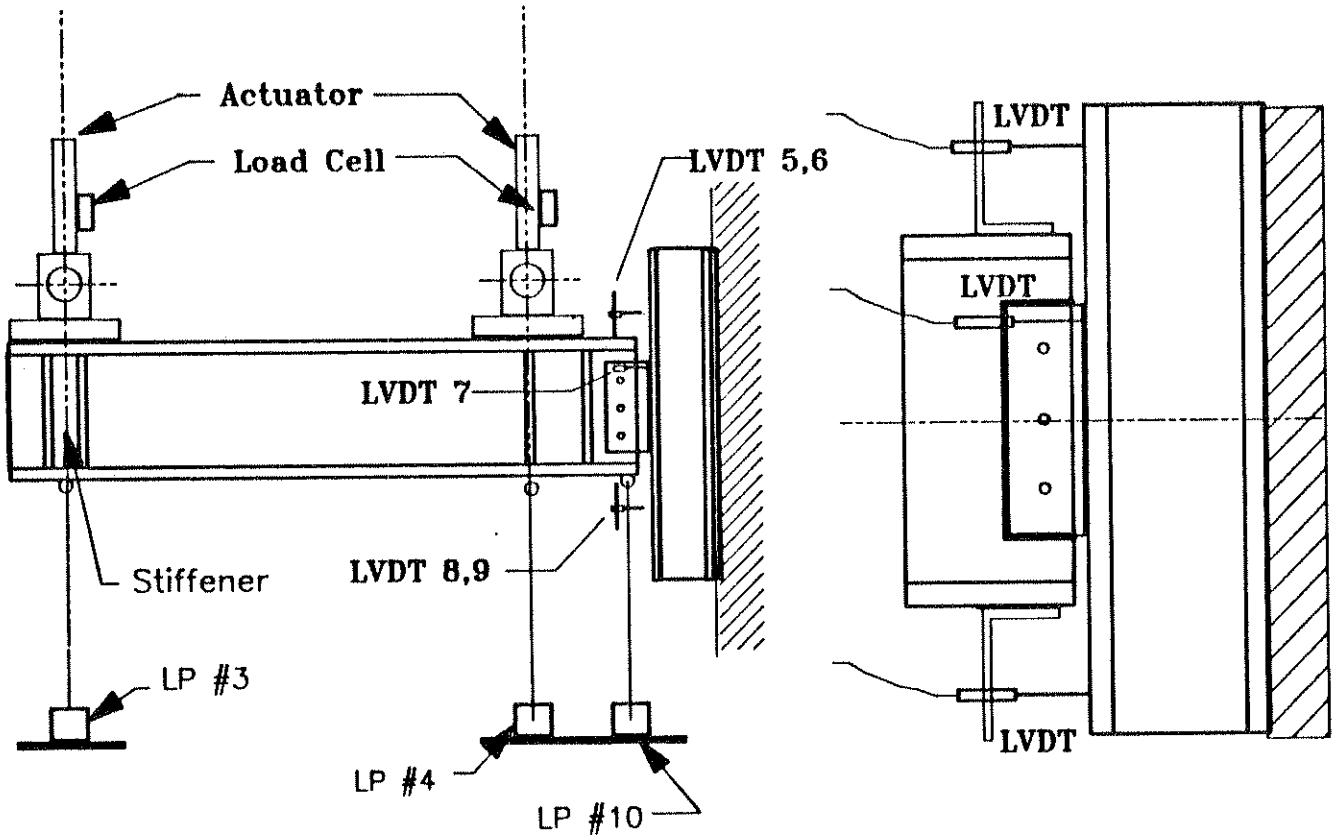

Figure 2.5 Diagram of Instrumentation Used During the Testing

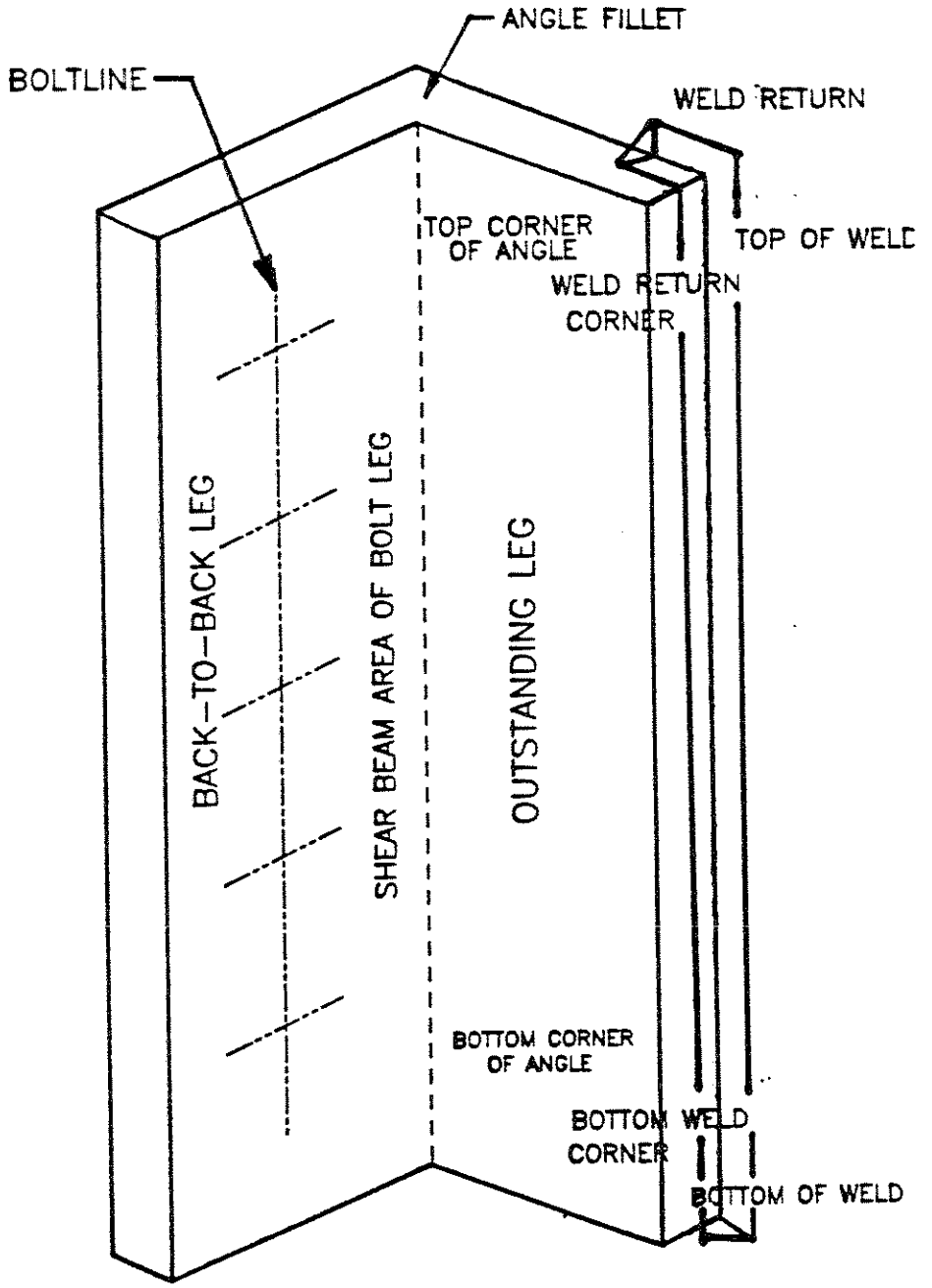

Figure 3.1 Nomenclature of Angle

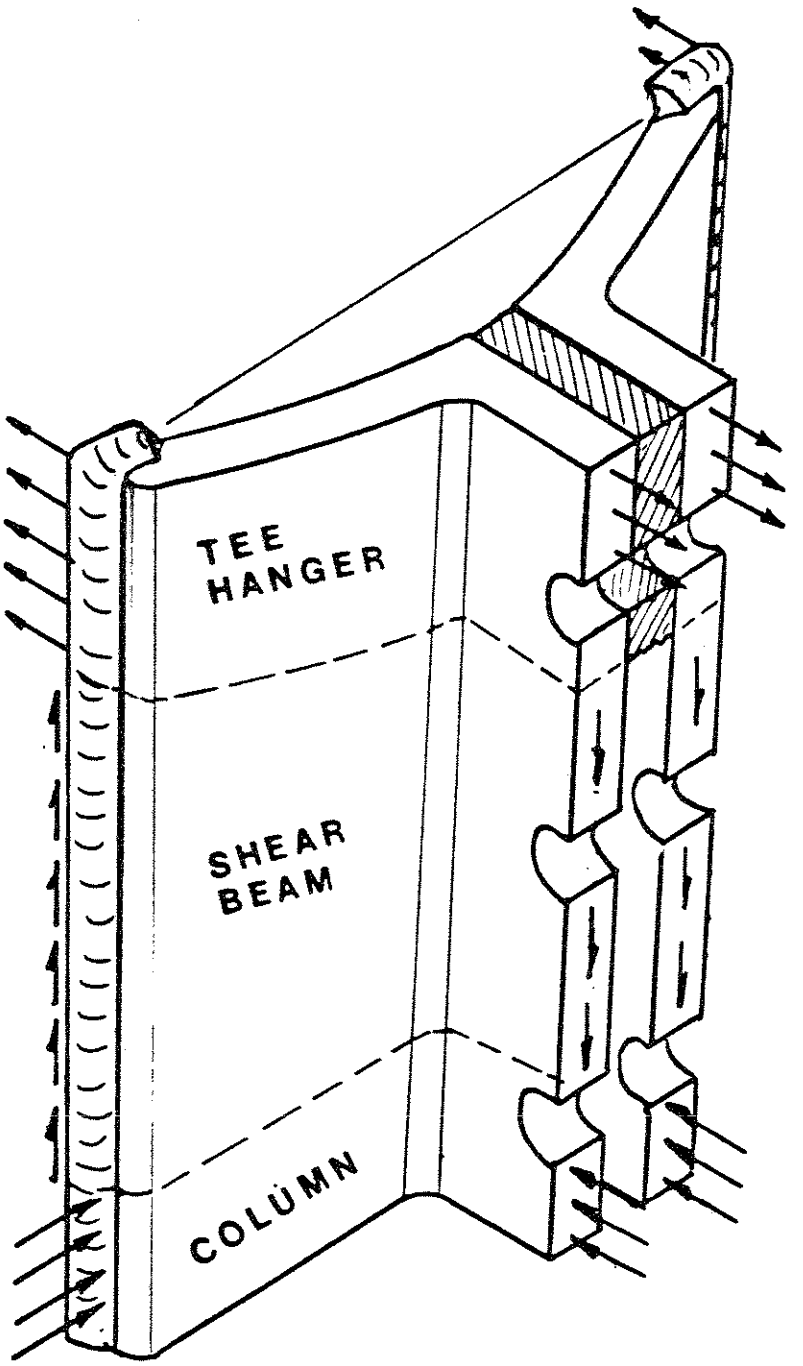

Figure 3.2 Double-Angle
Behavior

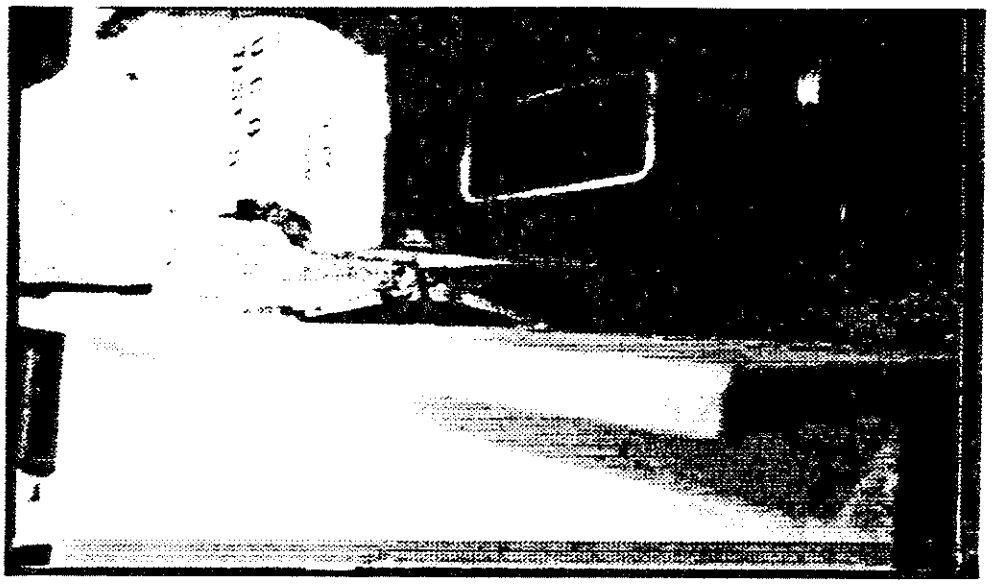

Figure 3.3 Tee-Hanger Region
of Connection

Figure 3.4 Compression Zone
of Connection

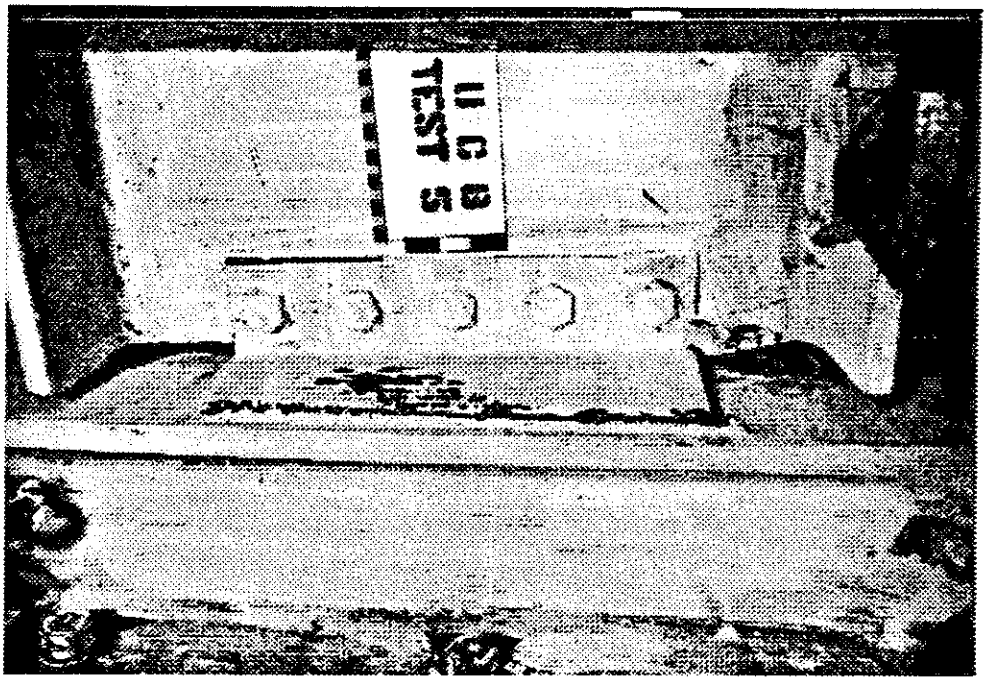

Figure 3.5 Failure of Double-Angle Connection

Figure 3.6 Fracturing of Weld in Double-Angle Connection

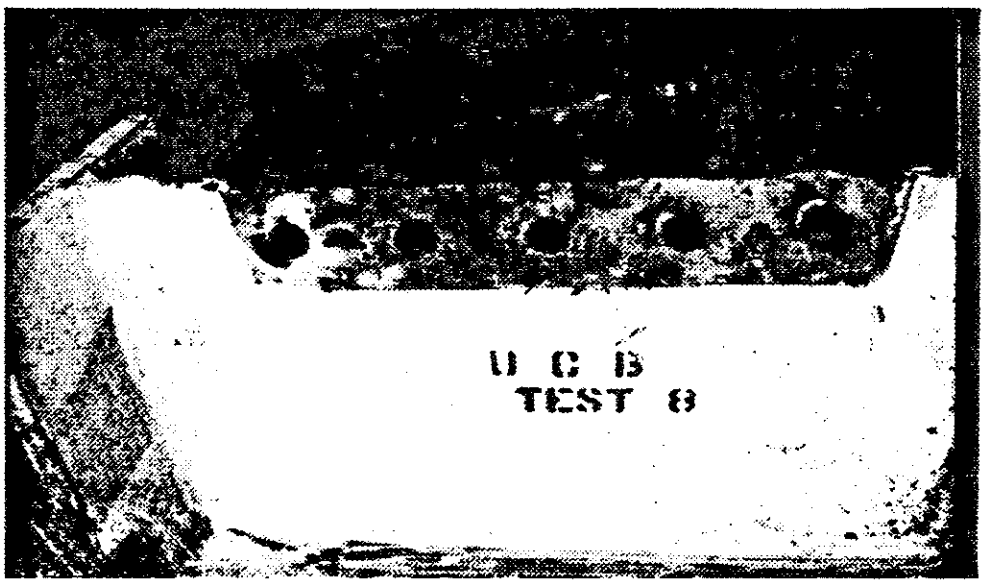

Figure 3.7 Bearing Damage to Web of Beam

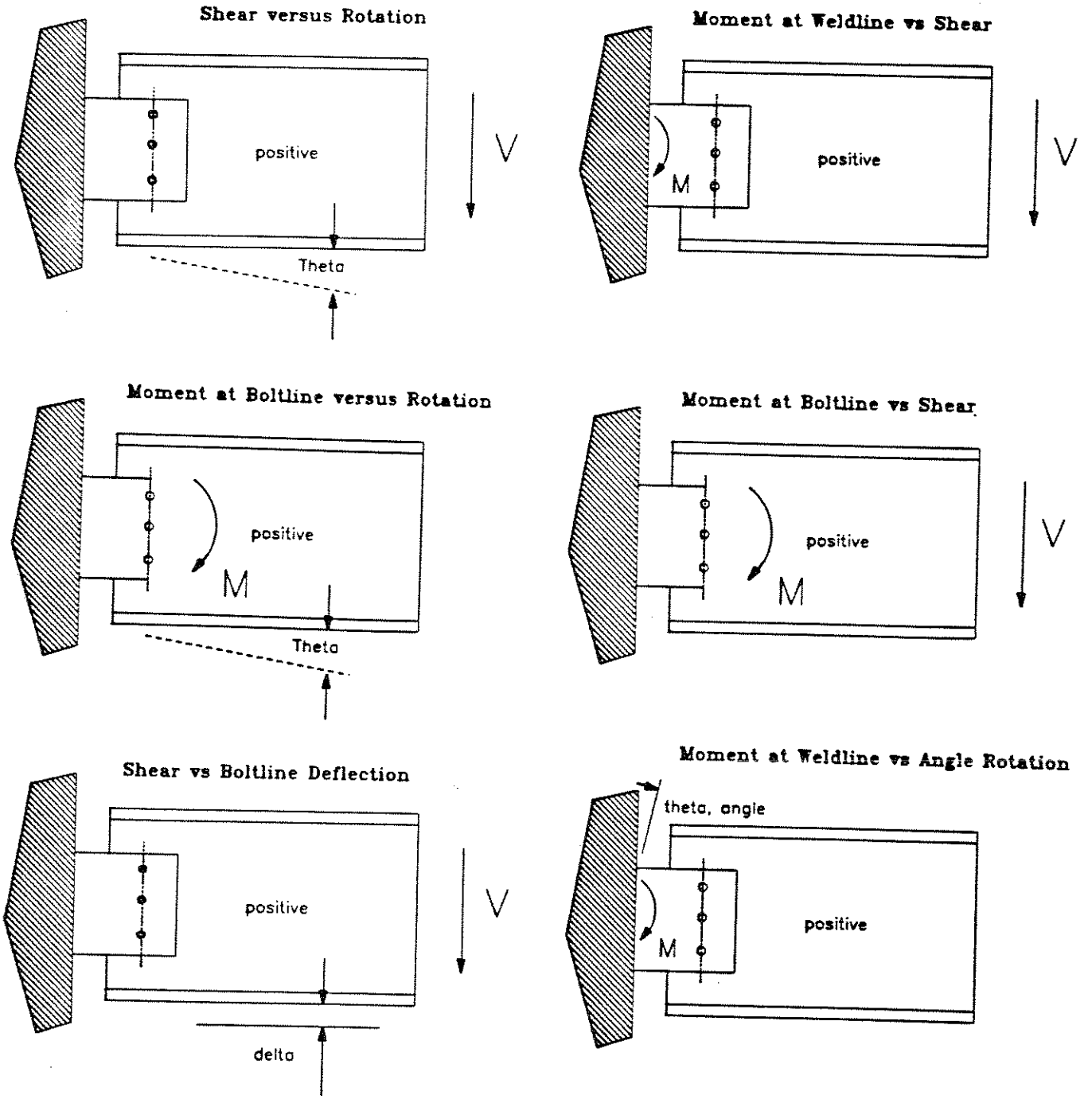

Figure 3.8 Sign Convention for Plots in Appendix B

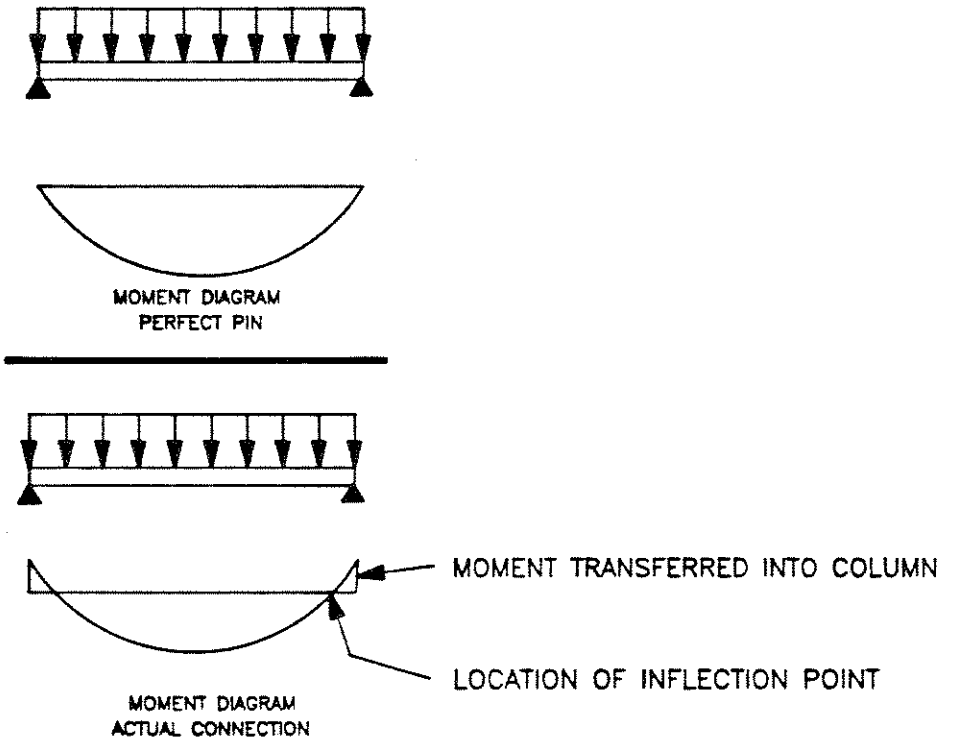

Figure 4.1 Moment Diagram for
Simply Supported Beam

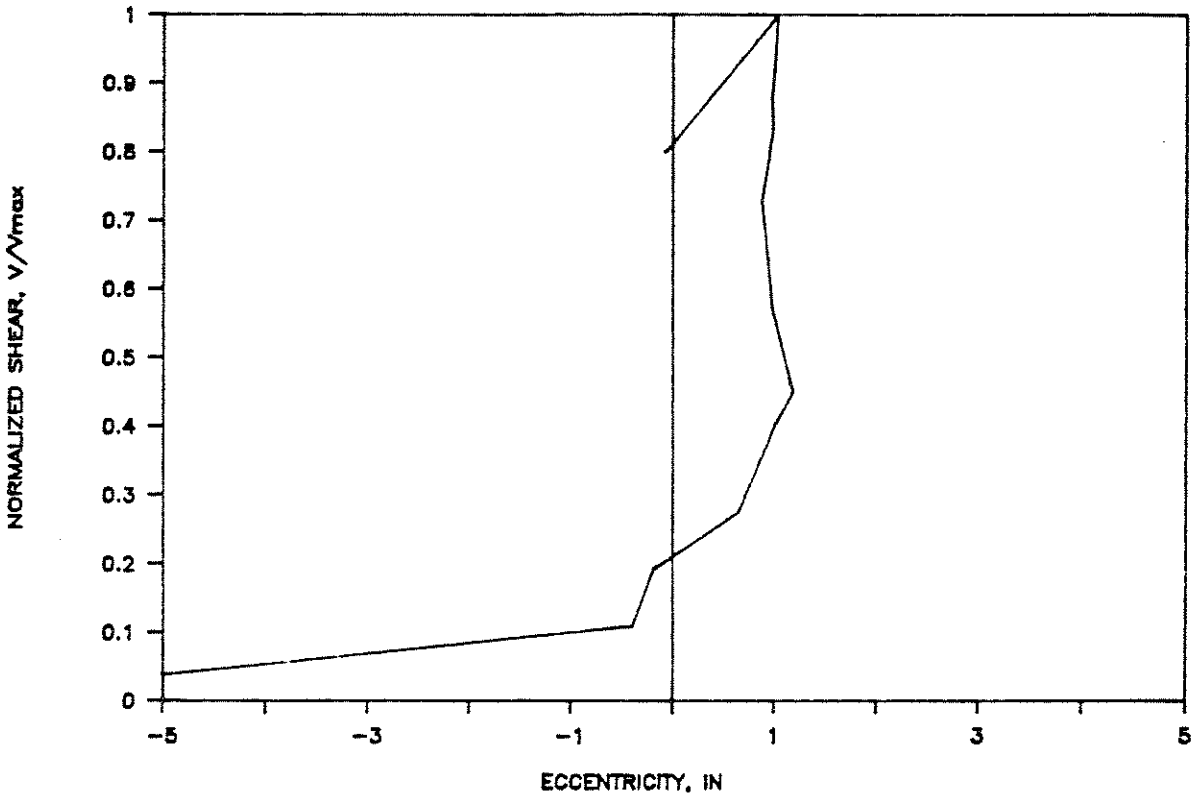

Figure 4.2
Eccentricity of Test #4

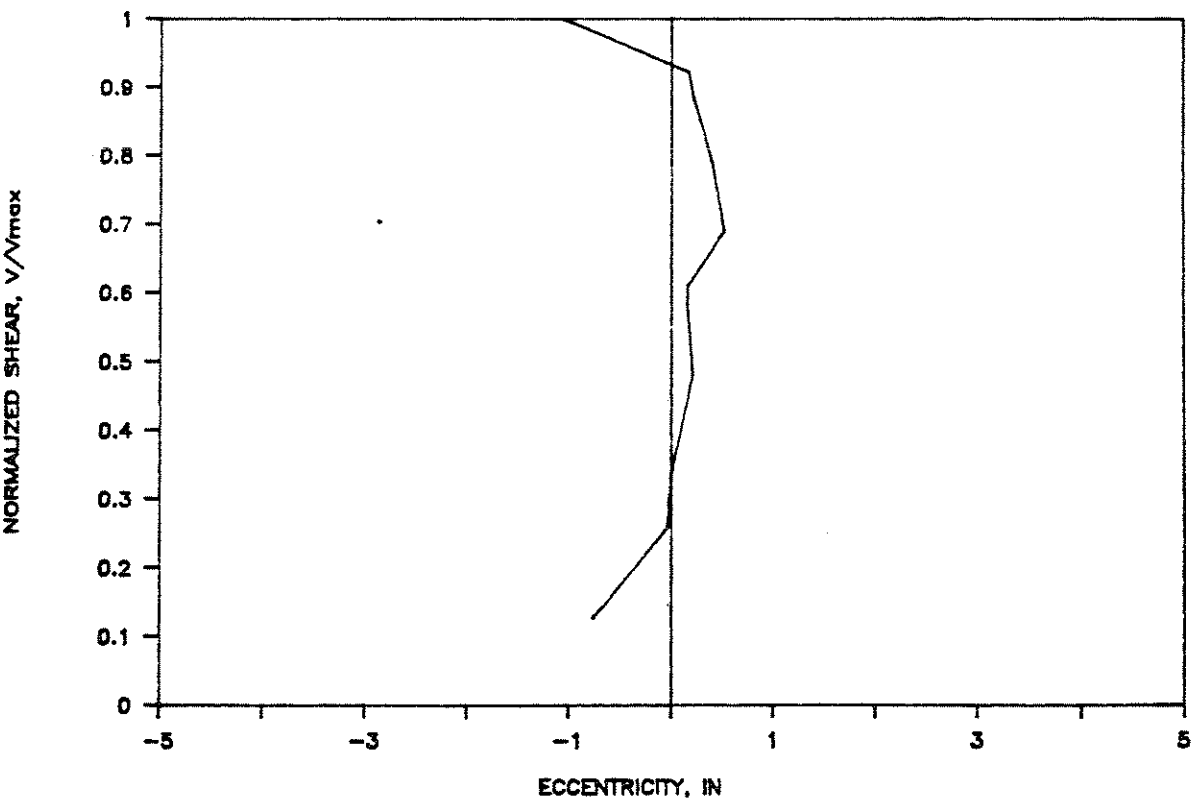

Figure 4.3
Eccentricity of Test #5

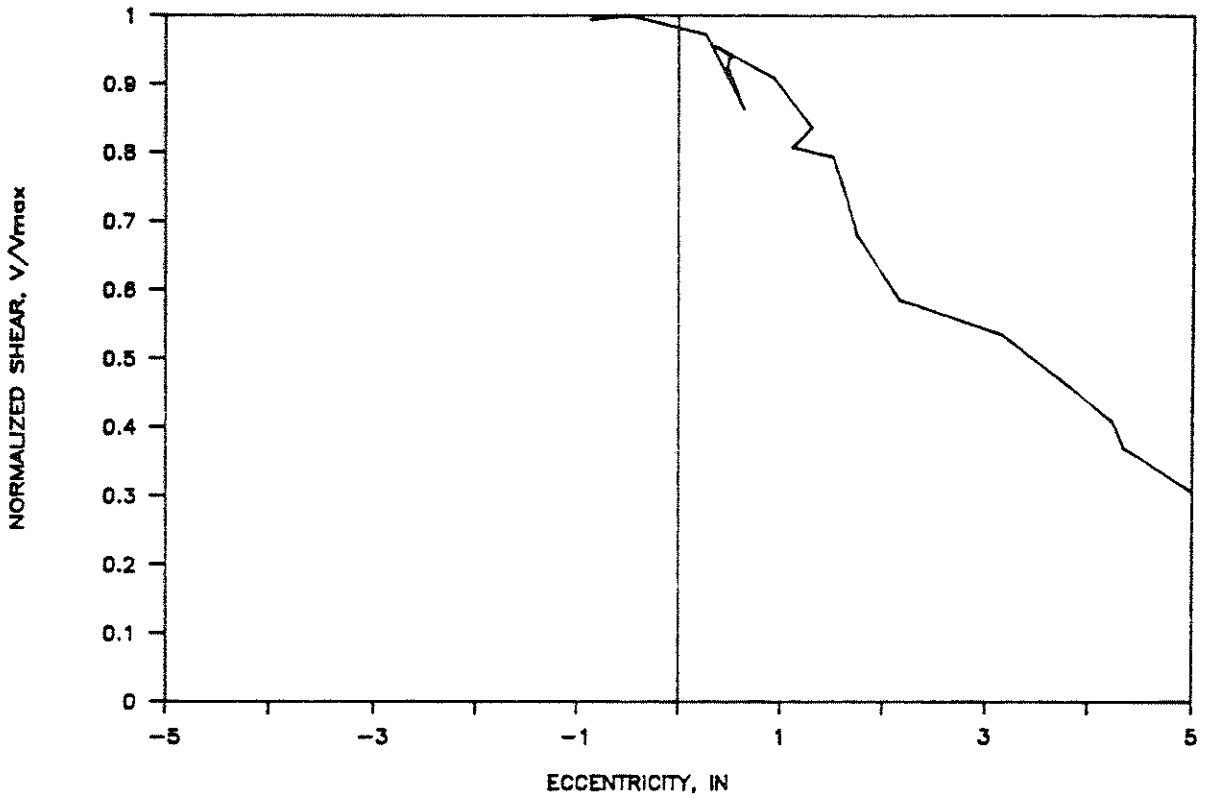

Figure 4.4

Eccentricity of Test #6

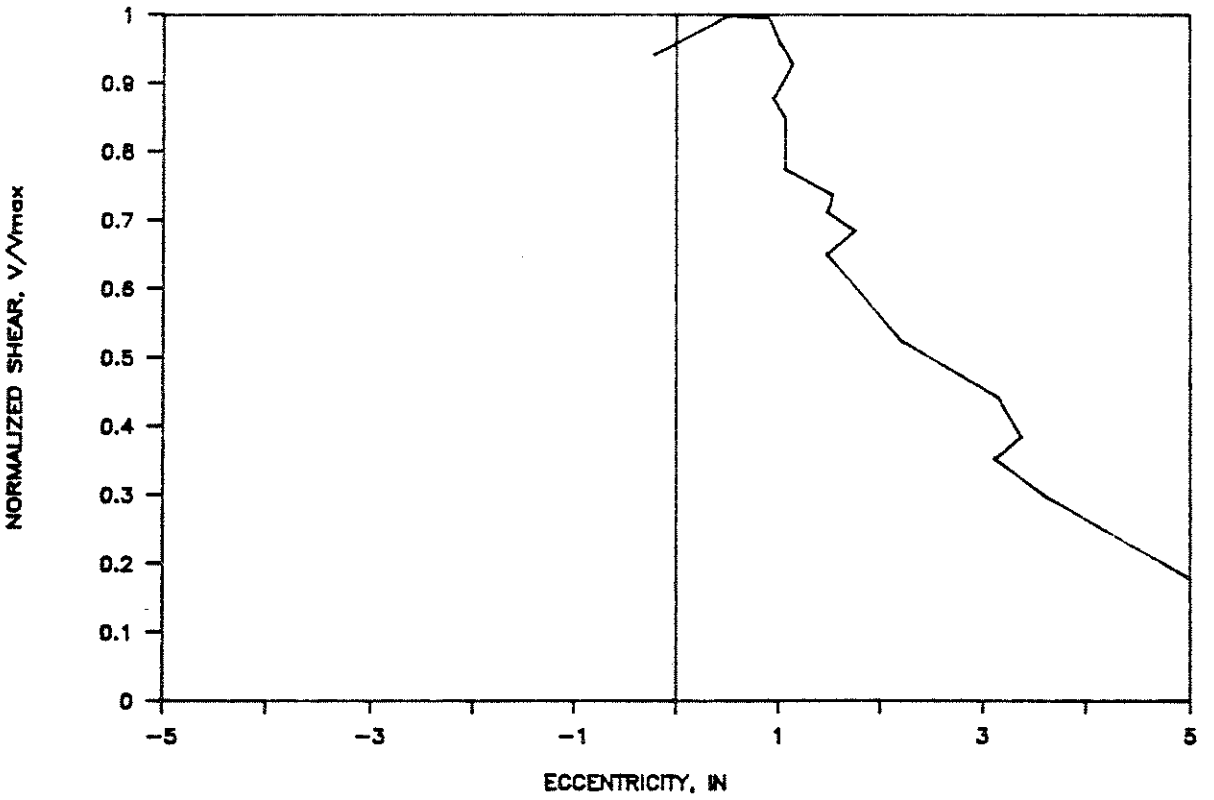

Figure 4.5

Eccentricity of Test #9

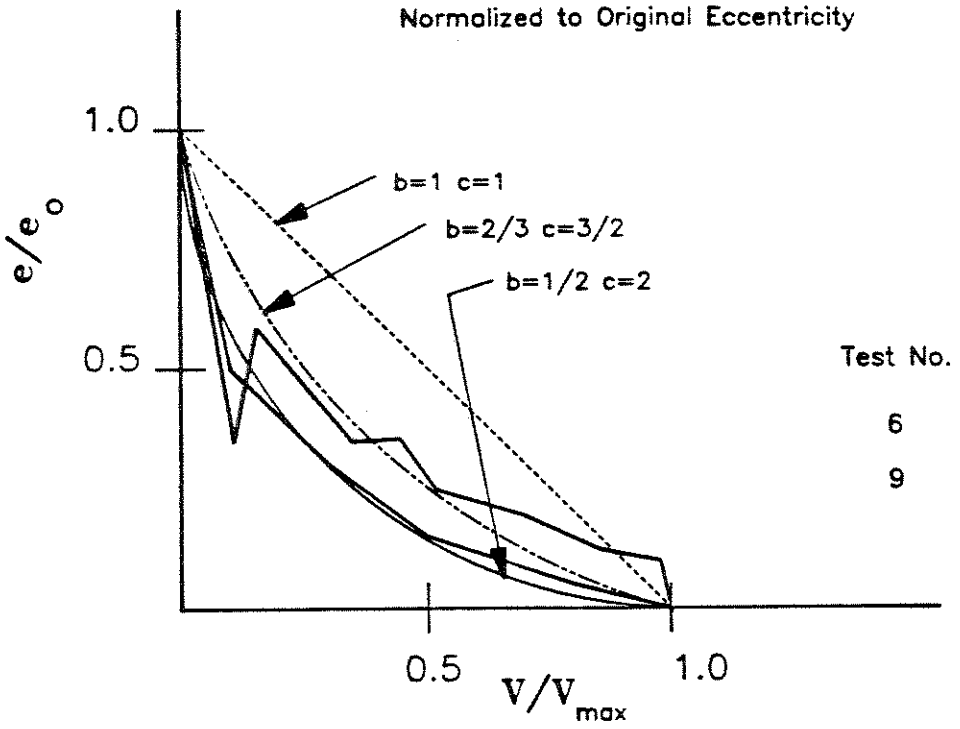

Test No.	e_o IN
6	20.13
9	8.85

Eccentricity vs. Shear

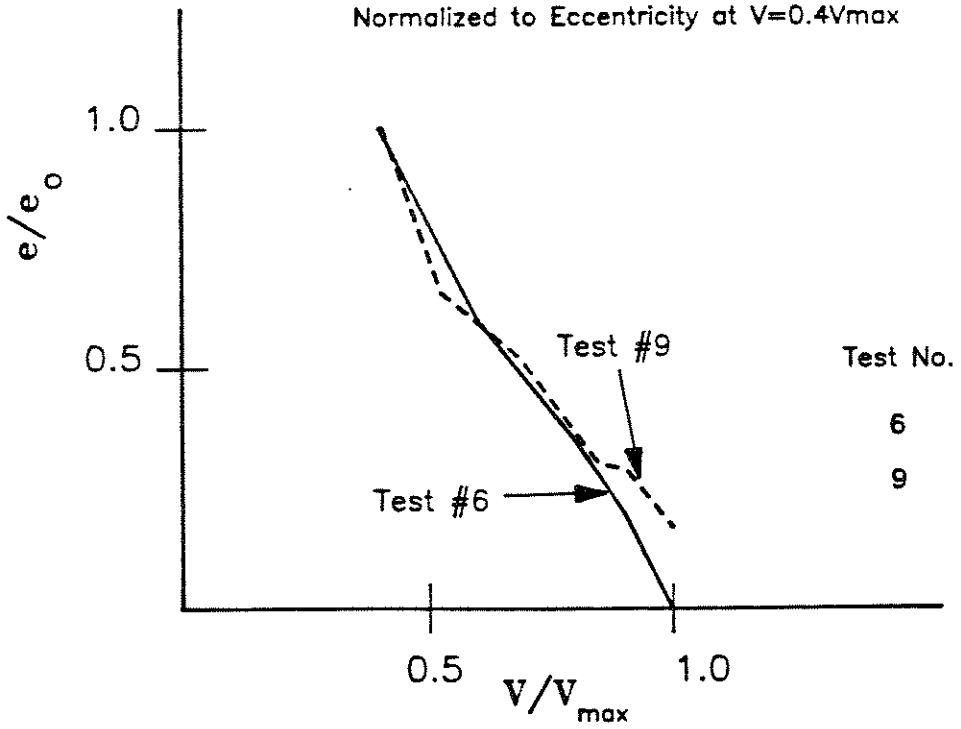

Test No.	e_o IN
6	4.22
9	3.30

Eccentricity vs. Shear

Figure 4.6

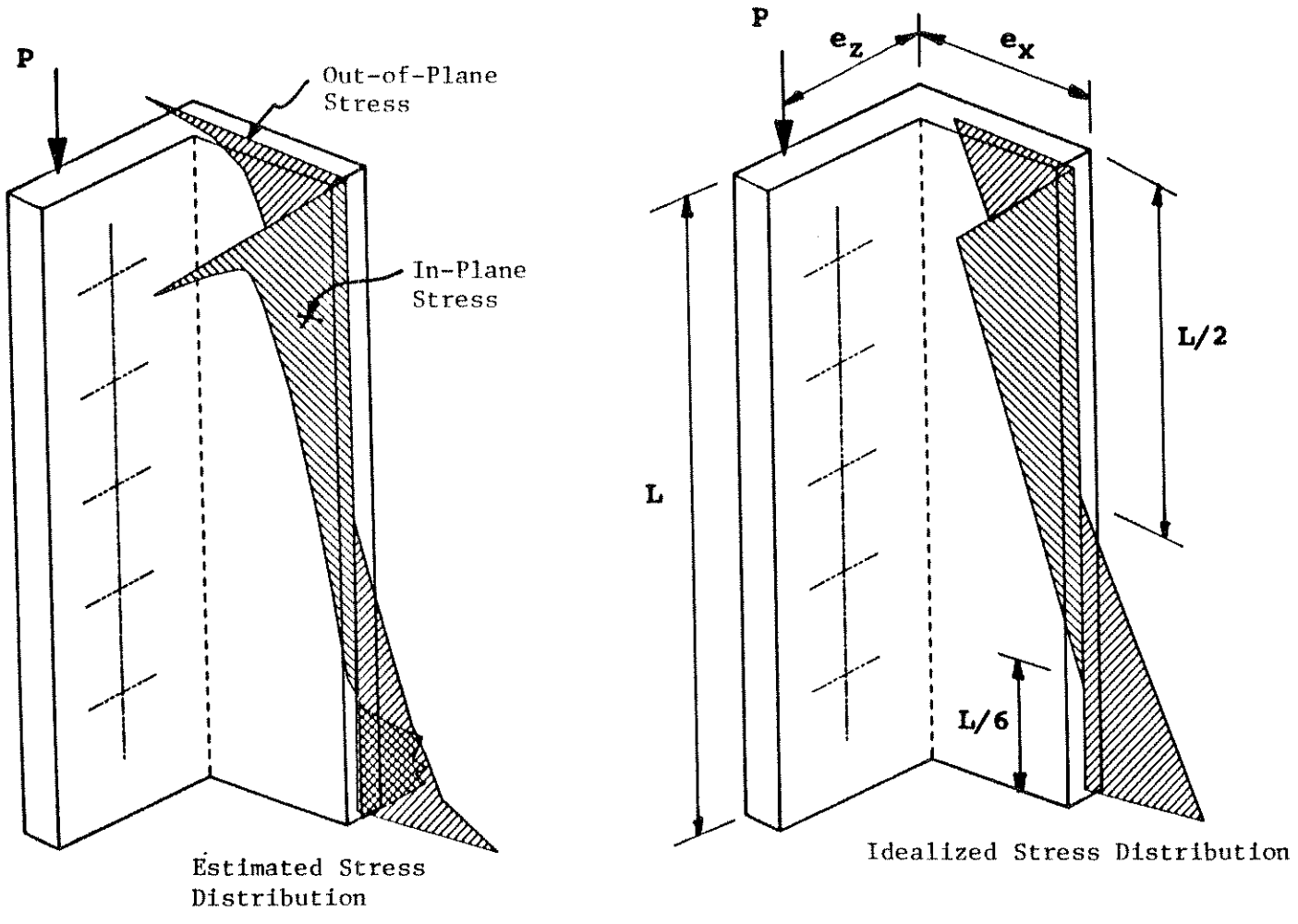

Figure 4.7 Distribution of Stress in a Double-Angle Connection

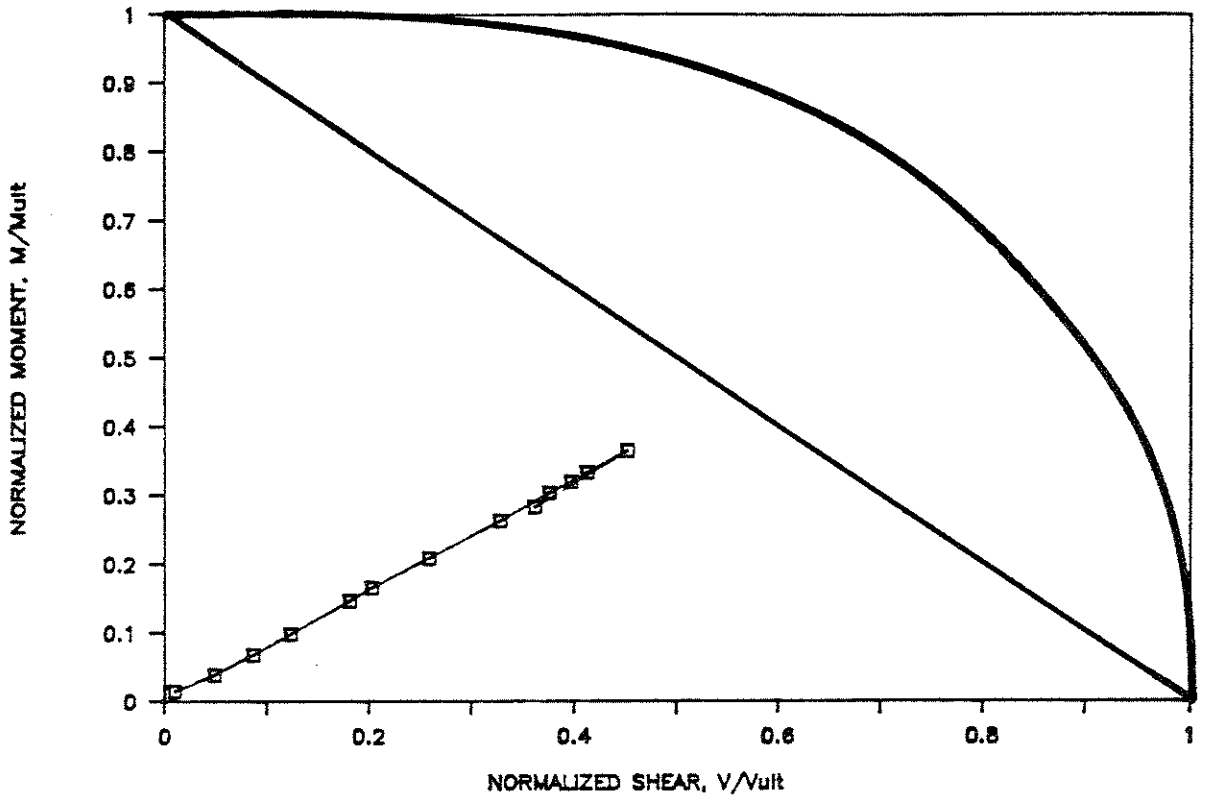

Figure 4.8 Plastic Analysis of of Test #4

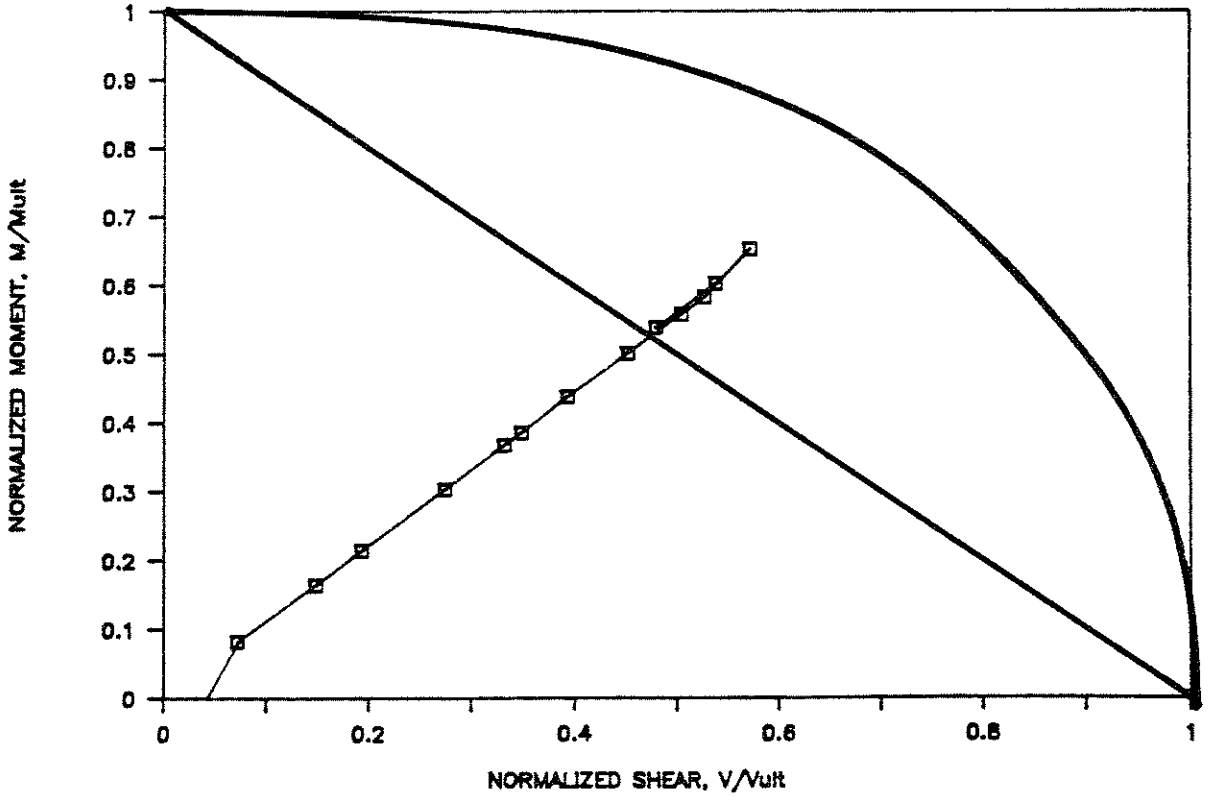

Figure 4.9 Plastic Analysis of Test #5

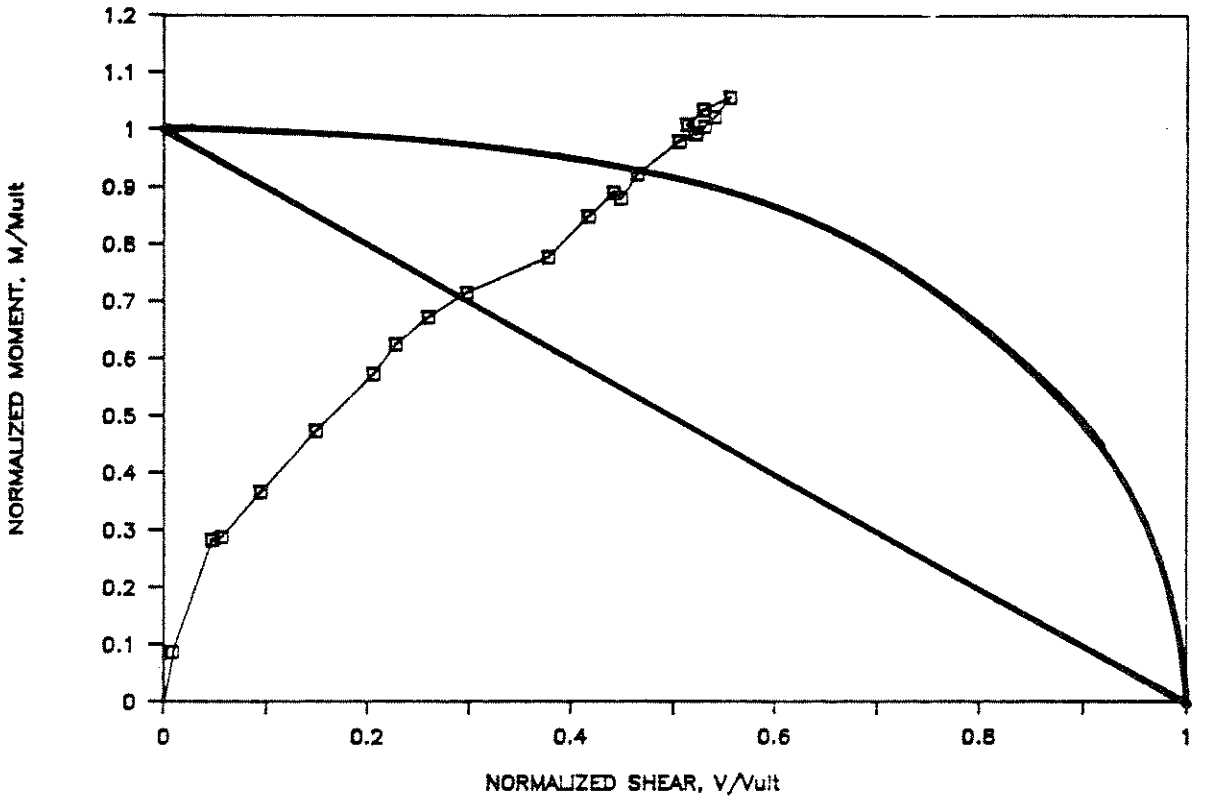

Figure 4.10 Plastic Analysis
of Test #6

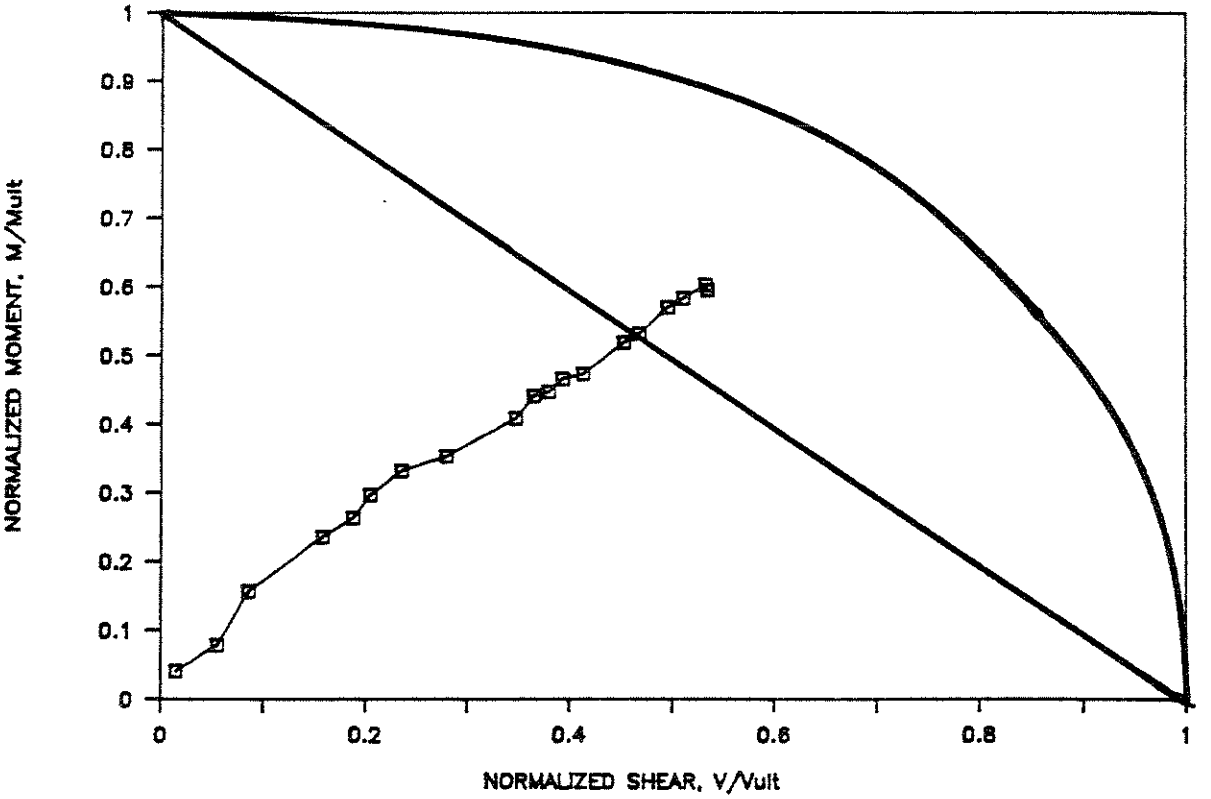

Figure 4.11 Plastic Analysis
of Test #9

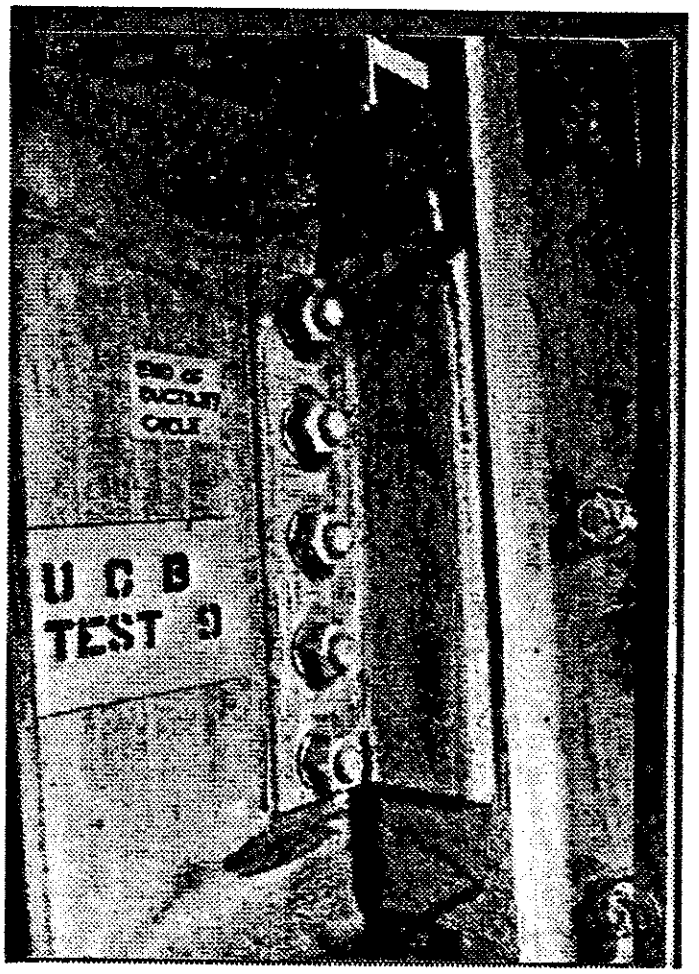

Figure 4.12 Specimen After Ductility Cycle

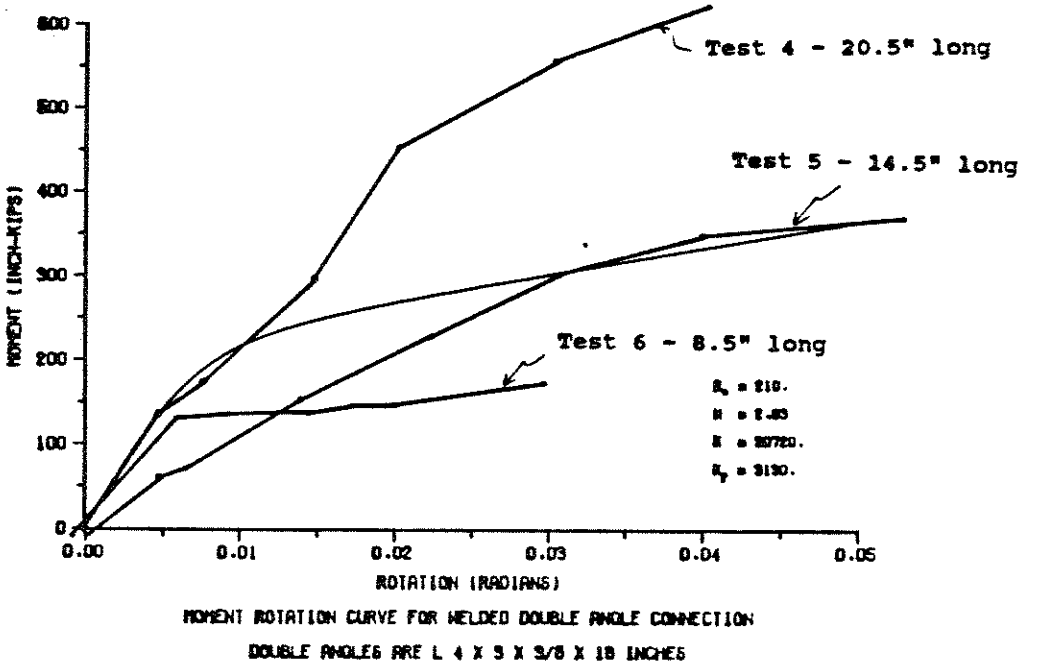

Figure 4.13 Comparison of Test Results With Richard's Equation

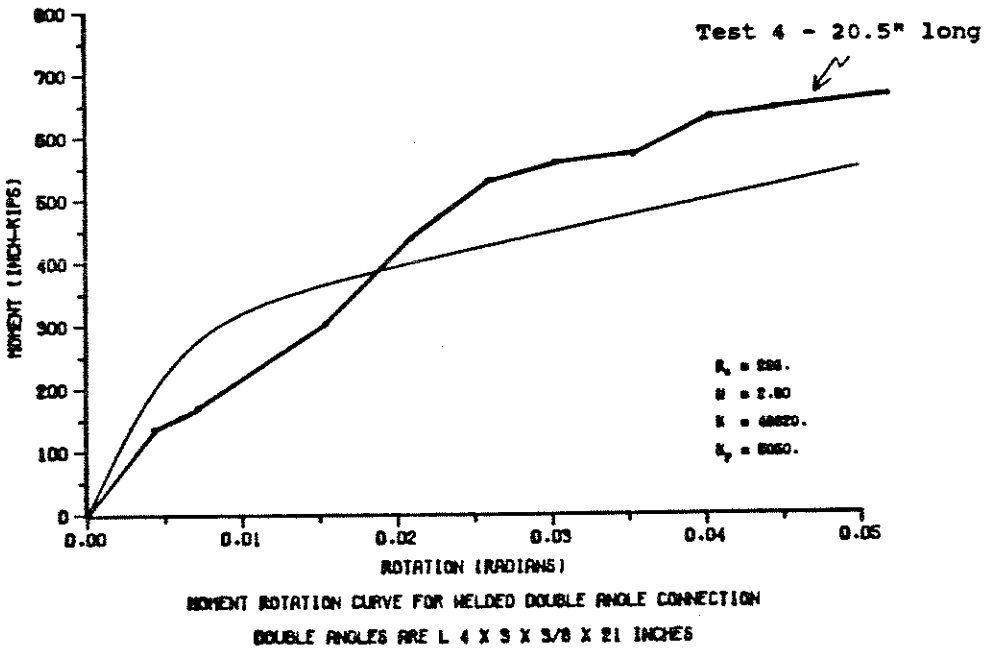

Figure 4.14 Comparison of Test Results With Richard's Equation

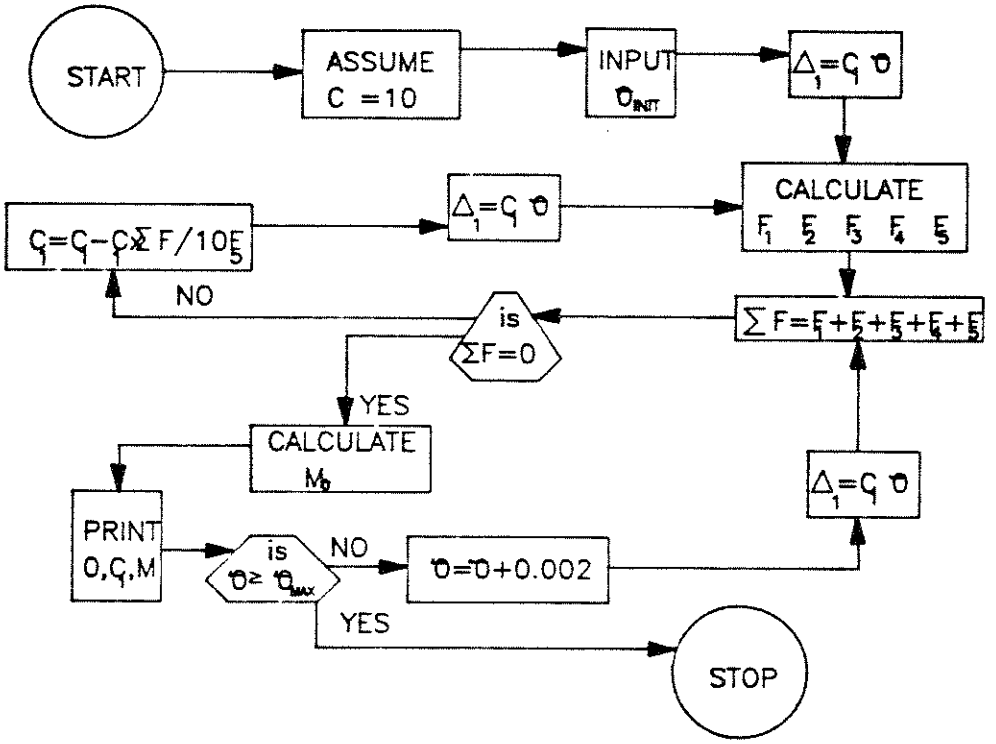

Figure 4.14 Flowchart for Richard's Model

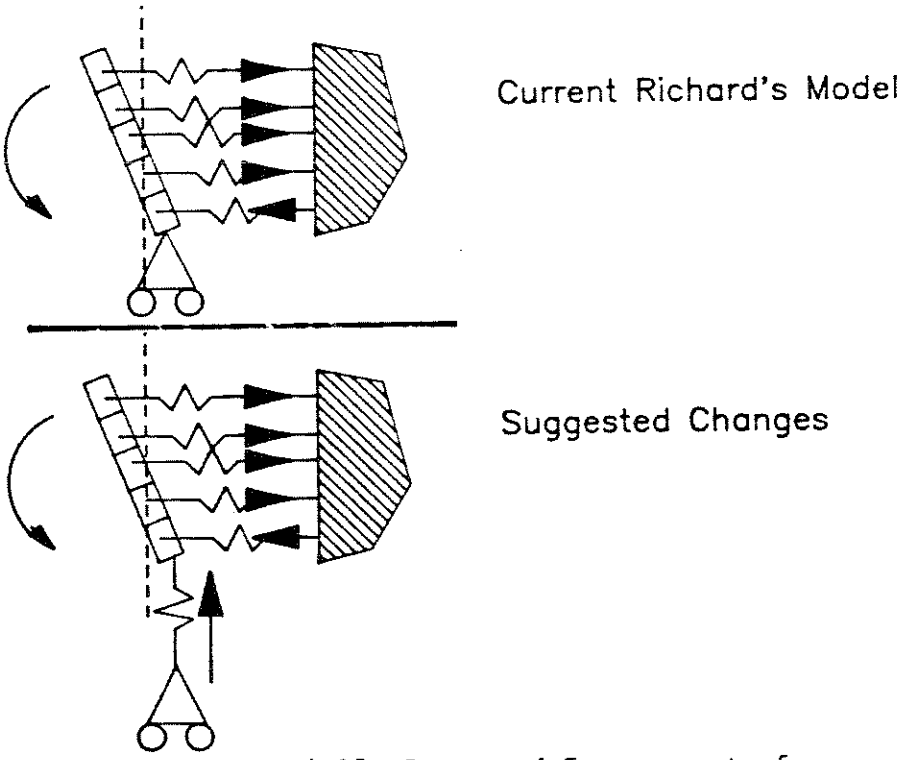

Figure 4.15 Suggested Improvements for Richard's Model

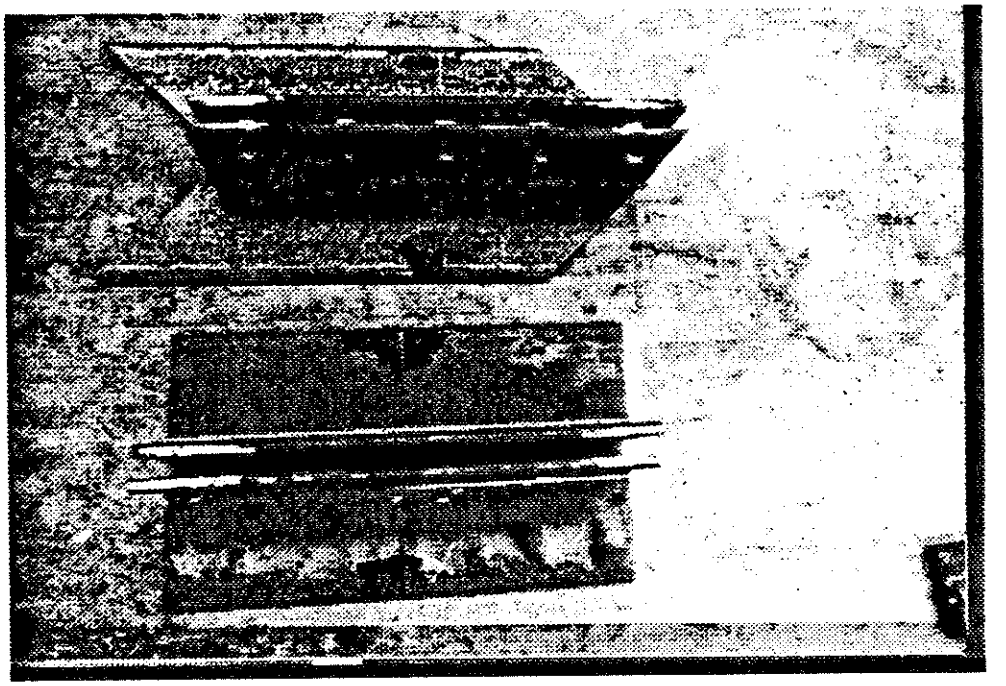

Figure 5.1 Test Specimens for Second Series of Tests

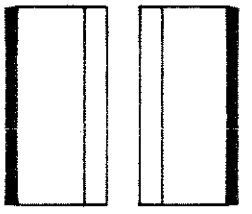

Traditional

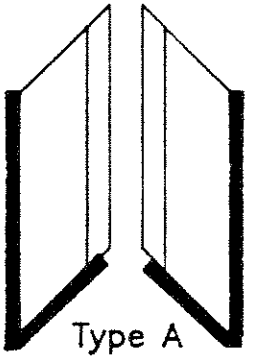

Type A

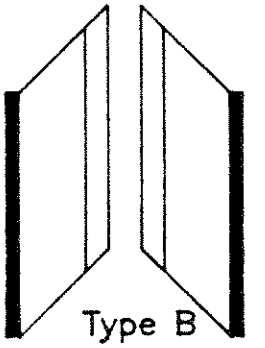

Type B

Figure 5.2 Detailing of Second Series of Tests

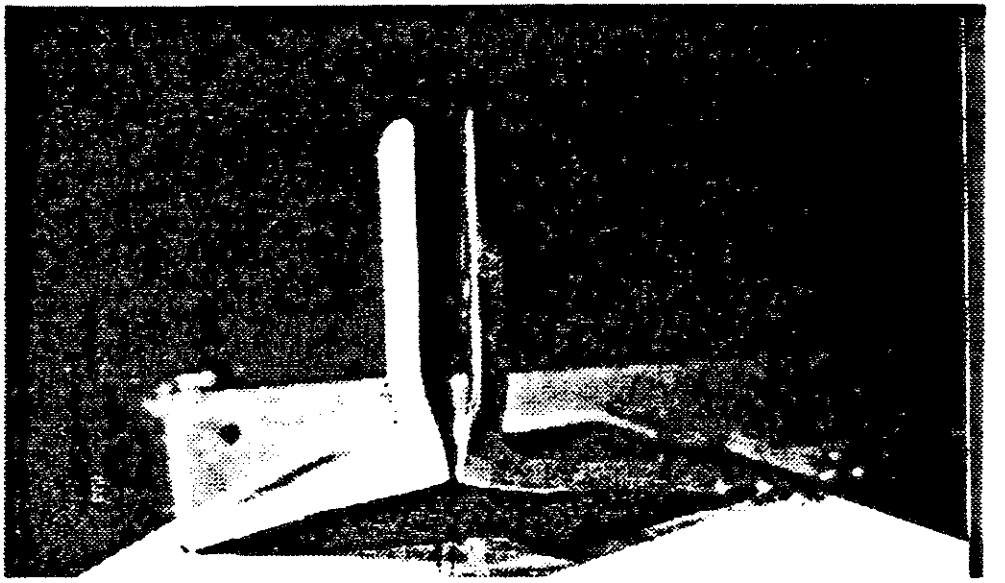

Figure 5.3 Effects of Removal of Tee-Hanger Region

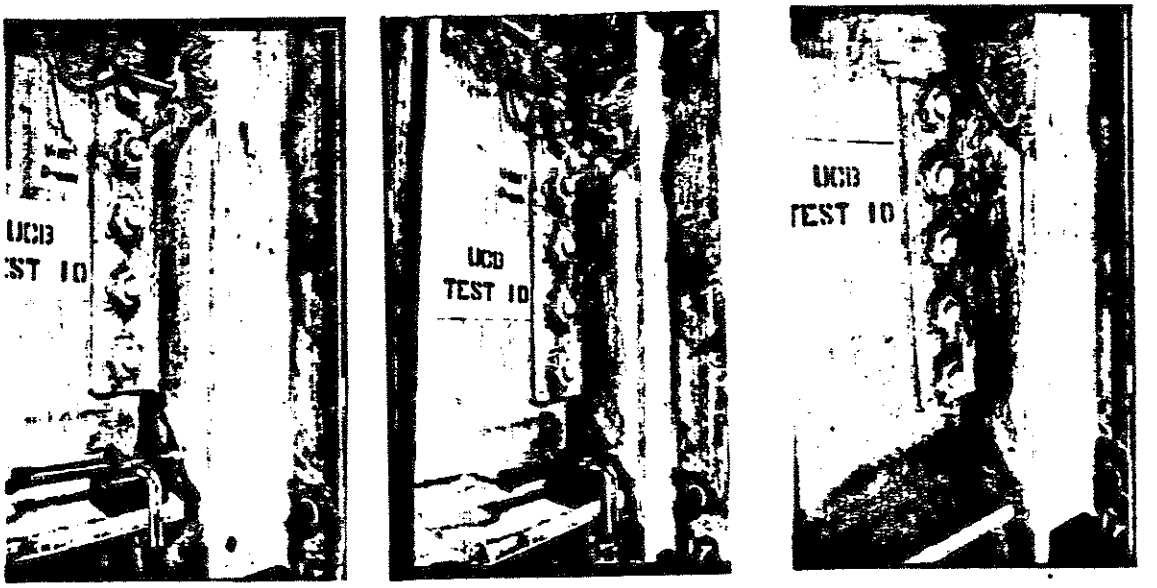

Figure 5.4 Progression of Failure for Specimen #10

APPENDIX A

TEST SUMMARIES

UCB DOUBLE-ANGLE FRAMING CONNECTION RESEARCH

SUMMARY OF TEST NUMBER 4

OBJECTIVE: Study the behavior of Double Angle Framing Connections
TEST DATE: Sept. 30, 1987
CONDUCTED BY: K. McMullin and A. Astaneh at the Univ. of Cal.-Berkeley
SPECIMEN NUMBER: UCB4-7B-0

PROPERTIES OF TEST SPECIMEN

DOUBLE ANGLES USED: 4 x 3 1/2 x 3/8 x 20.5 SLBB A36
NOMINAL BACK-TO-BACK LEG WIDTH: 3 1/2" THICKNESS: 3/8"
NOMINAL OUTSTANDING LEG WIDTH: 4" THICKNESS: 3/8"

NUMBER OF BOLTS: 7 DIAMETER OF BOLTS: 3/4"
TYPE OF BOLTS: A325-X
WELD SIZE: 1/4" WELDING ELECTRODE: E70XX

TEST RESULTS

A. ROTATION TEST CYCLE
MAXIMUM SHEAR: 10.2 kips MAXIMUM ROTATION: 0.0514 rad.
MAXIMUM MOMENT AT WELD: 697 k-in.
MAJOR OBSERVATION: yielding along top of weld and the middle bolt
B. STRENGTH TEST CYCLE
ULTIMATE SHEAR: 230.0 kips
ROTATION AT ULTIMATE SHEAR: 0.0257 rad.
MAXIMUM ROTATION: 0.0467 rad MAXIMUM MOMENT AT WELD: 404 k-in
FAILURE MODE: weld sheared along it's full length in the HAZ

UCB DOUBLE-ANGLE FRAMING CONNECTION RESEARCH

SUMMARY OF TEST NUMBER 5

OBJECTIVE: Study the behavior of Double Angle Framing Connections
TEST DATE: October 23, 1987
CONDUCTED BY: K. McMullin and A. Astaneh at the Univ. of Cal.-Berkeley
SPECIMEN NUMBER: UCB5-5B-0

PROPERTIES OF TEST SPECIMEN

DOUBLE ANGLES USED: 4 x 3 1/2 x 3/8 x 14.5 SLBB A36
NOMINAL BACK-TO-BACK LEG WIDTH: 3 1/2" THICKNESS: 3/8"
NOMINAL OUTSTANDING LEG WIDTH: 4" THICKNESS: 3/8"

NUMBER OF BOLTS: 5 DIAMETER OF BOLTS: 3/4"
TYPE OF BOLTS: A325-X
WELD SIZE: 1/4" WELDING ELECTRODE: E70XX

TEST RESULTS

A. ROTATION TEST CYCLE

MAXIMUM SHEAR: 5.30 kip MAXIMUM ROTATION: 0.0573 rad
MAXIMUM MOMENT AT WELD: 369 k-in
MAJOR OBSERVATION: weld return cracked during rotation cycle

B. STRENGTH TEST CYCLE

ULTIMATE SHEAR: 208 kip
ROTATION AT ULTIMATE SHEAR: 0.0323 rad
MAXIMUM ROTATION: 0.0359 MAXIMUM MOMENT AT WELD: 359 k-in
FAILURE MODE: weld cracked in HAZ of angle

GENERAL COMMENTS AND DISCUSSION

A. ROTATION CYCLE

B. STRENGTH CYCLE

-at 110 kips, yielding begins to show halfway down weld length where weld is thin

-at 150 kips, yielding appears at the top corner of the angle

-at 197 kips, the top third of the weld cracked

-load continued to climb to 208 kips, at which time there is very heavy yielding along the outstanding leg due to shear

-final failure occurred when the weld cracked along it's entire length

-after removing the beam there was heavy bearing damage to the holes in the beam's web

UCB DOUBLE-ANGLE FRAMING CONNECTION RESEARCH

SUMMARY OF TEST NUMBER 6

OBJECTIVE: Study the behavior of Double Angle Framing Connections
TEST DATE: November 12, 1987
CONDUCTED BY: K. McMullin and A. Astaneh at the Univ. of Cal.-Berkeley
SPECIMEN NUMBER: UCB6-3B-0

PROPERTIES OF TEST SPECIMEN

DOUBLE ANGLES USED: 4 x 3 1/2 x 3/8 x 8.5 SLBB A36
NOMINAL BACK-TO-BACK LEG WIDTH: 3 1/2" THICKNESS: 3/8"
NOMINAL OUTSTANDING LEG WIDTH: 4" THICKNESS: 3/8"

NUMBER OF BOLTS: 3 DIAMETER OF BOLTS: 3/4"
TYPE OF BOLTS: A325-X
WELD SIZE: 1/4" WELDING ELECTRODE: E70XX

TEST RESULTS

A. ROTATION TEST CYCLE
MAXIMUM SHEAR: 3.11 kip MAXIMUM ROTATION: 0.0310 rad
MAXIMUM MOMENT AT WELD: 171 k-in
MAJOR OBSERVATION: connection was so flexible that bottom flange of beam nearly contacted the column
B. STRENGTH TEST CYCLE
ULTIMATE SHEAR: 117.0 kip
ROTATION AT ULTIMATE SHEAR: 0.0414 rad
MAXIMUM ROTATION: 0.0449 rad MAXIMUM MOMENT AT WELD: 203 k-in
FAILURE MODE: weld cracked along the top length, compression edge of outstanding leg buckled

GENERAL COMMENTS AND DISCUSSION

A. ROTATION CYCLE

B. STRENGTH CYCLE

-at 28 kips, slight yielding shows at weld return corner

-at 68 kips, yielding appears along the shear beam area of the bolt leg

-at 87 kips, significant yielding at weld return corner and shear yielding along length of outstanding leg are evident

-at 113 kips, top of weld cracks 2" down it's length

-finally weld cracks 4", the compression zone of the outstanding leg buckles and the weld has failed by shear

UCB DOUBLE-ANGLE FRAMING CONNECTION RESEARCH

SUMMARY OF TEST NUMBER 7

OBJECTIVE: Study a new design of Double Angle framing connection
TEST DATE: November 20, 1987
CONDUCTED BY: K. McMullin and A. Astaneh at the Univ. of Cal.-Berkeley
SPECIMEN NUMBER: UCB7-7B-45

PROPERTIES OF TEST SPECIMEN

DOUBLE ANGLES USED: 4 x 4 x 3/8 x 20.5 A36, 45 cut - type A
NOMINAL BACK-TO-BACK LEG WIDTH: 4" THICKNESS: 3/8"
NOMINAL OUTSTANDING LEG WIDTH: 4" THICKNESS: 3/8"

NUMBER OF BOLTS: 7 DIAMETER OF BOLTS: 7/8"
TYPE OF BOLTS: A325-X
WELD SIZE: 5/16" WELDING ELECTRODE: E70XX

TEST RESULTS

A. ROTATION TEST CYCLE
MAXIMUM SHEAR: 8.62 kip MAXIMUM ROTATION: 0.0602 rad
MAXIMUM MOMENT AT WELD: 612 k-in
MAJOR OBSERVATION: weld return cracked

B. STRENGTH TEST CYCLE
ULTIMATE SHEAR: 300 kip
ROTATION AT ULTIMATE SHEAR: 0.0301 rad
MAXIMUM ROTATION: 0.0309 rad MAXIMUM MOMENT AT WELD: 547 k-in
FAILURE MODE: top of weld cracked and angle peels off from column

GENERAL COMMENTS AND DISCUSSION

A. ROTATION CYCLE

-a plastic hinge formed halfway between the weld return and the fillet of the angle

B. STRENGTH CYCLE

-at 83 kips, yielding appears in the shear beam area of the bolt leg

-at 120 kips, compression yielding appears in the area of the outstanding leg that is made by the 45 degree sawcut

-at 260 kips, very heavy yielding due to shear develops along the outstanding leg

-at 272 kips, weld has cracked at top about 3/4" from corner, yielding from weld return corner to bottom corner is very heavy

-finally the weld begins to crack along it's length due to shear; this allows the angle to move horizontally from the column; the weld cracks along it's length until it reaches the same elevation as the angle's bottom corner

-the weld at the bottom corner of angle cracks and now the angle begins to peel off the column

UCB DOUBLE-ANGLE FRAMING CONNECTION RESEARCH

SUMMARY OF TEST NUMBER 8

OBJECTIVE: Study a new design of Double Angle framing connection

TEST DATE: November 25, 1987

CONDUCTED BY: K. McMullin and A. Astaneh at the Univ. of Cal.-Berkeley

SPECIMEN NUMBER: UCB8-5B-45A

PROPERTIES OF TEST SPECIMEN

DOUBLE ANGLES USED: 4 x 4 x 3/8 x 14.5 A36, 45 cut - type A

NOMINAL BACK-TO-BACK LEG WIDTH: 4" THICKNESS: 3/8"

NOMINAL OUTSTANDING LEG WIDTH: 4" THICKNESS: 3/8"

NUMBER OF BOLTS: 5 DIAMETER OF BOLTS: 7/8"

TYPE OF BOLTS: A325-X

WELD SIZE: 5/16" WELDING ELECTRODE: E70XX

TEST RESULTS

A. ROTATION TEST CYCLE

MAXIMUM SHEAR: 3.88 kips MAXIMUM ROTATION: 0.0562 rad

MAXIMUM MOMENT AT WELD: 245 k-in

MAJOR OBSERVATION: yielding appears along the full length of the outstanding leg

B. STRENGTH TEST CYCLE

ULTIMATE SHEAR: 243 kip

ROTATION AT ULTIMATE SHEAR: 0.0326 rad

MAXIMUM ROTATION: 0.0331 rad MAXIMUM MOMENT AT WELD: 195 k-in

FAILURE MODE: bearing of bolts on web and buckling of web

GENERAL COMMENTS AND DISCUSSION

A. ROTATION CYCLE

-plastic hinge forms at top corner of angle during ductility cycle

B. STRENGTH CYCLE

-at 140 kips, significant yielding around the weld return and compression yielding in the lower triangle

-at 174 kips, angle has slight curvature developing along a yield line from the weld return to the bottom corner of the angle

-at 214.6 kips, yielding in shear beam area of bolt leg is at 45 degree angle to boltline, bearing of bolts on web is becoming evident, the weld return has cracked

-at 192 kips and 0.035 rads rotation, the web of the beam has buckled between the top flange and the angles, weld has cracked 1 1/2" along the top, upon removing the beam heavy bearing of the web is obvious

-the fillets of the two angles have bent around the beam's web in the tension zone, this happened because after removing the top tension zone of weld no T-hanger force could develop

UCB DOUBLE-ANGLE FRAMING CONNECTION RESEARCH

SUMMARY OF TEST NUMBER 9

OBJECTIVE: Study a new design of Double Angle framing connection

TEST DATE: December 14, 1987

CONDUCTED BY: K. McMullin and A. Astaneh at the Univ. of Cal.-Berkeley

SPECIMEN NUMBER: UCB9-5B-0

PROPERTIES OF TEST SPECIMEN

DOUBLE ANGLES USED: 4 x 4 x 3/8 x 14.5 A36

NOMINAL BACK-TO-BACK LEG WIDTH: 4" THICKNESS: 3/8"

NOMINAL OUTSTANDING LEG WIDTH: 4" THICKNESS: 3/8"

NUMBER OF BOLTS: 5 DIAMETER OF BOLTS: 7/8"

TYPE OF BOLTS: A325-X

WELD SIZE: 5/16" WELDING ELECTRODE: E70XX

TEST RESULTS

A. ROTATION TEST CYCLE

MAXIMUM SHEAR: 8.17 kips MAXIMUM ROTATION: 0.0563 rad

MAXIMUM MOMENT AT WELD: 507 k-in

MAJOR OBSERVATION: plastic hinge forming near fillet of angle, weld return cracked

B. STRENGTH TEST CYCLE

ULTIMATE SHEAR: 192 kip

ROTATION AT ULTIMATE SHEAR: 0.0332 rad

MAXIMUM ROTATION: 0.0341 rad MAXIMUM MOMENT AT WELD: 265 k-in

FAILURE MODE: weld cracks from top down

GENERAL COMMENTS AND DISCUSSION

A. ROTATION CYCLE

-during the ductility cycle a plastic hinge forms very close to the angle's fillet on the tension end of the connection; the outstanding leg shows much horizontal compression yielding and yielding at the weld return corner; weld return has cracked and top third of weld shows yielding

B. STRENGTH CYCLE

-at 72 kips, yielding occurs in shear beam area of bolt leg

-at 190 kips, weld cracks along top third of length; shear yielding is very heavy in shear beam area of bolt leg and along length of outstanding leg

UCB DOUBLE-ANGLE FRAMING CONNECTION RESEARCH

SUMMARY OF TEST NUMBER 10

OBJECTIVE: Study a new design of Double Angle framing connection
TEST DATE: December 15, 1987
CONDUCTED BY: K. McMullin and A. Astaneh at the Univ. of Cal.-Berkeley
SPECIMEN NUMBER: UCB10-5B-45B

PROPERTIES OF TEST SPECIMEN

DOUBLE ANGLES USED: 4 x 4 x 3/8 x 14.5 A36, 45 cut - type B
NOMINAL BACK-TO-BACK LEG WIDTH: 4" THICKNESS: 3/8"
NOMINAL OUTSTANDING LEG WIDTH: 4" THICKNESS: 3/8"

NUMBER OF BOLTS: 5 DIAMETER OF BOLTS: 7/8"
TYPE OF BOLTS: A325-X
WELD SIZE: 5/16" WELDING ELECTRODE: E70XX

TEST RESULTS

A. ROTATION TEST CYCLE
MAXIMUM SHEAR: 5.66 kip MAXIMUM ROTATION: 0.0535 rad
MAXIMUM MOMENT AT WELD: 285 k-in
MAJOR OBSERVATION: yielding at weld return corner and bottom corner of angle, but it is spread out over several sq. inches

B. STRENGTH TEST CYCLE
ULTIMATE SHEAR: 217 kip
ROTATION AT ULTIMATE SHEAR: 0.0344 rad
MAXIMUM ROTATION: 0.0423 rad MAXIMUM MOMENT AT WELD: 179 k-in
FAILURE MODE: weld has cracked, compression edge of outstanding leg is buckled

GENERAL COMMENTS AND DISCUSSION

A. ROTATION CYCLE

-a yield line develops from the weld return corner to the bottom corner of the angle

B. STRENGTH CYCLE

-at 105 kips, yielding grows at the bottom corner of the angle

-at 140 kips, yielding in shear beam of outstanding leg

-at 155 kips, weld return cracks, yielding occurring along boltline

-at 205 kips, very distributed yielding through outstanding leg

-at 199 kips and 0.033 rad rotation, top 3" of weld has cracked

-finally weld cracks 5" and the compression edge of outstanding leg buckles

APPENDIX B

PLOTS OF TEST DATA

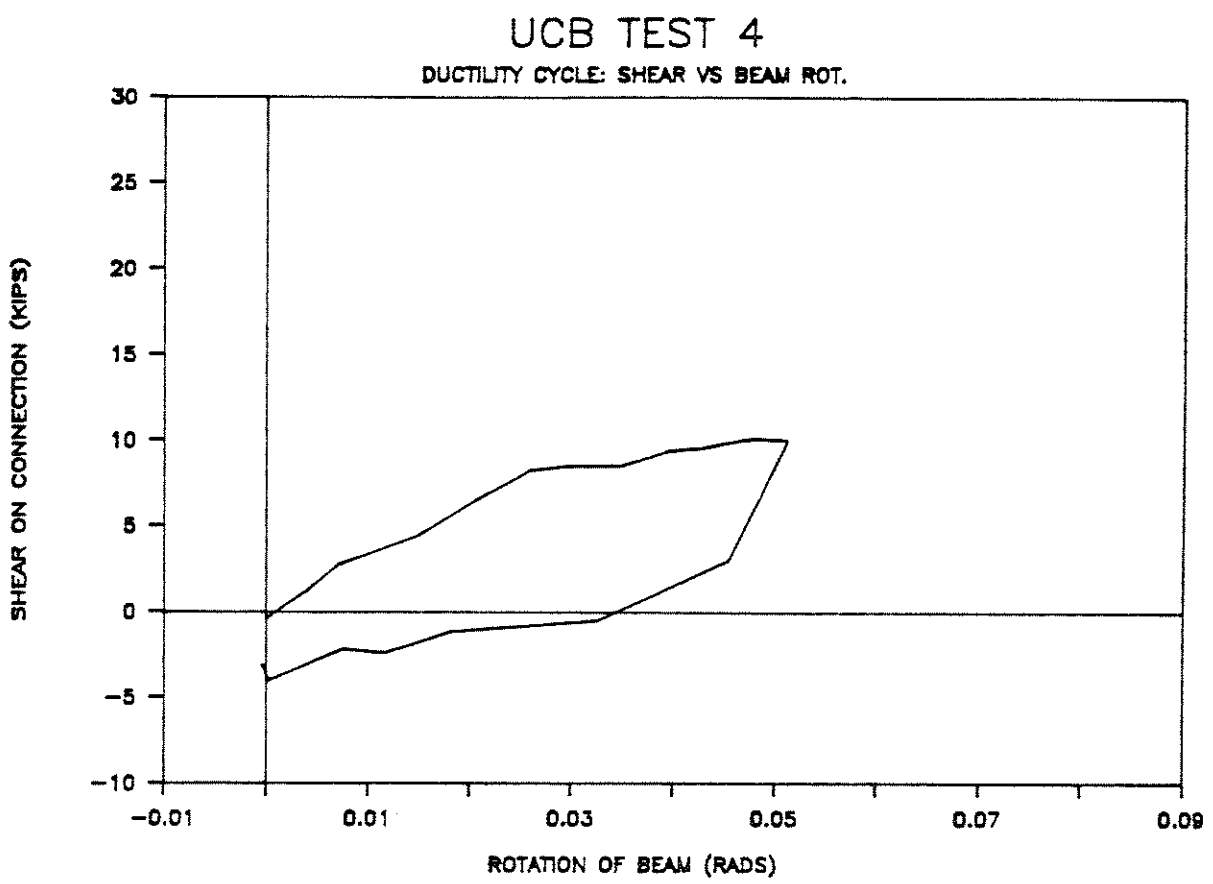
UCB TEST 4
DUCTILITY CYCLE: SHEAR VS BEAM ROT.
SHEAR ON CONNECTION (KIPS)
30
25
20
15
10
5
0
−5
−10
−0.01
0.01
0.03
0.05
0.07
0.09
ROTATION OF BEAM (RADS)

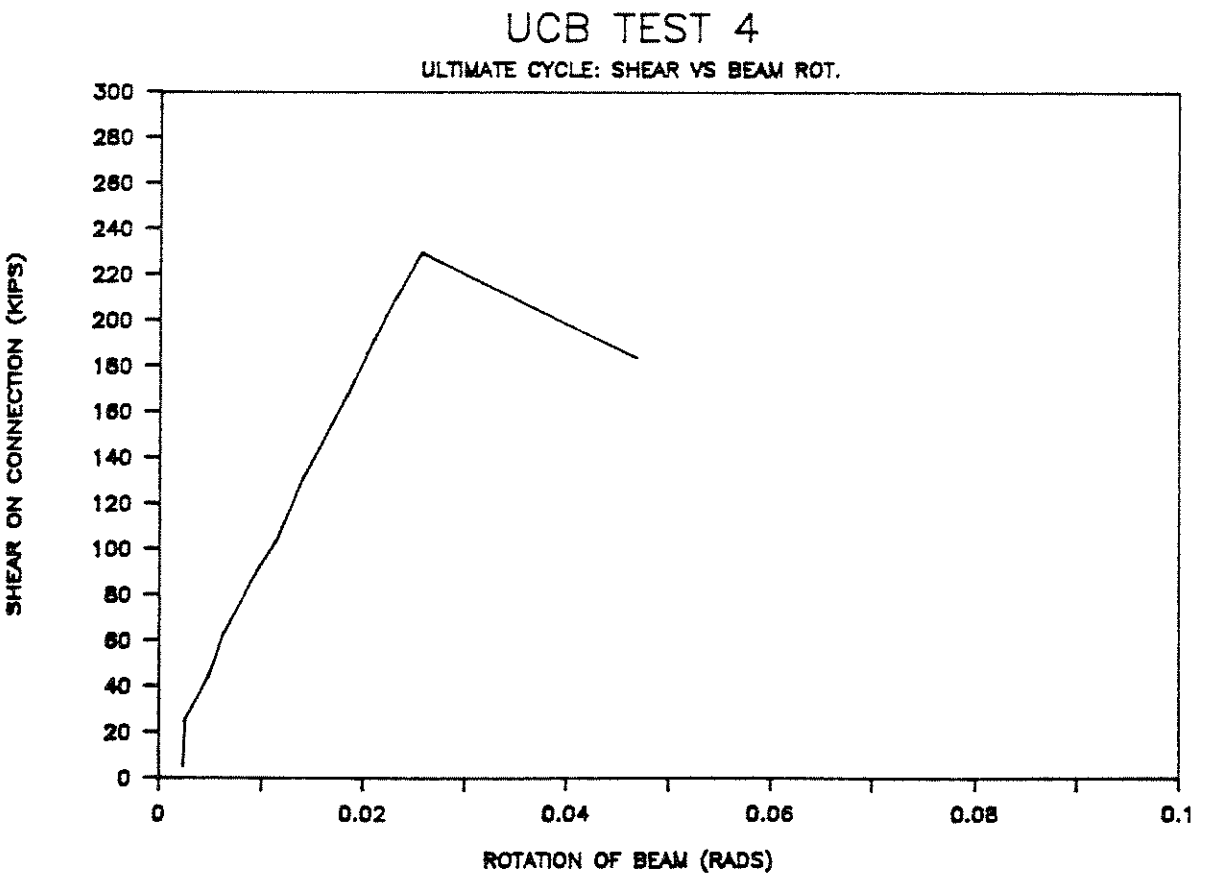
UCB TEST 4
ULTIMATE CYCLE: SHEAR VS BEAM ROT.
SHEAR ON CONNECTION (KIPS)
300
280
260
240
220
200
180
160
140
120
100
80
60
40
20
0
0
0.02
0.04
0.06
0.08
0.1
ROTATION OF BEAM (RADS)

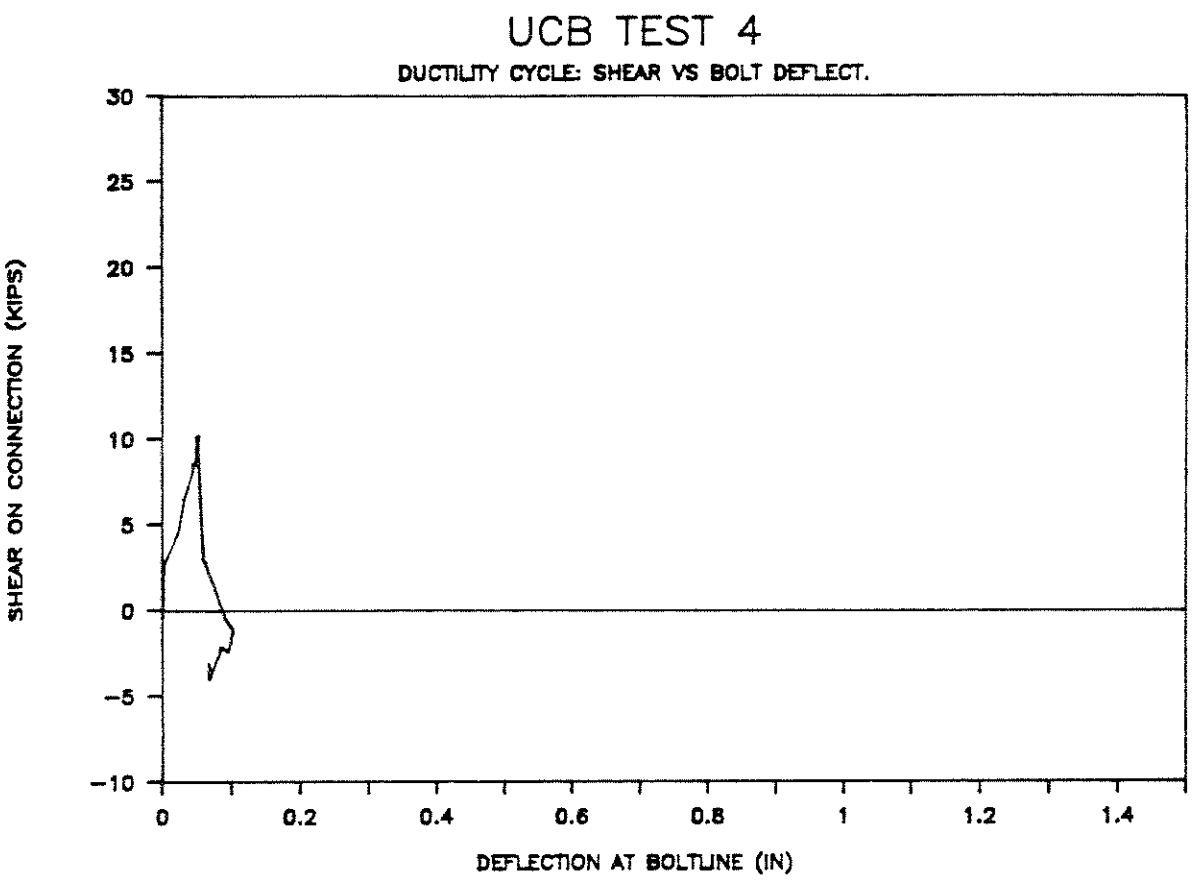
UCB TEST 4
DUCTILITY CYCLE: SHEAR VS BOLT DEFLECT.
SHEAR ON CONNECTION (KIPS)
30
25
20
15
10
5
0
-5
-10
0
0.2
0.4
0.6
0.8
1
1.2
1.4
DEFLECTION AT BOLTLINE (IN)

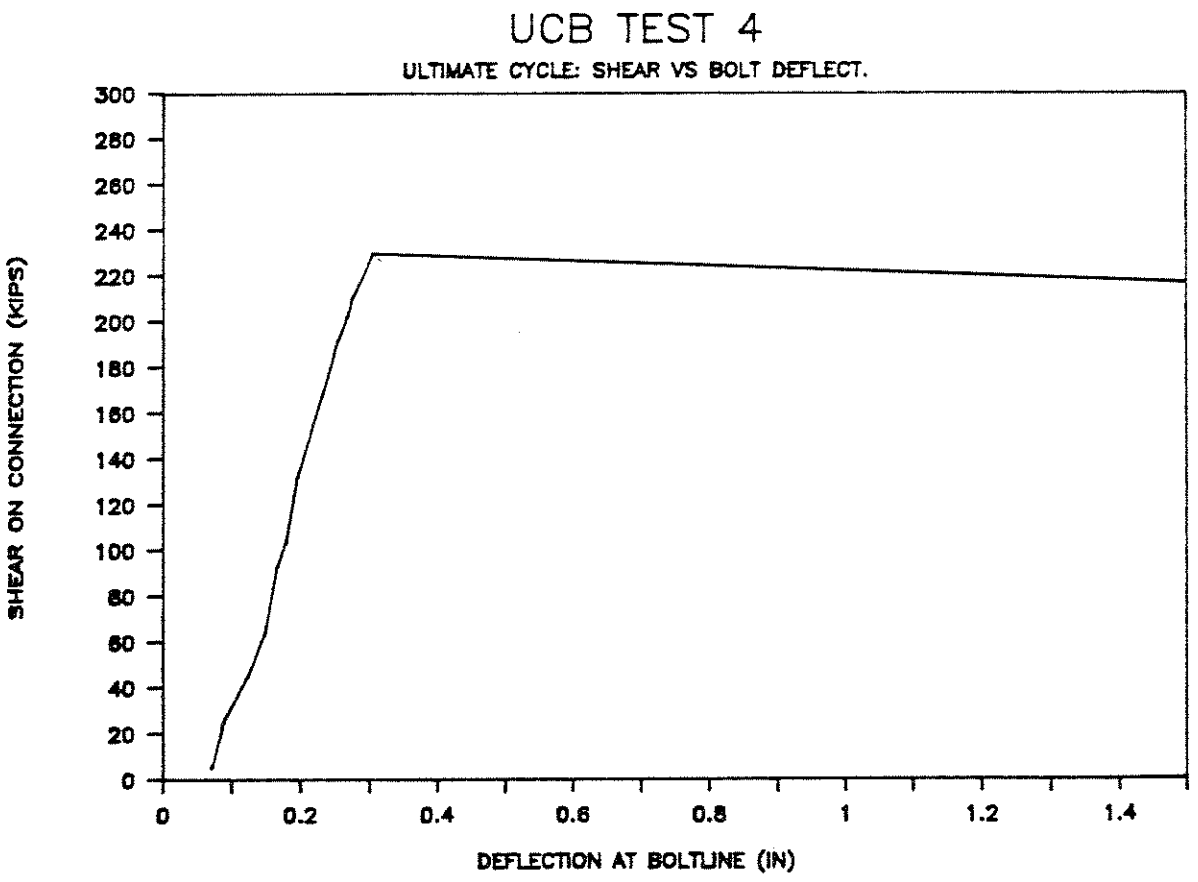
UCB TEST 4
ULTIMATE CYCLE: SHEAR VS BOLT DEFLECT.
SHEAR ON CONNECTION (KIPS)
300
280
260
240
220
200
180
160
140
120
100
80
60
40
20
0
0
0.2
0.4
0.6
0.8
1
1.2
1.4
DEFLECTION AT BOLTLINE (IN)

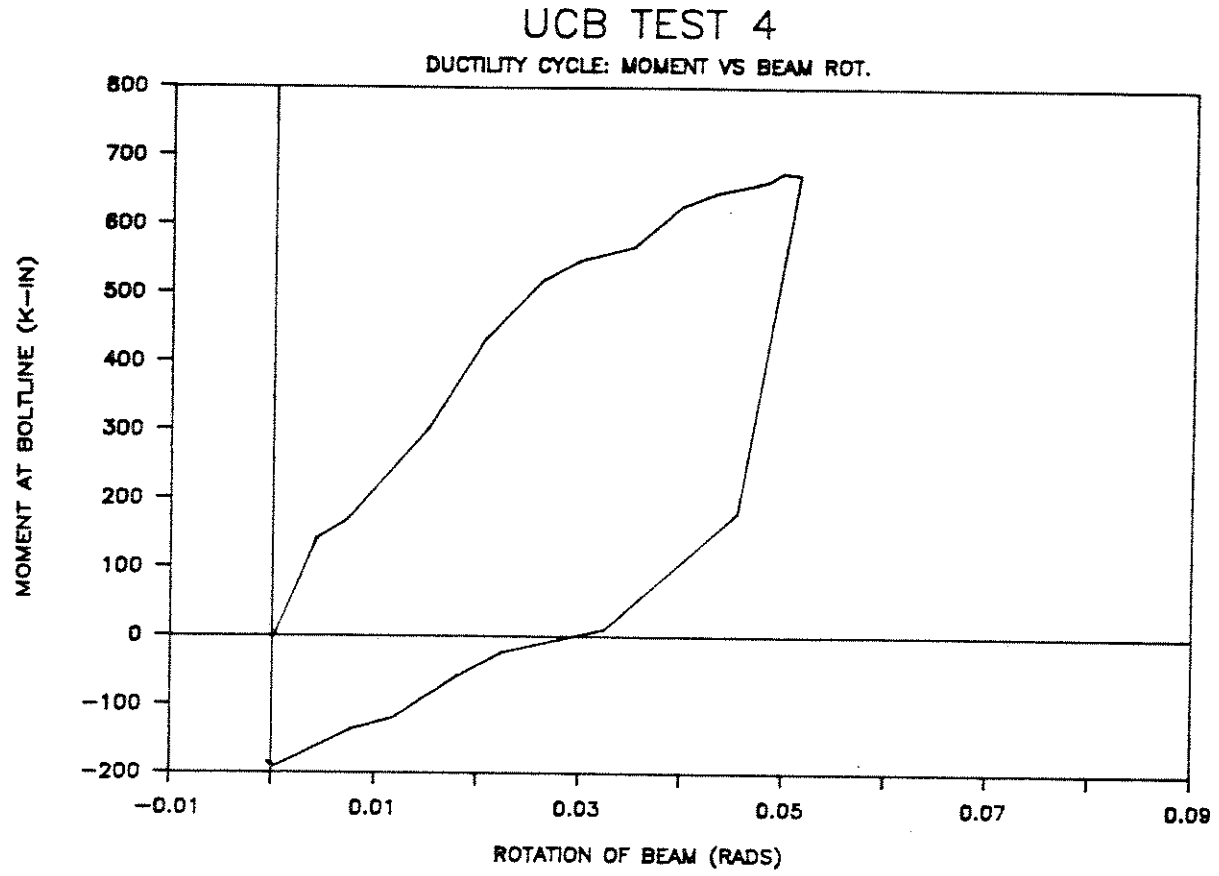
UCB TEST 4
DUCTILITY CYCLE: MOMENT VS BEAM ROT.
MOMENT AT BOLTLINE (K-IN)
800
700
600
500
400
300
200
100
0
-100
-200
-0.01
0.01
0.03
0.05
0.07
0.09
ROTATION OF BEAM (RADS)

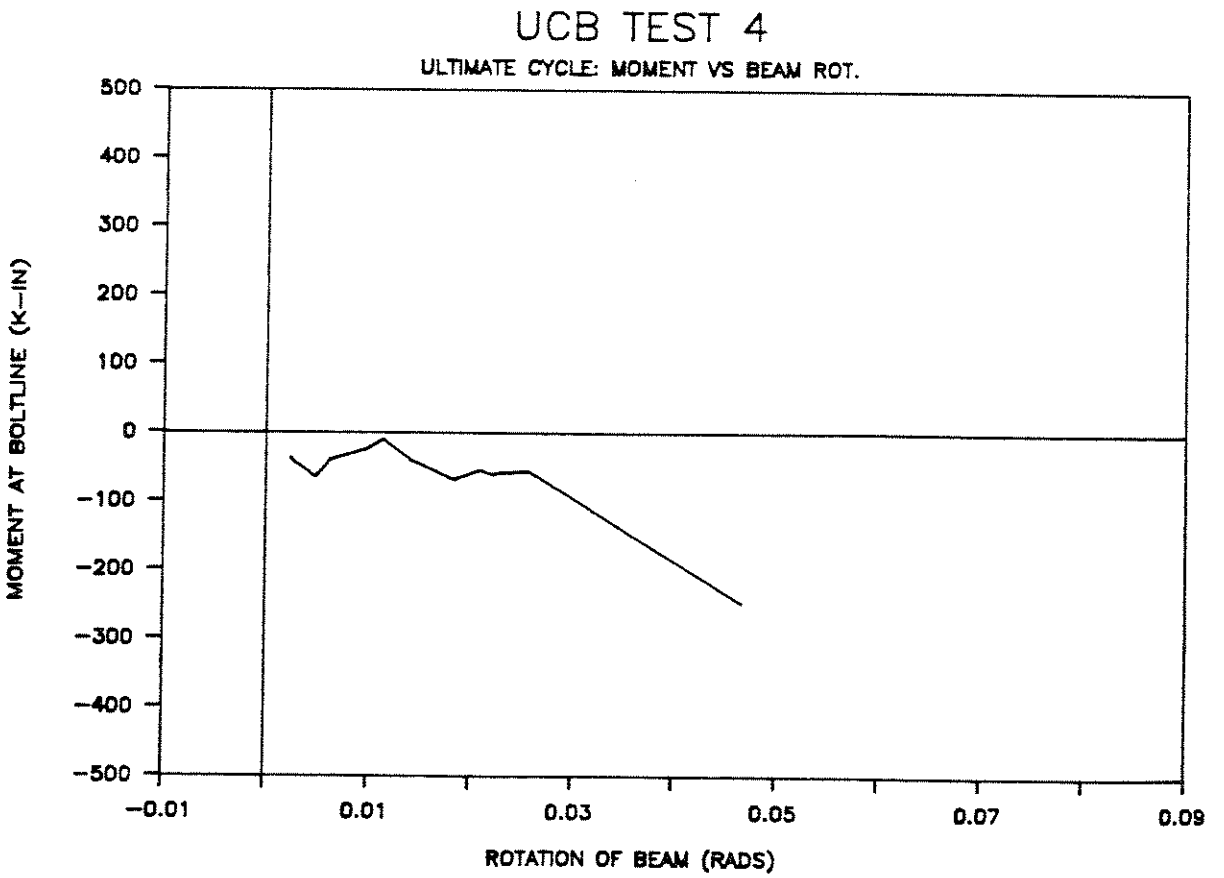
UCB TEST 4
ULTIMATE CYCLE: MOMENT VS BEAM ROT.
MOMENT AT BOLTLINE (K-IN)
500
400
300
200
100
0
-100
-200
-300
-400
-500
-0.01
0.01
0.03
0.05
0.07
0.09
ROTATION OF BEAM (RADS)

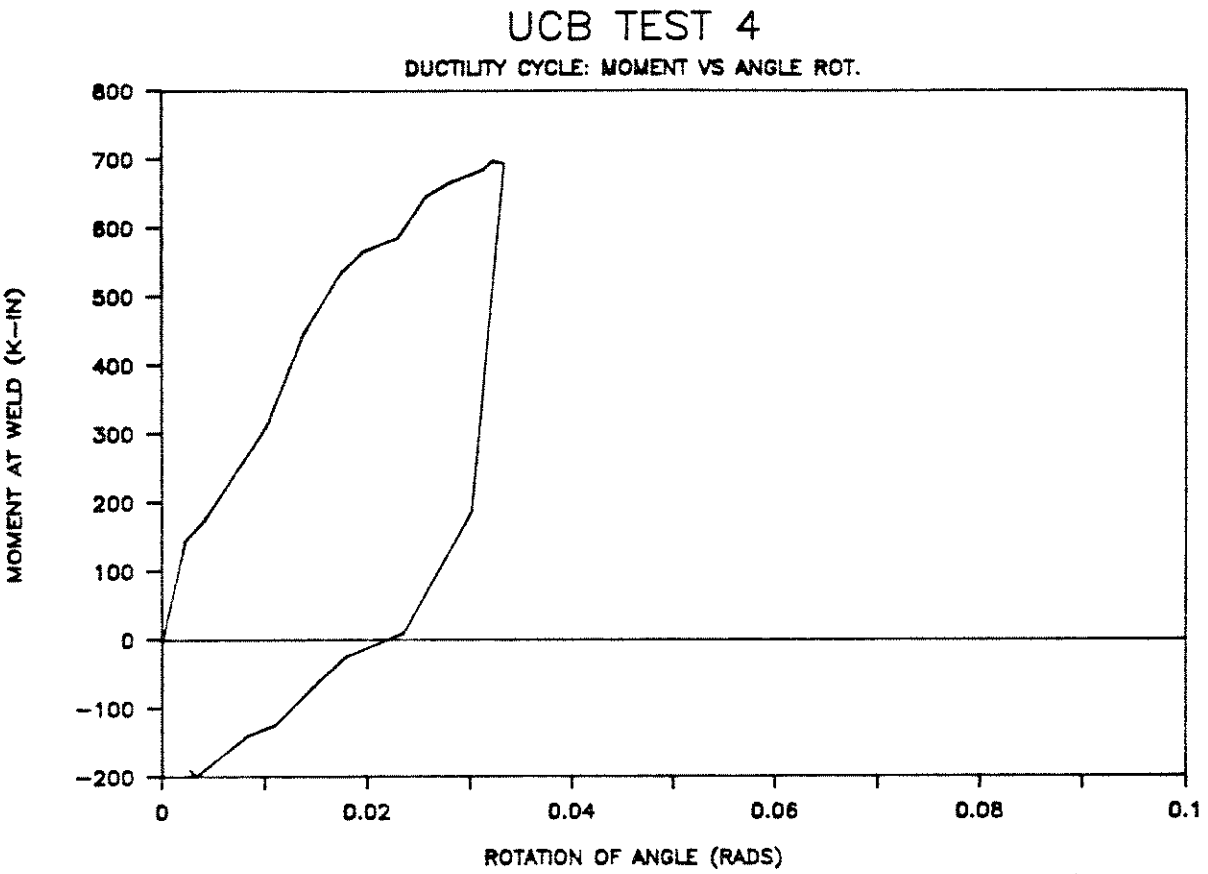
UCB TEST 4
DUCTILITY CYCLE: MOMENT VS ANGLE ROT.
MOMENT AT WELD (K-IN)
800
700
600
500
400
300
200
100
0
-100
-200
0
0.02
0.04
0.06
0.08
0.1
ROTATION OF ANGLE (RADS)

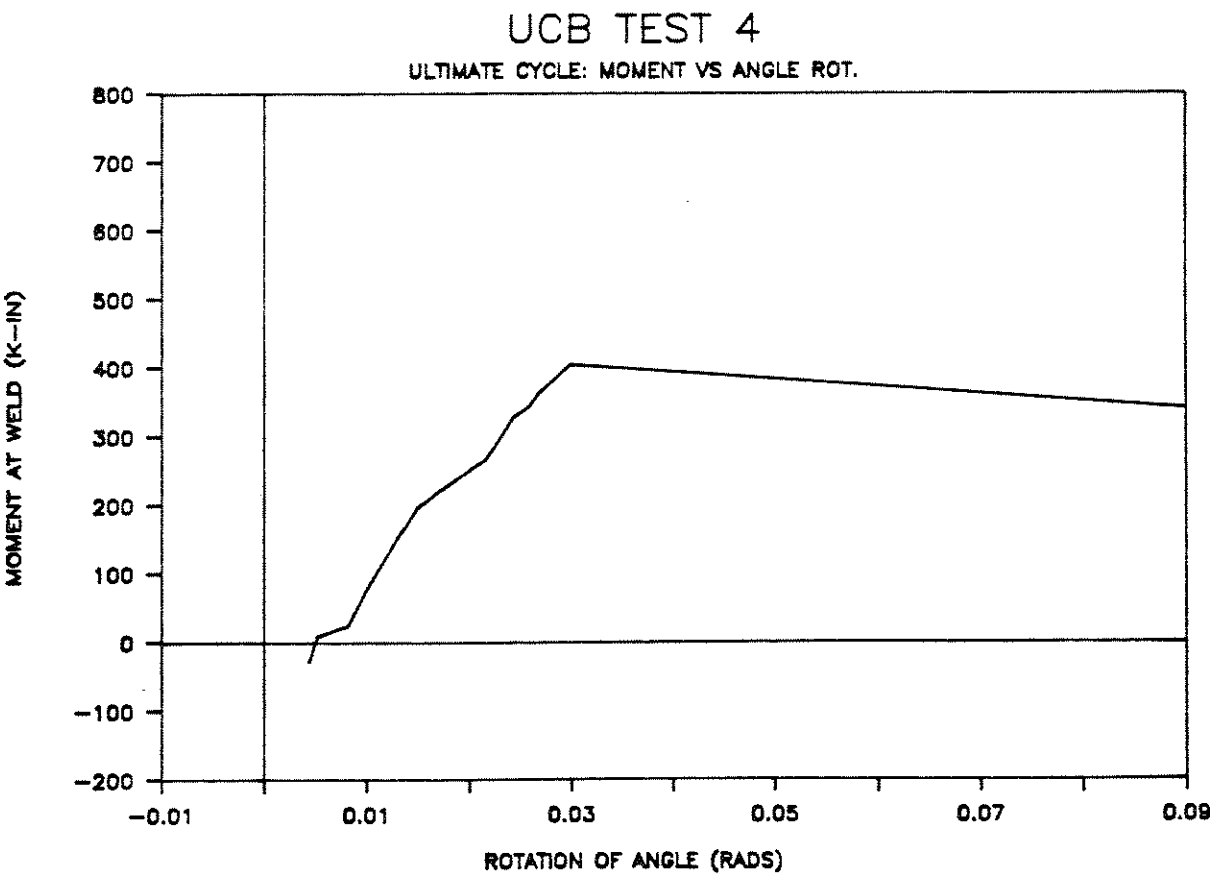
UCB TEST 4
ULTIMATE CYCLE: MOMENT VS ANGLE ROT.
MOMENT AT WELD (K-IN)
800
700
600
500
400
300
200
100
0
-100
-200
-0.01
0.01
0.03
0.05
0.07
0.09
ROTATION OF ANGLE (RADS)

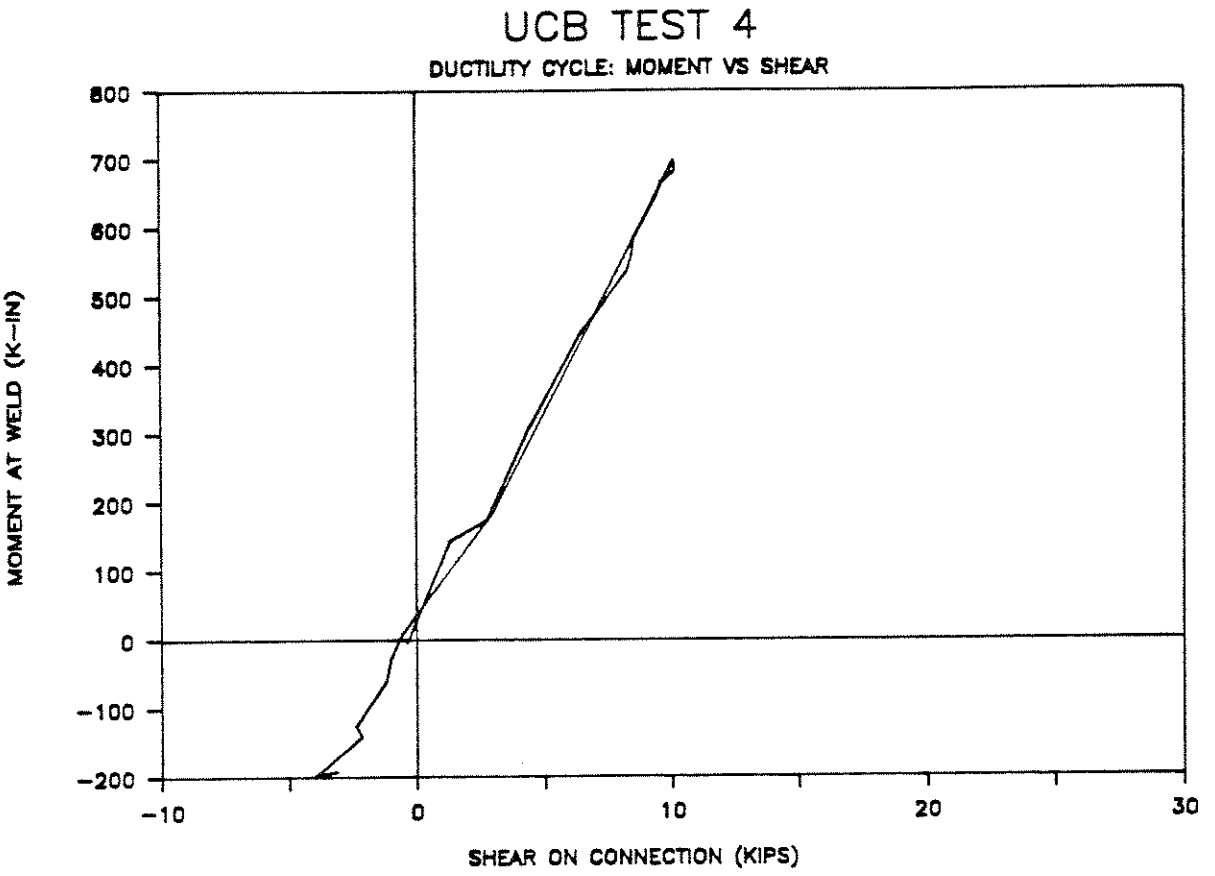
UCB TEST 4
DUCTILITY CYCLE: MOMENT VS SHEAR
MOMENT AT WELD (K-IN)
800
700
600
500
400
300
200
100
0
-100
-200
-10
0
10
20
30
SHEAR ON CONNECTION (KIPS)

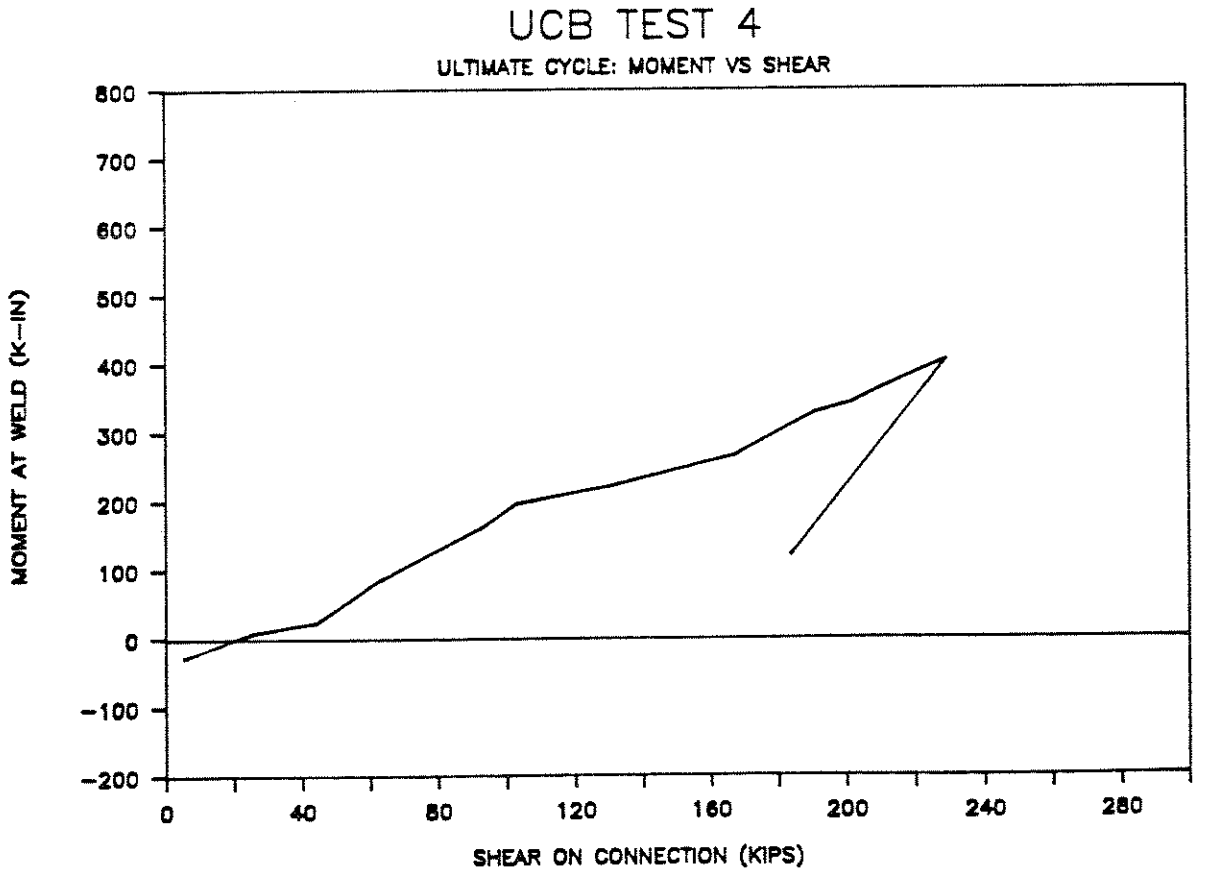
UCB TEST 4
ULTIMATE CYCLE: MOMENT VS SHEAR
MOMENT AT WELD (K-IN)
800
700
600
500
400
300
200
100
0
-100
-200
0
40
80
120
160
200
240
280
SHEAR ON CONNECTION (KIPS)

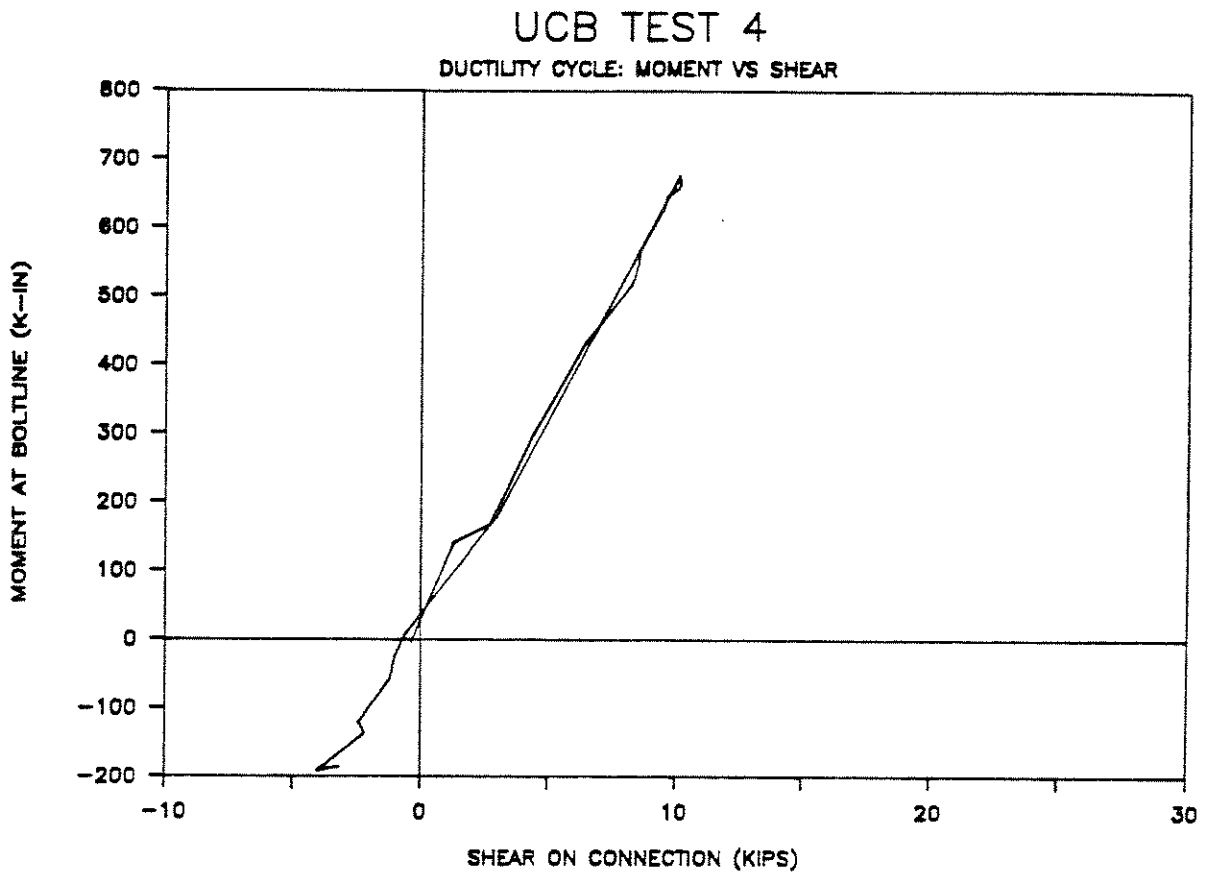
UCB TEST 4
DUCTILITY CYCLE: MOMENT VS SHEAR
MOMENT AT BOLTLINE (K-IN)
800
700
600
500
400
300
200
100
0
-100
-200
-10
0
10
20
30
SHEAR ON CONNECTION (KIPS)

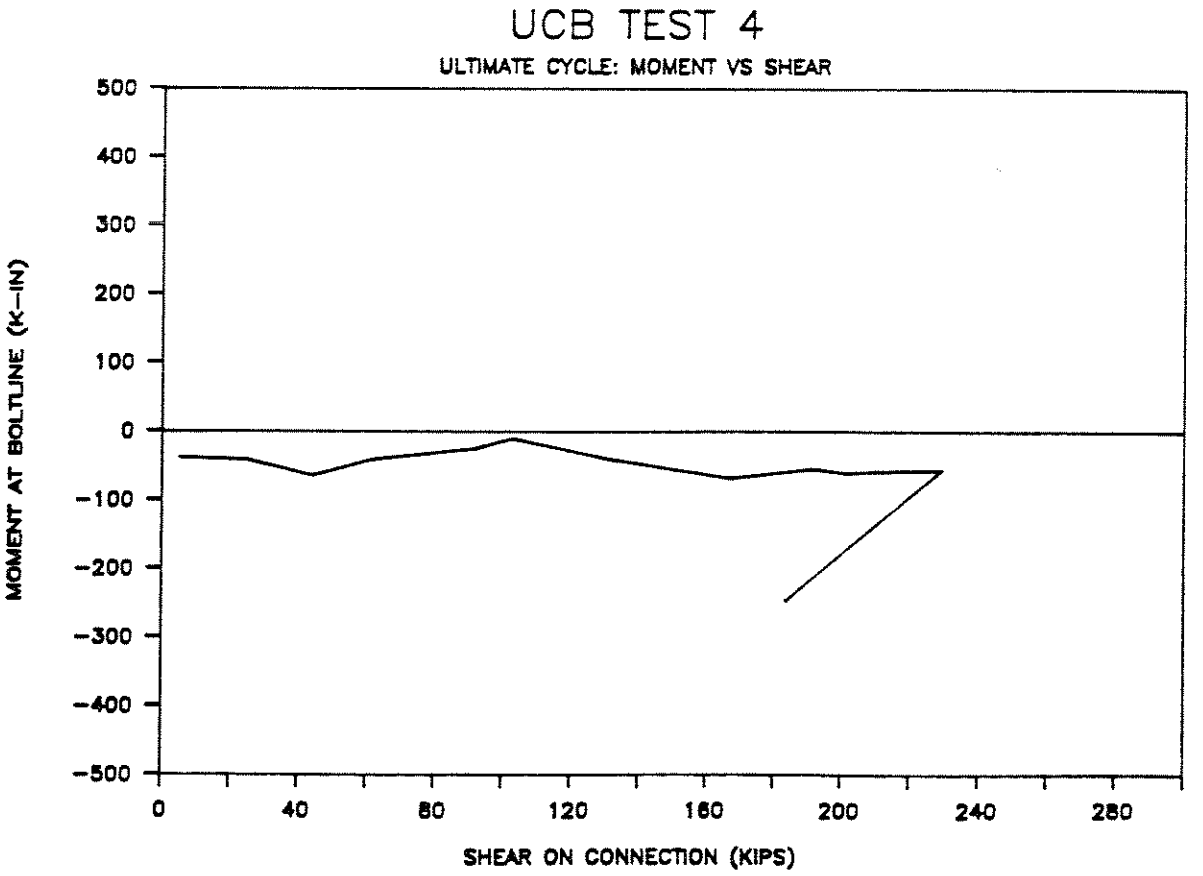
UCB TEST 4
ULTIMATE CYCLE: MOMENT VS SHEAR
MOMENT AT BOLTLINE (K-IN)
500
400
300
200
100
0
-100
-200
-300
-400
-500
0
40
80
120
160
200
240
280
SHEAR ON CONNECTION (KIPS)

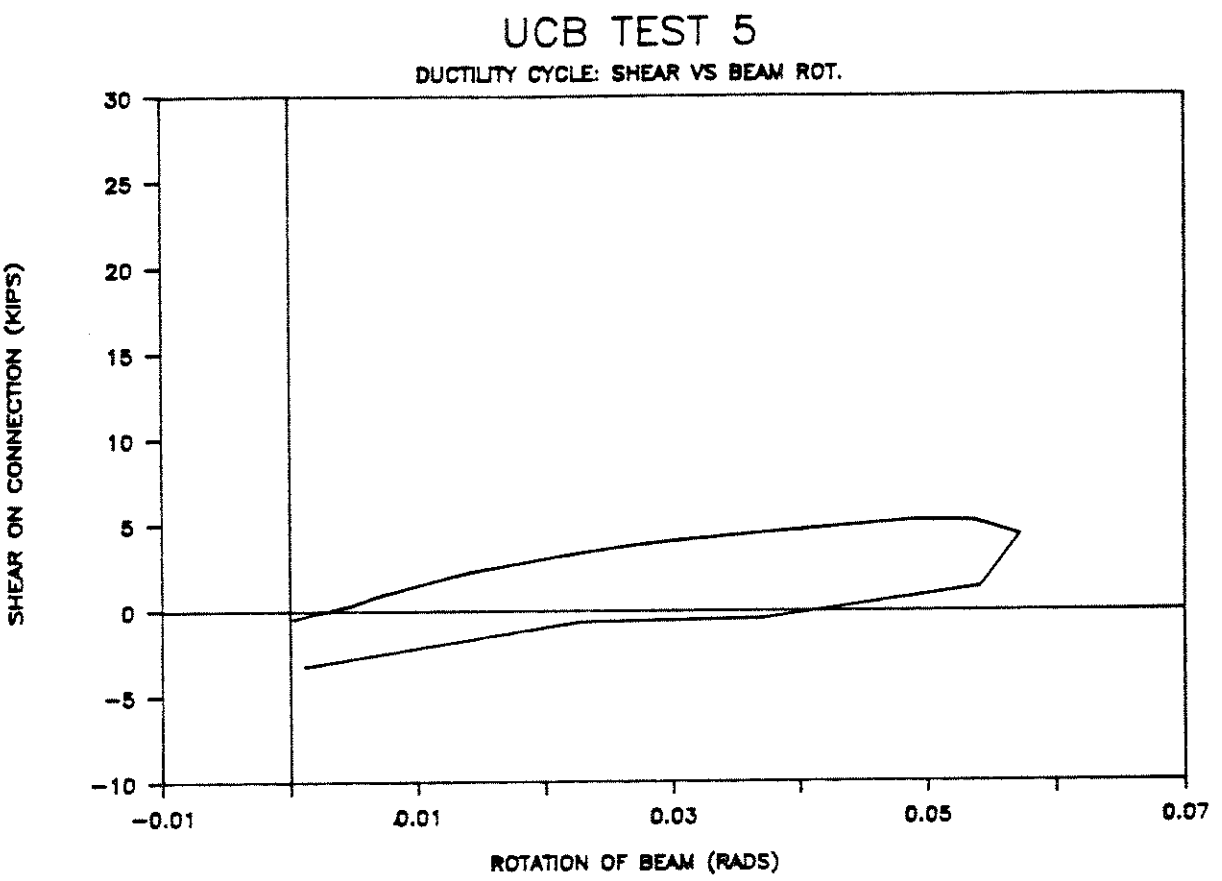
UCB TEST 5
DUCTILITY CYCLE: SHEAR VS BEAM ROT.
SHEAR ON CONNECTION (KIPS)
30
25
20
15
10
5
0
-5
-10
-0.01
0.01
0.03
0.05
0.07
ROTATION OF BEAM (RADS)

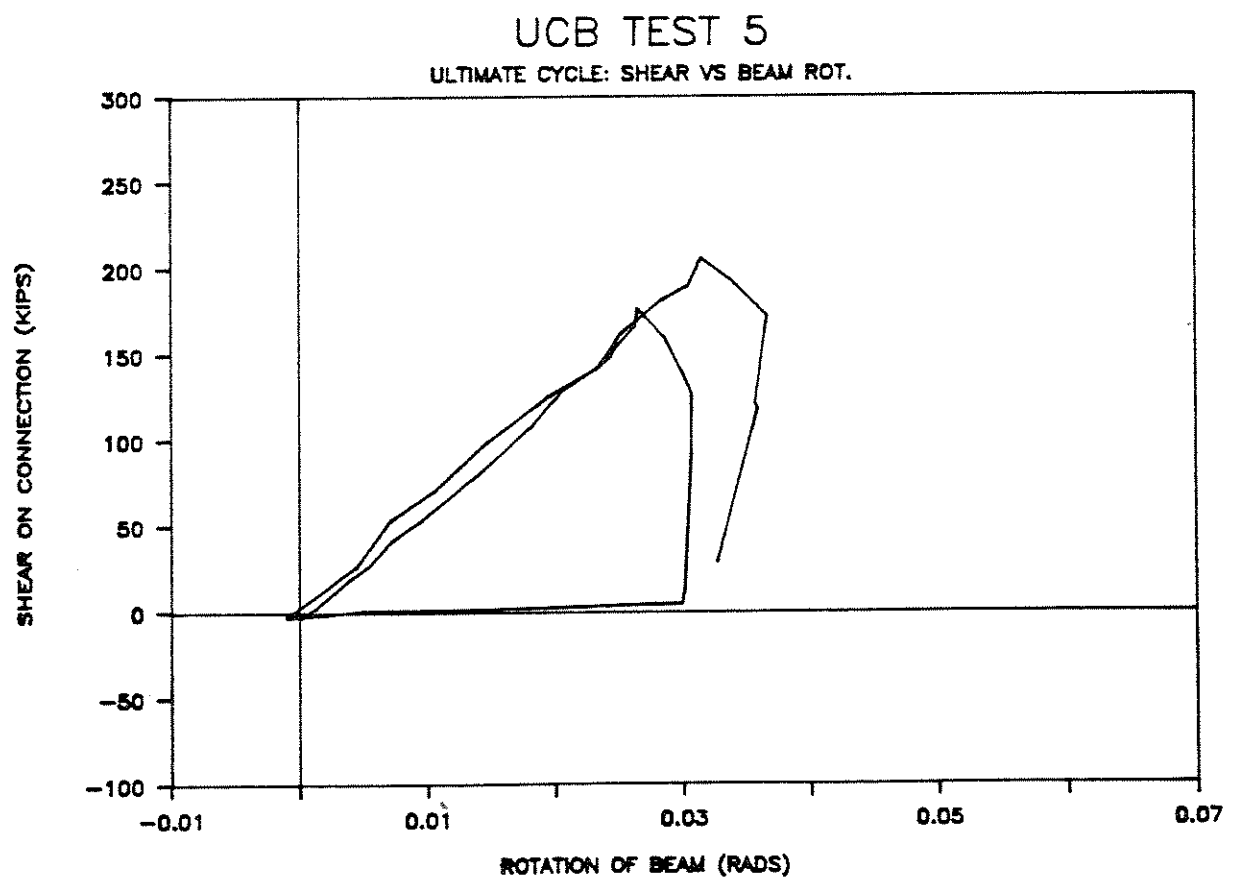
UCB TEST 5
ULTIMATE CYCLE: SHEAR VS BEAM ROT.
SHEAR ON CONNECTION (KIPS)
300
250
200
150
100
50
0
-50
-100
-0.01
0.01
0.03
0.05
0.07
ROTATION OF BEAM (RADS)

UCB TEST 5

DUCTILITY CYCLE: SHEAR VS BOLT DEFLECT.

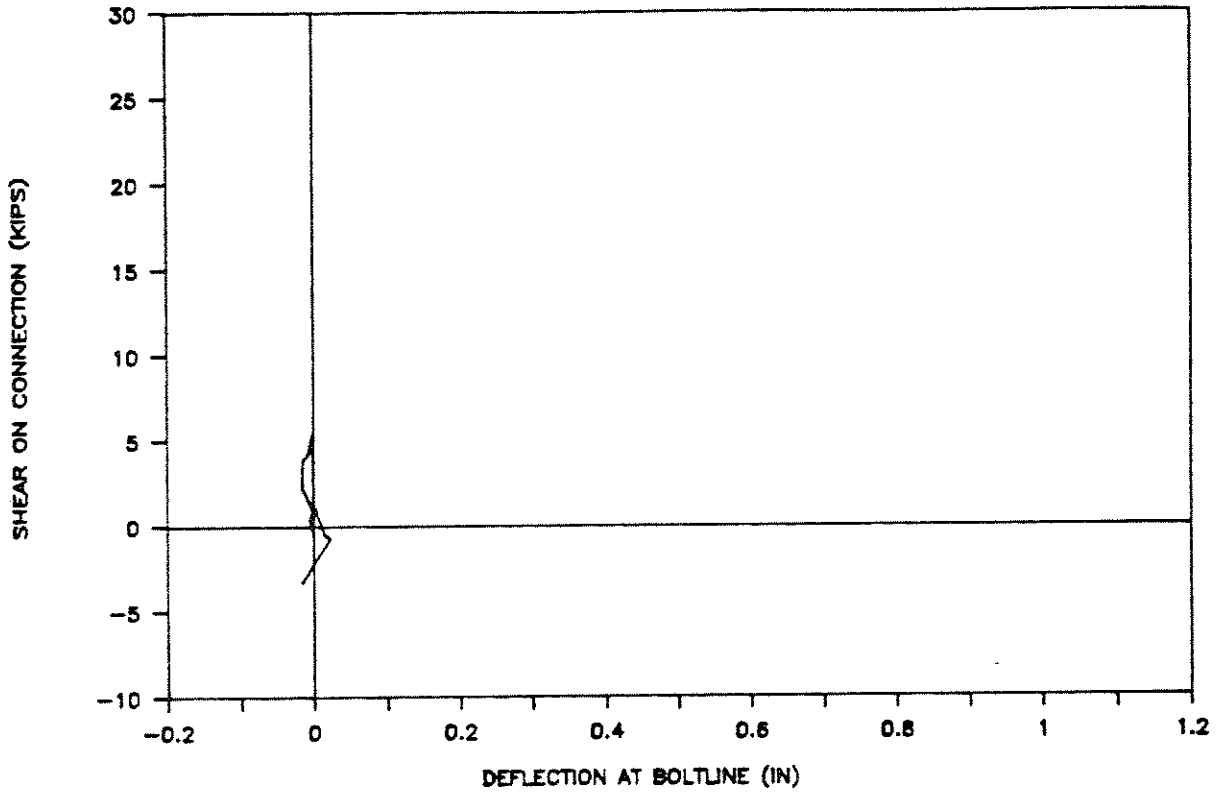

UCB TEST 5

ULTIMATE CYCLE: SHEAR VS BOLT DEFLECT.

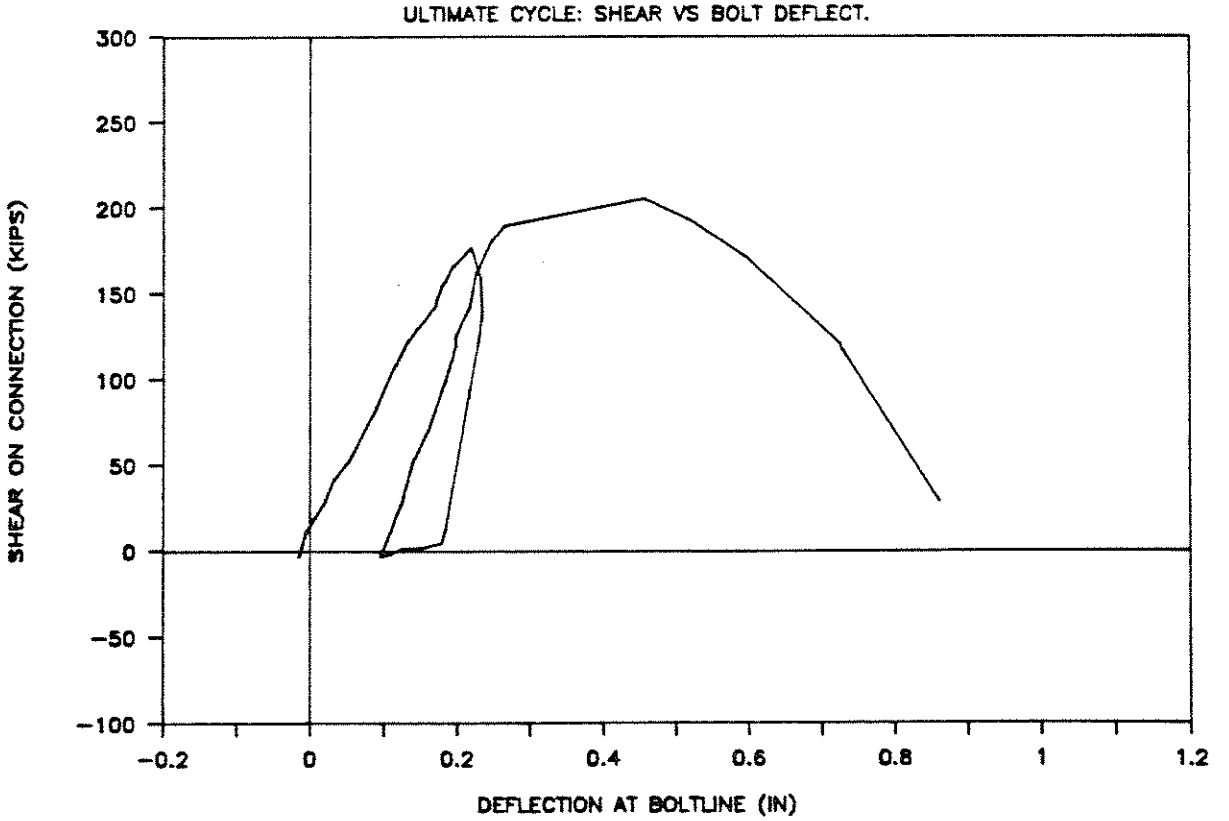

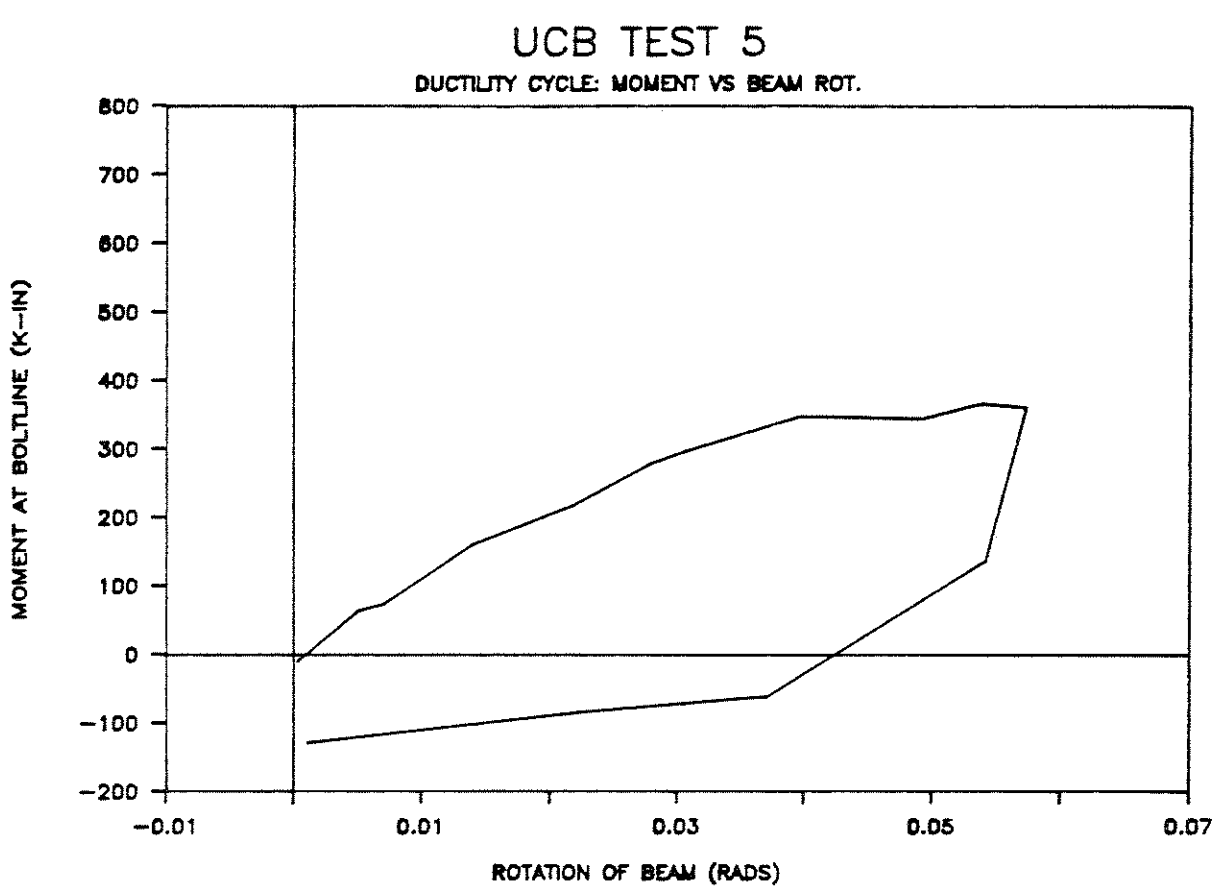
UCB TEST 5
DUCTILITY CYCLE: MOMENT VS BEAM ROT.
MOMENT AT BOLTLINE (K-IN)
800
700
600
500
400
300
200
100
0
-100
-200
-0.01
0.01
0.03
0.05
0.07
ROTATION OF BEAM (RADS)

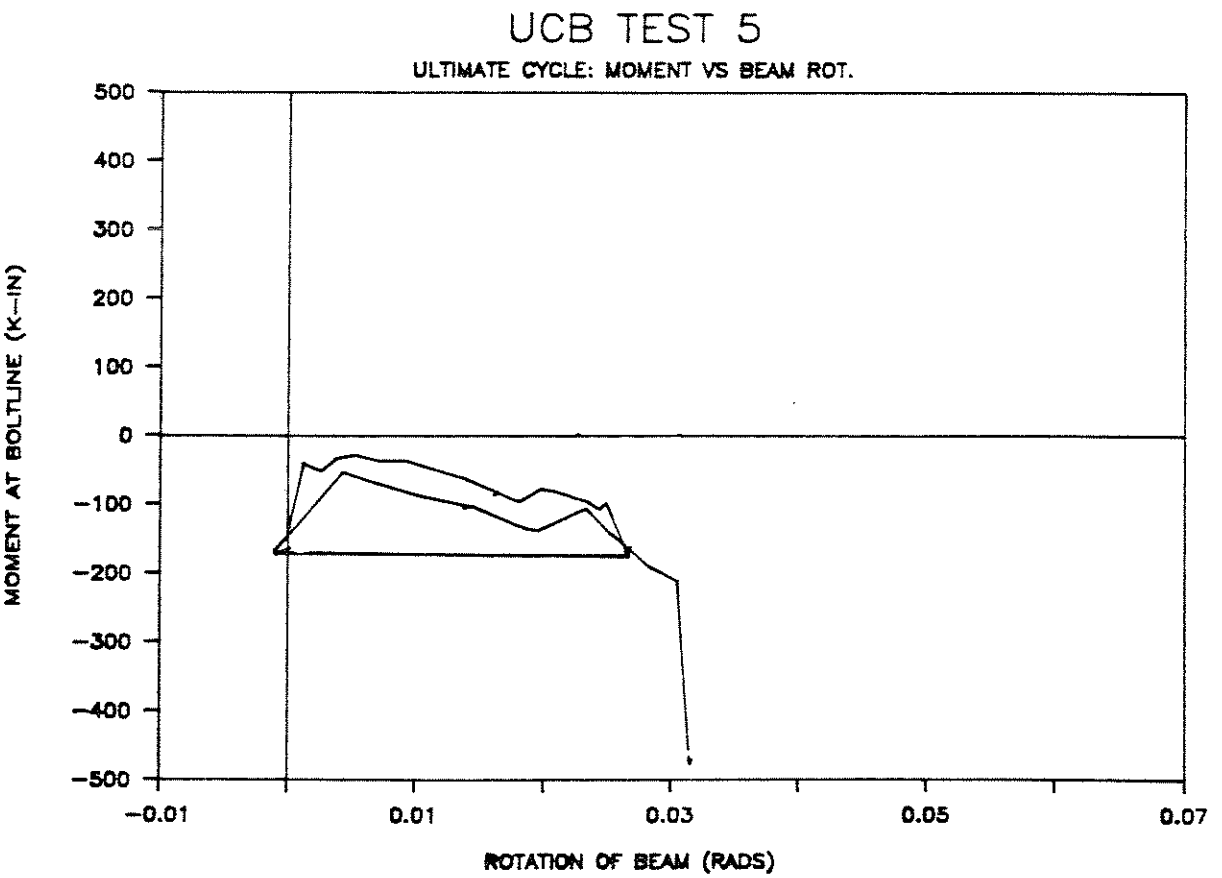
UCB TEST 5
ULTIMATE CYCLE: MOMENT VS BEAM ROT.
MOMENT AT BOLTLINE (K-IN)
500
400
300
200
100
0
-100
-200
-300
-400
-500
-0.01
0.01
0.03
0.05
0.07
ROTATION OF BEAM (RADS)

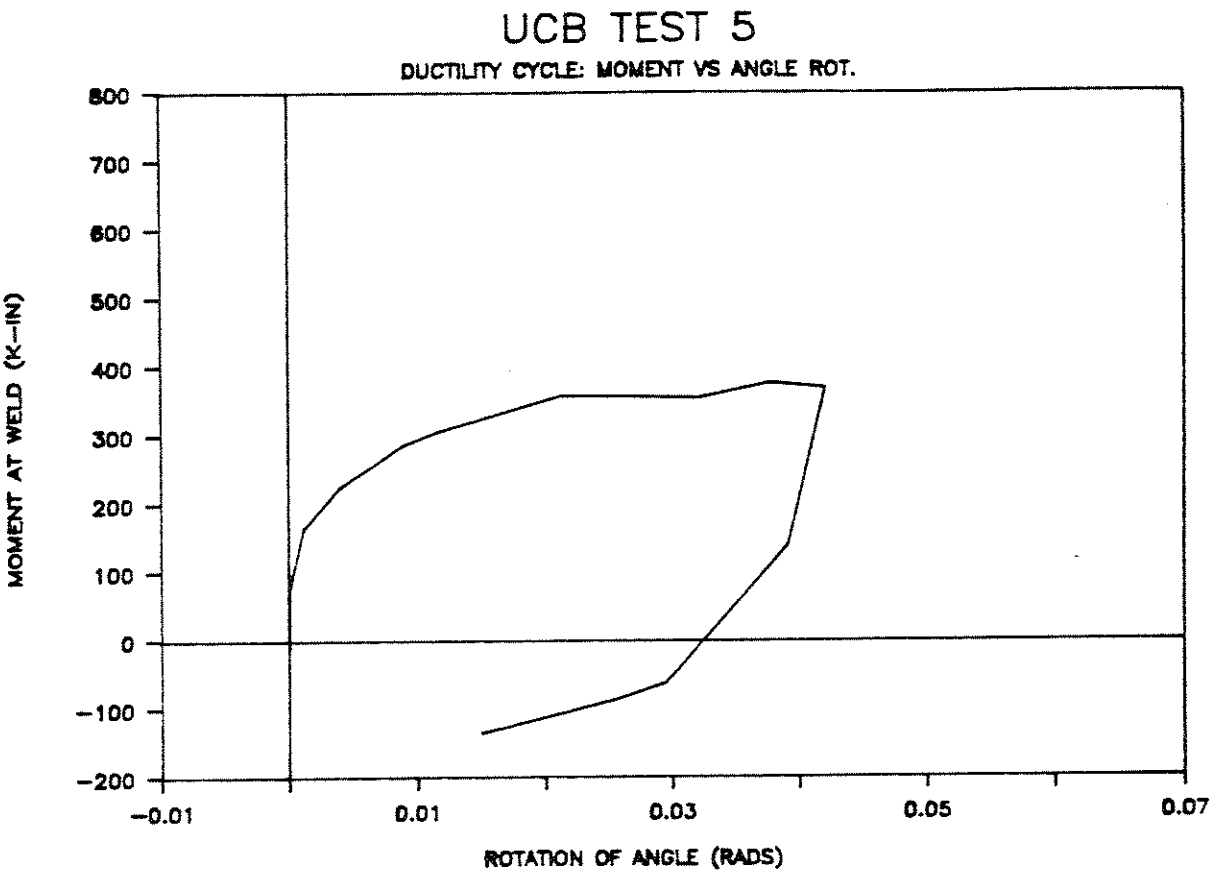
UCB TEST 5
DUCTILITY CYCLE: MOMENT VS ANGLE ROT.
MOMENT AT WELD (K-IN)
800
700
600
500
400
300
200
100
0
-100
-200
-0.01
0.01
0.03
0.05
0.07
ROTATION OF ANGLE (RADS)

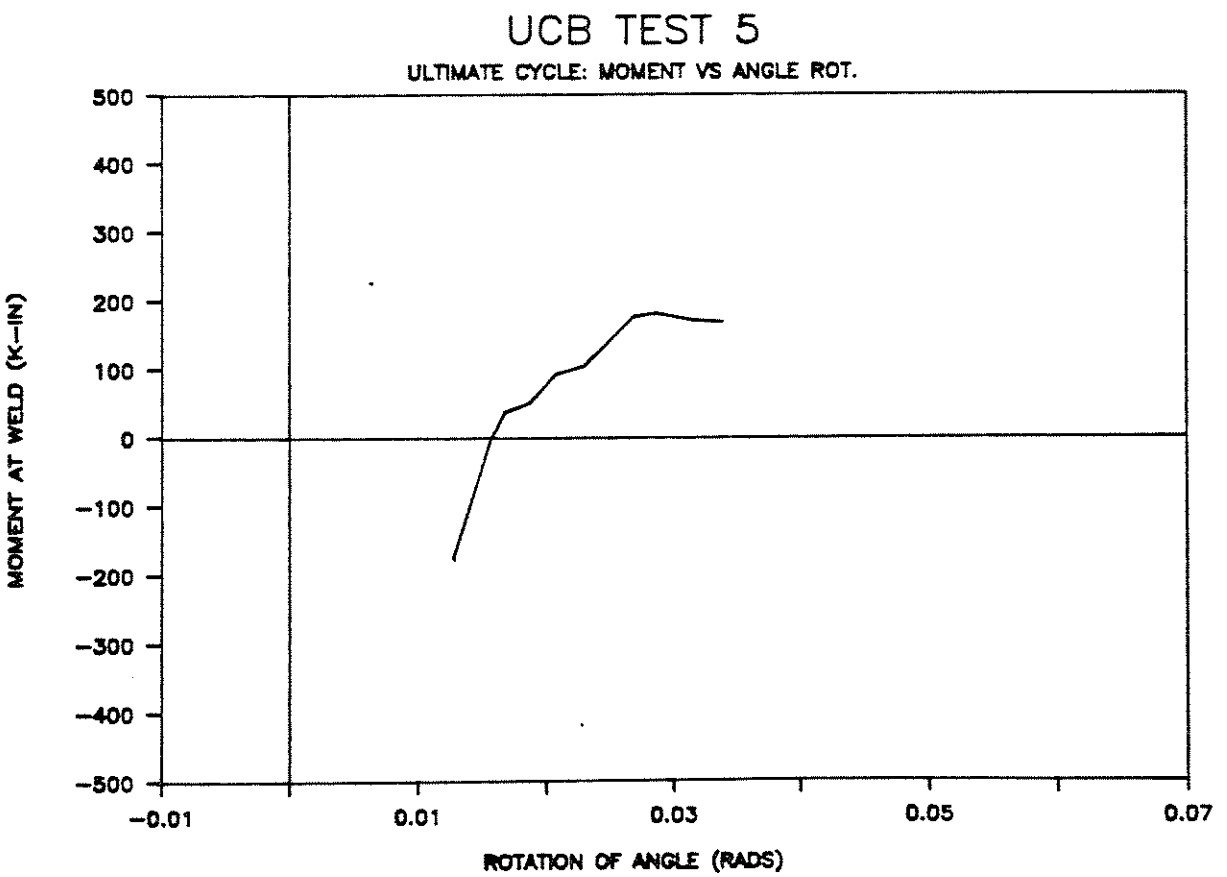
UCB TEST 5
ULTIMATE CYCLE: MOMENT VS ANGLE ROT.
MOMENT AT WELD (K-IN)
500
400
300
200
100
0
-100
-200
-300
-400
-500
-0.01
0.01
0.03
0.05
0.07
ROTATION OF ANGLE (RADS)

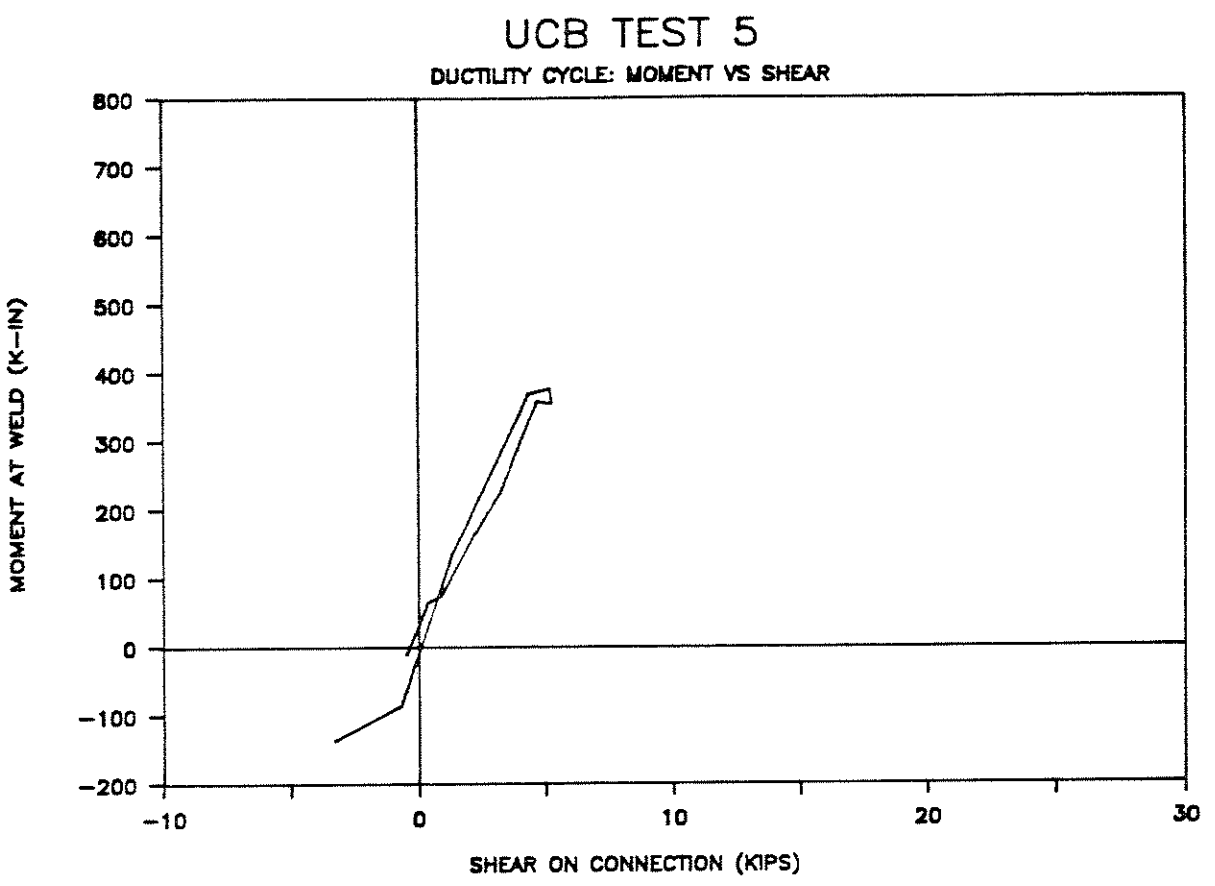
UCB TEST 5
DUCTILITY CYCLE: MOMENT VS SHEAR
MOMENT AT WELD (K-IN)
800
700
600
500
400
300
200
100
0
-100
-200
-10
0
10
20
30
SHEAR ON CONNECTION (KIPS)

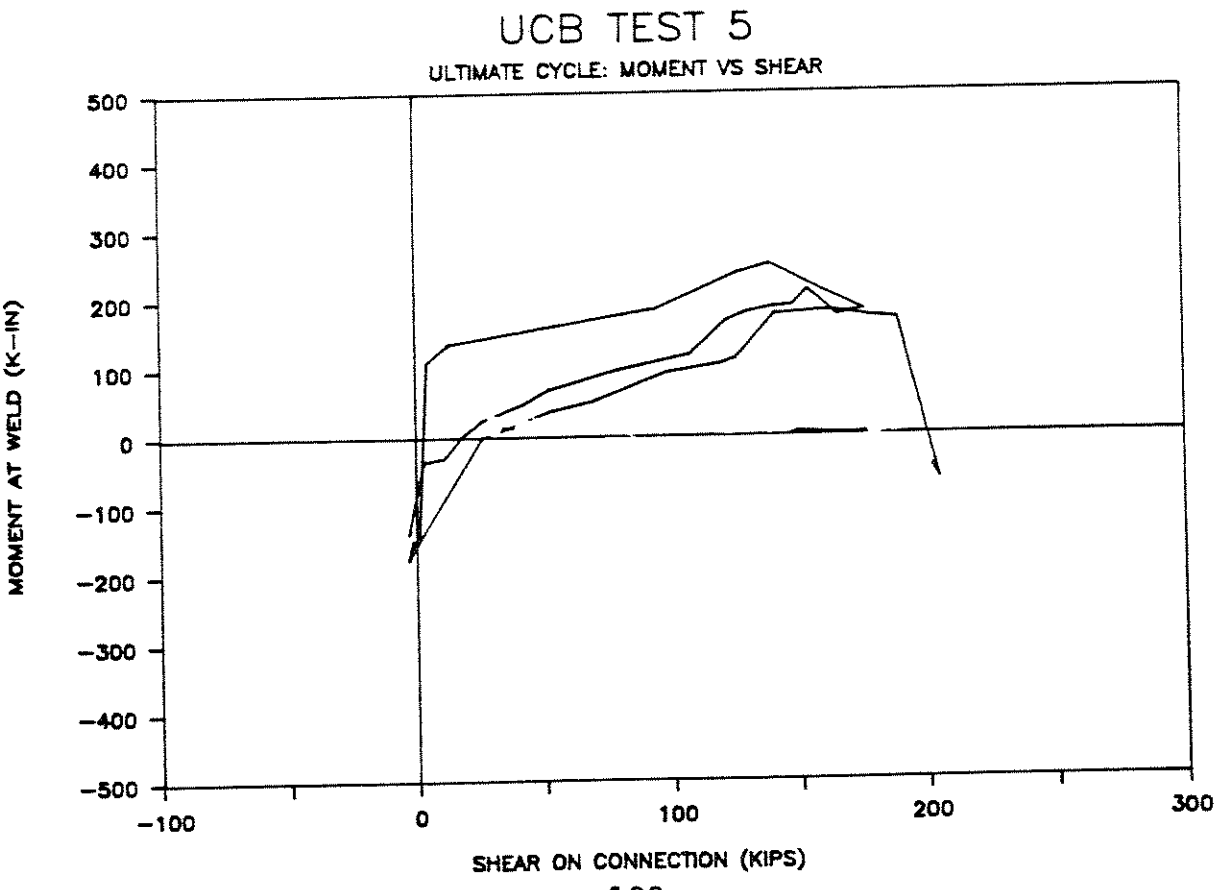
UCB TEST 5
ULTIMATE CYCLE: MOMENT VS SHEAR
MOMENT AT WELD (K-IN)
500
400
300
200
100
0
-100
-200
-300
-400
-500
-100
0
100
200
300
SHEAR ON CONNECTION (KIPS)

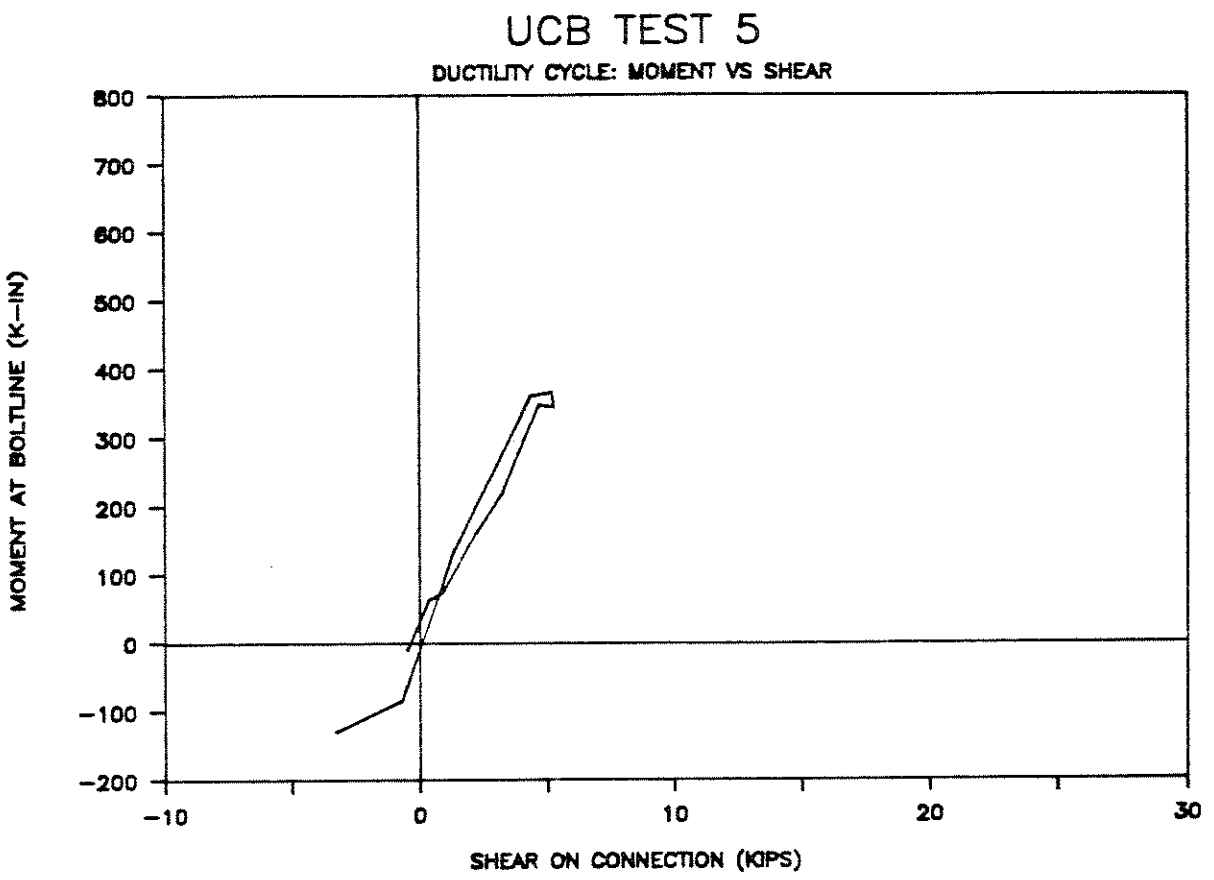
UCB TEST 5
DUCTILITY CYCLE: MOMENT VS SHEAR
MOMENT AT BOLTLINE (K-IN)
800
700
600
500
400
300
200
100
0
-100
-200
-10
0
10
20
30
SHEAR ON CONNECTION (KIPS)

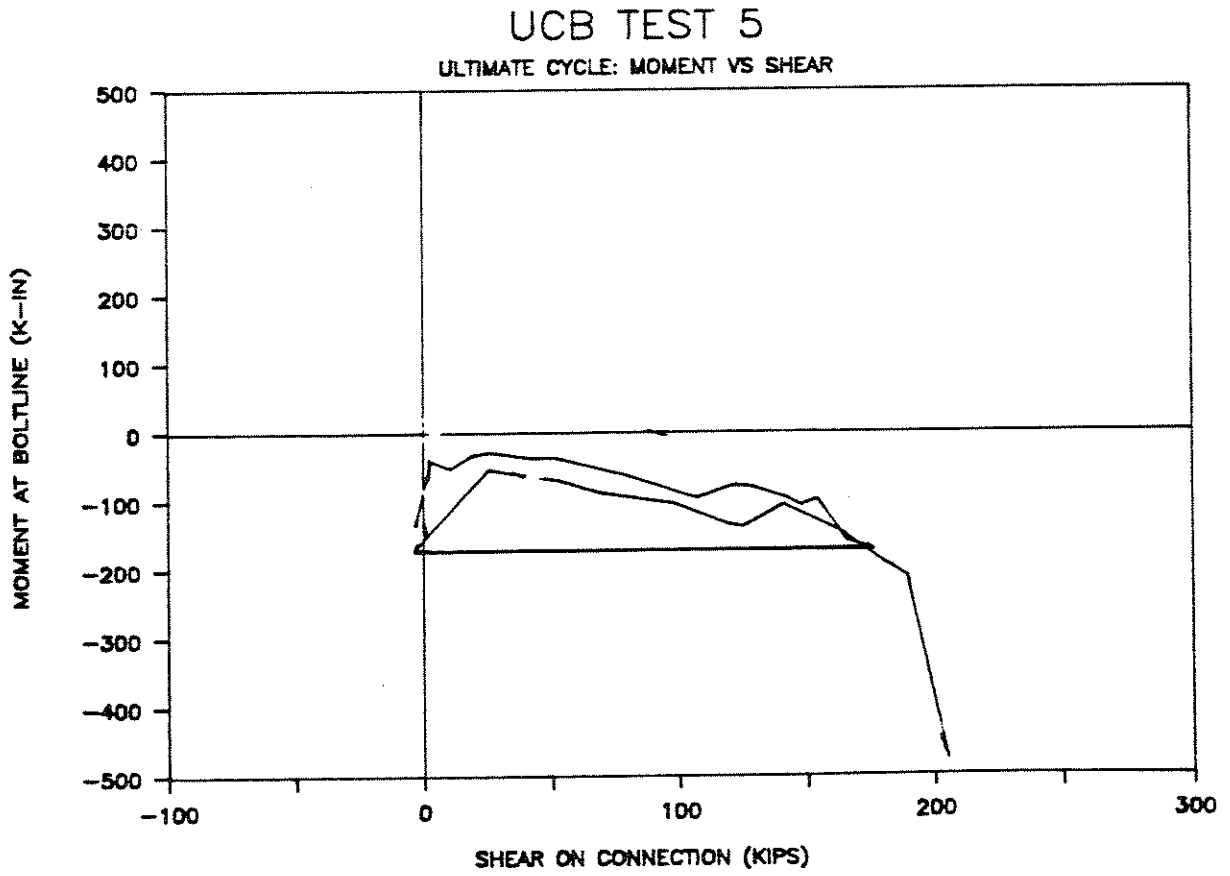
UCB TEST 5
ULTIMATE CYCLE: MOMENT VS SHEAR
MOMENT AT BOLTLINE (K-IN)
500
400
300
200
100
0
-100
-200
-300
-400
-500
-100
0
100
200
300
SHEAR ON CONNECTION (KIPS)

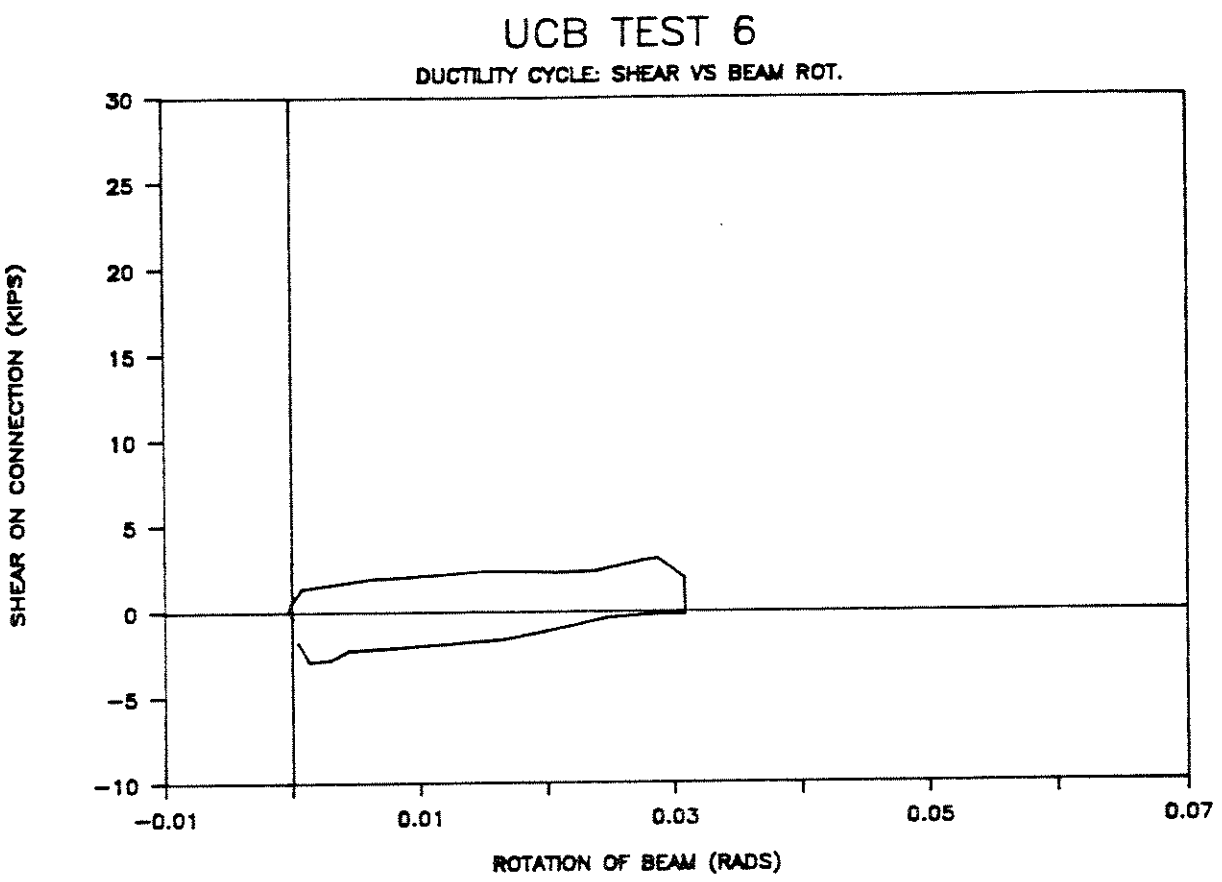
UCB TEST 6
DUCTILITY CYCLE: SHEAR VS BEAM ROT.
SHEAR ON CONNECTION (KIPS)
30
25
20
15
10
5
0
-5
-10
-0.01
0.01
0.03
0.05
0.07
ROTATION OF BEAM (RADS)

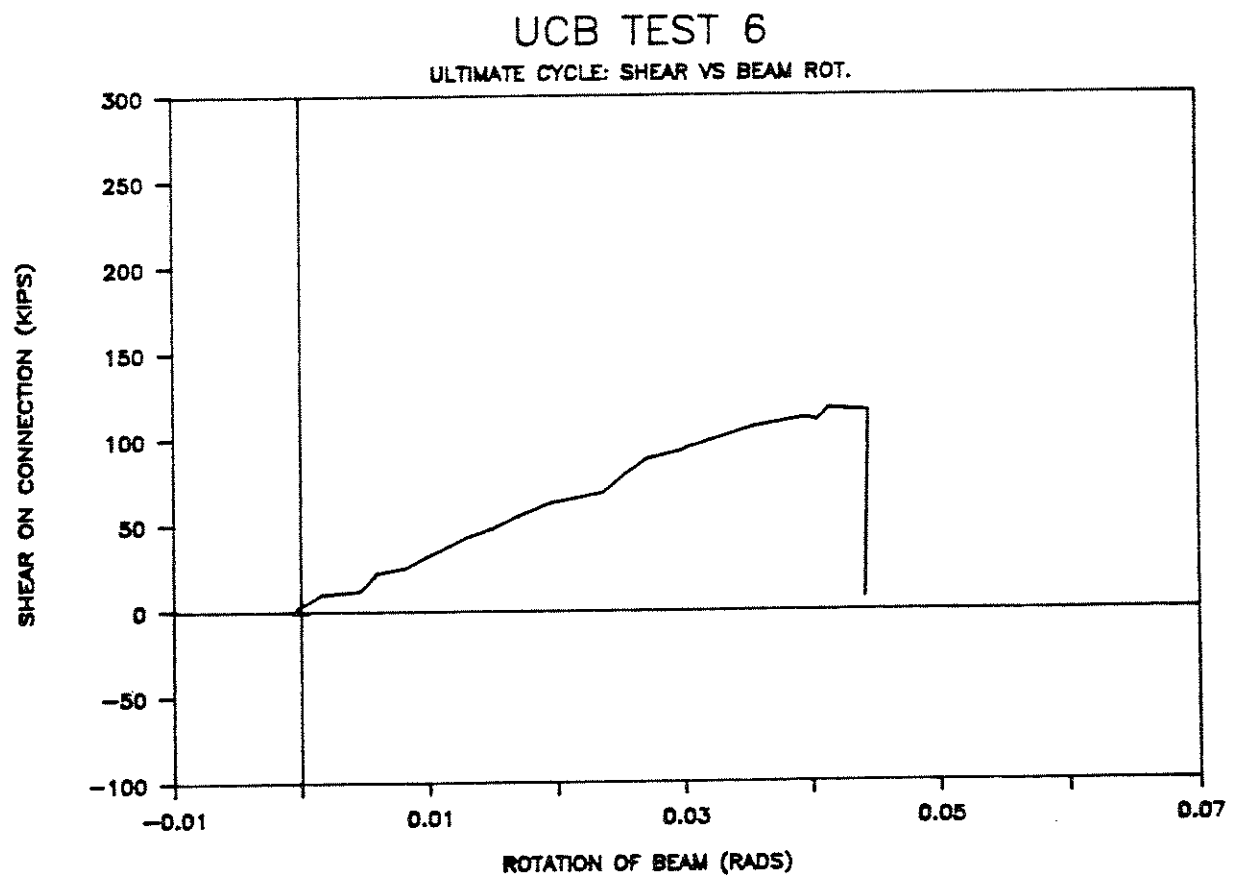
UCB TEST 6
ULTIMATE CYCLE: SHEAR VS BEAM ROT.
SHEAR ON CONNECTION (KIPS)
300
250
200
150
100
50
0
-50
-100
-0.01
0.01
0.03
0.05
0.07
ROTATION OF BEAM (RADS)

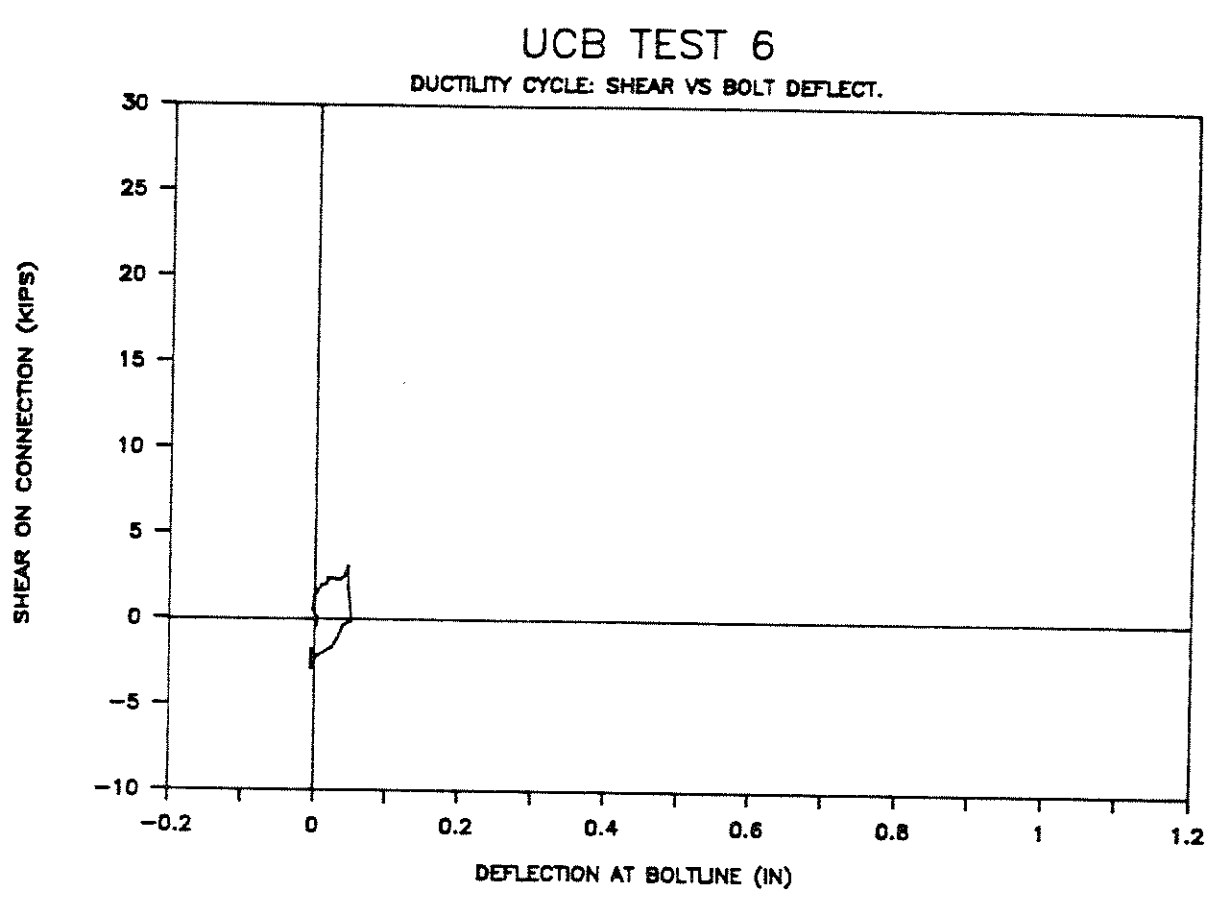
UCB TEST 6
DUCTILITY CYCLE: SHEAR VS BOLT DEFLECT.
SHEAR ON CONNECTION (KIPS)
30
25
20
15
10
5
0
−5
−10
−0.2
0
0.2
0.4
0.6
0.8
1
1.2
DEFLECTION AT BOLTLINE (IN)

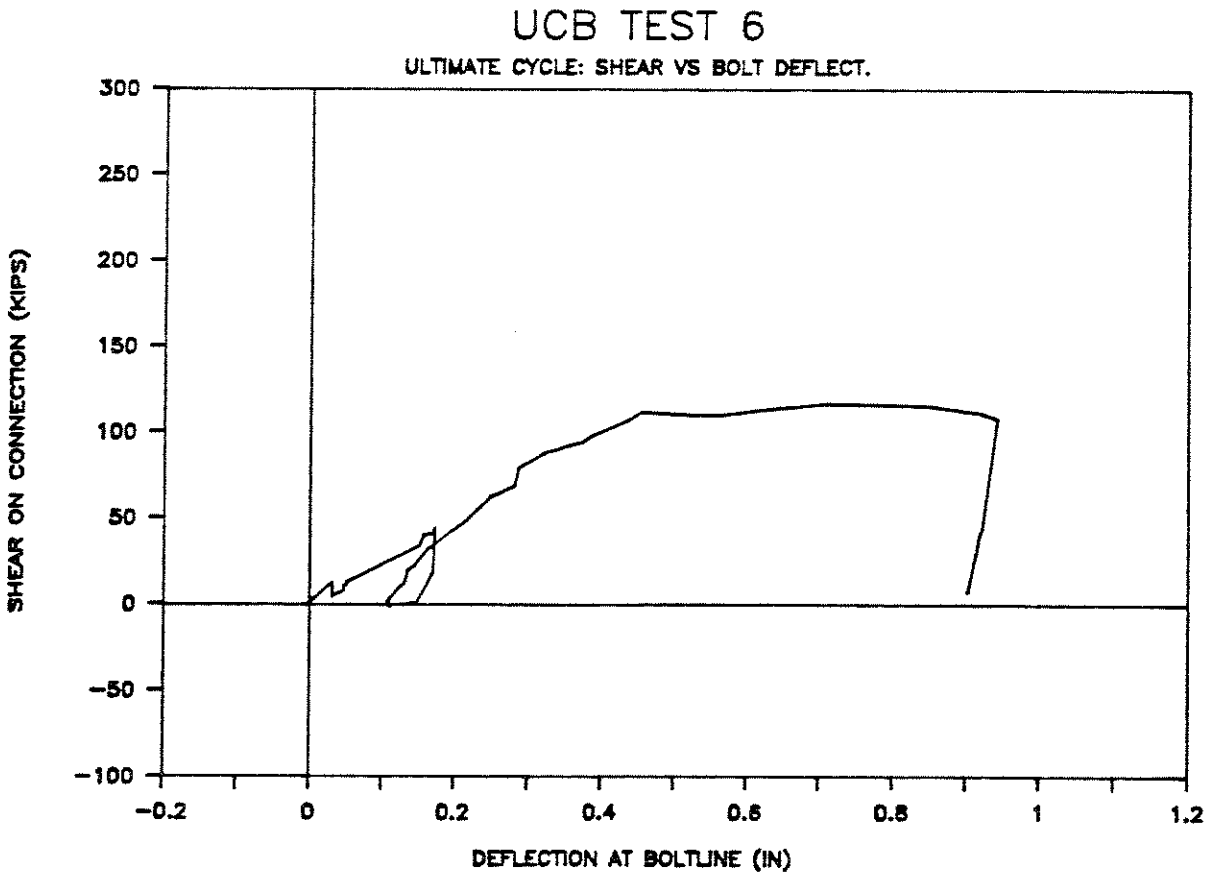
UCB TEST 6
ULTIMATE CYCLE: SHEAR VS BOLT DEFLECT.
SHEAR ON CONNECTION (KIPS)
300
250
200
150
100
50
0
−50
−100
−0.2
0
0.2
0.4
0.6
0.8
1
1.2
DEFLECTION AT BOLTLINE (IN)

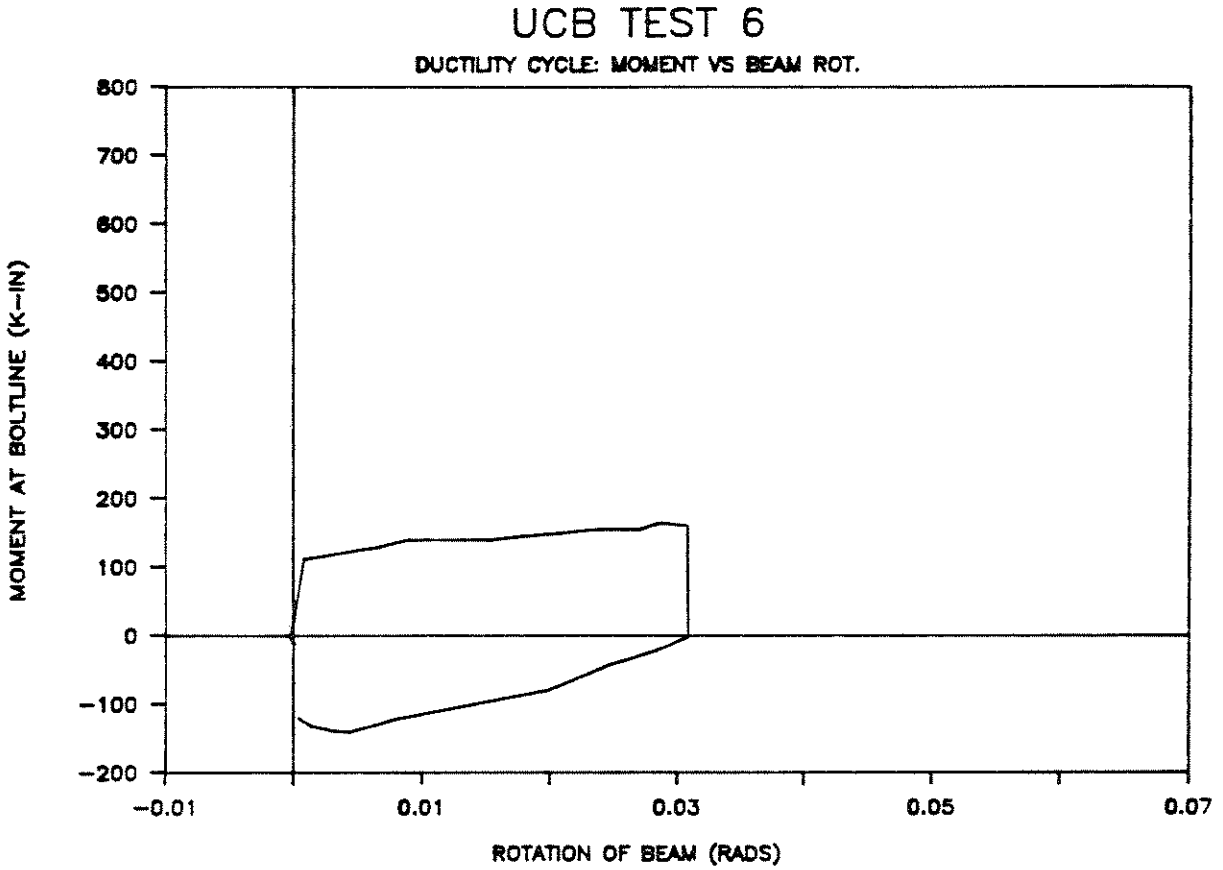
UCB TEST 6
DUCTILITY CYCLE: MOMENT VS BEAM ROT.
MOMENT AT BOLTLINE (K-IN)
800
700
600
500
400
300
200
100
0
-100
-200
-0.01
0.01
0.03
0.05
0.07
ROTATION OF BEAM (RADS)

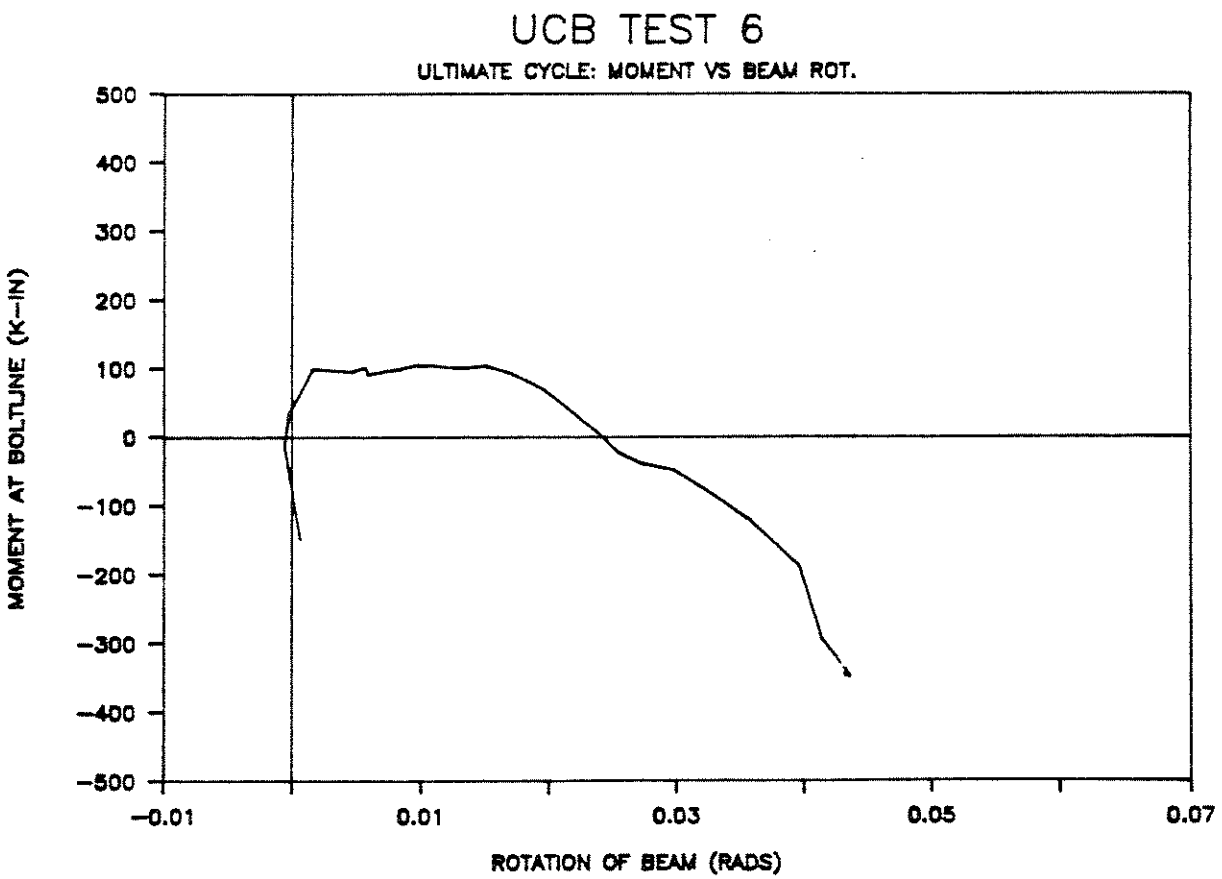
UCB TEST 6
ULTIMATE CYCLE: MOMENT VS BEAM ROT.
MOMENT AT BOLTLINE (K-IN)
500
400
300
200
100
0
-100
-200
-300
-400
-500
-0.01
0.01
0.03
0.05
0.07
ROTATION OF BEAM (RADS)

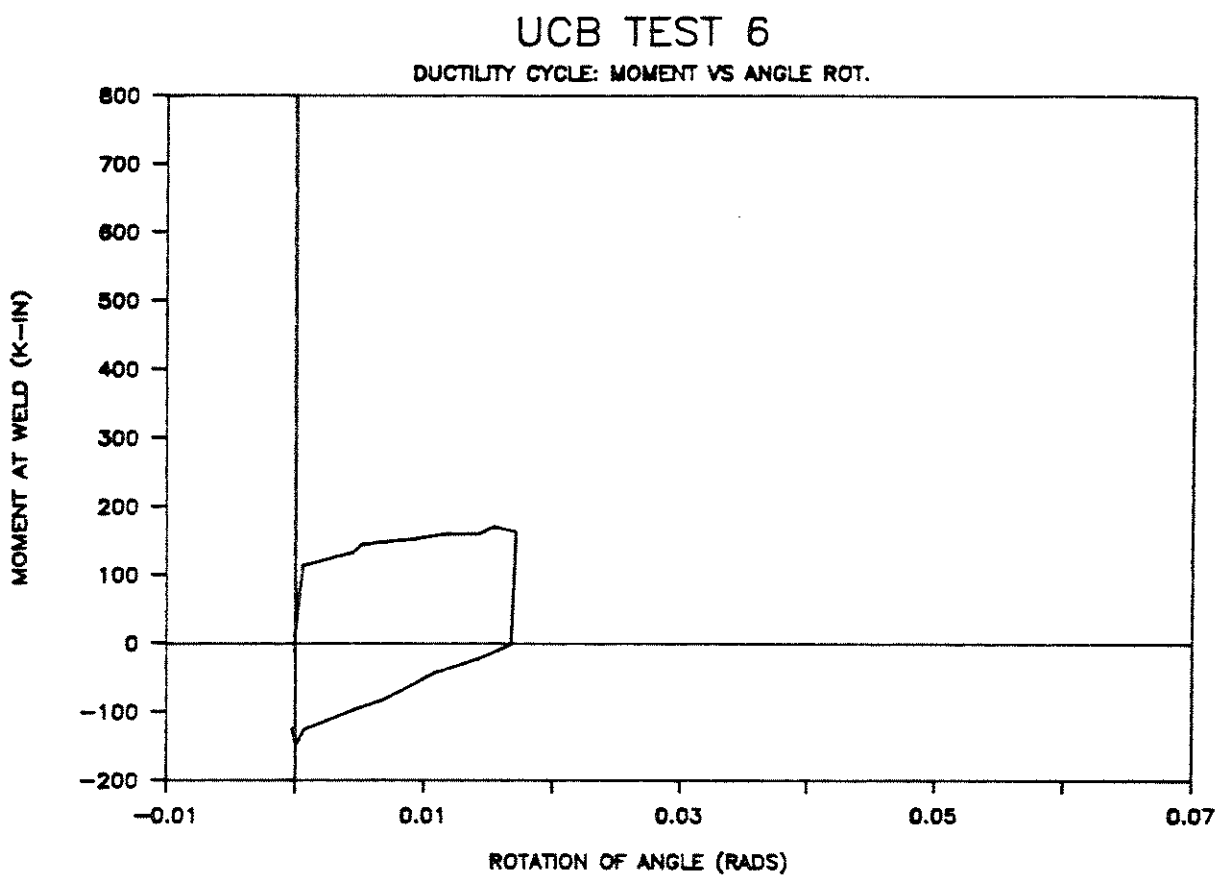
UCB TEST 6
DUCTILITY CYCLE: MOMENT VS ANGLE ROT.
MOMENT AT WELD (K-IN)
800
700
600
500
400
300
200
100
0
-100
-200
-0.01
0.01
0.03
0.05
0.07
ROTATION OF ANGLE (RADS)

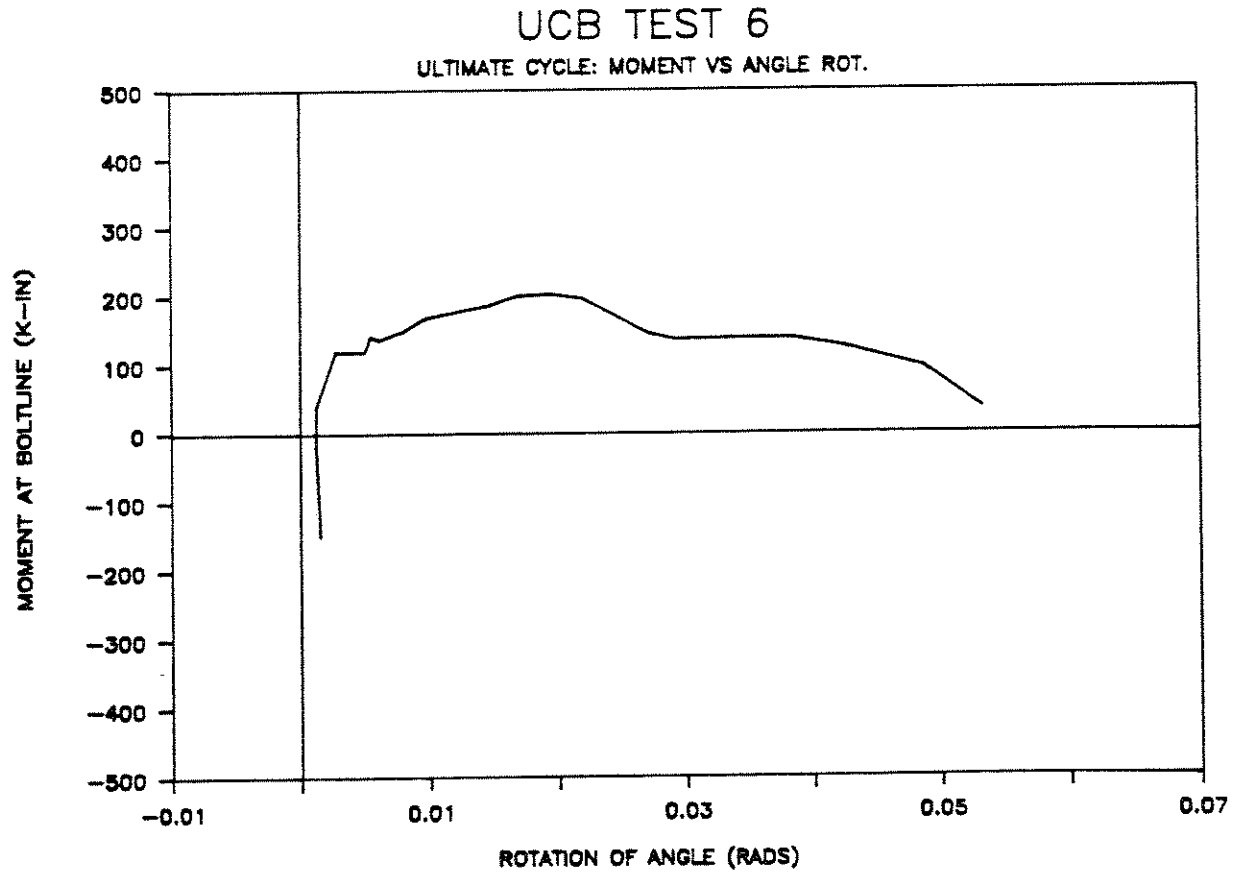
UCB TEST 6
ULTIMATE CYCLE: MOMENT VS ANGLE ROT.
MOMENT AT BOLTLINE (K-IN)
500
400
300
200
100
0
-100
-200
-300
-400
-500
-0.01
0.01
0.03
0.05
0.07
ROTATION OF ANGLE (RADS)

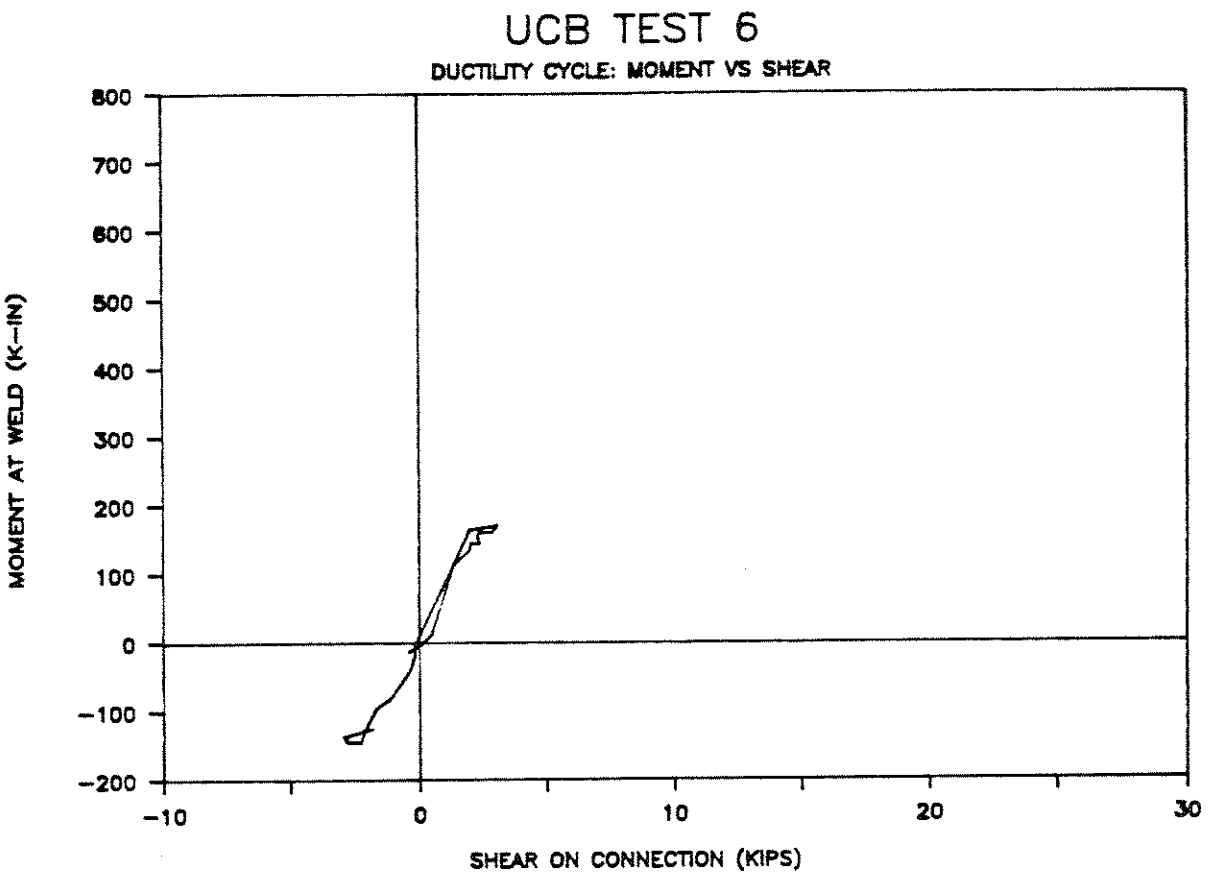
UCB TEST 6
DUCTILITY CYCLE: MOMENT VS SHEAR
MOMENT AT WELD (K-IN)
800
700
600
500
400
300
200
100
0
-100
-200
-10
0
10
20
30
SHEAR ON CONNECTION (KIPS)

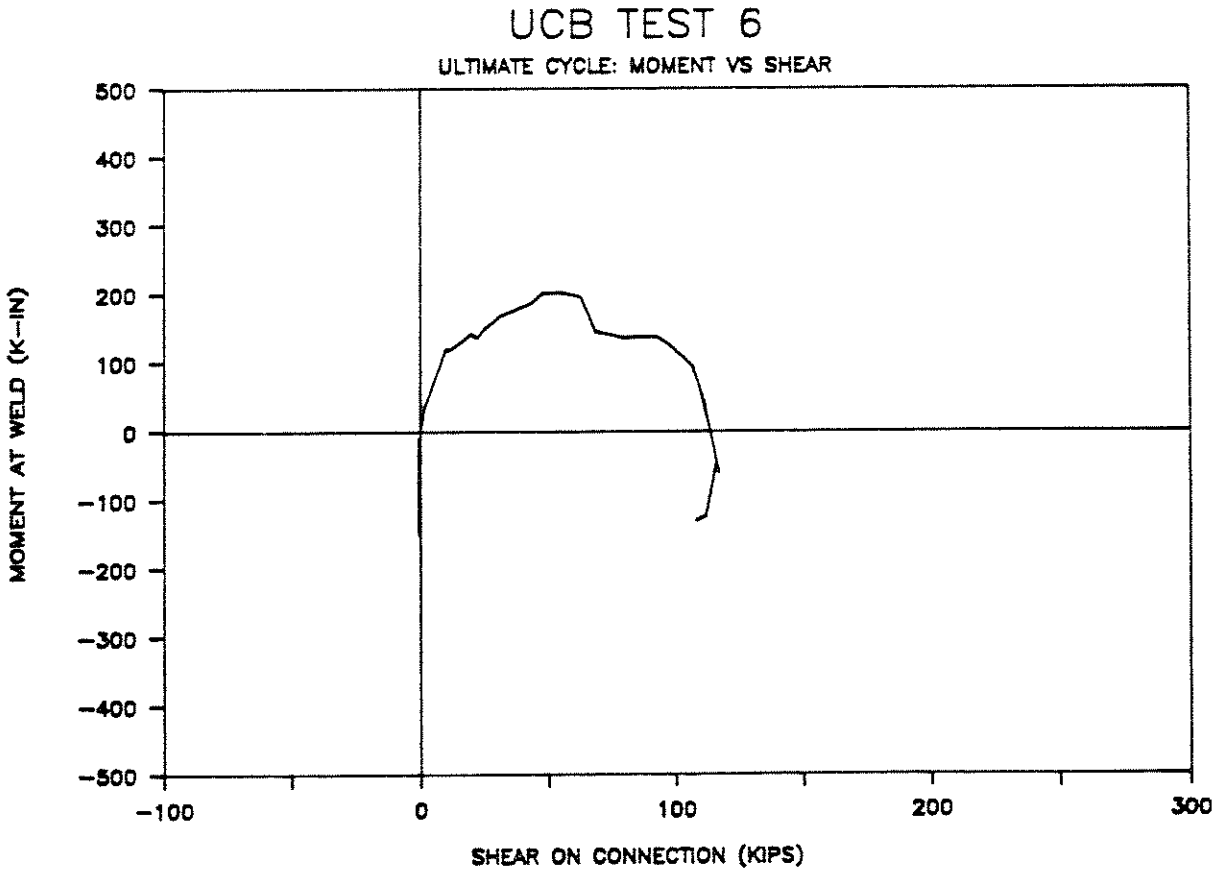
UCB TEST 6
ULTIMATE CYCLE: MOMENT VS SHEAR
MOMENT AT WELD (K-IN)
500
400
300
200
100
0
-100
-200
-300
-400
-500
-100
0
100
200
300
SHEAR ON CONNECTION (KIPS)

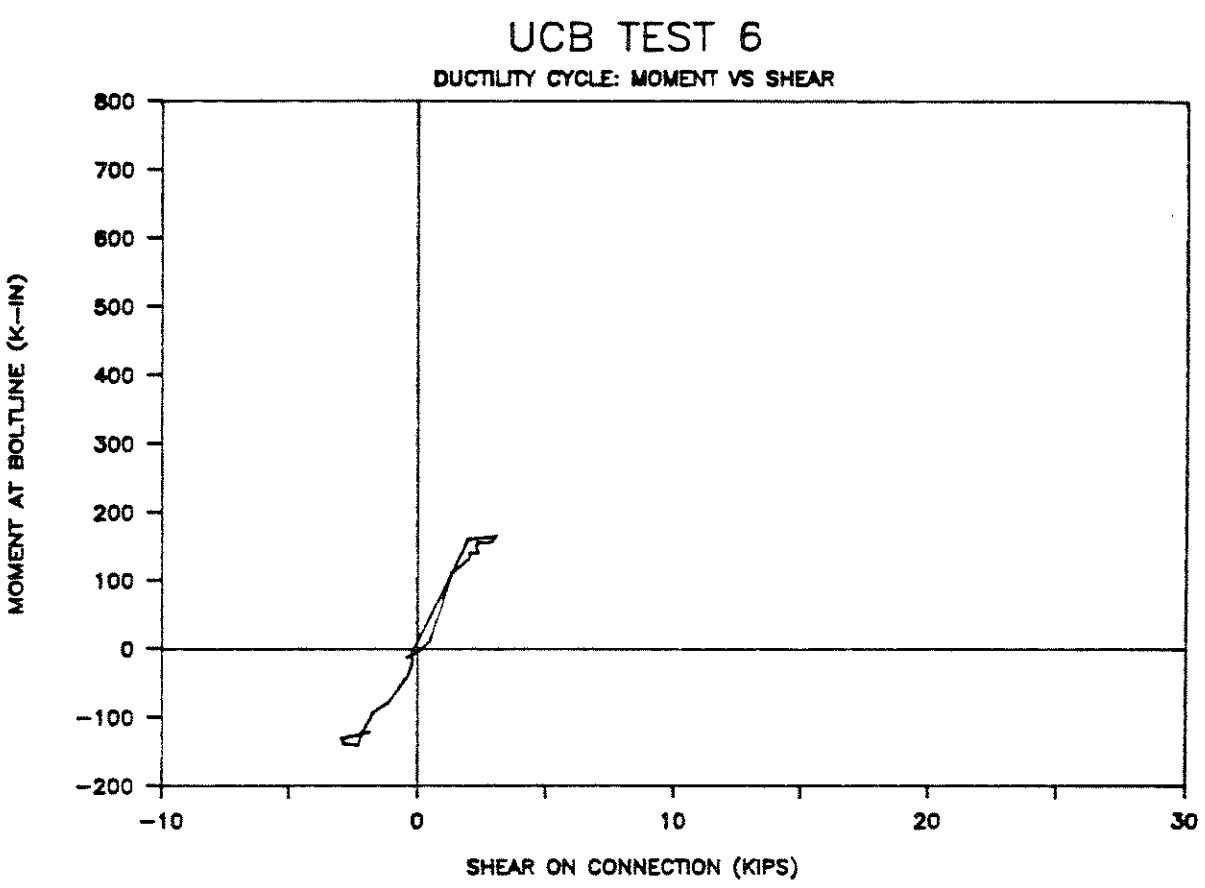
UCB TEST 6
DUCTILITY CYCLE: MOMENT VS SHEAR
MOMENT AT BOLTLINE (K-IN)
800
700
600
500
400
300
200
100
0
-100
-200
-10
0
10
20
30
SHEAR ON CONNECTION (KIPS)

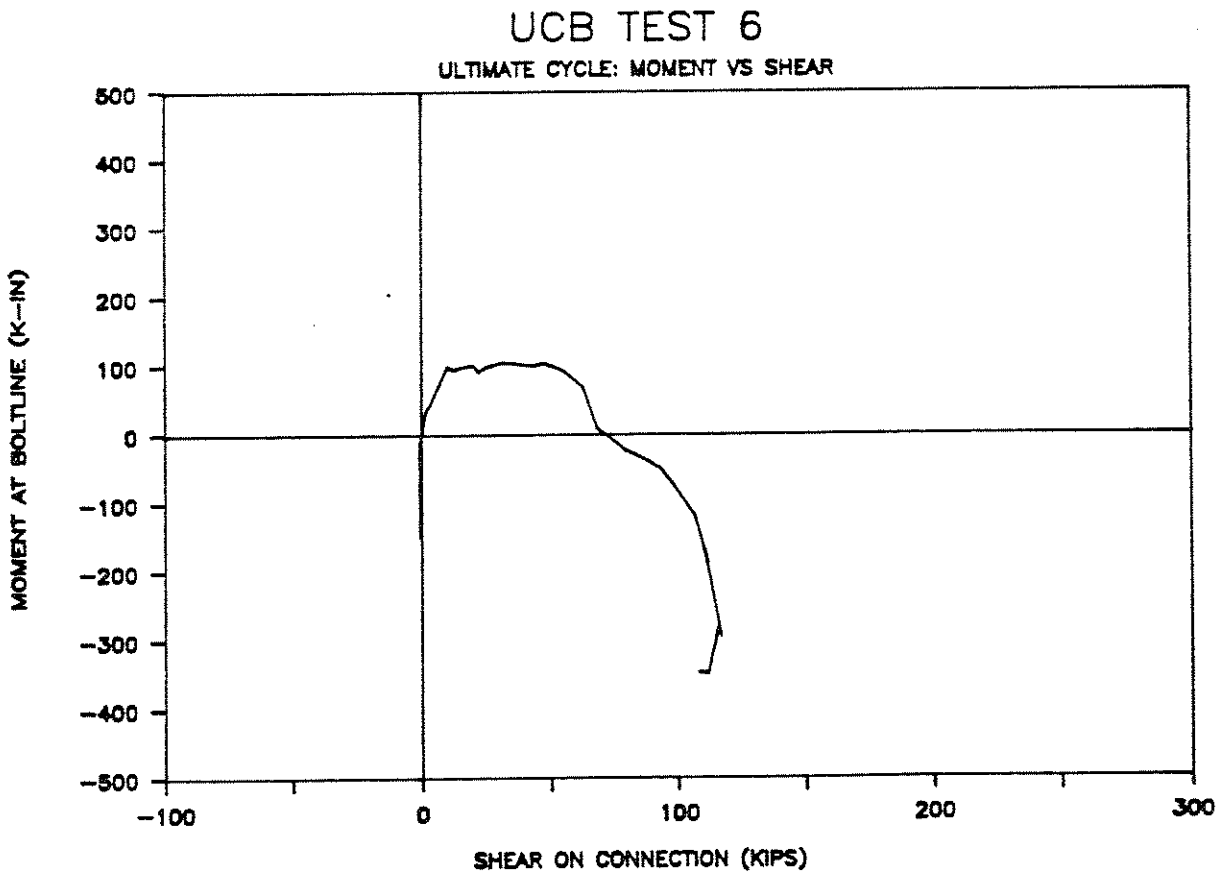
UCB TEST 6
ULTIMATE CYCLE: MOMENT VS SHEAR
MOMENT AT BOLTLINE (K-IN)
500
400
300
200
100
0
-100
-200
-300
-400
-500
-100
0
100
200
300
SHEAR ON CONNECTION (KIPS)

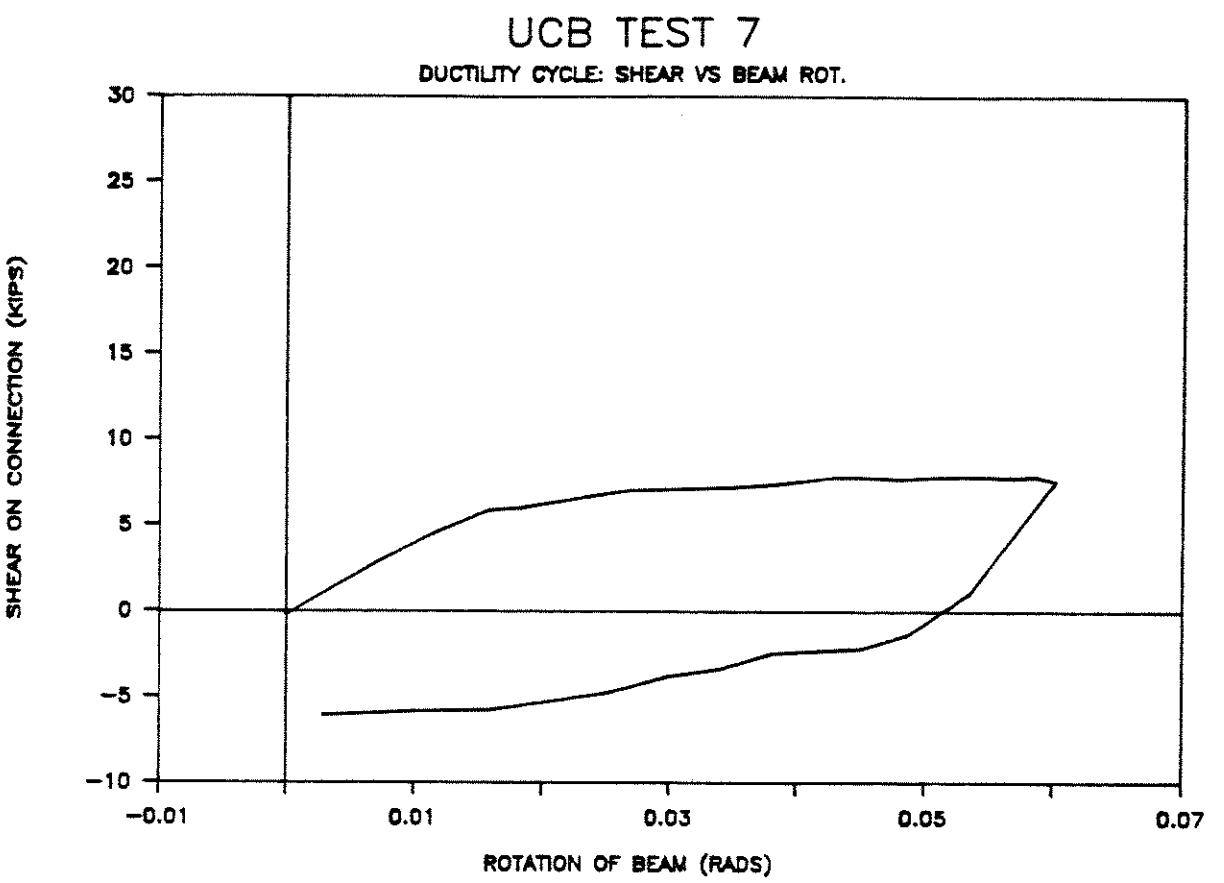
UCB TEST 7
DUCTILITY CYCLE: SHEAR VS BEAM ROT.
SHEAR ON CONNECTION (KIPS)
30
25
20
15
10
5
0
-5
-10
-0.01
0.01
0.03
0.05
0.07
ROTATION OF BEAM (RADS)

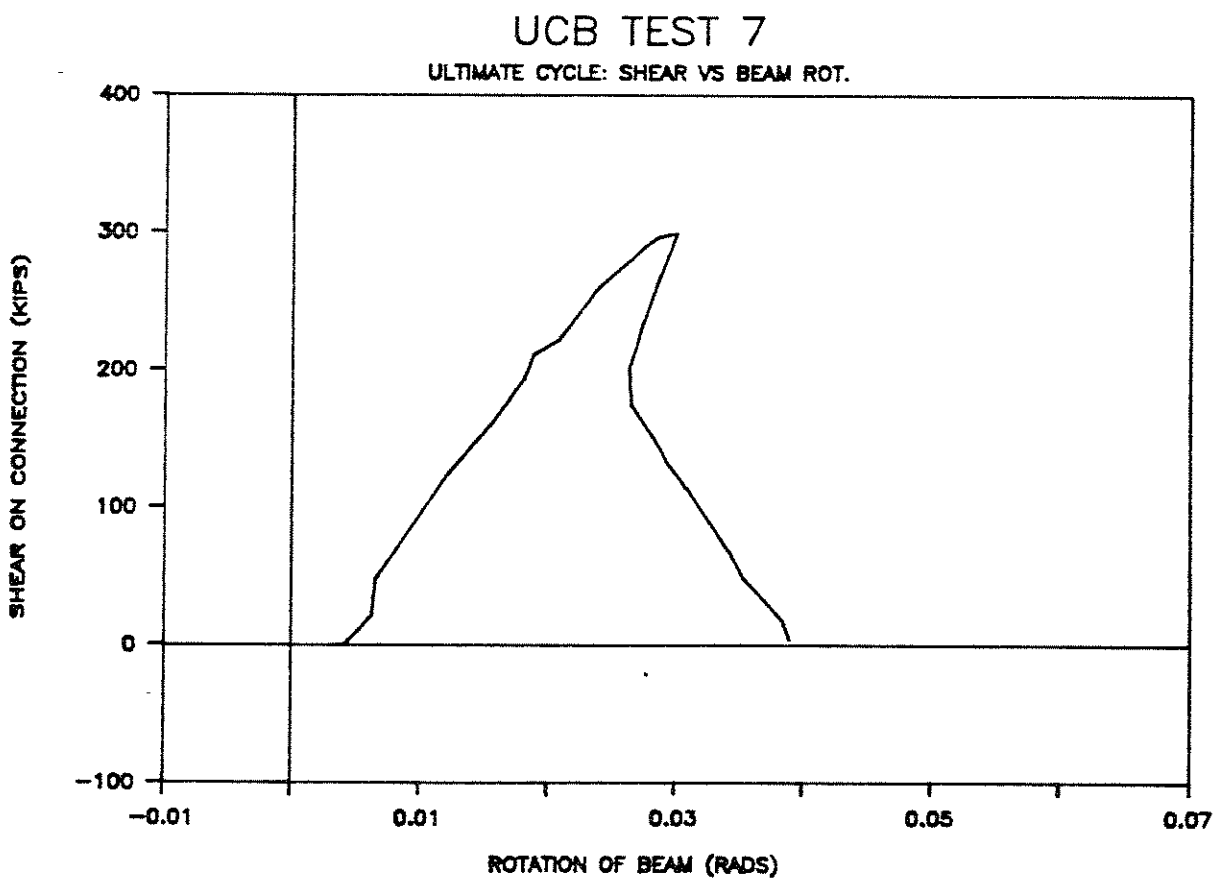
UCB TEST 7
ULTIMATE CYCLE: SHEAR VS BEAM ROT.
SHEAR ON CONNECTION (KIPS)
400
300
200
100
0
-100
-0.01
0.01
0.03
0.05
0.07
ROTATION OF BEAM (RADS)

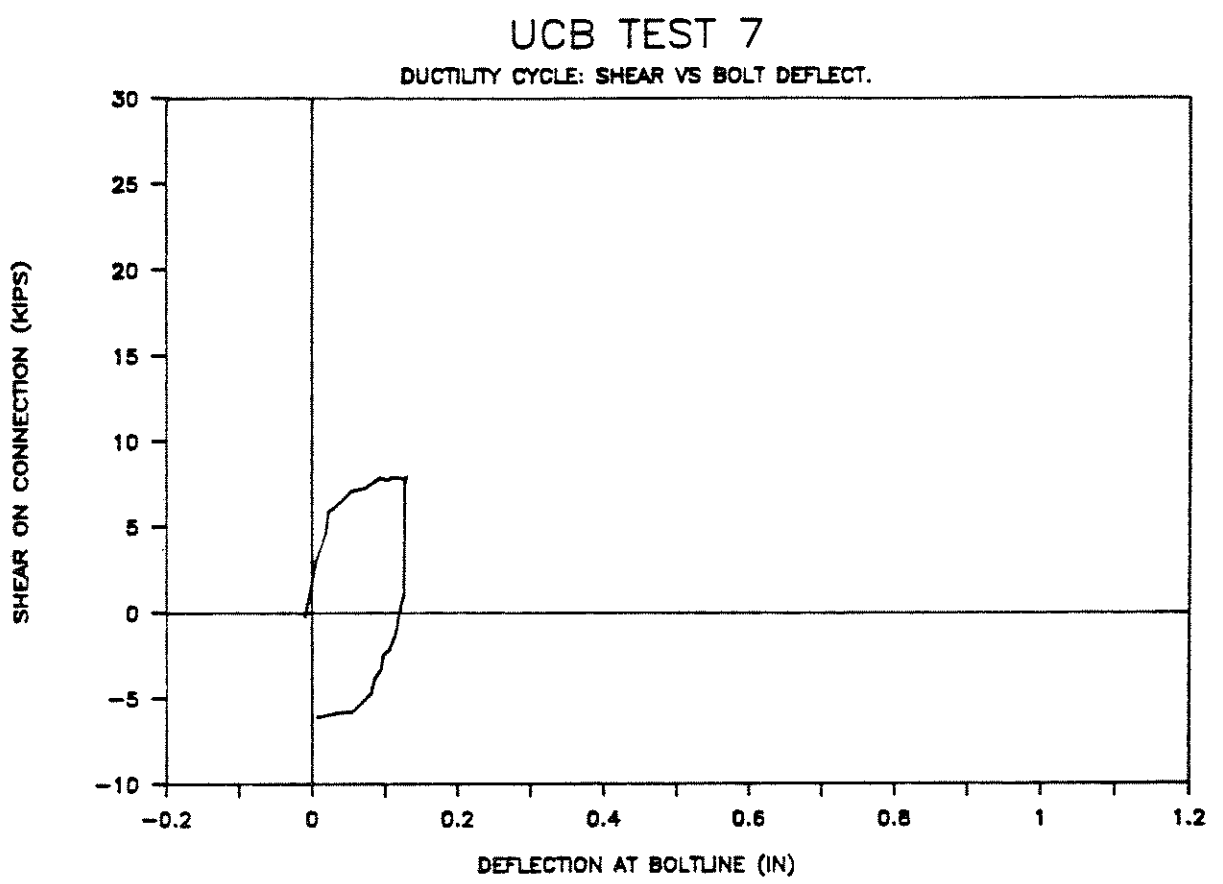
UCB TEST 7
DUCTILITY CYCLE: SHEAR VS BOLT DEFLECT.
SHEAR ON CONNECTION (KIPS)
30
25
20
15
10
5
0
−5
−10
−0.2
0
0.2
0.4
0.6
0.8
1
1.2
DEFLECTION AT BOLTLINE (IN)

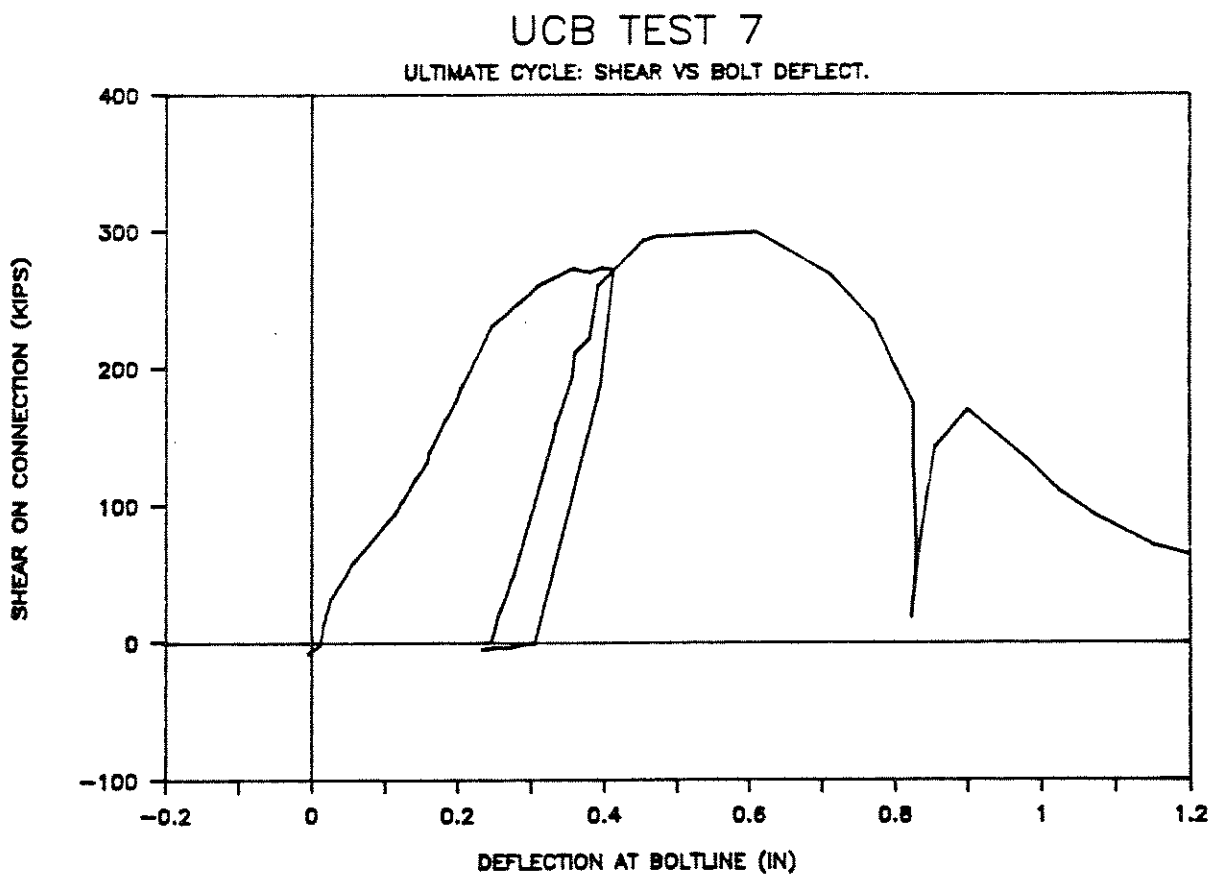
UCB TEST 7
ULTIMATE CYCLE: SHEAR VS BOLT DEFLECT.
SHEAR ON CONNECTION (KIPS)
400
300
200
100
0
−100
−0.2
0
0.2
0.4
0.6
0.8
1
1.2
DEFLECTION AT BOLTLINE (IN)

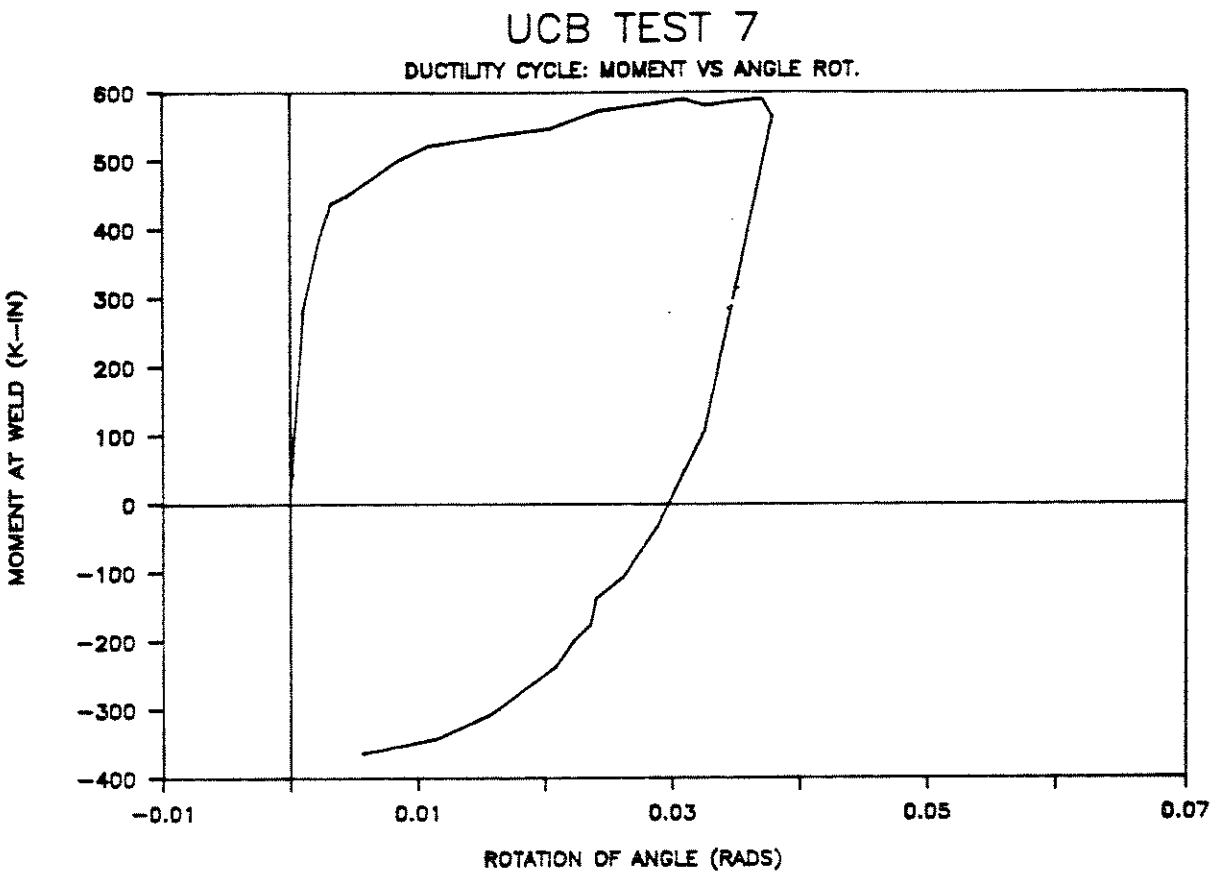
UCB TEST 7
DUCTILITY CYCLE: MOMENT VS ANGLE ROT.
MOMENT AT WELD (K-IN)
600
500
400
300
200
100
0
-100
-200
-300
-400
-0.01
0.01
0.03
0.05
0.07
ROTATION OF ANGLE (RADS)

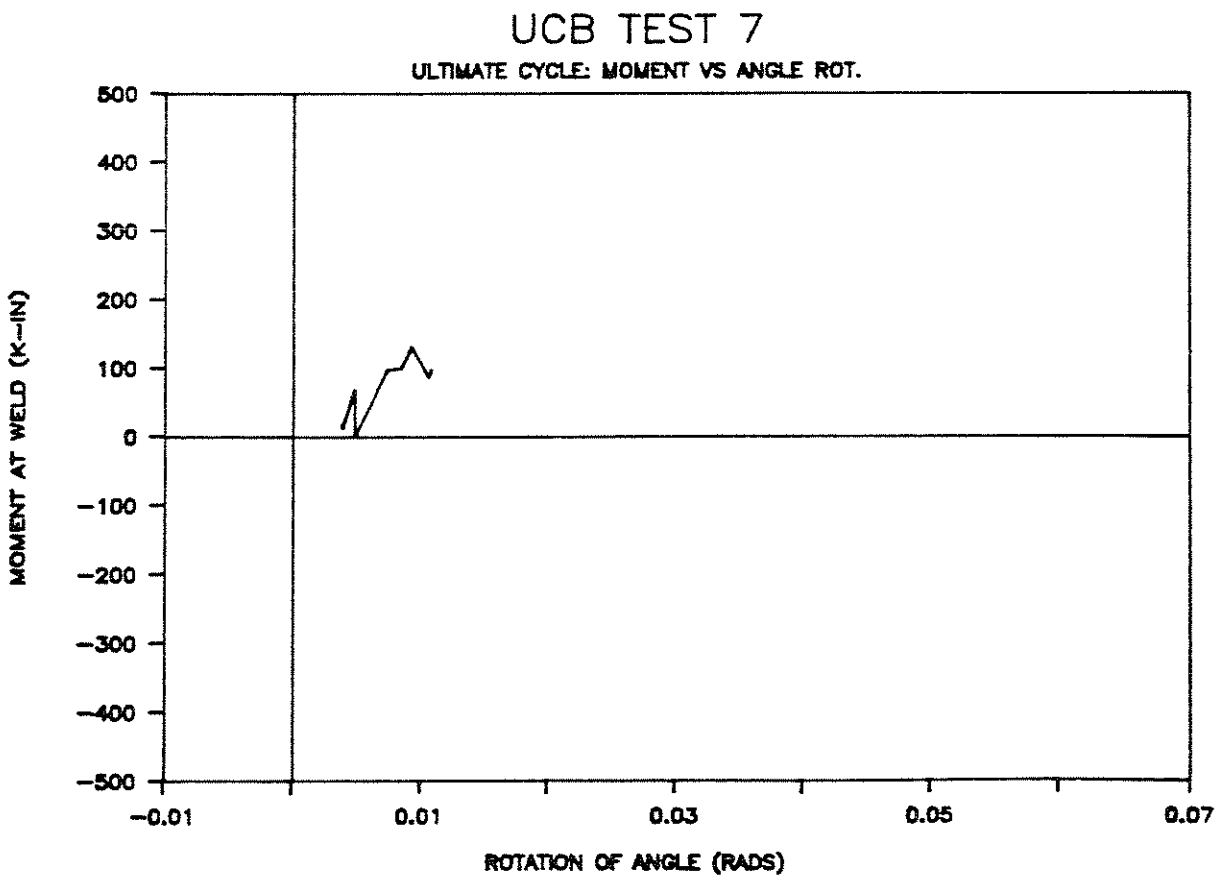
UCB TEST 7
ULTIMATE CYCLE: MOMENT VS ANGLE ROT.
MOMENT AT WELD (K-IN)
500
400
300
200
100
0
-100
-200
-300
-400
-500
-0.01
0.01
0.03
0.05
0.07
ROTATION OF ANGLE (RADS)

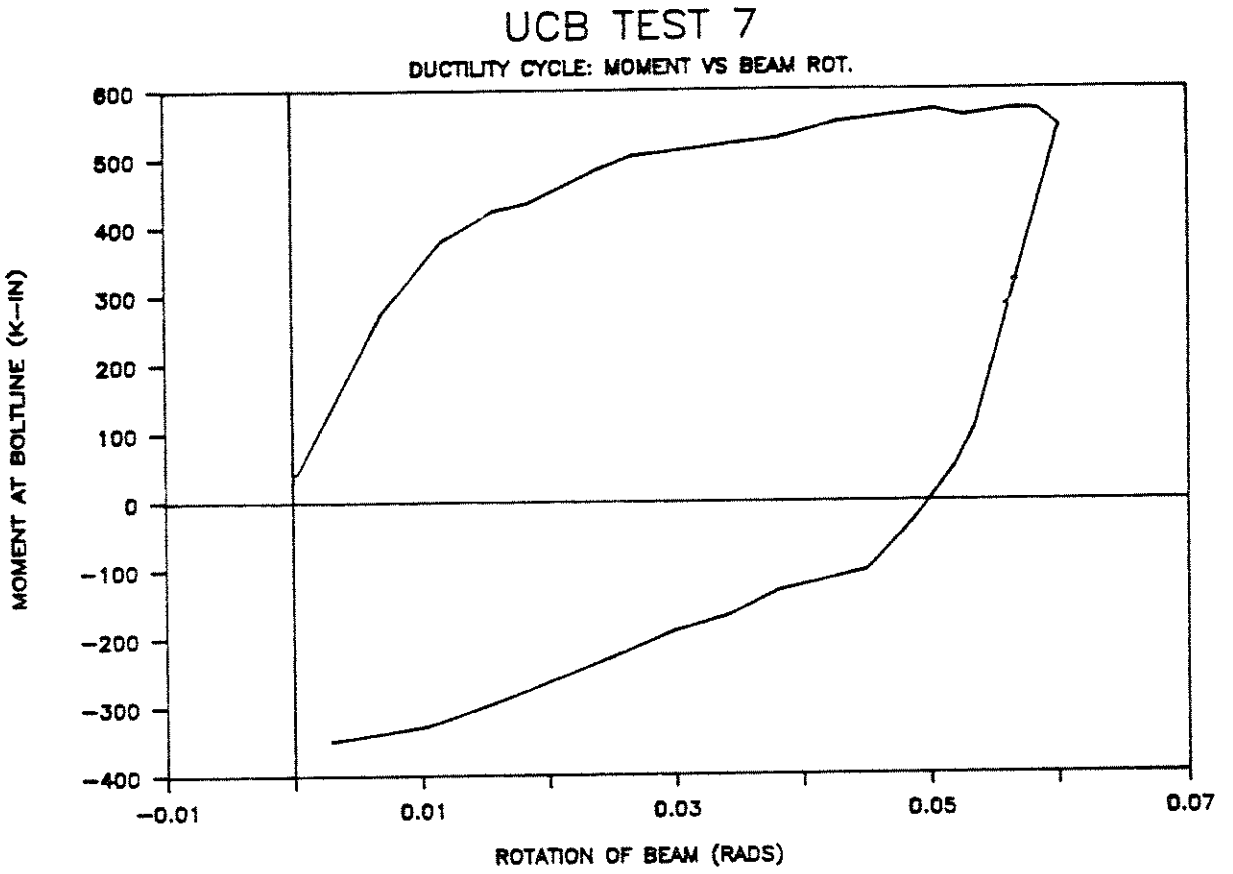
UCB TEST 7
DUCTILITY CYCLE: MOMENT VS BEAM ROT.
MOMENT AT BOLTLINE (K-IN)
600
500
400
300
200
100
0
-100
-200
-300
-400
-0.01
0.01
0.03
0.05
0.07
ROTATION OF BEAM (RADS)

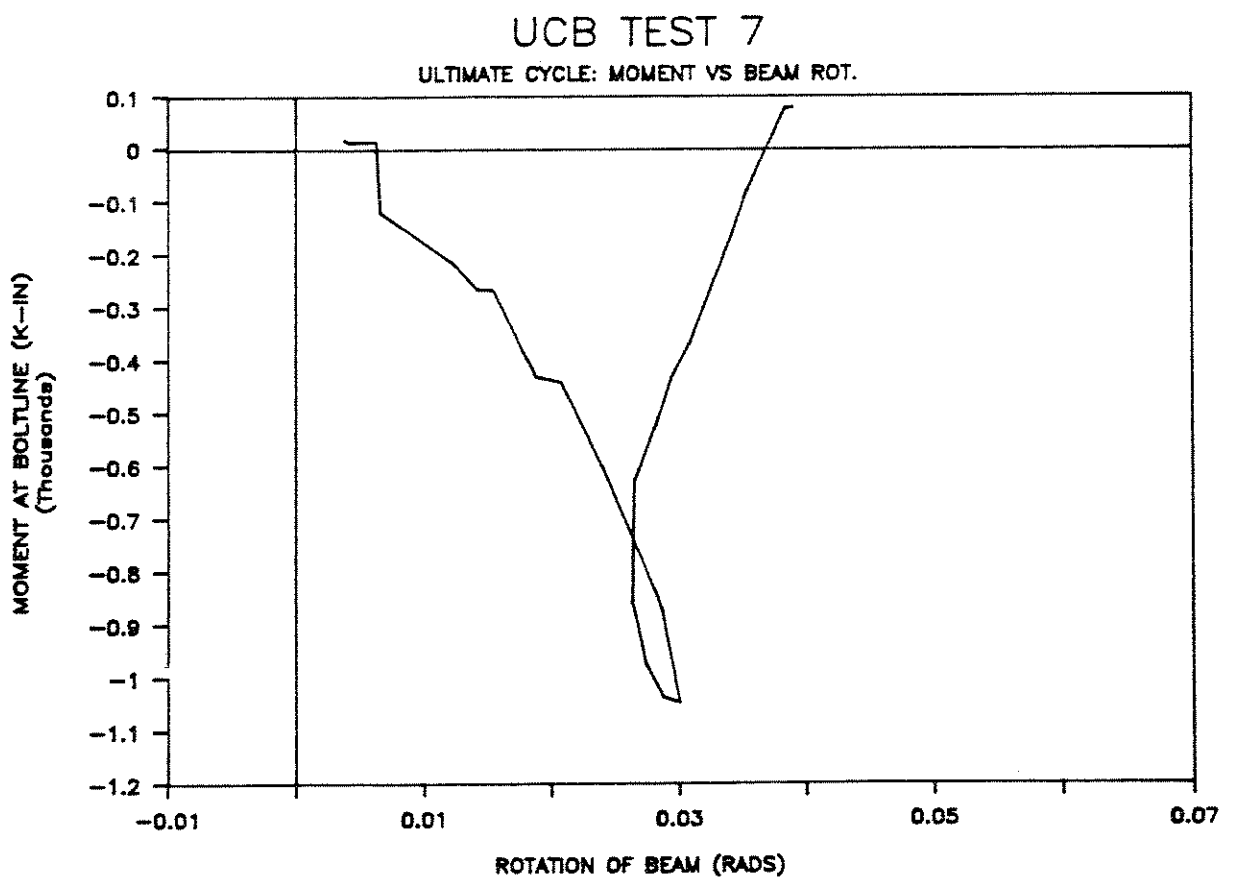
UCB TEST 7
ULTIMATE CYCLE: MOMENT VS BEAM ROT.
MOMENT AT BOLTLINE (K-IN)
(Thousands)
0.1
0
-0.1
-0.2
-0.3
-0.4
-0.5
-0.6
-0.7
-0.8
-0.9
-1
-1.1
-1.2
-0.01
0.01
0.03
0.05
0.07
ROTATION OF BEAM (RADS)

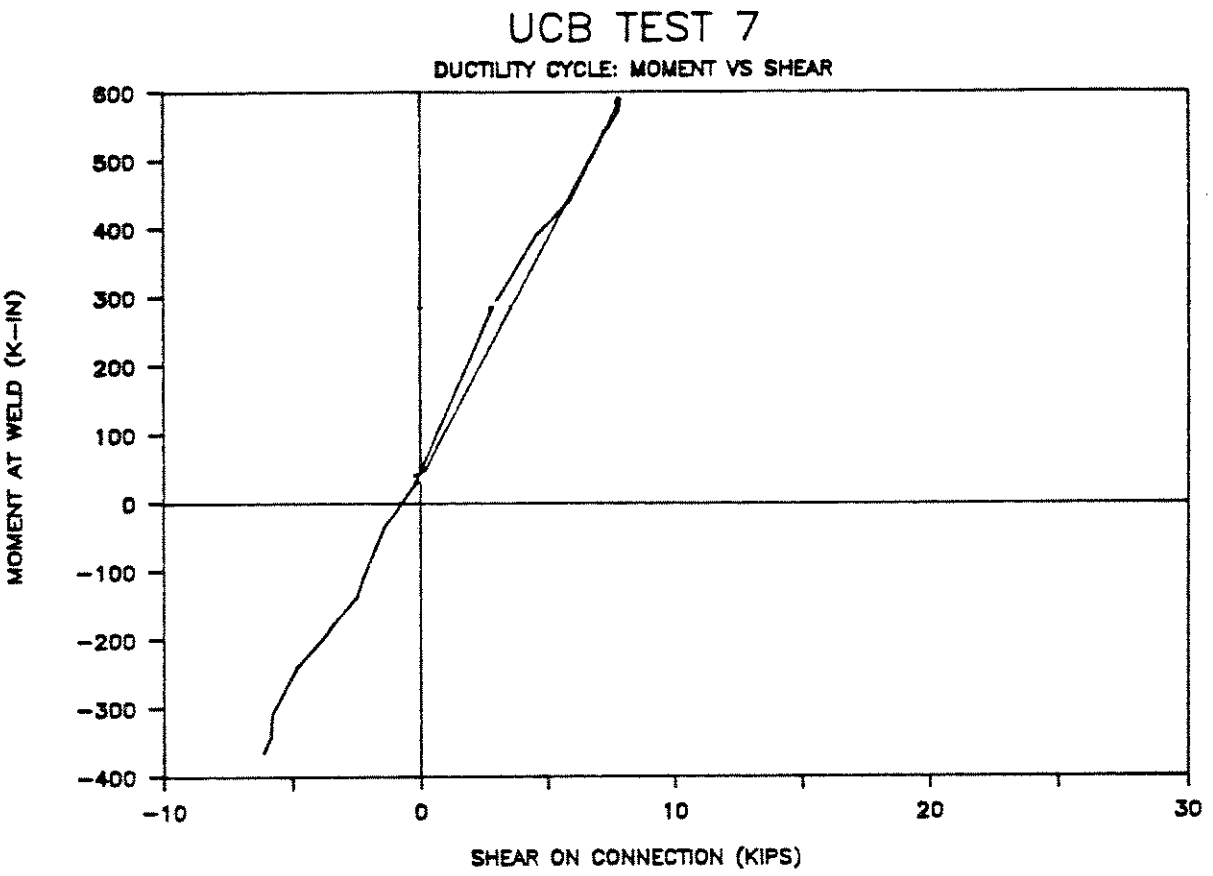
UCB TEST 7
DUCTILITY CYCLE: MOMENT VS SHEAR
MOMENT AT WELD (K--IN)
600
500
400
300
200
100
0
-100
-200
-300
-400
-10
0
10
20
30
SHEAR ON CONNECTION (KIPS)

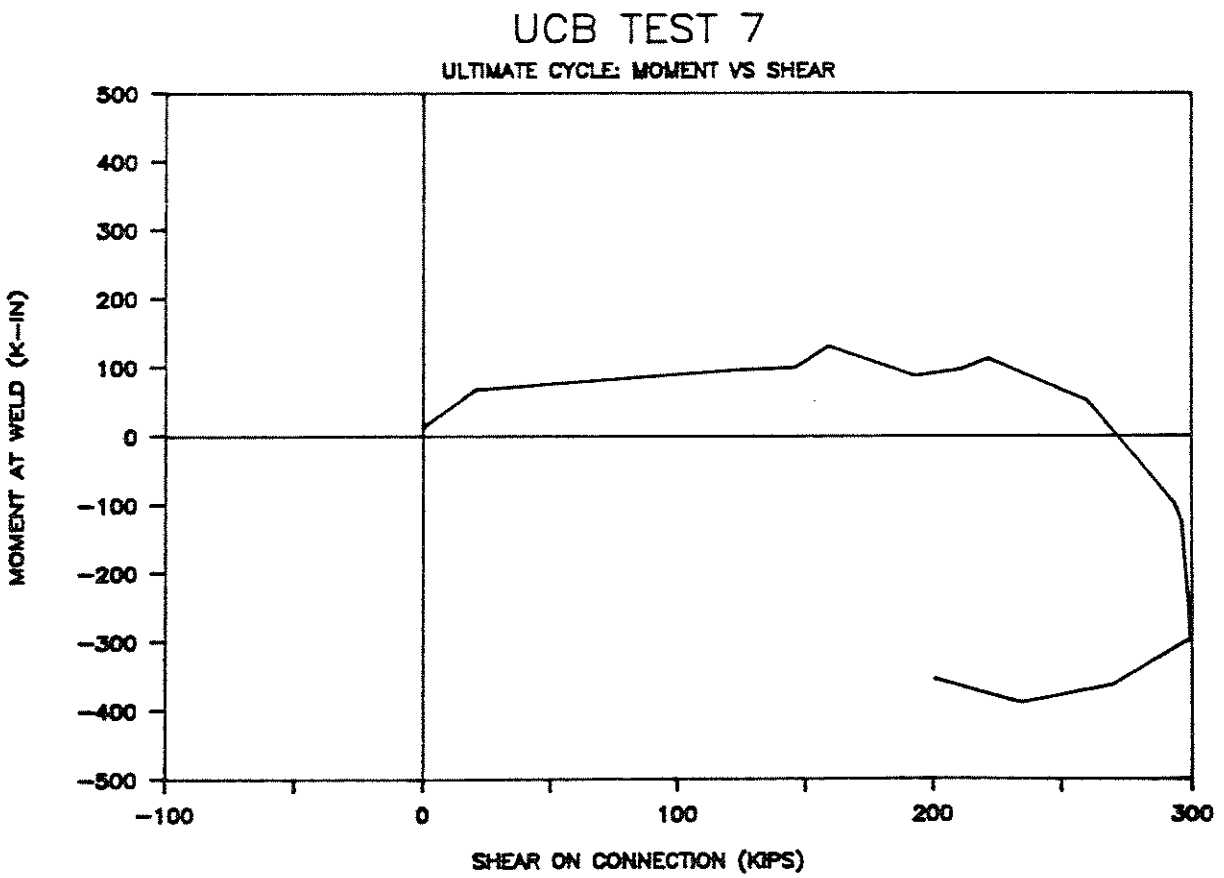
UCB TEST 7
ULTIMATE CYCLE: MOMENT VS SHEAR
MOMENT AT WELD (K--IN)
500
400
300
200
100
0
-100
-200
-300
-400
-500
-100
0
100
200
300
SHEAR ON CONNECTION (KIPS)

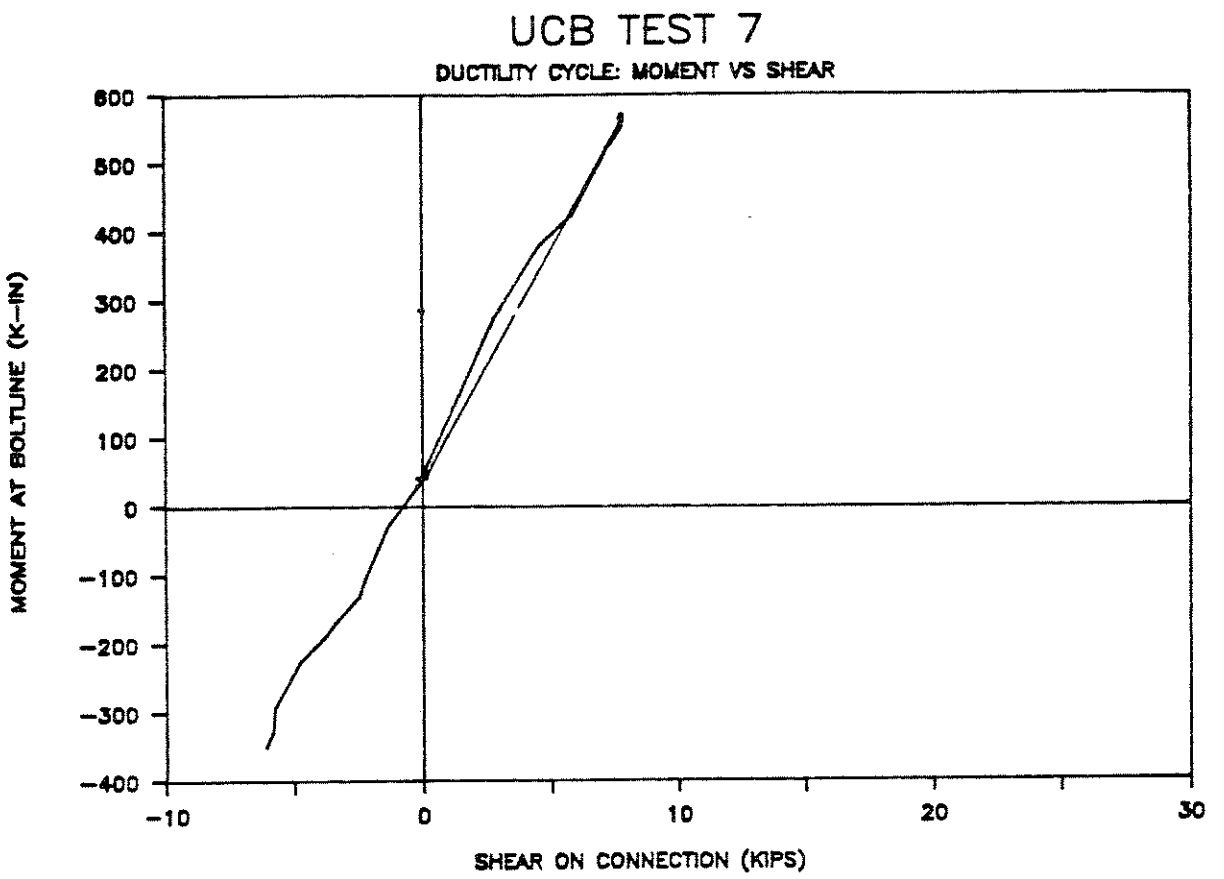
UCB TEST 7
DUCTILITY CYCLE: MOMENT VS SHEAR
MOMENT AT BOLTLINE (K-IN)
600
500
400
300
200
100
0
-100
-200
-300
-400
-10
0
10
20
30
SHEAR ON CONNECTION (KIPS)

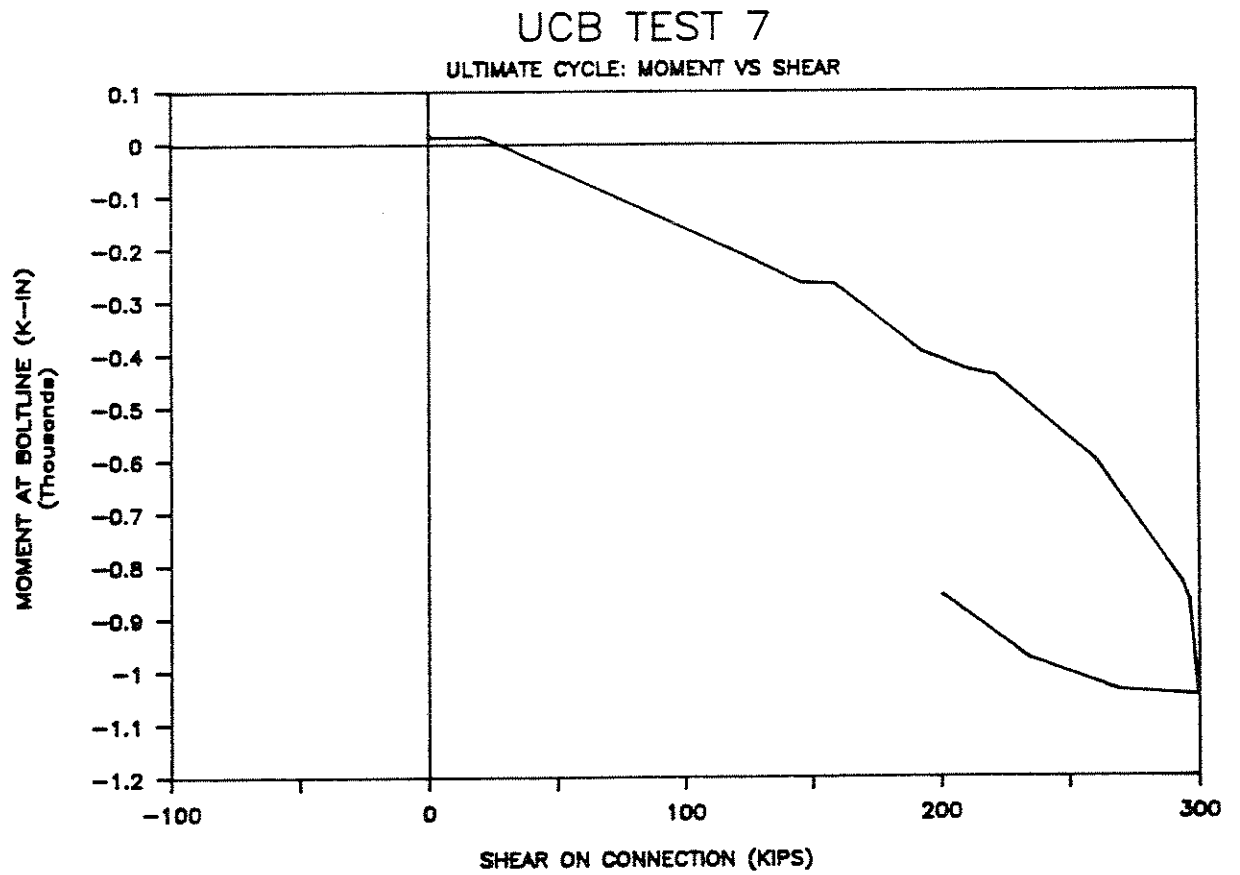
UCB TEST 7
ULTIMATE CYCLE: MOMENT VS SHEAR
MOMENT AT BOLTLINE (K-IN)
(Thousands)
0.1
0
-0.1
-0.2
-0.3
-0.4
-0.5
-0.6
-0.7
-0.8
-0.9
-1
-1.1
-1.2
-100
0
100
200
300
SHEAR ON CONNECTION (KIPS)

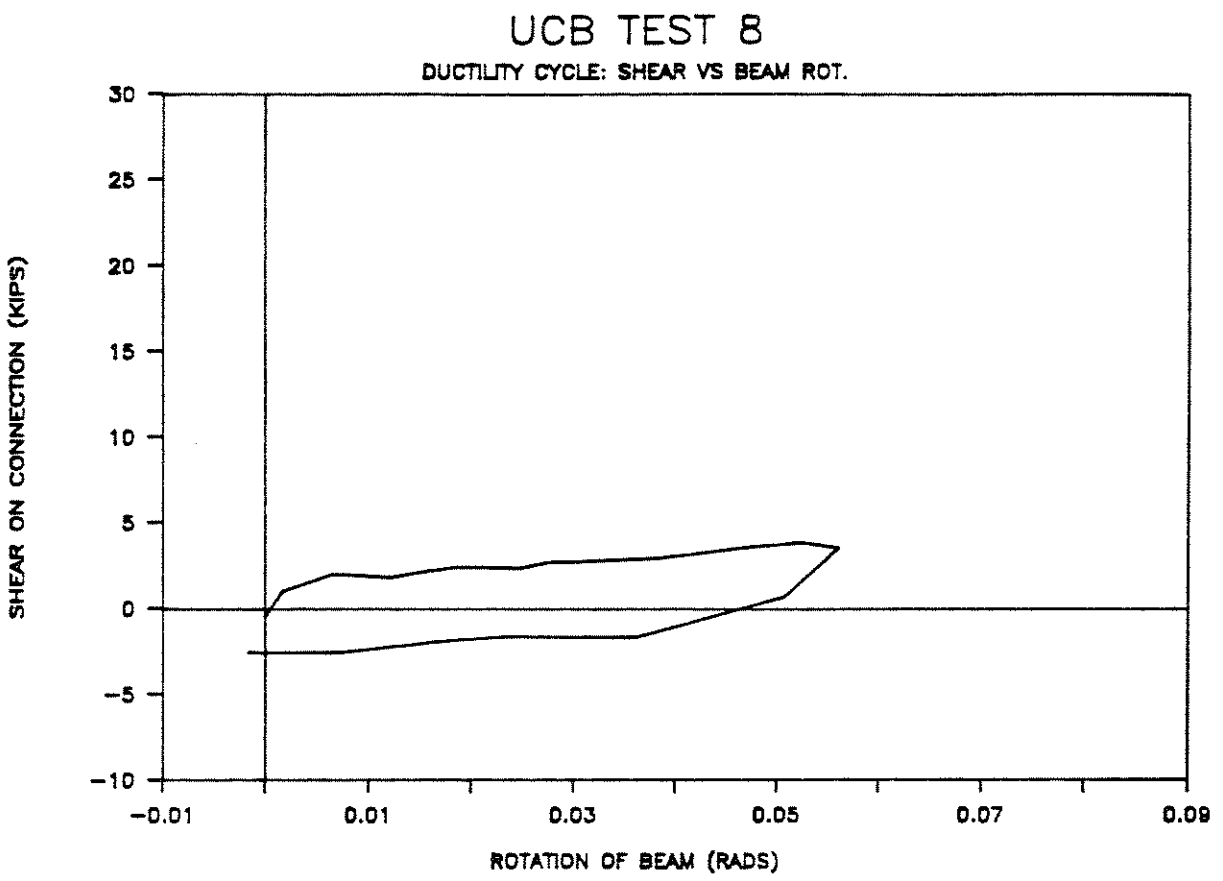
UCB TEST 8
DUCTILITY CYCLE: SHEAR VS BEAM ROT.
SHEAR ON CONNECTION (KIPS)
30
25
20
15
10
5
0
-5
-10
-0.01
0.01
0.03
0.05
0.07
0.09
ROTATION OF BEAM (RADS)

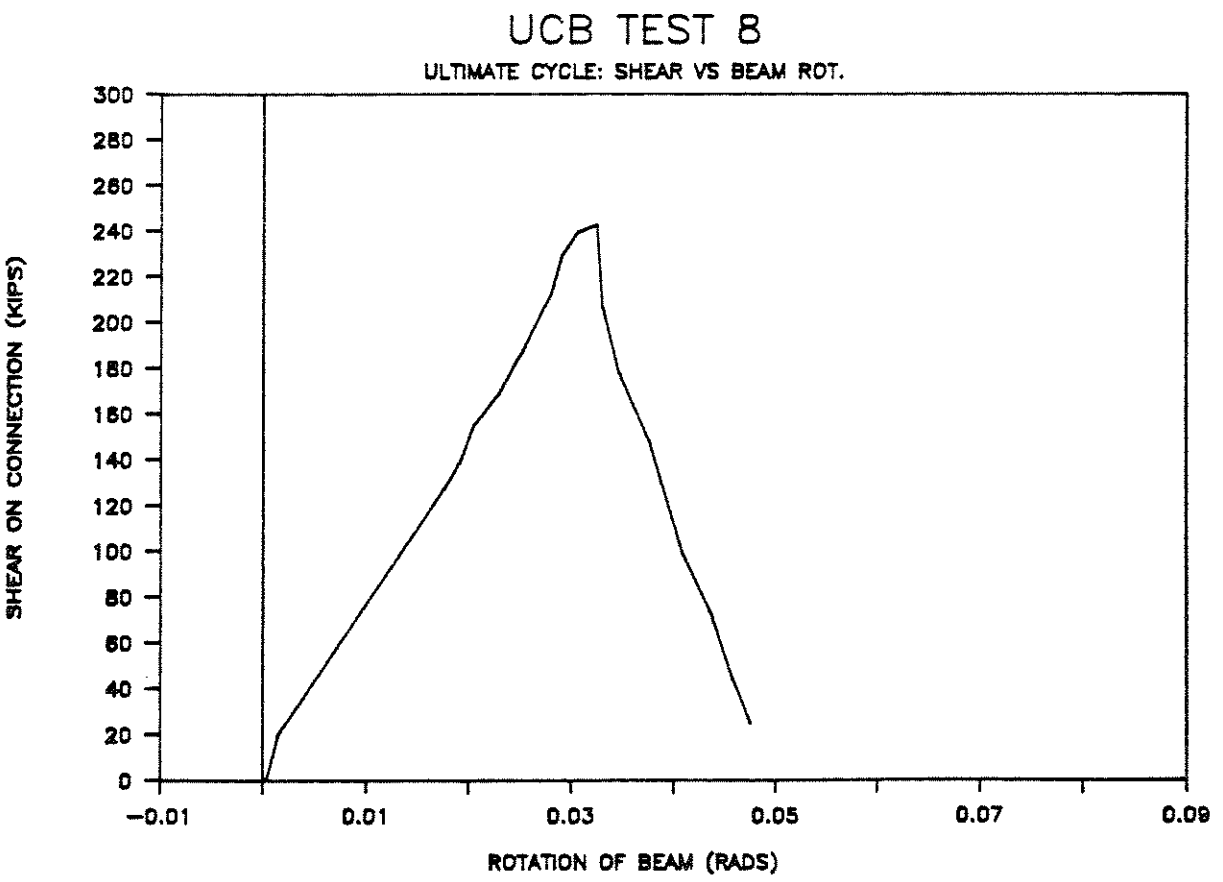
UCB TEST 8
ULTIMATE CYCLE: SHEAR VS BEAM ROT.
SHEAR ON CONNECTION (KIPS)
300
280
260
240
220
200
180
160
140
120
100
80
60
40
20
0
-0.01
0.01
0.03
0.05
0.07
0.09
ROTATION OF BEAM (RADS)

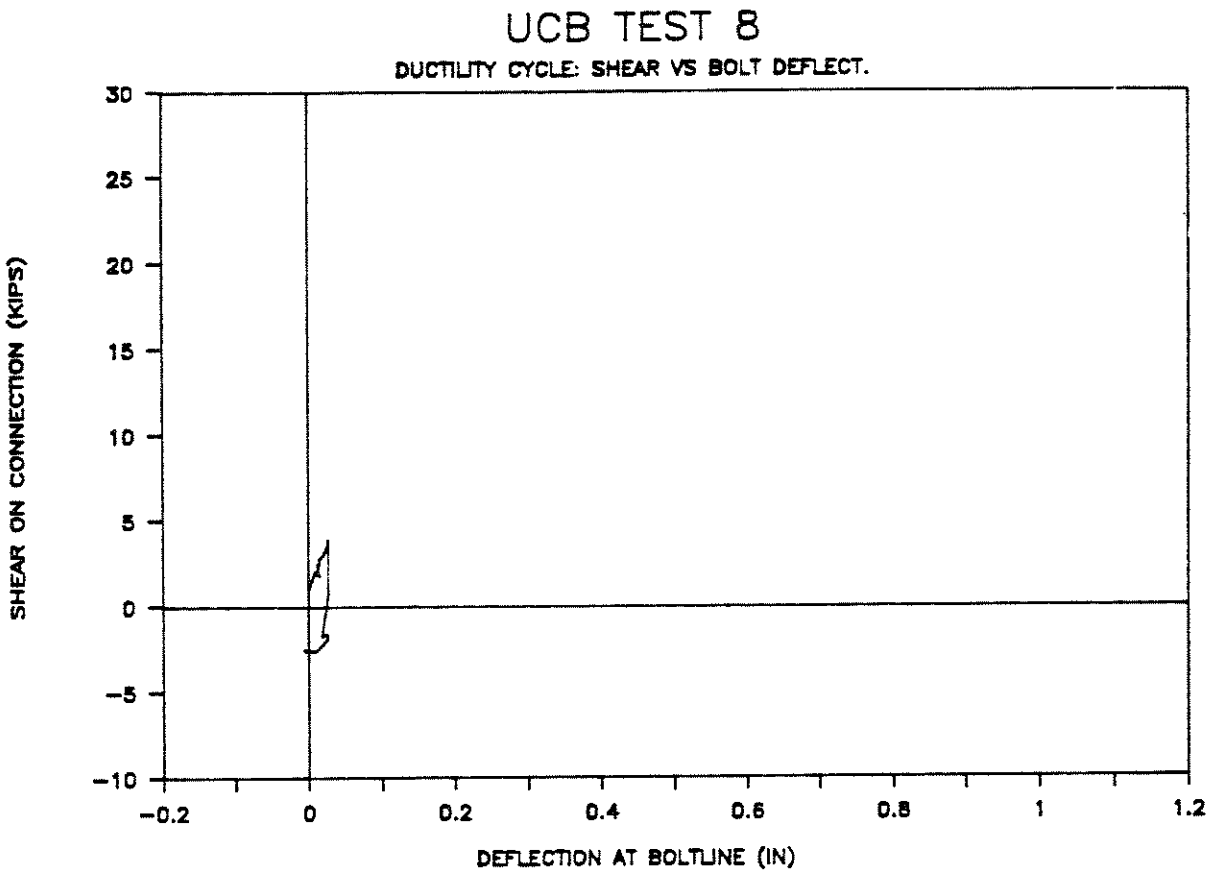
UCB TEST 8
DUCTILITY CYCLE: SHEAR VS BOLT DEFLECT.
SHEAR ON CONNECTION (KIPS)
30
25
20
15
10
5
0
−5
−10
−0.2
0
0.2
0.4
0.6
0.8
1
1.2
DEFLECTION AT BOLTLINE (IN)

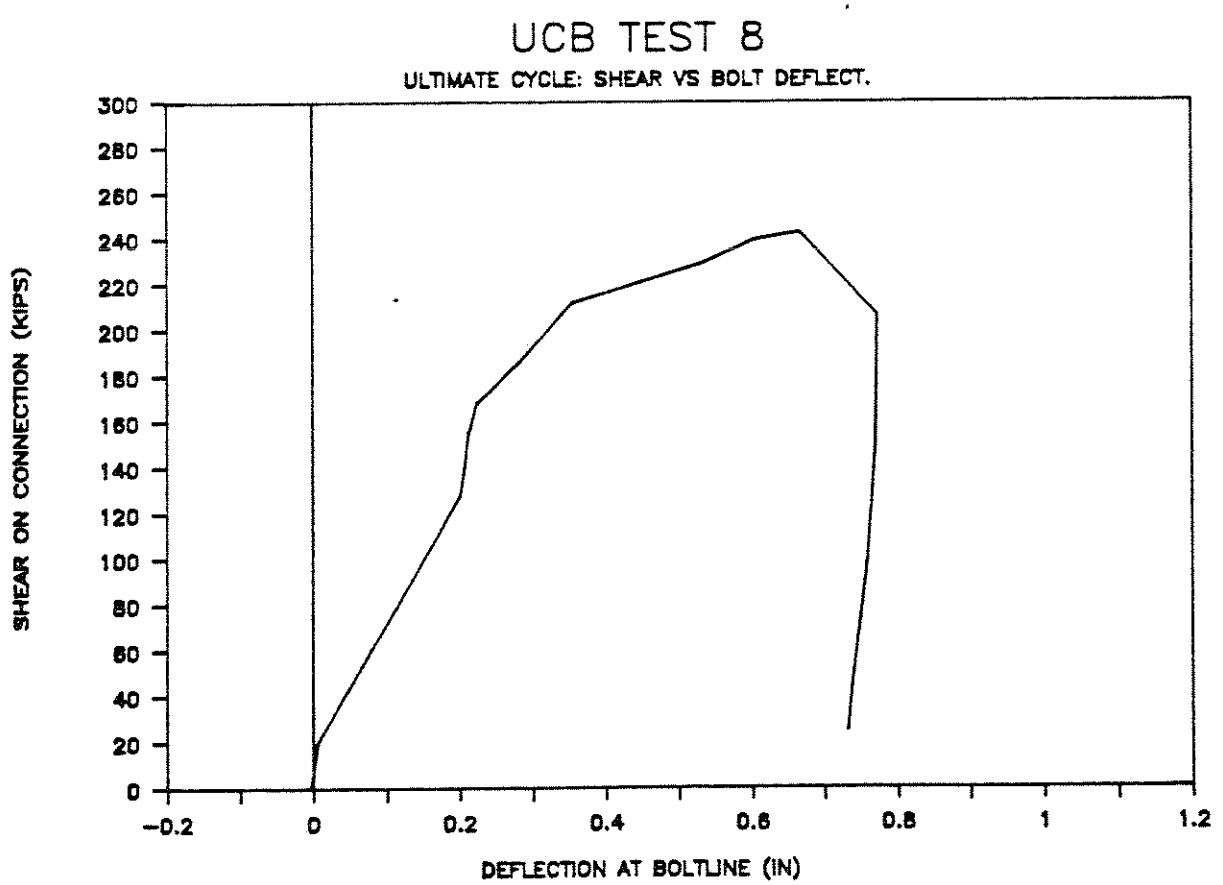
UCB TEST 8
ULTIMATE CYCLE: SHEAR VS BOLT DEFLECT.
SHEAR ON CONNECTION (KIPS)
300
280
260
240
220
200
180
160
140
120
100
80
60
40
20
0
−0.2
0
0.2
0.4
0.6
0.8
1
1.2
DEFLECTION AT BOLTLINE (IN)

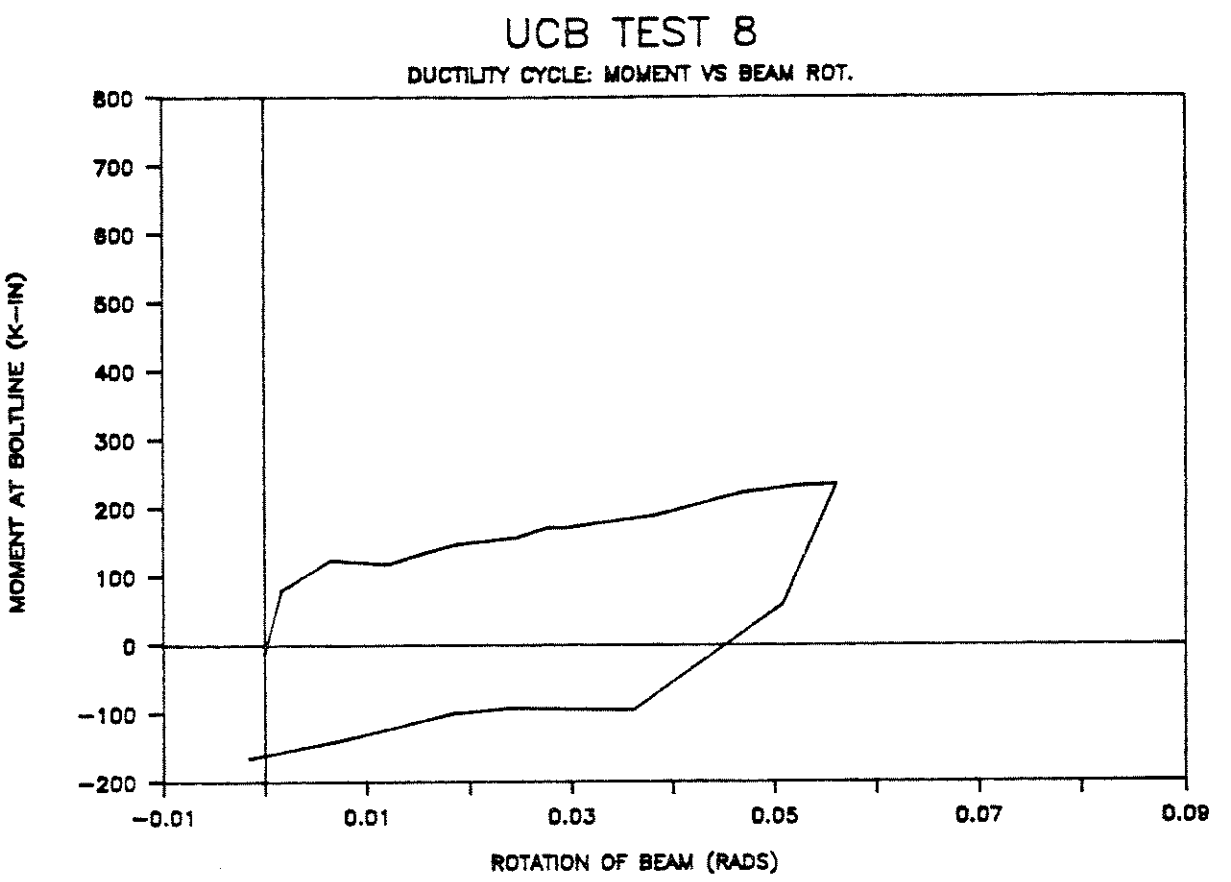
UCB TEST 8
DUCTILITY CYCLE: MOMENT VS BEAM ROT.
MOMENT AT BOLTLINE (K-IN)
800
700
600
500
400
300
200
100
0
-100
-200
-0.01
0.01
0.03
0.05
0.07
0.09
ROTATION OF BEAM (RADS)

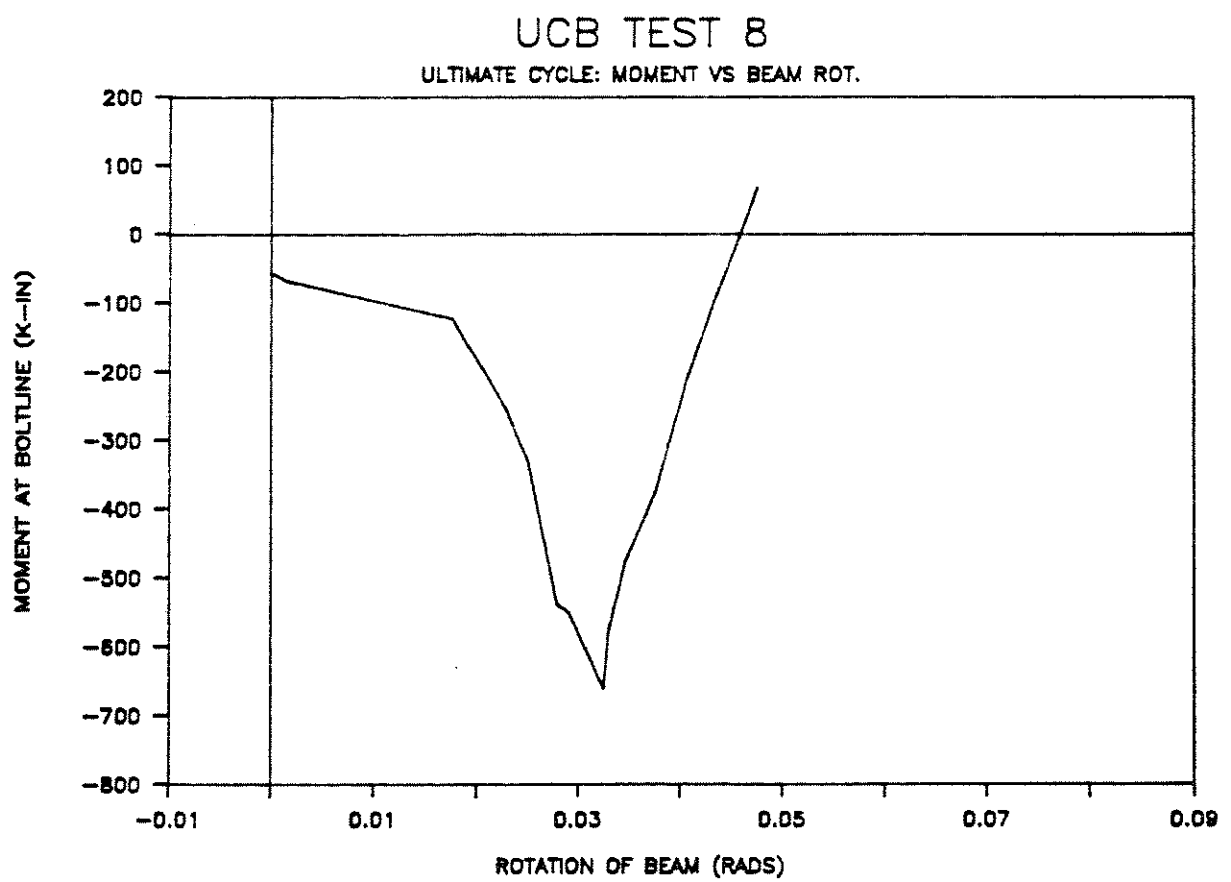
UCB TEST 8
ULTIMATE CYCLE: MOMENT VS BEAM ROT.
MOMENT AT BOLTLINE (K-IN)
200
100
0
-100
-200
-300
-400
-500
-600
-700
-800
-0.01
0.01
0.03
0.05
0.07
0.09
ROTATION OF BEAM (RADS)

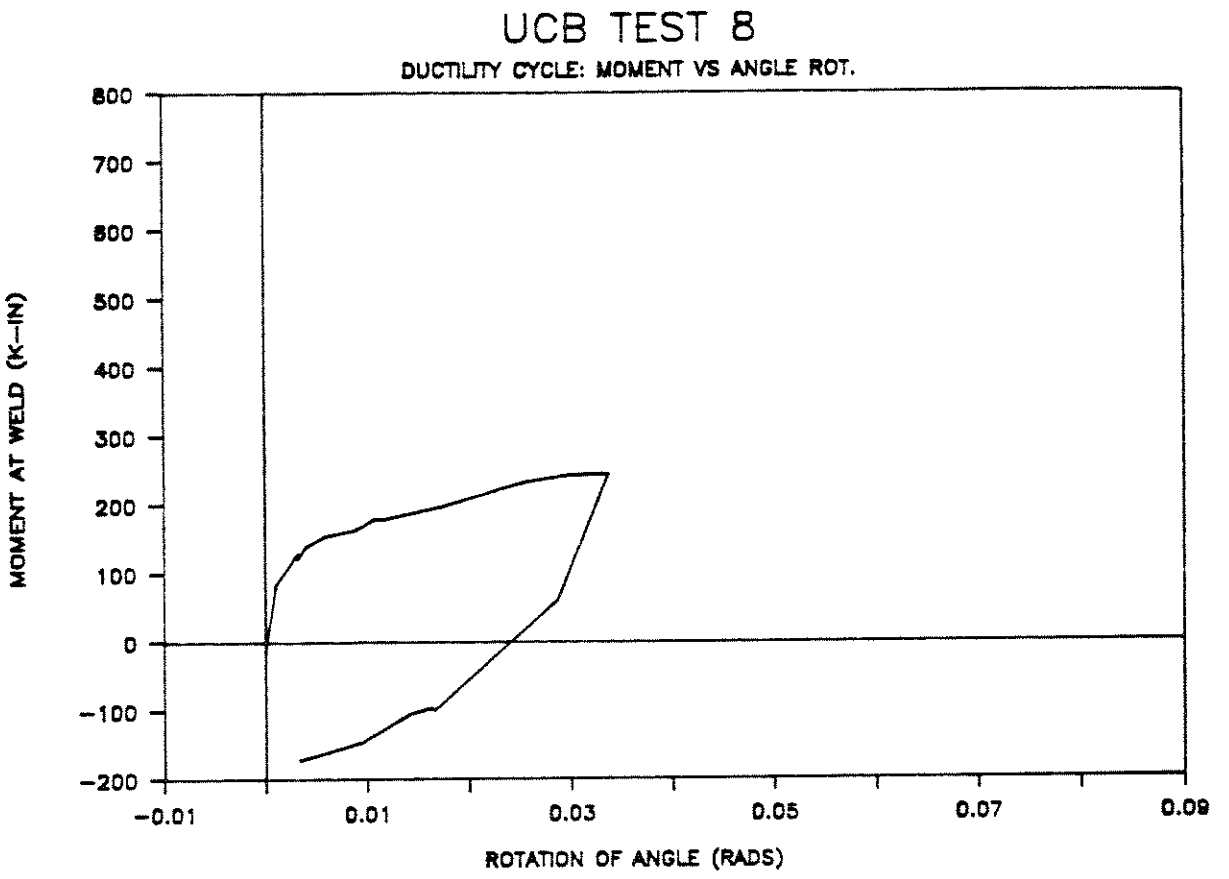
UCB TEST 8
DUCTILITY CYCLE: MOMENT VS ANGLE ROT.
MOMENT AT WELD (K-IN)
800
700
600
500
400
300
200
100
0
-100
-200
-0.01
0.01
0.03
0.05
0.07
0.09
ROTATION OF ANGLE (RADS)

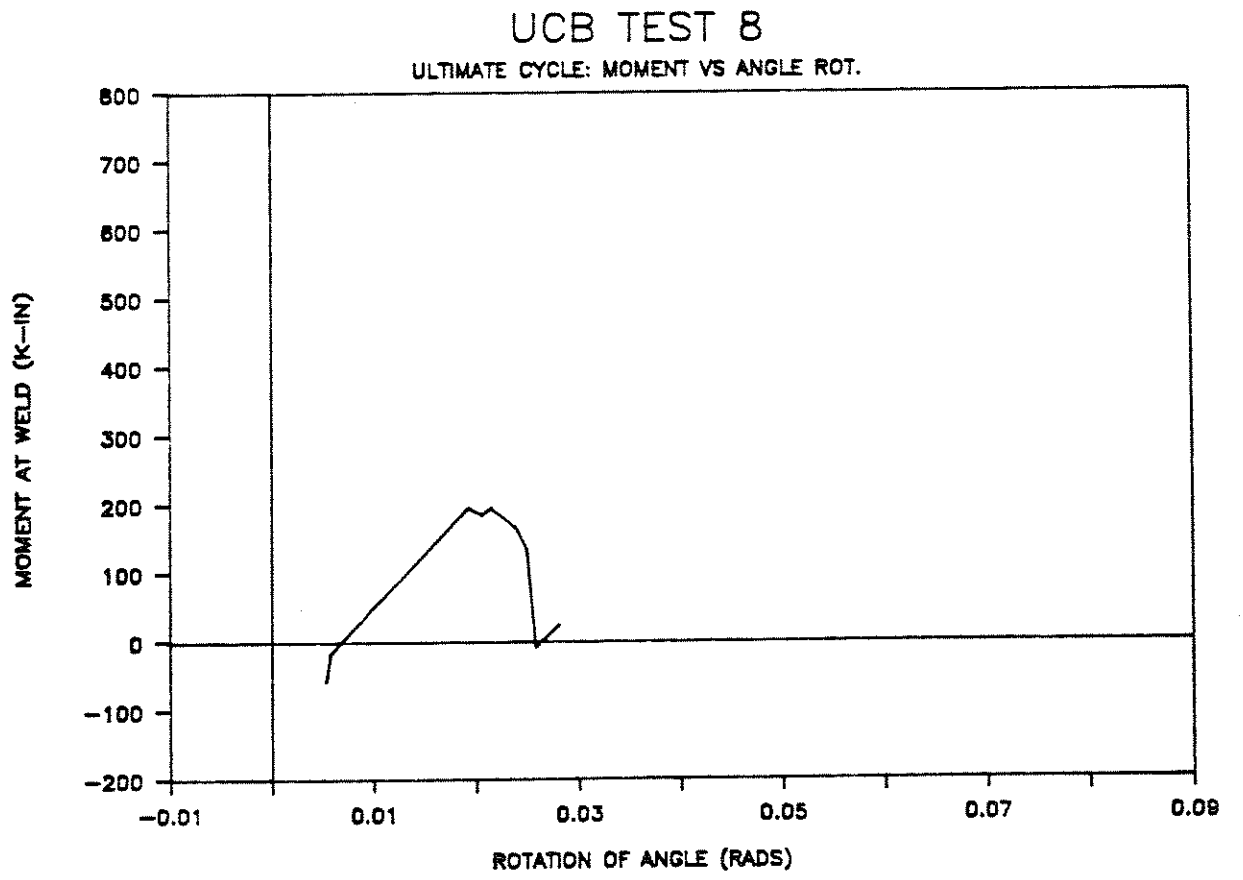
UCB TEST 8
ULTIMATE CYCLE: MOMENT VS ANGLE ROT.
MOMENT AT WELD (K-IN)
800
700
600
500
400
300
200
100
0
-100
-200
-0.01
0.01
0.03
0.05
0.07
0.09
ROTATION OF ANGLE (RADS)

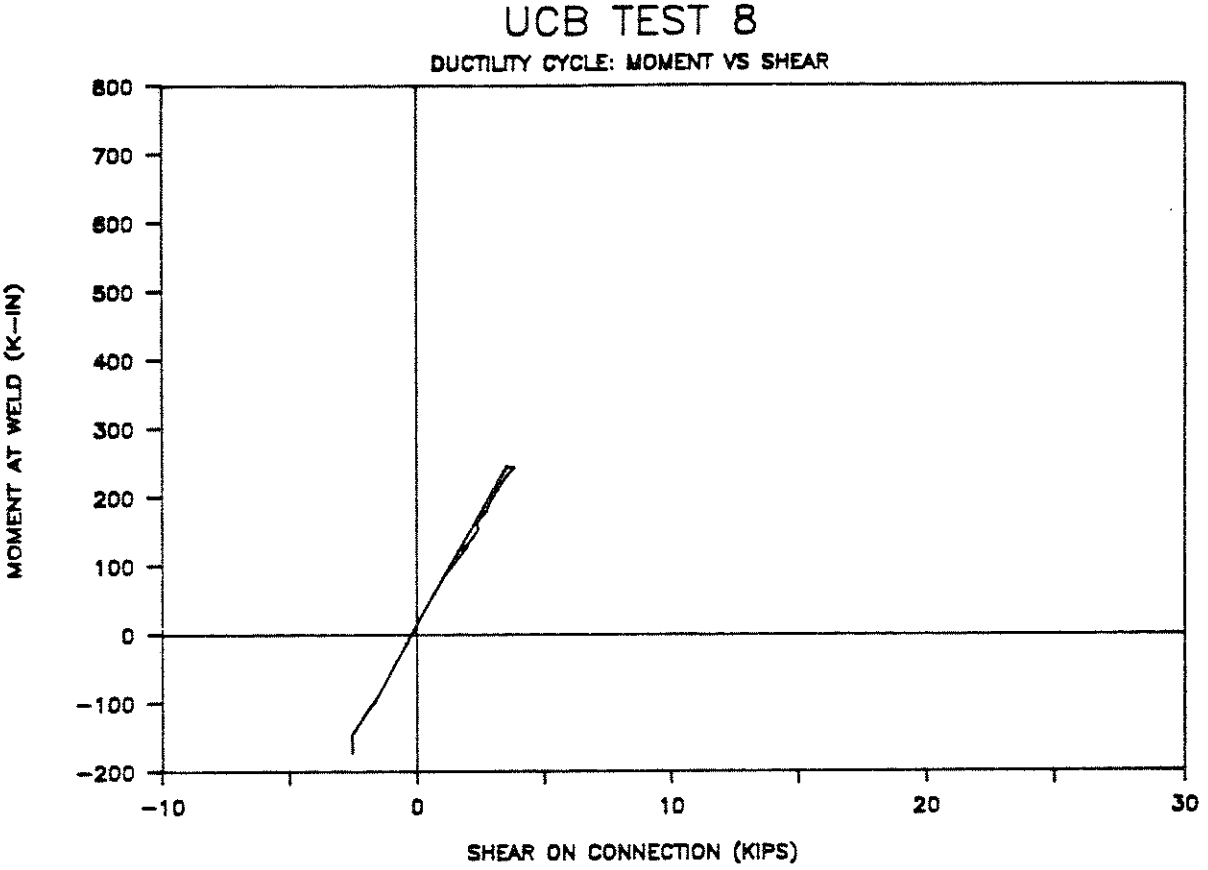
UCB TEST 8
DUCTILITY CYCLE: MOMENT VS SHEAR
MOMENT AT WELD (K-IN)
800
700
600
500
400
300
200
100
0
-100
-200
-10
0
10
20
30
SHEAR ON CONNECTION (KIPS)

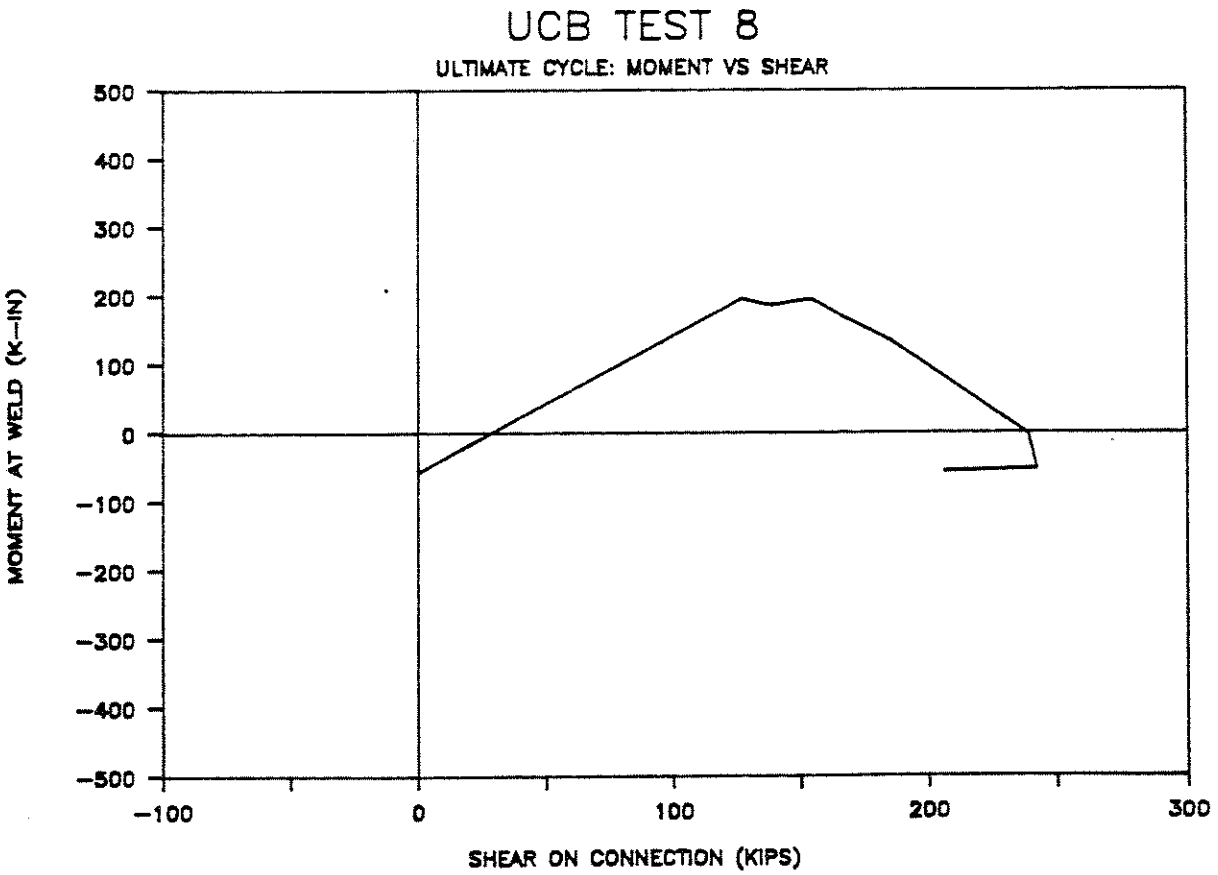
UCB TEST 8
ULTIMATE CYCLE: MOMENT VS SHEAR
MOMENT AT WELD (K-IN)
500
400
300
200
100
0
-100
-200
-300
-400
-500
-100
0
100
200
300
SHEAR ON CONNECTION (KIPS)

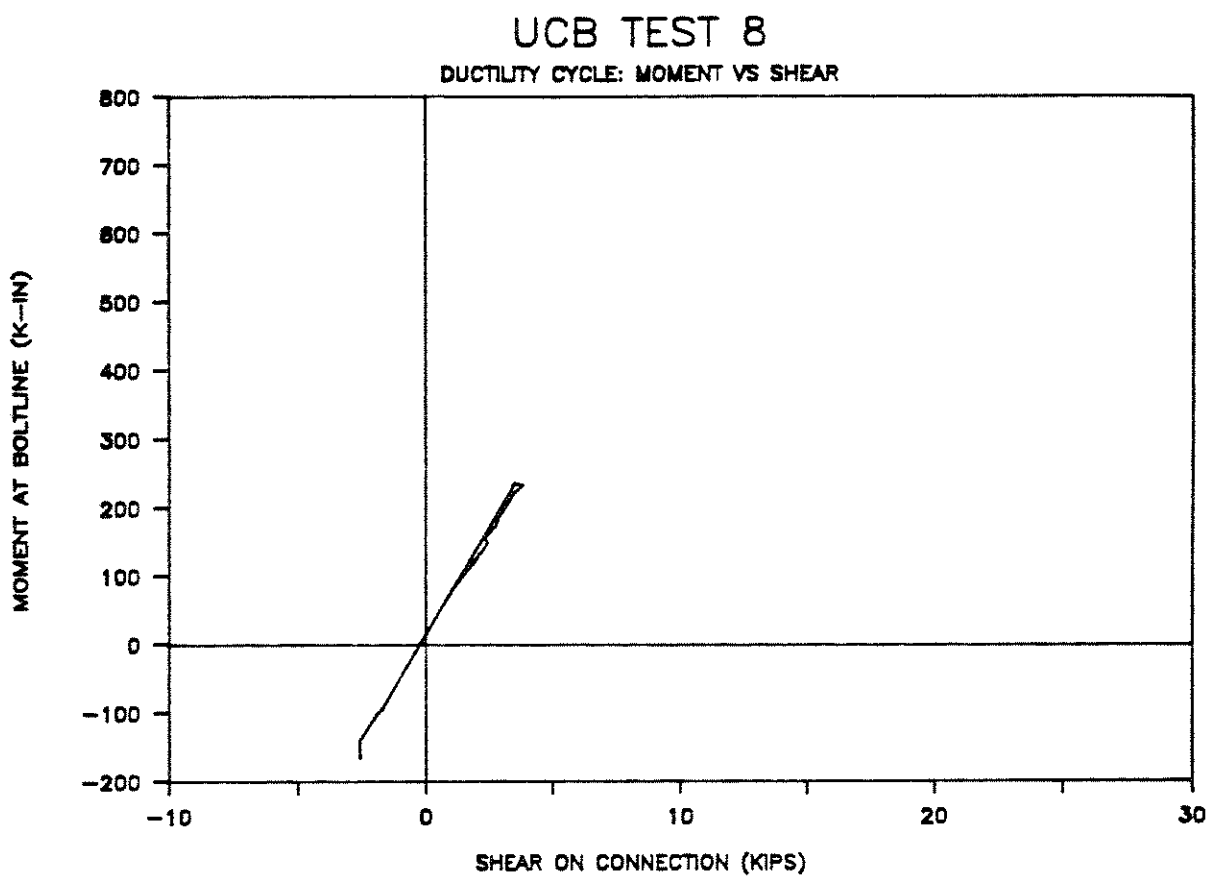
UCB TEST 8
DUCTILITY CYCLE: MOMENT VS SHEAR
MOMENT AT BOLTLINE (K-IN)
800
700
600
500
400
300
200
100
0
-100
-200
-10
0
10
20
30
SHEAR ON CONNECTION (KIPS)

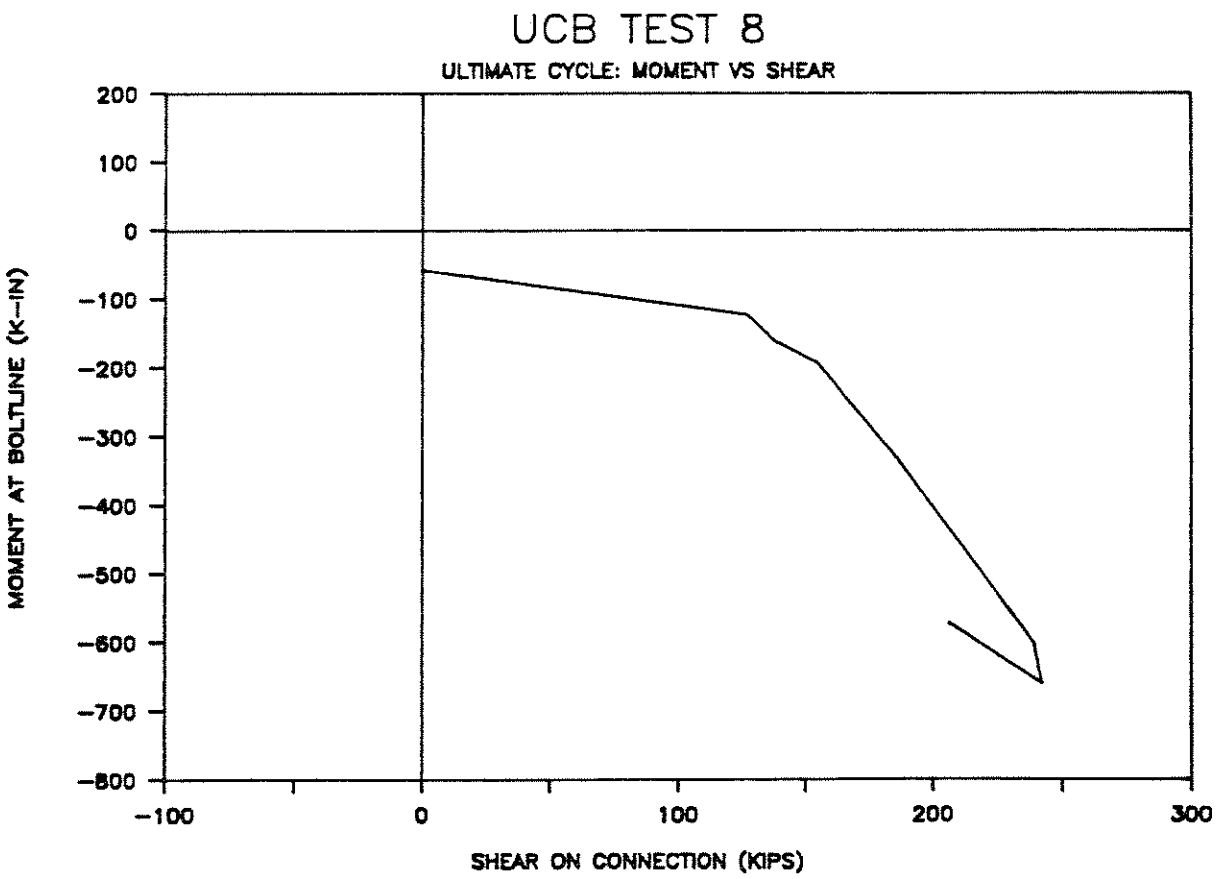
UCB TEST 8
ULTIMATE CYCLE: MOMENT VS SHEAR
MOMENT AT BOLTLINE (K-IN)
200
100
0
-100
-200
-300
-400
-500
-600
-700
-800
-100
0
100
200
300
SHEAR ON CONNECTION (KIPS)

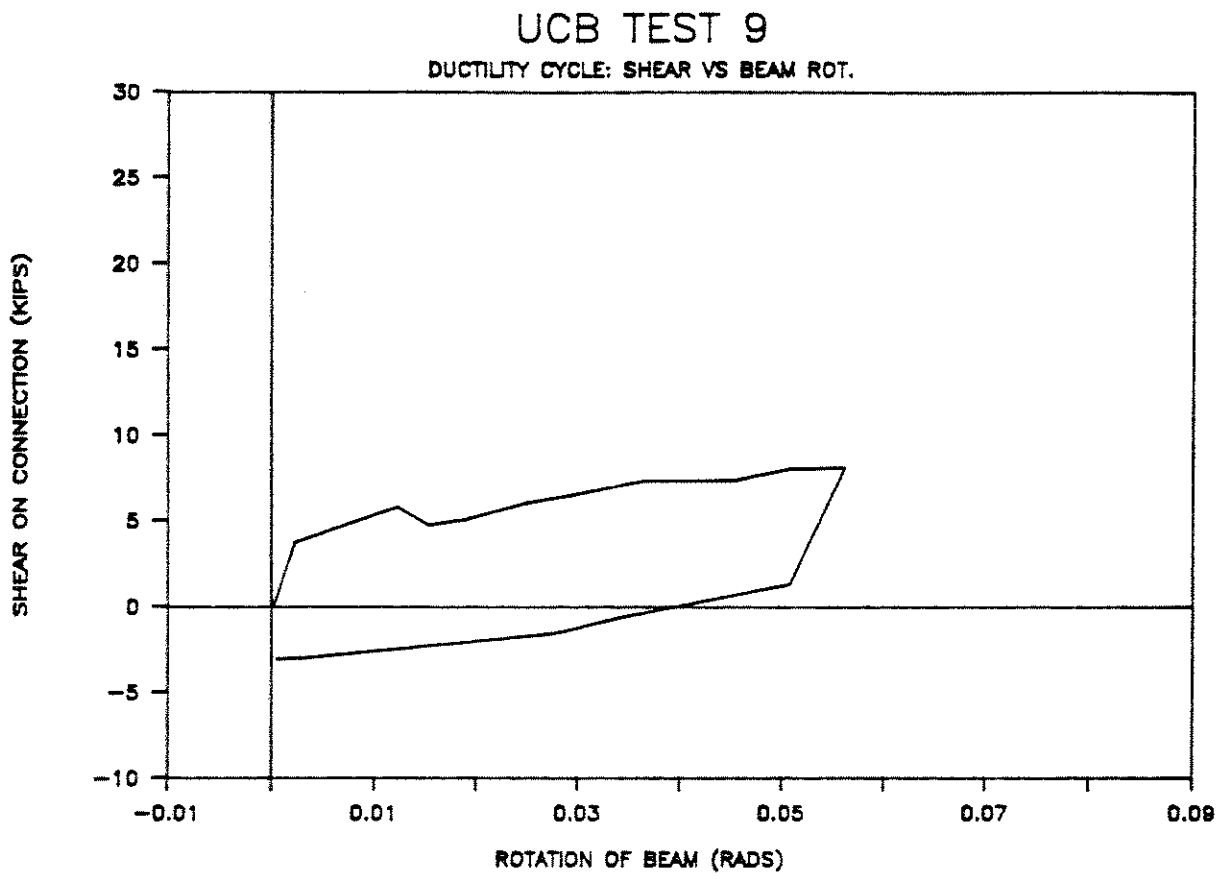
UCB TEST 9
DUCTILITY CYCLE: SHEAR VS BEAM ROT.
SHEAR ON CONNECTION (KIPS)
30
25
20
15
10
5
0
-5
-10
-0.01
0.01
0.03
0.05
0.07
0.09
ROTATION OF BEAM (RADS)

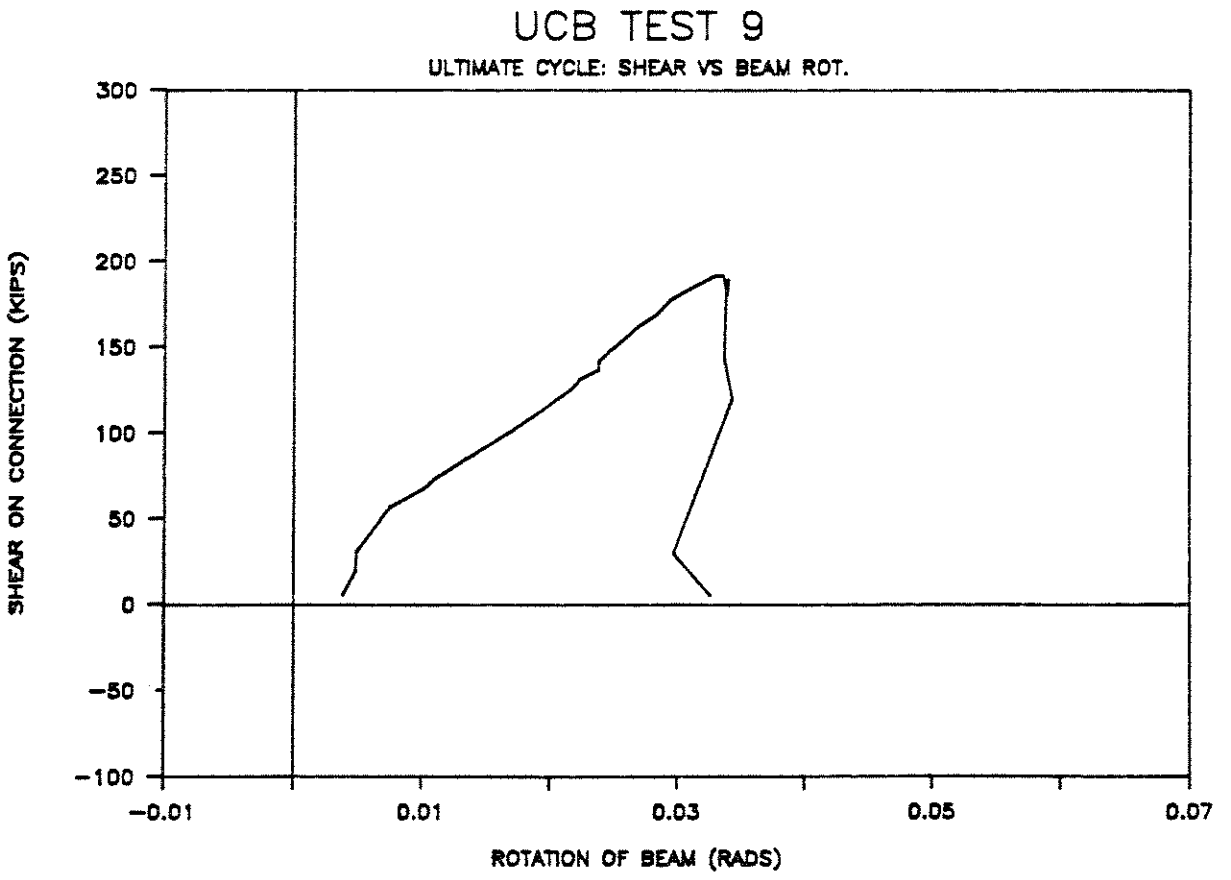
UCB TEST 9
ULTIMATE CYCLE: SHEAR VS BEAM ROT.
SHEAR ON CONNECTION (KIPS)
300
250
200
150
100
50
0
-50
-100
-0.01
0.01
0.03
0.05
0.07
ROTATION OF BEAM (RADS)

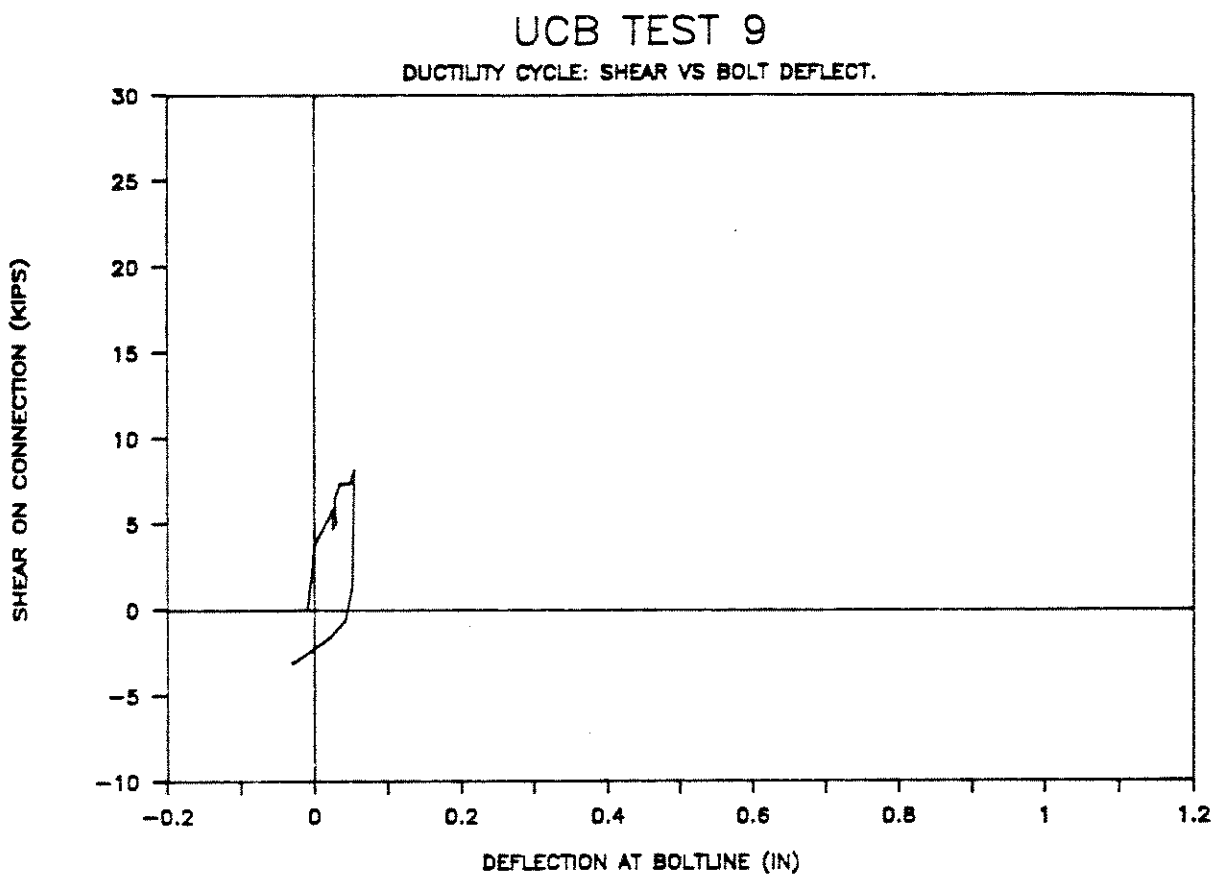
UCB TEST 9
DUCTILITY CYCLE: SHEAR VS BOLT DEFLECT.
SHEAR ON CONNECTION (KIPS)
30
25
20
15
10
5
0
−5
−10
−0.2
0
0.2
0.4
0.6
0.8
1
1.2
DEFLECTION AT BOLTLINE (IN)

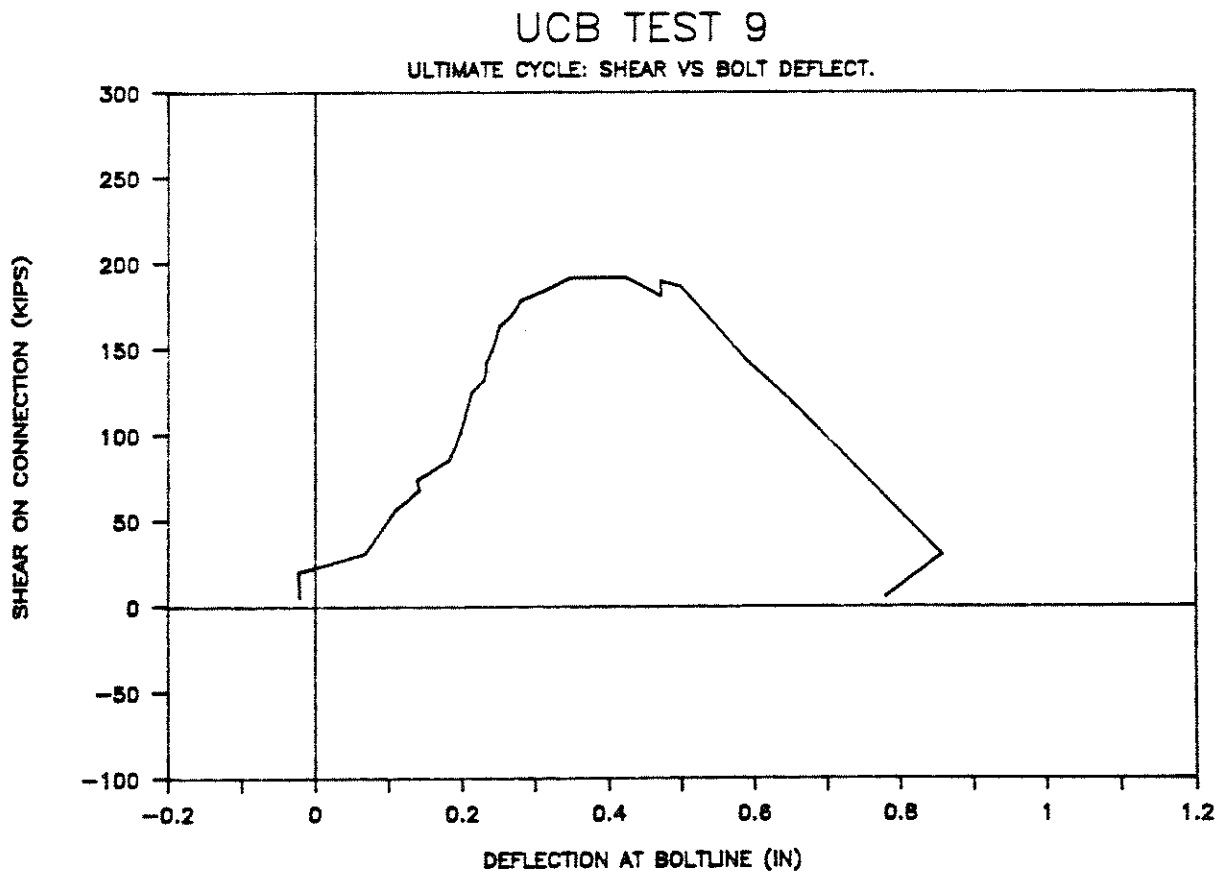
UCB TEST 9
ULTIMATE CYCLE: SHEAR VS BOLT DEFLECT.
SHEAR ON CONNECTION (KIPS)
300
250
200
150
100
50
0
−50
−100
−0.2
0
0.2
0.4
0.6
0.8
1
1.2
DEFLECTION AT BOLTLINE (IN)

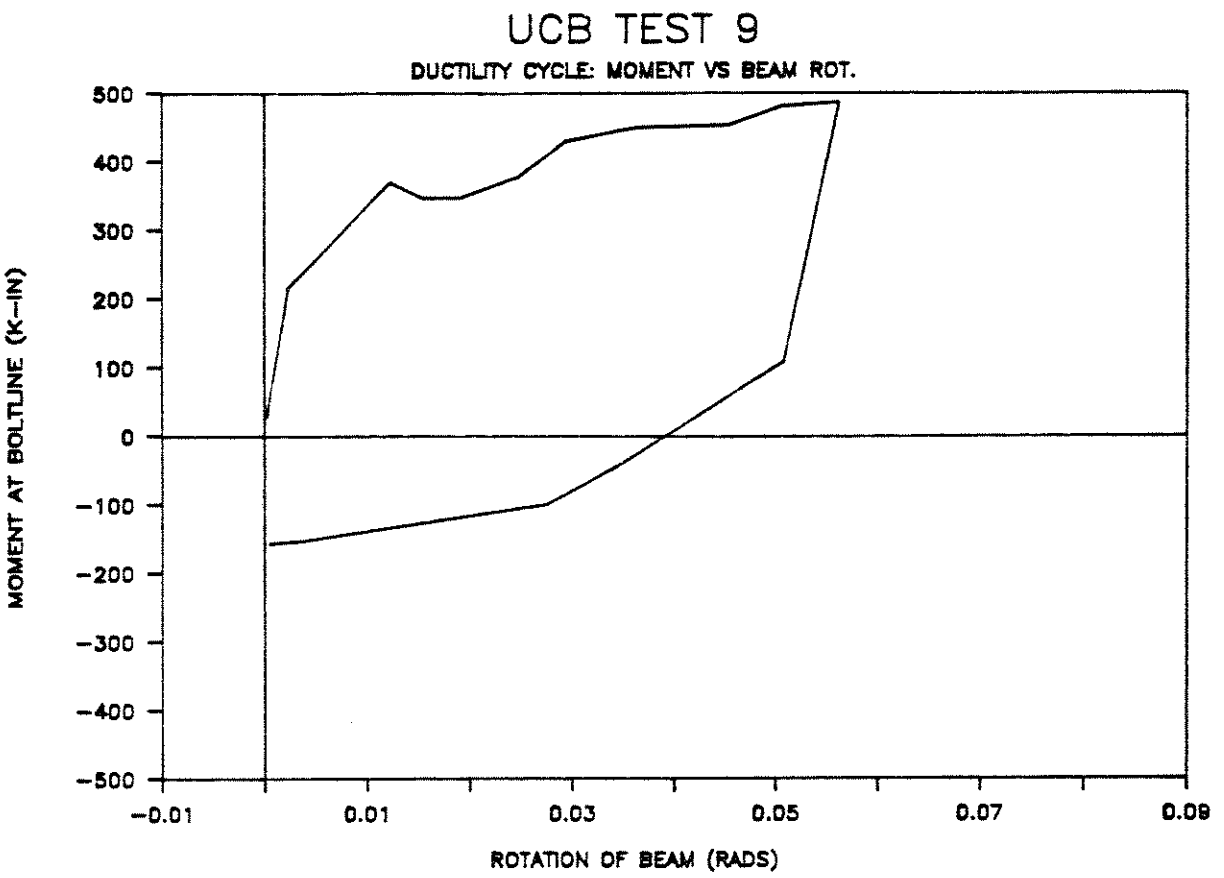
UCB TEST 9
DUCTILITY CYCLE: MOMENT VS BEAM ROT.
MOMENT AT BOLTLINE (K-IN)
500
400
300
200
100
0
-100
-200
-300
-400
-500
-0.01
0.01
0.03
0.05
0.07
0.09
ROTATION OF BEAM (RADS)

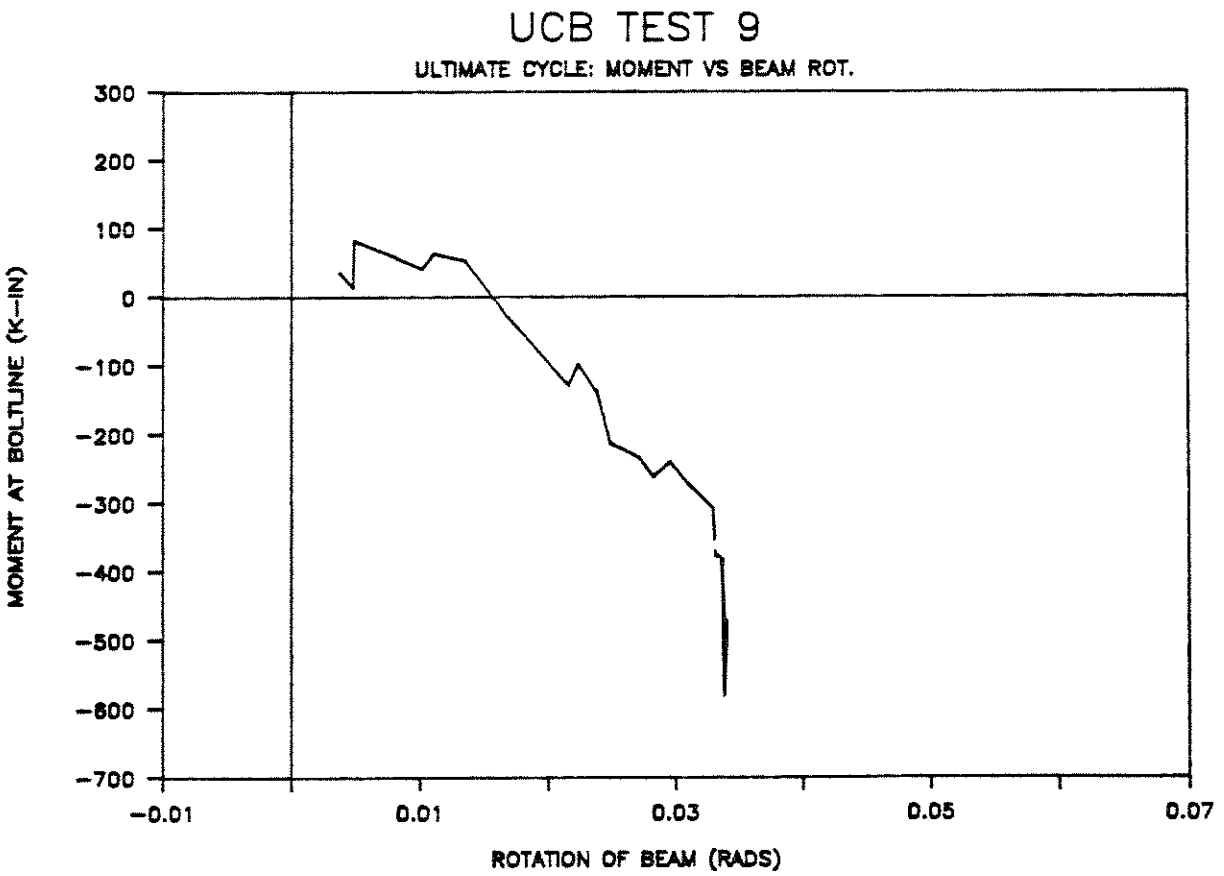
UCB TEST 9
ULTIMATE CYCLE: MOMENT VS BEAM ROT.
MOMENT AT BOLTLINE (K-IN)
300
200
100
0
-100
-200
-300
-400
-500
-600
-700
-0.01
0.01
0.03
0.05
0.07
ROTATION OF BEAM (RADS)

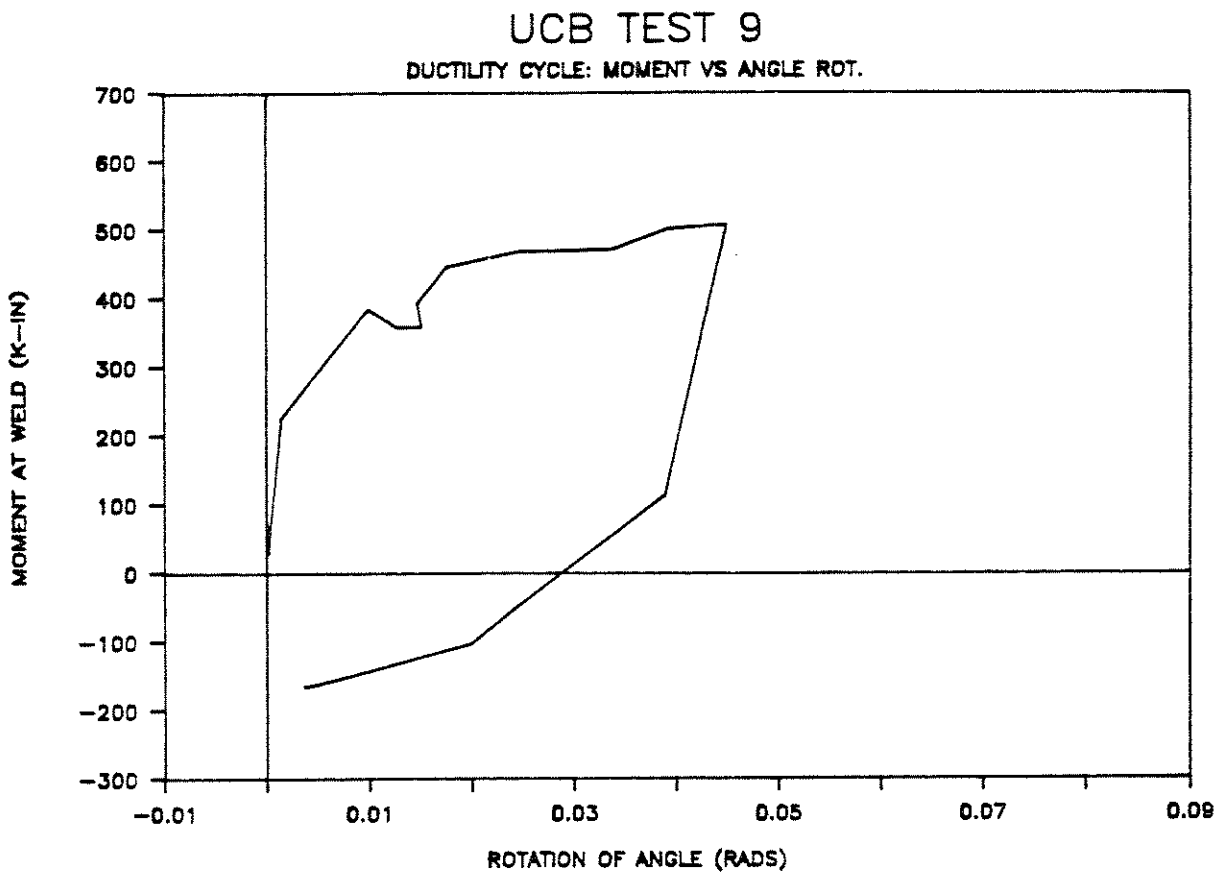
UCB TEST 9
DUCTILITY CYCLE: MOMENT VS ANGLE ROT.
MOMENT AT WELD (K-IN)
700
600
500
400
300
200
100
0
-100
-200
-300
-0.01
0.01
0.03
0.05
0.07
0.09
ROTATION OF ANGLE (RADS)

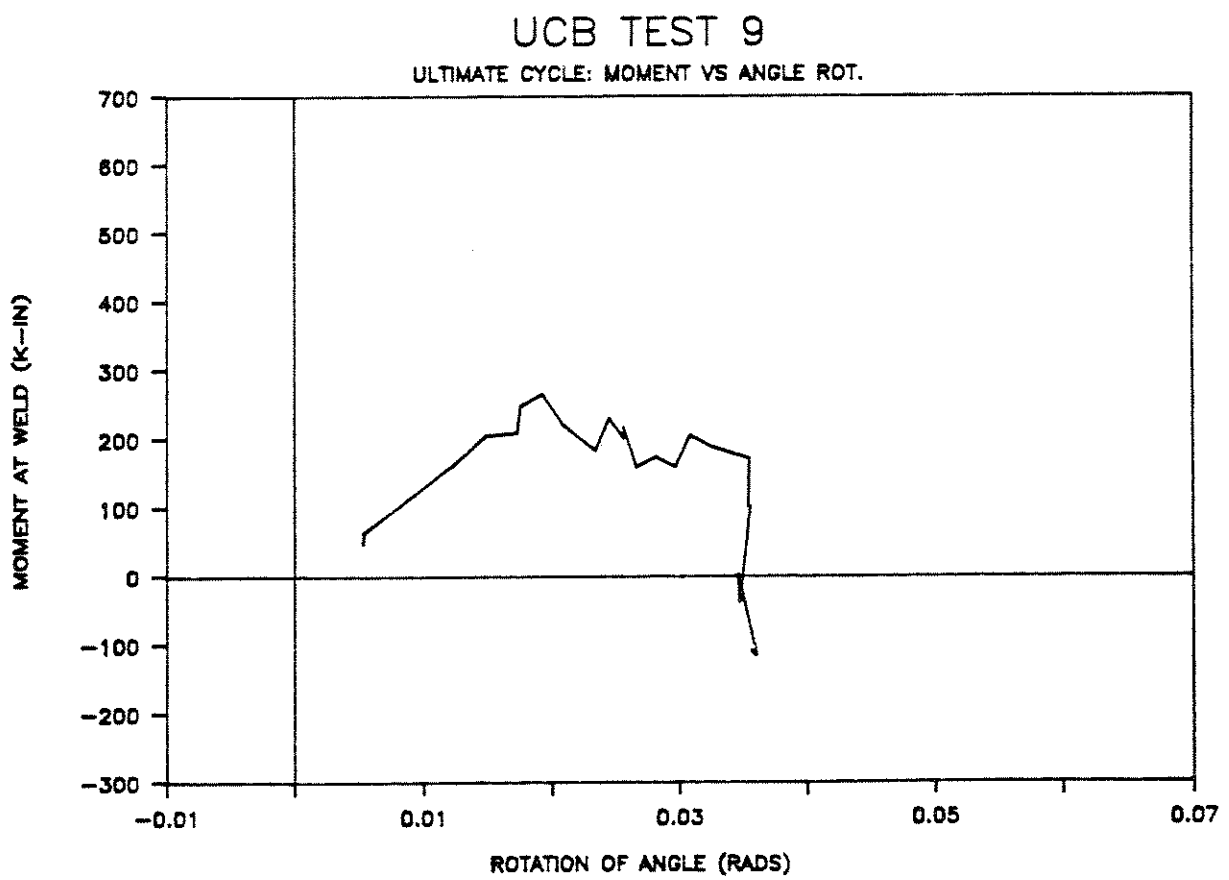
UCB TEST 9
ULTIMATE CYCLE: MOMENT VS ANGLE ROT.
MOMENT AT WELD (K-IN)
700
600
500
400
300
200
100
0
-100
-200
-300
-0.01
0.01
0.03
0.05
0.07
ROTATION OF ANGLE (RADS)

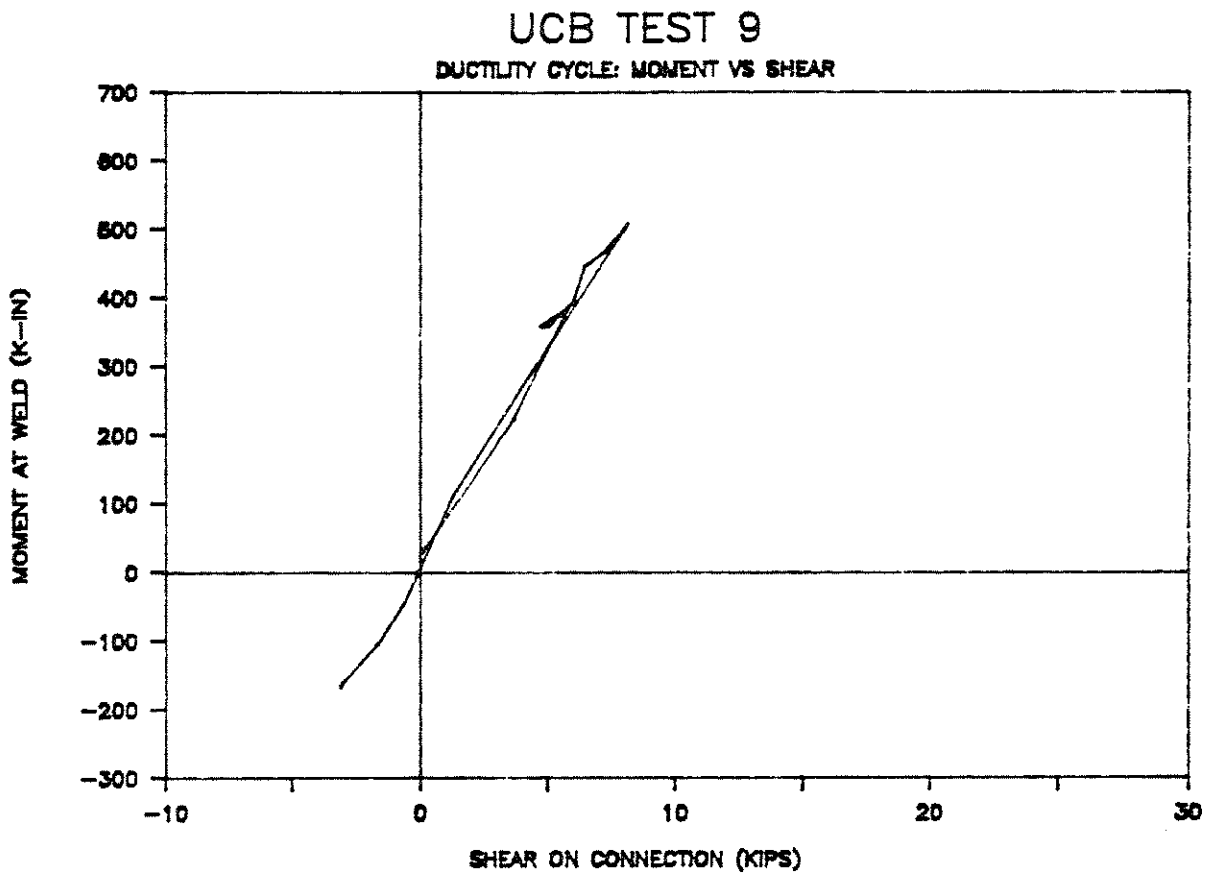
UCB TEST 9
DUCTILITY CYCLE: MOMENT VS SHEAR
MOMENT AT WELD (K-IN)
700
600
500
400
300
200
100
0
-100
-200
-300
-10
0
10
20
30
SHEAR ON CONNECTION (KIPS)

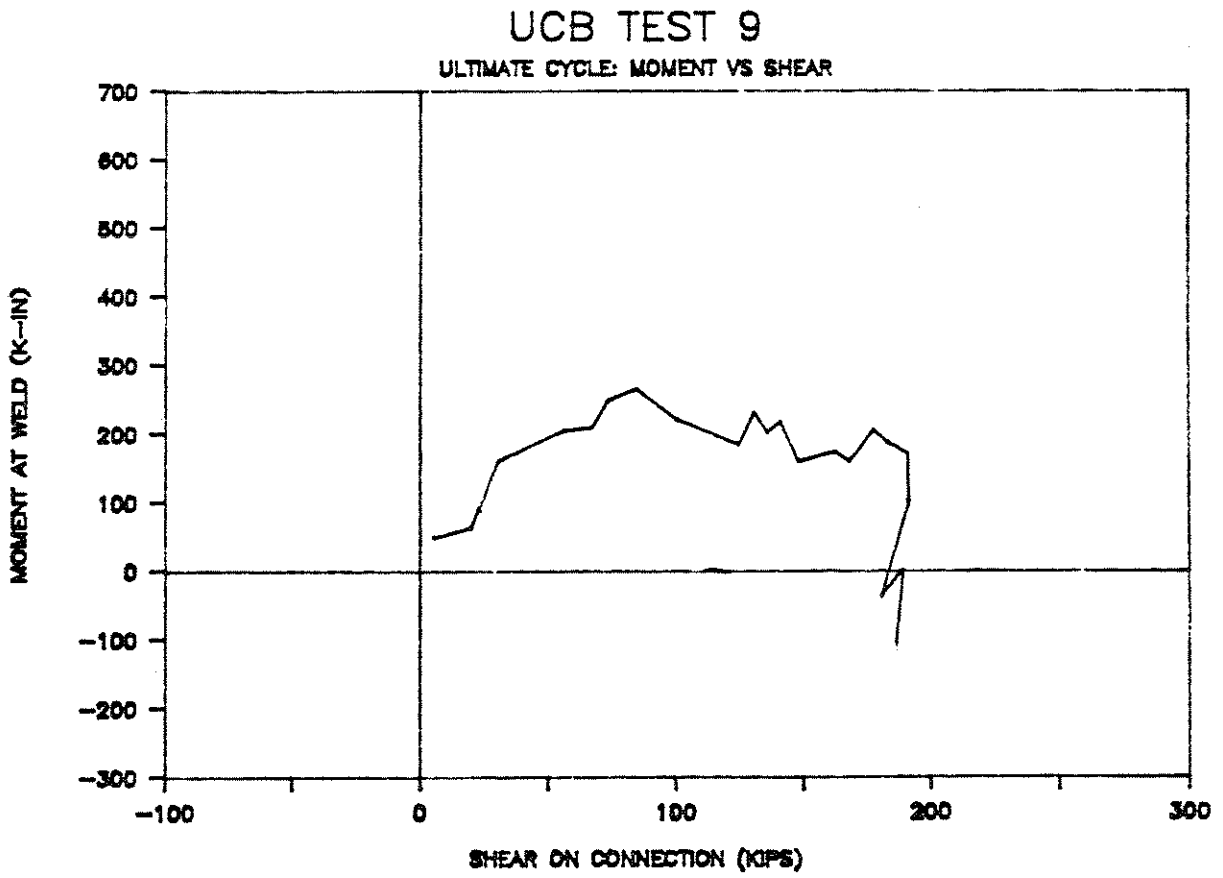
UCB TEST 9
ULTIMATE CYCLE: MOMENT VS SHEAR
MOMENT AT WELD (K-IN)
700
600
500
400
300
200
100
0
-100
-200
-300
-100
0
100
200
300
SHEAR ON CONNECTION (KIPS)

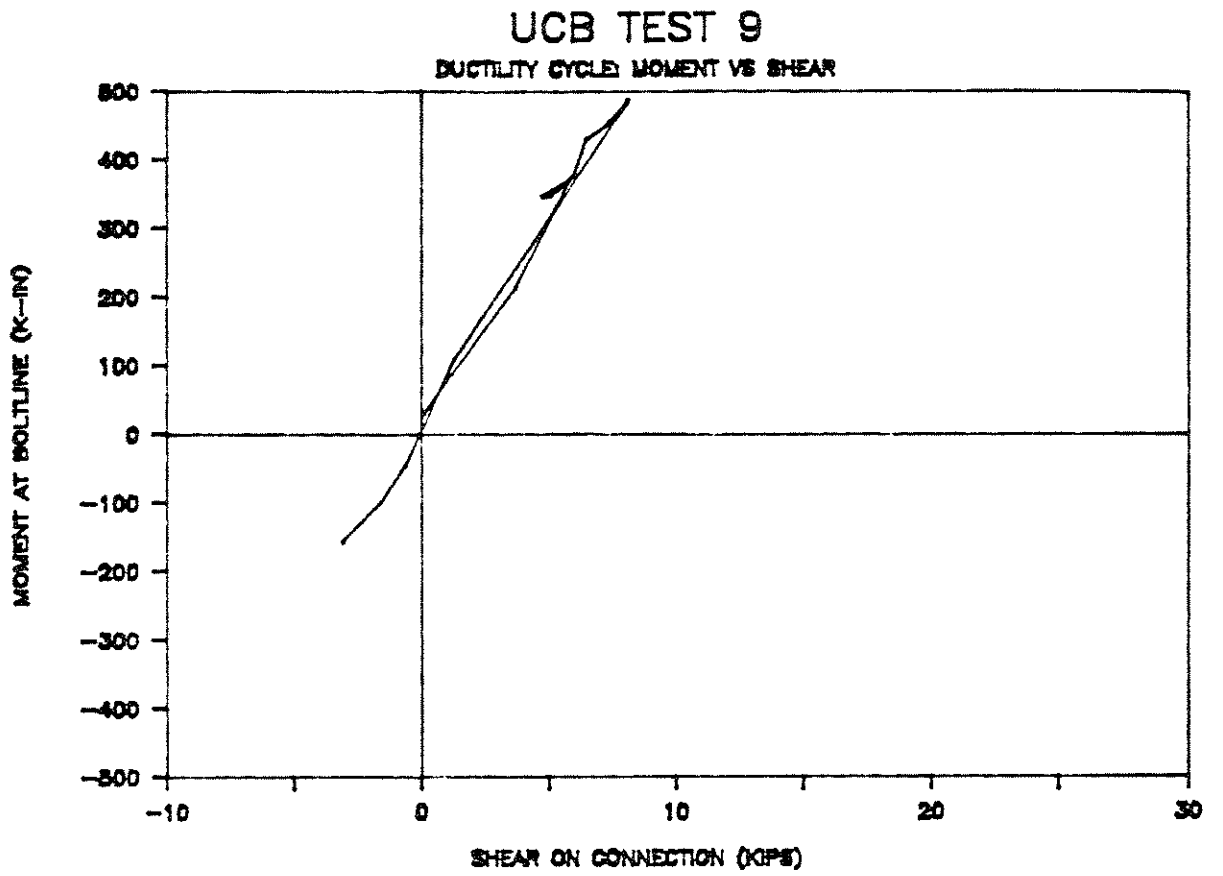
UCB TEST 9
DUCTILITY CYCLE: MOMENT VS SHEAR
MOMENT AT BOLTLINE (K--IN)
500
400
300
200
100
0
-100
-200
-300
-400
-500
-10
0
10
20
30
SHEAR ON CONNECTION (KIPS)

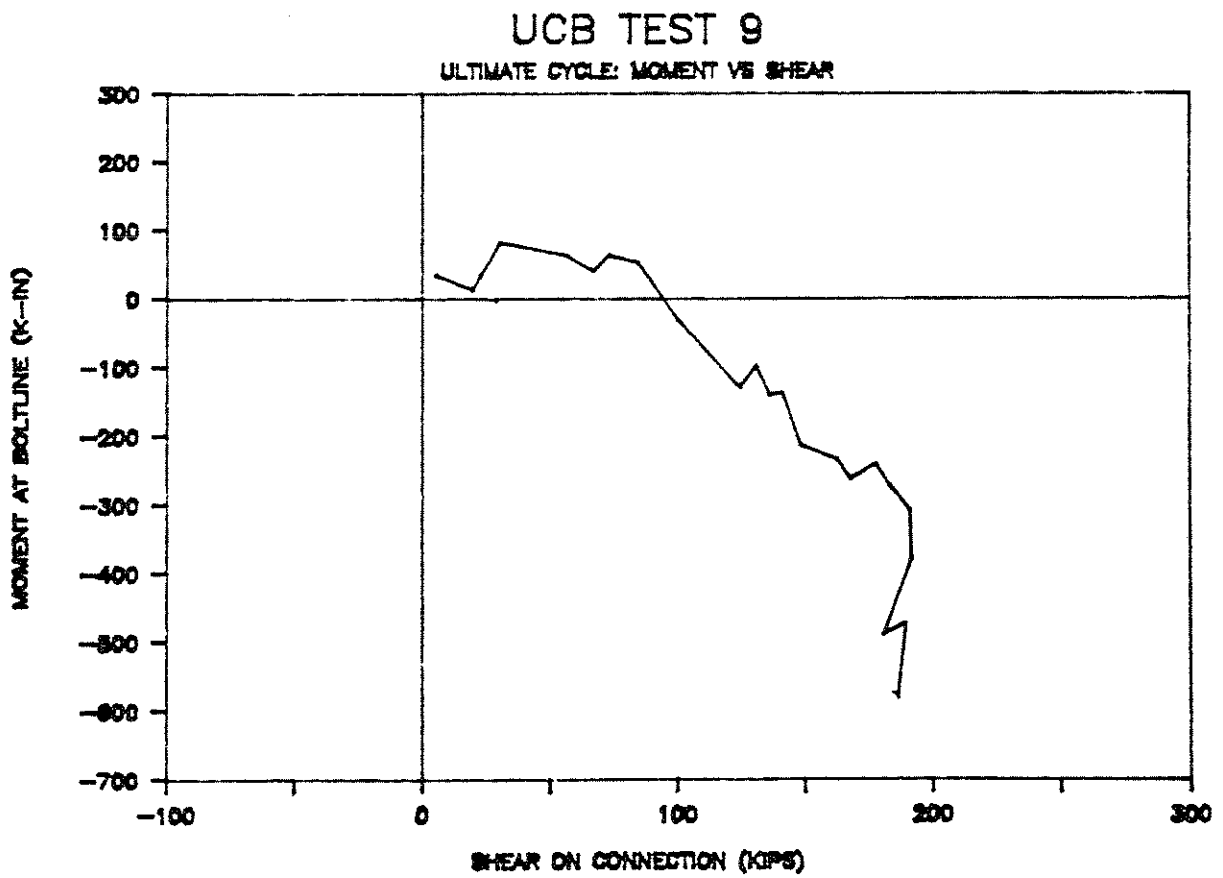
UCB TEST 9
ULTIMATE CYCLE: MOMENT VS SHEAR
MOMENT AT BOLTLINE (K--IN)
300
200
100
0
-100
-200
-300
-400
-500
-600
-700
-100
0
100
200
300
SHEAR ON CONNECTION (KIPS)

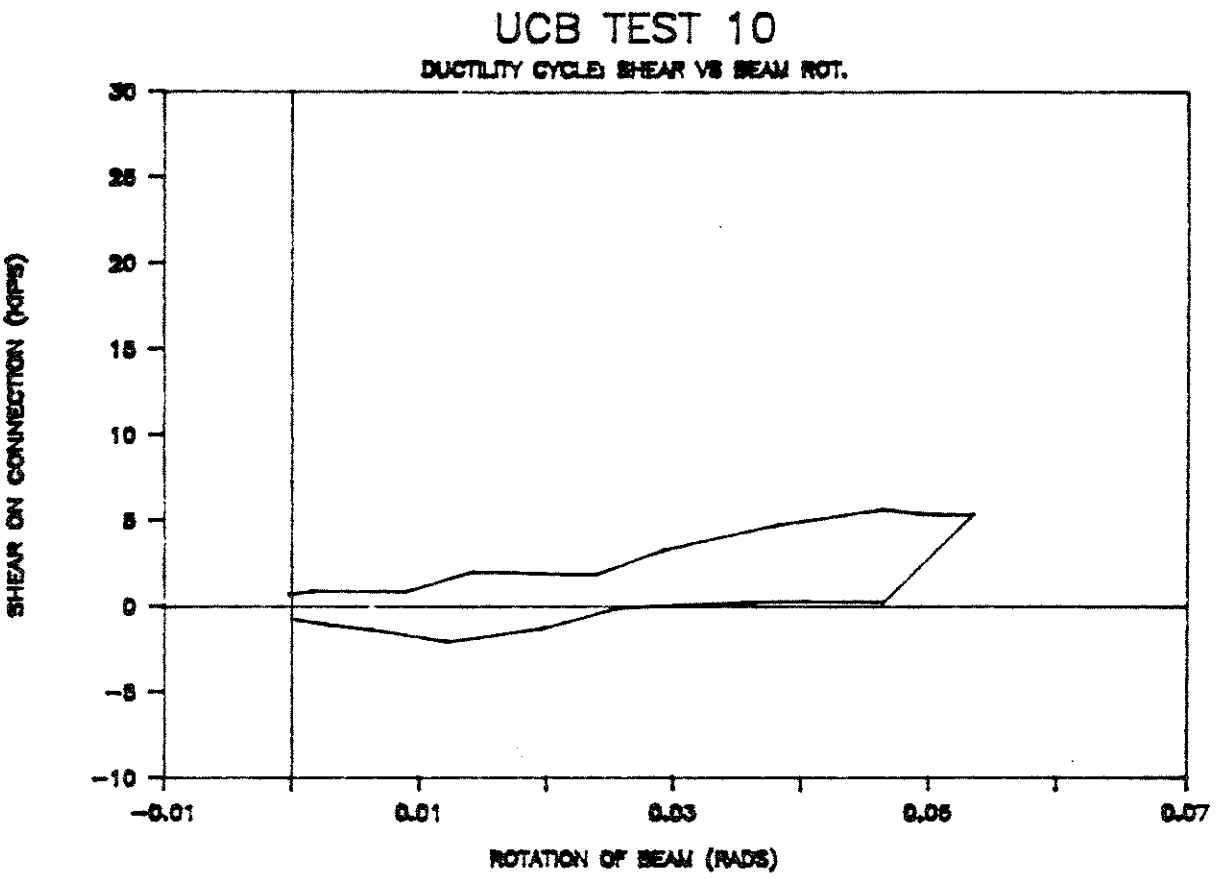
UCB TEST 10
DUCTILITY CYCLE: SHEAR VS BEAM ROT.
SHEAR ON CONNECTION (KIPS)
30
25
20
15
10
5
0
-5
-10
-0.01
0.01
0.03
0.05
0.07
ROTATION OF BEAM (RADS)

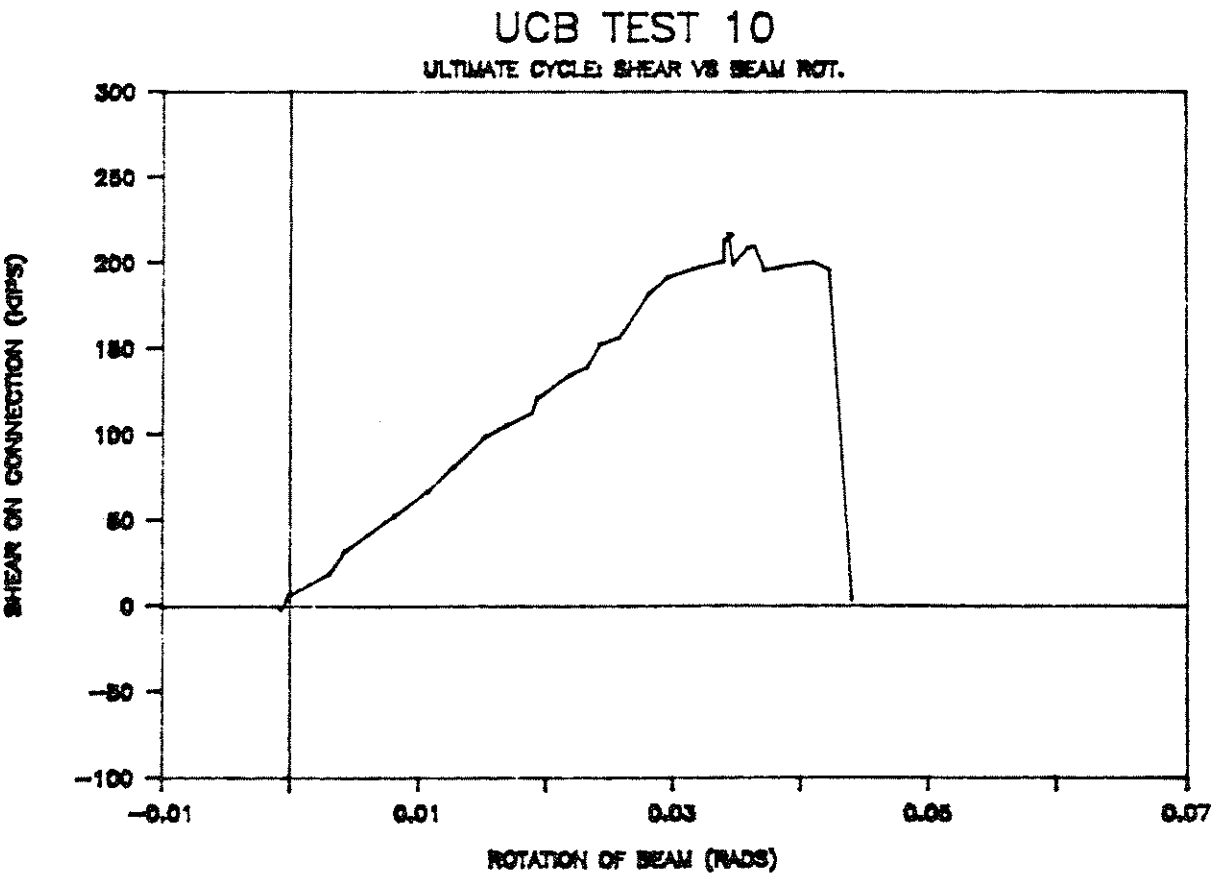
UCB TEST 10
ULTIMATE CYCLE: SHEAR VS BEAM ROT.
SHEAR ON CONNECTION (KIPS)
300
250
200
150
100
50
0
-50
-100
-0.01
0.01
0.03
0.05
0.07
ROTATION OF BEAM (RADS)

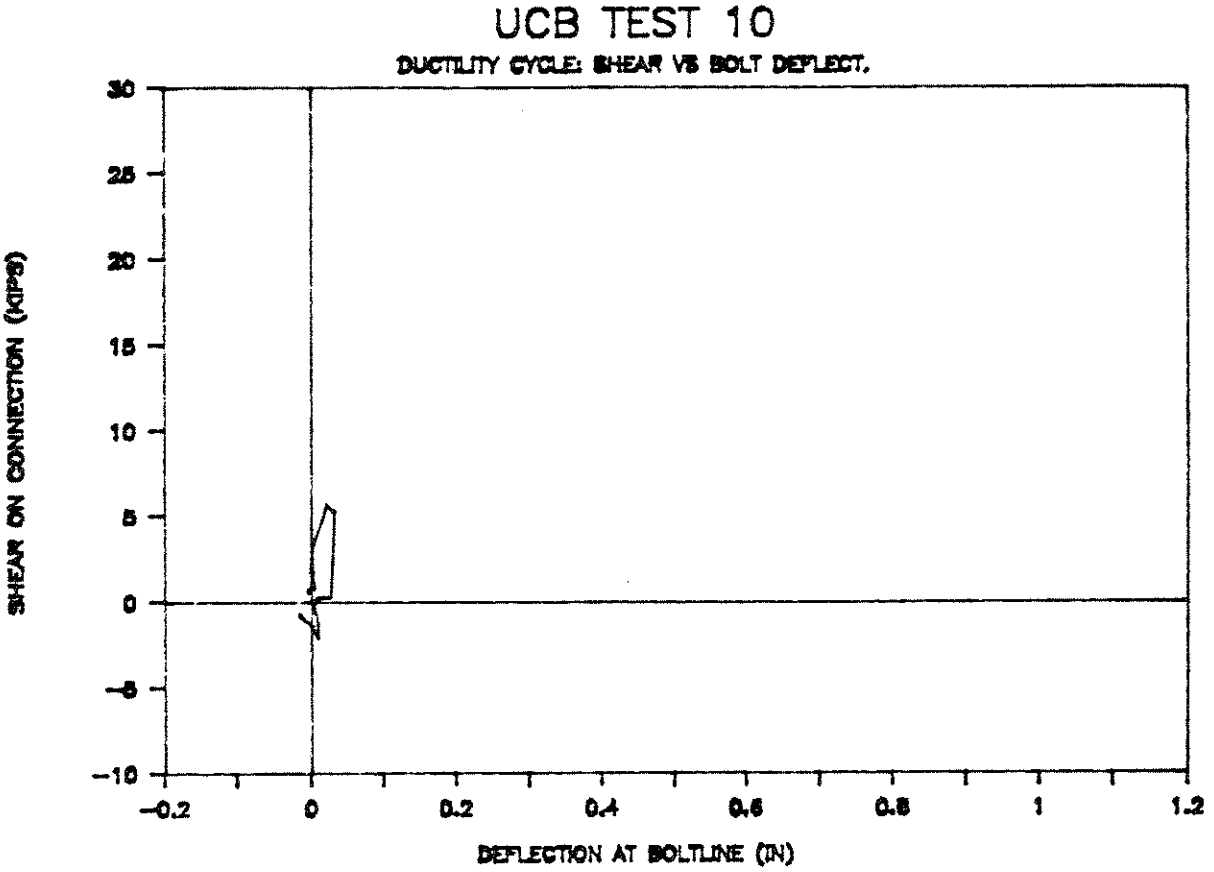
UCB TEST 10
DUCTILITY CYCLE: SHEAR VS BOLT DEFLECT.
SHEAR ON CONNECTION (KIPS)
30
25
20
15
10
5
0
-5
-10
-0.2
0
0.2
0.4
0.6
0.8
1
1.2
DEFLECTION AT BOLTLINE (IN)

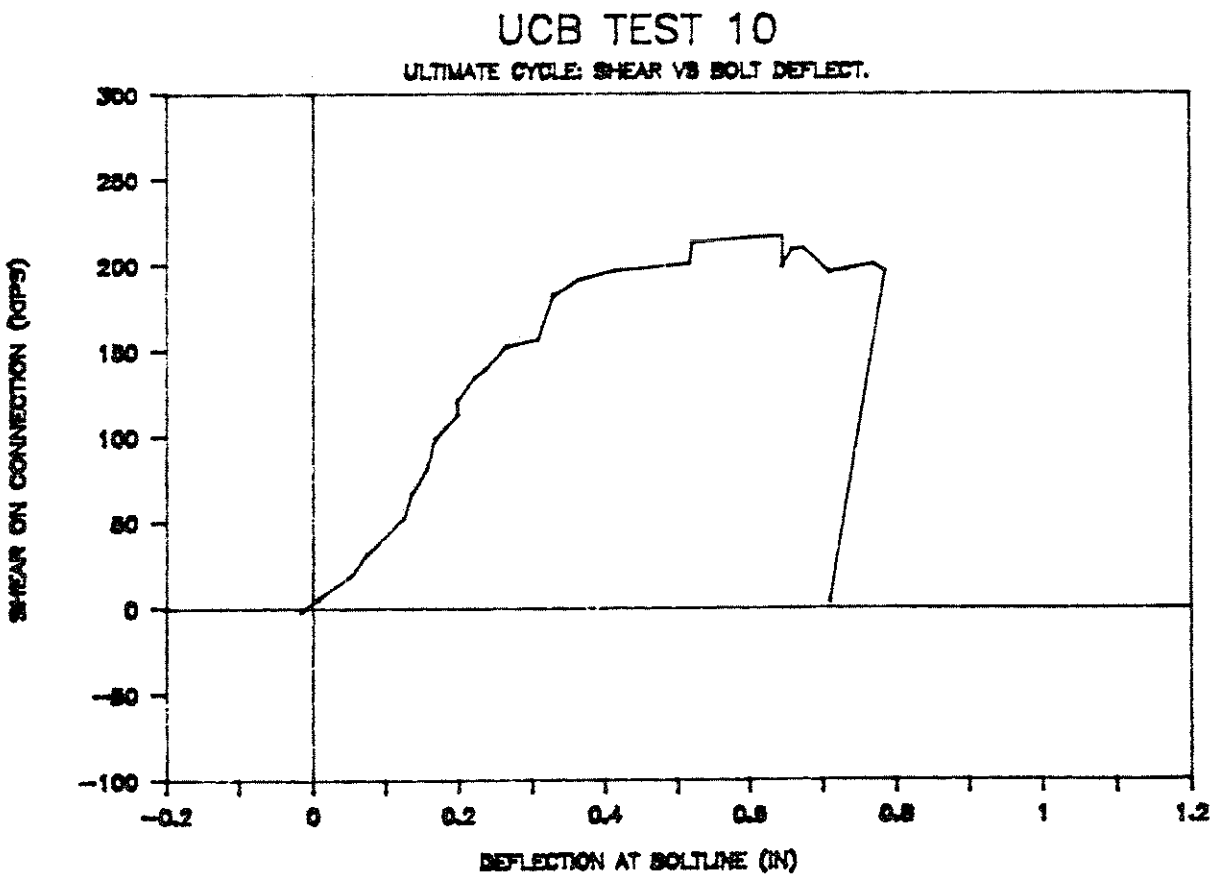
UCB TEST 10
ULTIMATE CYCLE: SHEAR VS BOLT DEFLECT.
SHEAR ON CONNECTION (KIPS)
300
250
200
150
100
50
0
-50
-100
-0.2
0
0.2
0.4
0.6
0.8
1
1.2
DEFLECTION AT BOLTLINE (IN)

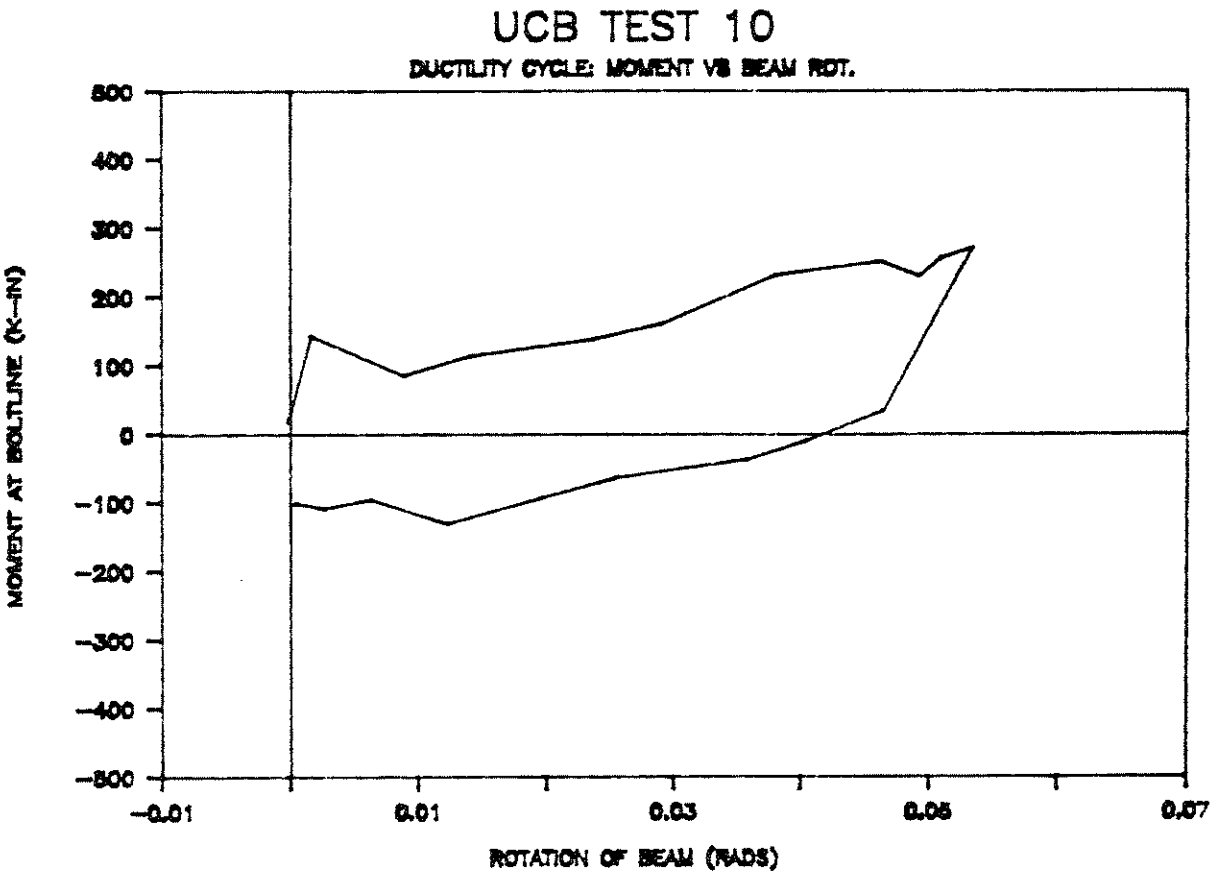
UCB TEST 10
DUCTILITY CYCLE: MOMENT VS BEAM ROT.
MOMENT AT BOLTLINE (K--IN)
500
400
300
200
100
0
-100
-200
-300
-400
-500
-0.01
0.01
0.03
0.05
0.07
ROTATION OF BEAM (RADS)

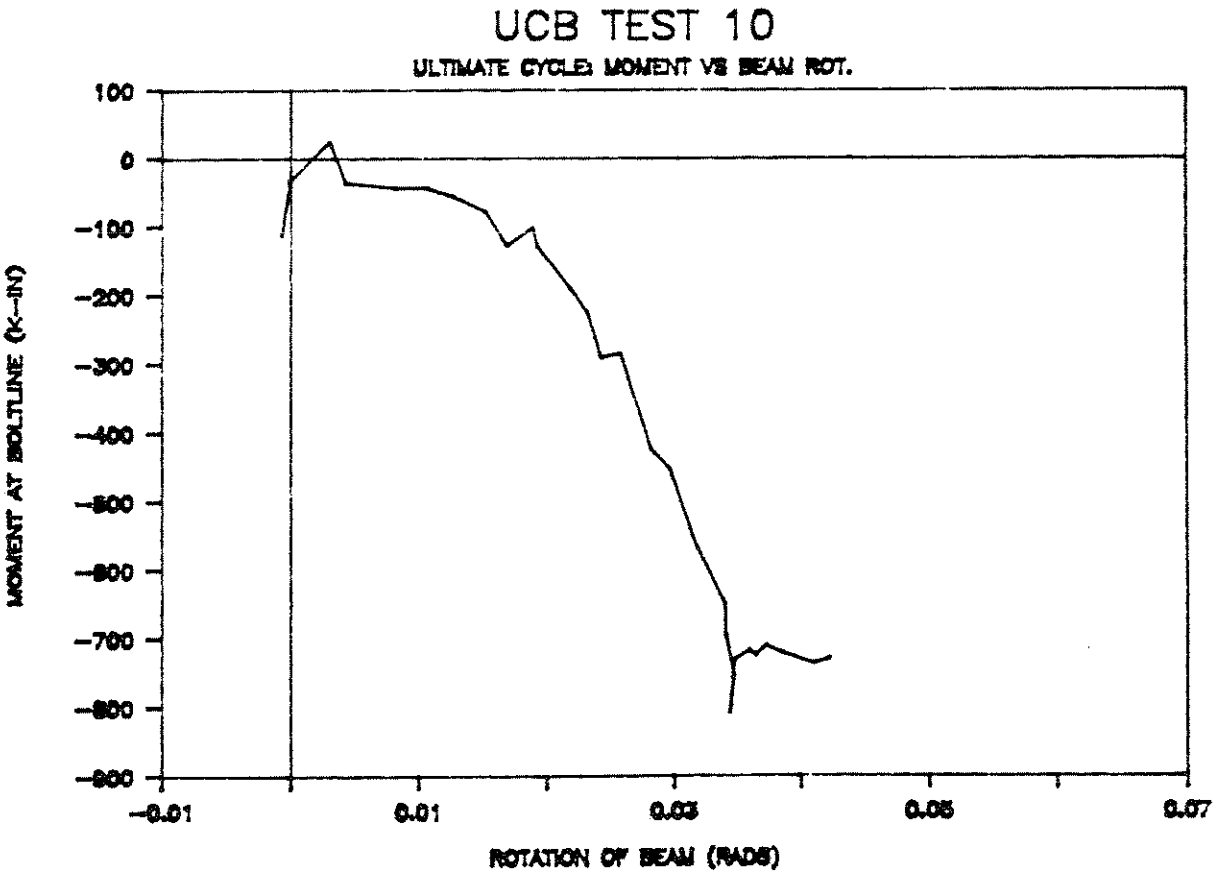
UCB TEST 10
ULTIMATE CYCLE: MOMENT VS BEAM ROT.
MOMENT AT BOLTLINE (K--IN)
100
0
-100
-200
-300
-400
-500
-600
-700
-800
-900
-0.01
0.01
0.03
0.05
0.07
ROTATION OF BEAM (RADS)

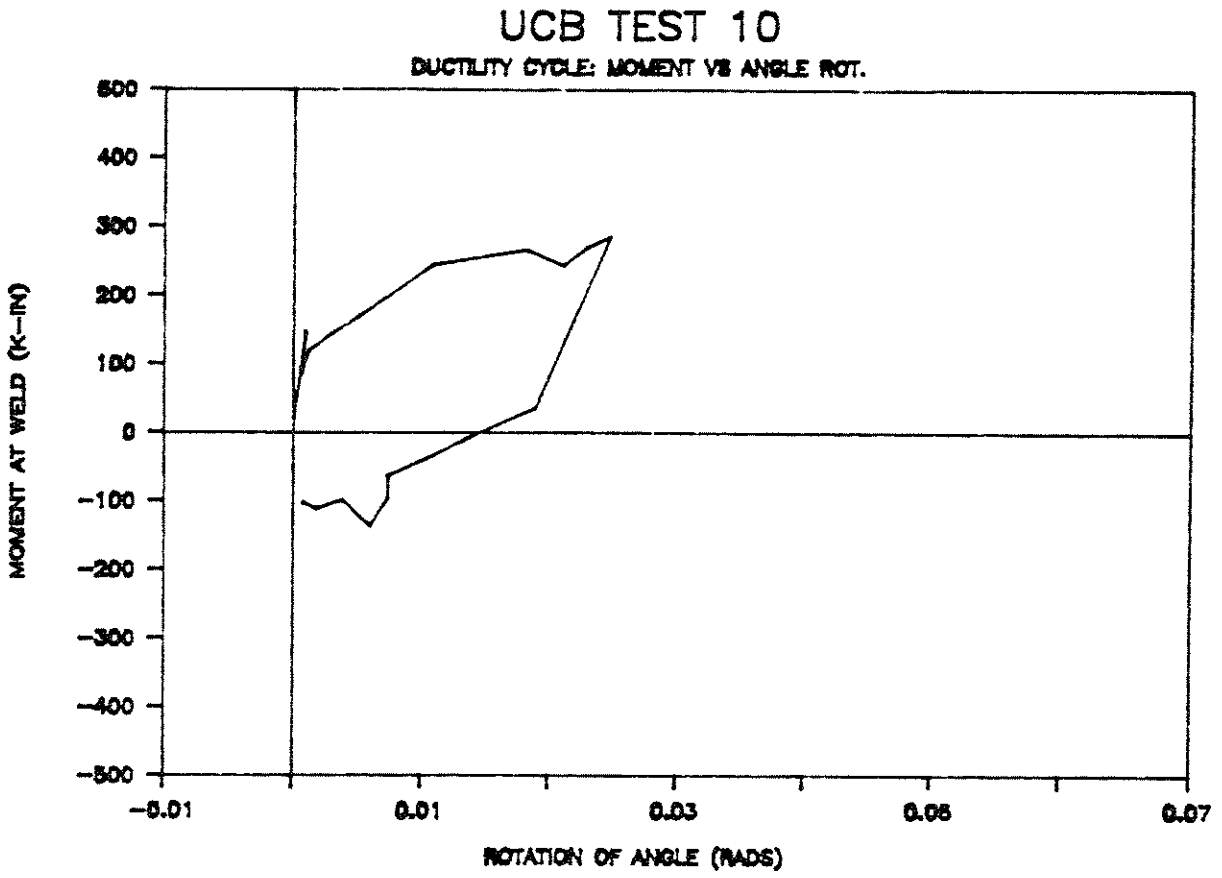
UCB TEST 10
DUCTILITY CYCLE: MOMENT VS ANGLE ROT.
MOMENT AT WELD (K--IN)
500
400
300
200
100
0
-100
-200
-300
-400
-500
-0.01
0.01
0.03
0.05
0.07
ROTATION OF ANGLE (RADS)

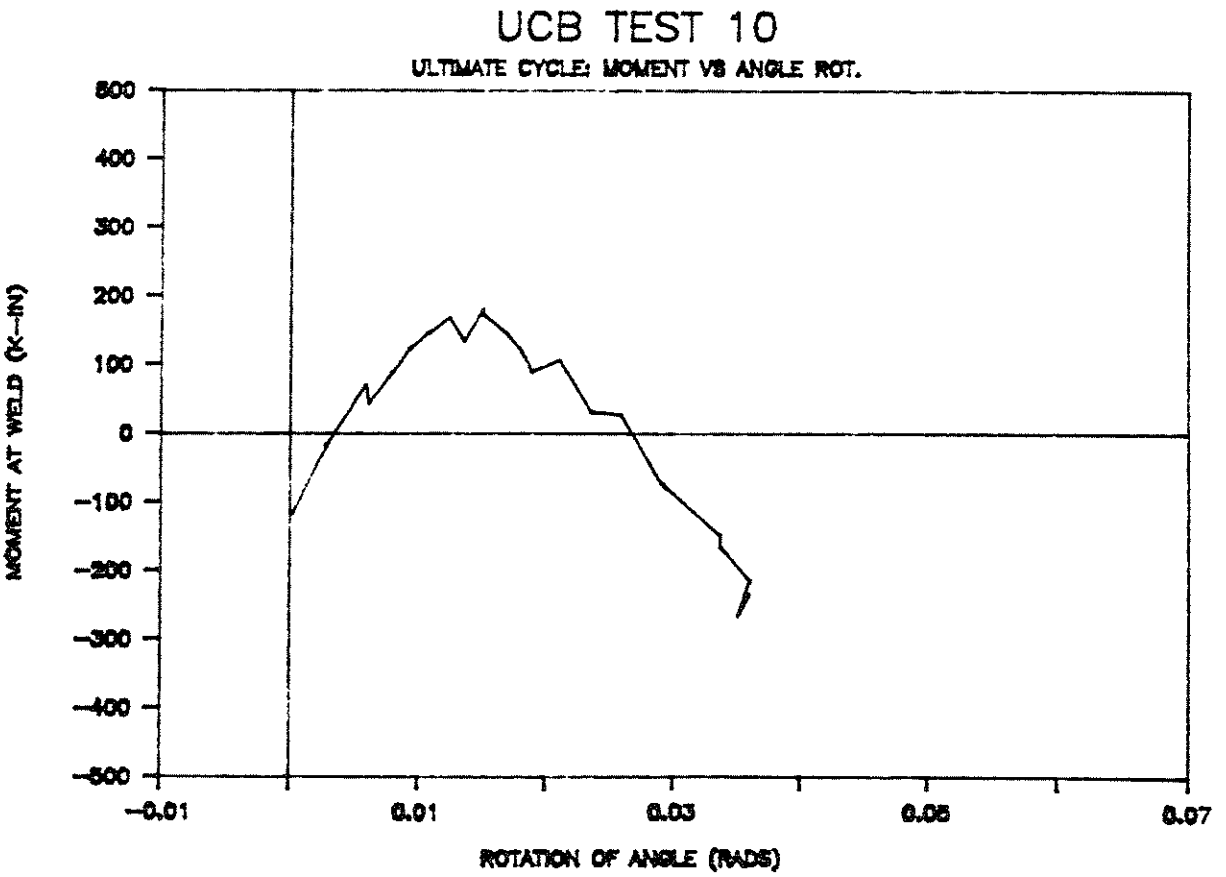
UCB TEST 10
ULTIMATE CYCLE: MOMENT VS ANGLE ROT.
MOMENT AT WELD (K--IN)
500
400
300
200
100
0
-100
-200
-300
-400
-500
-0.01
0.01
0.03
0.05
0.07
ROTATION OF ANGLE (RADS)

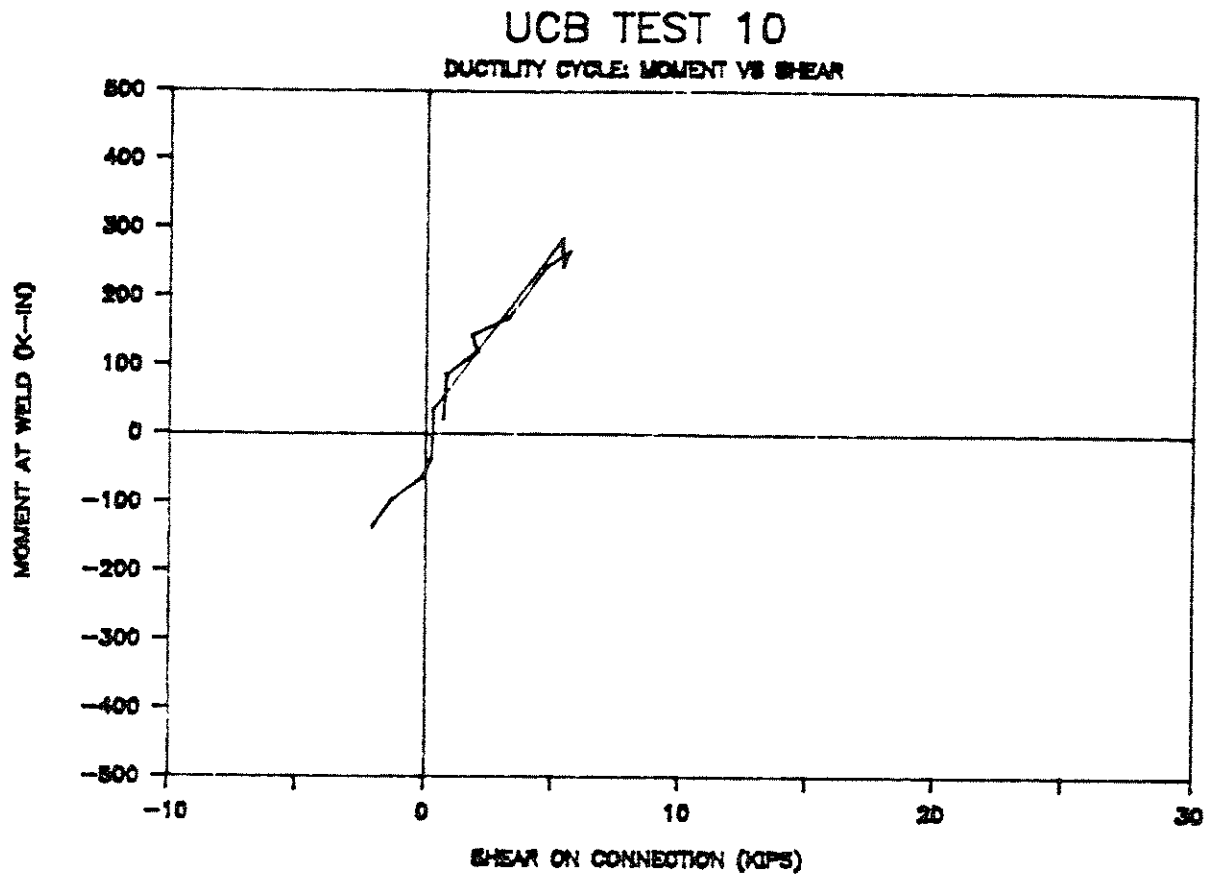
UCB TEST 10
DUCTILITY CYCLE: MOMENT VS SHEAR
MOMENT AT WELD (K--IN)
500
400
300
200
100
0
-100
-200
-300
-400
-500
-10
0
10
20
30
SHEAR ON CONNECTION (KIPS)

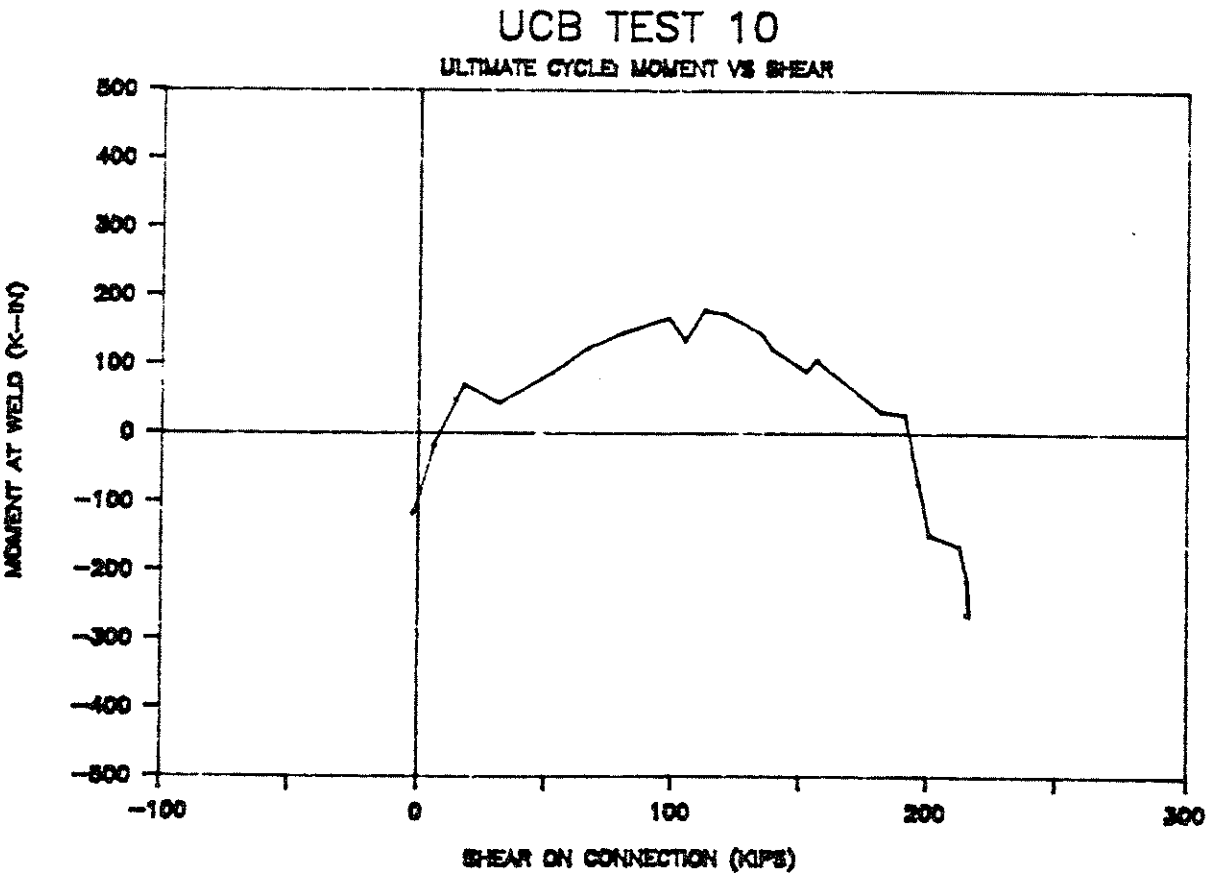
UCB TEST 10
ULTIMATE CYCLE: MOMENT VS SHEAR
MOMENT AT WELD (K--IN)
500
400
300
200
100
0
-100
-200
-300
-400
-500
-100
0
100
200
300
SHEAR ON CONNECTION (KIPS)

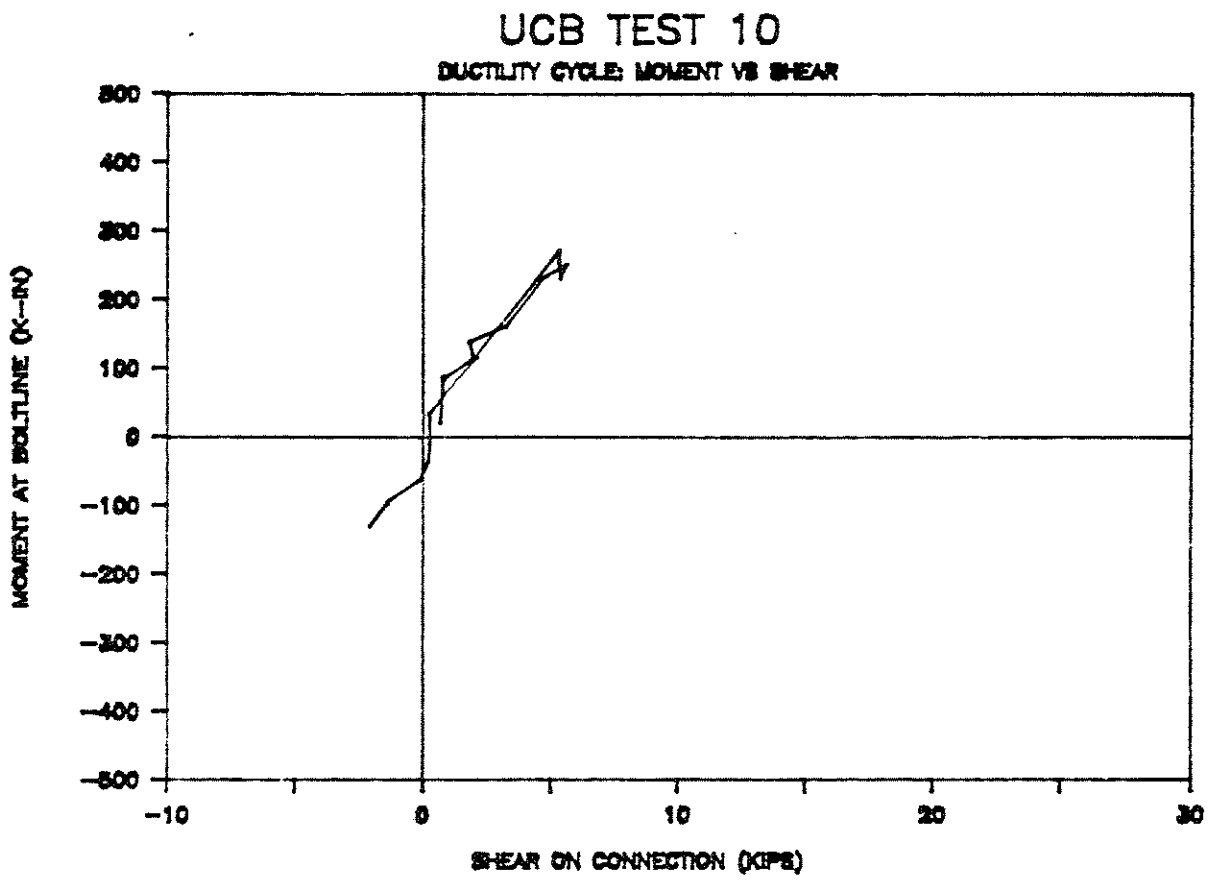
UCB TEST 10
DUCTILITY CYCLE: MOMENT VS SHEAR
MOMENT AT BOLTLINE (K-IN)
SHEAR ON CONNECTION (KIPS)
500
400
300
200
100
0
-100
-200
-300
-400
-500
-10
0
10
20
30

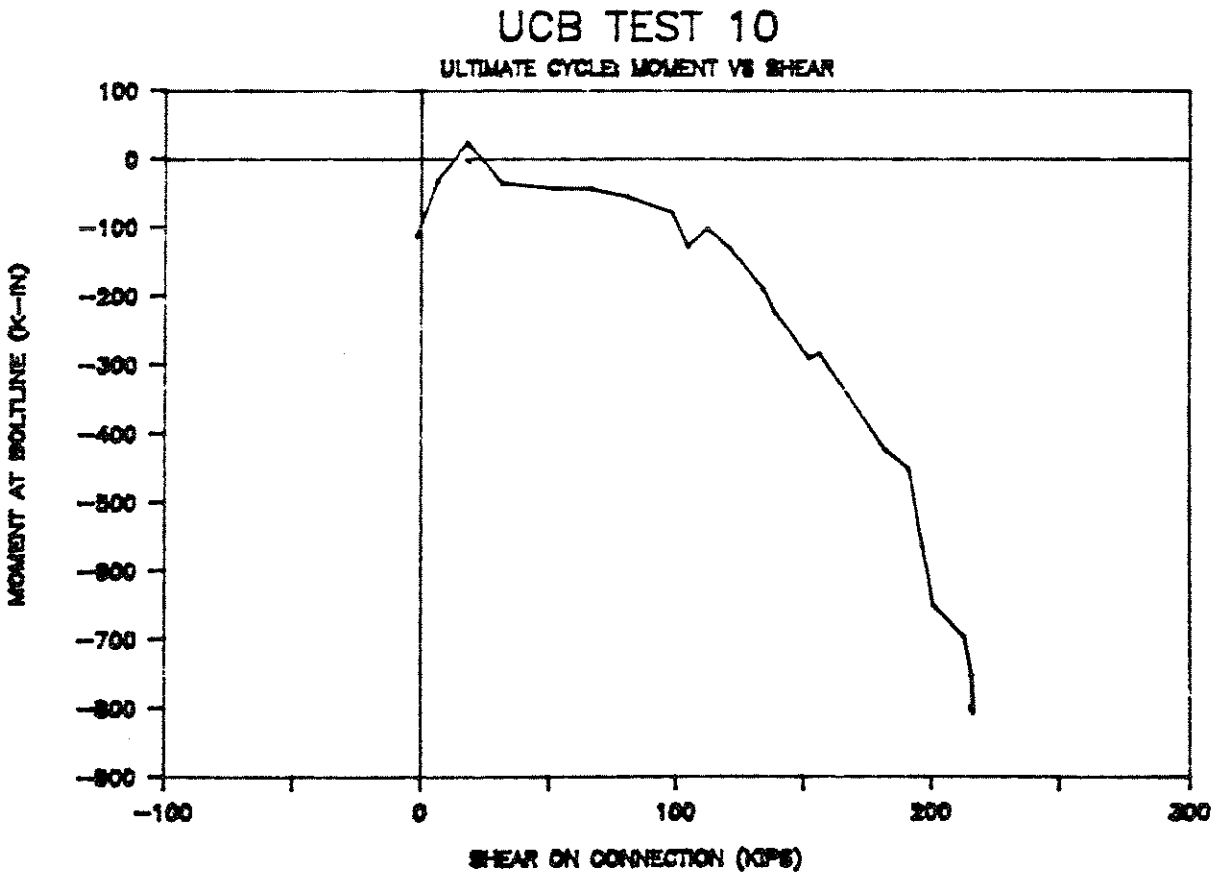
UCB TEST 10
ULTIMATE CYCLE: MOMENT VS SHEAR
MOMENT AT BOLTLINE (K-IN)
SHEAR ON CONNECTION (KIPS)
100
0
-100
-200
-300
-400
-500
-600
-700
-800
-900
-100
0
100
200
300

APPENDIX C

THE RICHARD'S MODEL

The Richard Equations were developed to analyze the non-linear load-deformation relationship of a structural system. The equation was originally published by Richard and Abbott in 1975 and has been used to model connections by LeBouton and Richard, Blewitt and Richard and Hsia and Richard.

The Richard Equation is based on four parameters that are developed from the analysis of test data. The numeric value of these parameters differ for various configurations and types of structures.

Richard Equation

$$M = \frac{(K - KP) \times \Theta}{\left[1 + \left|\frac{(K - KP) \times \Theta}{Rc}\right|^{N}\right]^{1/N}} + (KP \times \Theta)$$

M = Load (moment or force)
Θ = Deformation (rotation or displacement)
K = Elastic Stiffness
KP = Plastic Stiffness
N = Shape Parameter — Based on sharpness of transition between K and KP
Rc = Reference Load